The one-dimensional spin-1/2 ANNNI model in non-commuting magnetic fields

Von der Universität Bayreuth
zur Erlangung des Grades eines
Doktors der Naturwissenschaften (Dr. rer. nat.)
genehmigte Abhandlung

von

Adekunle M. Adegoke

geboren in Lagos, Nigeria

1. Gutachter: Prof. Dr. Helmut Büttner
2. Gutachter: Prof. Dr. Werner Pesch

Tag der Einreichung: 06. 06. 2006
Tag des Kolloquiums:19. 07. 2006

„Gedruckt mit Unterstützung des Deutschen Akademischen Austauschdienstes“

Abstract

In this thesis we have investigated the one-dimensional spin-1/2 Axial Next Nearest Neighbour Ising (ANNNI) model in non-commuting magnetic fields. As a starting point we obtained an estimate of the phase diagram of the model by treating the spins as classical vectors. This was followed by an investigation of the zero temperature ground state of the one-dimensional spin-1/2 ANNNI model in a longitudinal magnetic field. By using the symmetries of the Hamiltonian, we were able to diagonalize the longitudinal ANNNI model exactly. We found that there are four different possible ground state configurations for the longitudinal ANNNI model, in the thermodynamic limit. Rayleigh Schroedinger perturbation series for the ground state energy of the ANNNI model in non-commuting fields were then developed in each of the four ordered regions. Order parameters and the associated susceptibilities as well as specific heats were calculated. By application of the finite-size scaling technique it was possible to obtain the phase boundaries of the model numerically. For certain limits of the full Hamiltonian we compared the obtained results with the existing literature and we got good agreement.

Zussamenfassung

Gegenstand dieser Arbeit war die Untersuchung des eindimensionalen Spin-1/2 Ising Modells mit Übernächster - Nachbar Wechselwirkung (das sog. ANNNI Modell) in nichtkommutierenden magnetischen Feldern.Als Ausgangspunkt behandelten wir die Spins als klassische Vektoren um eine Abschaetzung des Phasendiagramms zu erhalten. Diesem folgte eine Untersuchung des T=0 Grundzustandes des eindimensionalen Spin-1/2 ANNNI Modells mit longitudinalem Feld. Durch Ausnutzen der Symmetrieeigenschaften des Hamiltonians, war es möglich das longitudinale Modell exakt zu diagonalisieren. Wir fanden heraus, dass es im thermodynamischen Limes vier mögliche, voneinander verschiedene Grundzustandskonfigurationen gibt.Dann wurde für das ANNNI Modell mit nichtkommutierenden Feldern die Grundzustandsenergie in den vier geordneten Regionen mittels Raleigh Schrödinger Störungsentwicklung entwickelt. Sowohl Ordnugsparameter mit zugehörigen Suszeptibilitäten als auch spezifische Wärmen wurden berechnet. Durch Anwendung der finite-size scaling Technik war es möglich die Phasengrenzen des Modells numerisch zu erhalten. Für gewisse Grenzfälle des gesamten Hamiltonians wurde ein Vergleich mit Literaturdaten durchgeführt und gute Übereinstimmung erzielt.

Contents

Chapter 1

Introduction

Frustration as a result of competitive interactions in magnetic models has remained a subject of active research [1, 2, 3]. The most popular model in which the effects of regular frustration on spin models have been extensively studied is the axial next nearest neighbour Ising (ANNNI) model [4, 5]. The ANNNI model is described by a system of Ising spins with nearest neighbour interactions along all the lattice directions (x, y and z) as well as a competing next nearest neighbour interaction in one axial (*e.g.* z) direction.

Recently, there has been an increased interest in transverse Ising models in which the competition is generated by the presence of an external longitudinal field [3, 5]. The phase transitions in the transverse field Ising model in a competing periodic longitudinal field have been studied in [5] using numerical diagonalization of finite systems and finite size scaling procedure. The transition line between the ordered and disordered phases was found and the model was found to belong to the universality class of the two dimensional Ising model. In reference [3] the antiferromagnetic transverse Ising chain in a uniform longitudinal field was studied. Combining the technique of Density Matrix Renormalization group (DMRG) and finite size scaling the authors of [3] came to conclusions similar to those of [5].

In this work we have investigated an Ising system in which frustration is due to the presence of an external transverse field as well as competitive interactions from next nearest neighbour spins and the influence of an external longitudinal field. Specifically, we have studied the one-dimensional ANNNI model in an external transverse magnetic field h_x and a uniform longitudinal field h_z. The system is described by the Hamiltonian

$$H = \sum_i S_i^z S_{i+1}^z + j \sum_i S_i^z S_{i+2}^z - h_x \sum_i S_i^x - h_z \sum_i S_i^z \tag{1.1}$$

where j is the next nearest neighbour exchange interaction, S_i are the usual spin-$\frac{1}{2}$ operators and the fields h_x and h_z are measured in units where the splitting factor and Bohr magneton are unity.

While so far almost exclusively ferromagnetically coupled spins have been discussed in the literature, we will focus this thesis on the antiferromagnetic coupling.

To the best of our knowledge the model (1.1) has never been investigated before. We have employed symmetry considerations [6] to diagonalize the Hamiltonian (1.1) for finite systems and we have used the finite size scaling technique to determine the phase boundaries, after the fashion of [7].

The ANNNI model in non-commuting fields is particularly interesting because it is a rather complete model in the following sense: various special cases of the model have either been exactly solved or their phase diagrams obtained using numerical and approximate techniques. In particular we would like to mention the following cases:

- $h_z = 0$, $h_x = 0$ in Hamiltonian (1.1) is the well-known and well-studied one-dimensional ANNNI model. The ANNNI model was proposed by Elliot [8] to account for the existence of modulated phases in some rare-earth compounds. The ANNNI model is the simplest non-trivial model that exhibits spatially modulated phases [9, 10, 11, 12]. The ground state of the model at zero temperature is well known in all dimensions [13, 14]: the two-fold degenerate antiferromagnetic state for $j < 1/2$ and the four-fold degenerate antiphase configuration for $j > 0.5$. The model is infinitely degenerate at $j = 1/2$, with the degeneracy being of the order of τ^N for a system of N spins, τ being the golden ratio. An excellent review of the ANNNI model can be found in Selke [13].

- The case $h_z = 0$, $j = 0$ corresponds to the Ising model in a transverse field. This model belongs to the same universality class of the two-dimensional Ising model [3, 5]. The transverse Ising model has been solved analytically by Pfeuty [15], who obtained the ground state energy of the model using a technique developed by Lieb et al. [16] and employed the results of McCoy [17] to investigate the order in the system. The model is gapped at $h_x < 0.5$ with non-zero staggered magnetization, with the ground state being two-fold degenerate in the thermodynamic limit. The transverse Ising model becomes gapless at $h_x = 1/2$ and the order parameter (staggered magnetization) vanishes as function of $h_x = -1/2$ with the critical exponent $\frac{1}{8}$.

- When $h_z = 0$ in Hamiltonian (1.1), we have the one-dimensional ANNNI model in a transverse field. Again, this is a well-studied model, and one which has continued to arouse interest among researchers. The reason this model has been extensively studied is probably due to the fact that the zero temperature (quantum) critical behaviour of a quantum spin Ising system in d-dimension is usually related to the thermal behaviour of the corresponding classical system in $d+1$-dimension, and vice versa [4, 18]. For spin-1/2, the relation between the quantum d-dimensional transverse Ising model and the $(d+1)$-dimensional classical Ising model is most clearly seen by considering the Ising model in an extremely anisotropic limit of the exchange couplings [19, 20]. Following Fradkin and Susskind [21], Barber and Duxbury [22] were able to relate the one-dimensional quantum ANNNI model to the transfer matrix of the two-dimensional ANNNI model and then carry out a detailed investigation of the phase diagram. The two-dimensional ANNNI model (whose critical properties should be equivalent to that of the one-dimensional quantum model) was investigated for the first time by the transfer matrix technique for semi-infinite strips by Pesch and Kroemer [23], thereby obtaining the correlation functions and the structure factor. It is not clear if the transverse ANNNI model can be solved exactly, although there have been several attempts in this direction. Ruján [24] and later Sen and Chakrabarti [25] expressed the Hamiltonian for the transverse field ANNNI model in terms of interacting fermions in order to apply Jordan-Wigner transformations to diagonalize the system exactly (apparently following in the footsteps of Lieb et al. [16] and Pfeuty [15]). The next nearest neighbour interaction term however introduced a four-fermion operator term in the Hamiltonian which precludes its exact diagonalization. Sen and Chakrabarti [25] employed a mean field approximation to cope with the quartic coupling of the fermion operators and arrived thus to an approximate solution of the model. Sen and Chakrabarti [2] attempted to improve on this method by using a self-consistent Hartree-Fock method [26] to write the Jordan-Wigner transformed Hamiltonian in a diagonal form and obtained the critical boundary for order-disorder transitions for $j \leq 0.5$. The method failed to produce results for $j > 0.5$. As part of the quest to understand the transverse ANNNI model, Rieger and Uimin [1] considered, instead of the original Hamiltonian, a reduced model which they showed to be a reasonable modification when the competition parameter j, as well as the frustration parameter h_x are small. They were able to obtain the excitation spectrum for the reduced model. One should also mention the Real Space Renormalization Group (RSRG) calculations [25] using the truncation method [27, 28] (in which a number of spins are grouped in a block and the Hamiltonian for a single block is diagonalized exactly). The RSRG methods, frequently employed to study phase

transitions in classical systems, were extended to study the critical properties of quantum systems at $T = 0$ [29, 30]. Also worthy to mention are the Field-Theoretic Renormalization Group calculations which give direct evidence for the existence of a floating phase with algebraically decaying correlations [31]. So far the most detailed phase diagrams for the transverse ANNNI model have been obtained using numerical or approximate calculations such as perturbation expansions and finite size scaling [9, 22, 24, 32, 33], the Strong Coupling Eigenstate Method (SCEM) [34, 35, 36] and Monte Carlo methods [11, 37]. The phase diagram of the transverse ANNNI model obtained from systematic perturbation expansions and finite size scaling [22] has the same general topology as that found in Monte Carlo calculations. The results also suggest that a Lifshitz point exists at around $j \approx 0.35$ for the ferromagnetic model. Villain and Bak [12] and Coopersmith et al. [38] however argued that the ferromagnetic and floating phases do not coexist but are always separated by a paramagnetic phase. Peschel and Emery [39] found a particular line (the so-called one-dimensional line) along which the ground state energy and the correlation length can be determined exactly, the latter being everywhere finite. More recent investigations (for example Guimarães et al. [33], Sen [40]) corroborate the earlier results.

- When $j = 0$ in Hamiltonian (1.1), the model is the Ising model in two external magnetic fields, longitudinal and transverse. While it is true that field-induced effects in low-dimensional quantum spin systems have been studied for a long time [41, 42], one should remark however that in the past, the longitudinal field was often introduced mainly as an artifice to facilitate the calculation of order parameter and associated susceptibility as can be seen for example in references [20, 22, 34]. Models incorporating two noncommuting fields are gaining popularity, however, among experimentalists as well as theoreticians as is evident for example in references [3, 5, 43, 44]. Sen [5] investigated the quantum phase transitions in the ferromagnetic transverse Ising model in a spatially modulated longitudinal field and obtained the phase diagram of the model at zero temperature, using finite size scaling techniques. It was found that a continuous phase transition occurs everywhere except at the multiphase point $h_x = 0$ where a first order transition exists. The values of the critical exponents obtained in reference [5] are identical to those of the transverse Ising model, putting the model in the same universality class as the two-dimensional classical Ising model. Ovchinnikov et al. [3] investigated the antiferromagnetic Ising chain in the presence of a transverse magnetic field and a longitudinal magnetic field, and showed that the quantum phase transition existing in the transverse Ising model remains in the presence of the longitudinal field. Using the Density Matrix Renormalization Group (DMRG) technique of White [45], they found the critical line in the (h_x, h_z) plane where the mass

gap disappears and the staggered magnetizations along the X and Z axes vanish. The authors of reference [3] established that the Ising model in non-commuting fields belongs to the universality class of the transverse Ising model.

- The case $h_x = 0$ in the Hamiltonian (1.1) corresponds to the ANNNI model in a longitudinal field. This is a classical model in the sense that all operators involved commute. The longitudinal ANNNI model has interesting properties and its investigation is the subject of chapter 3 of this thesis where we show that there are four possible ground state configurations, the ferromagnetic, antiferromagnetic, antiphase and the three-fold degenerate $\uparrow\uparrow\downarrow$ ground states. We note that this is a classical model with competitive interaction from the nearest neighbours, next nearest neighbours and the longitudinal field. The effect of the transverse field in the general Hamiltonian (1.1) is therefore to introduce quantum fluctuations in the system. As will be seen in chapters 4 and 5, the existing order of the longitudinal ANNNI model is destroyed by quantum fluctuations.

The organization of the thesis is as follows. In chapter 2 we will present a study of the classical ANNNI model in mixed fields. The idea is to have an insight into what to expect at the quantum level. In chapter 3 we shall obtain the phase diagram of the longitudinal ANNNI model. The discussions will also include the various symmetries that can be gainfully employed for reducing the dimension of the Hilbert space for exact diagonalization. Chapter 4 will be concerned with perturbation expansions of the ground state energy of the Hamiltonian (1.1) around $h_x = 0$. The associated order parameters will also be calculated. In Chapter 5 we will employ the finite size scaling technique to estimate the phase diagram of the ANNNI model in the presence of two non-commuting external magnetic fields. A summary of our results as well as suggestions for future investigation are presented in chapter 6.

Chapter 2

Classical approach to the ANNNI model in mixed fields

Given a quantum system, it is often of benefit to first examine the theory in the large $\hbar$ limit. In many cases, this often gives one an idea or a general overview of what to expect at the quantum level. Of course one has to exercise some caution in interpreting the classical results and in drawing conclusions since the behaviour of a system may be very different at the quantum level than the results one obtains classically. Nonetheless, a classical treatment of a model usually sheds some light on the system. In the first part of this chapter we will give a spin waves theory treatment of the one dimensional ANNNI model while the second part will be concerned with a classical mechanical theory.

2.1 Spin waves treatment of the antiferromagnetic ground state

The analytical determination of the exact ground state of Ising-like models has proved and has remained difficult. Consequently one often has to resort to various approximate theories. One such theory is the spin waves theory introduced by Bloch [46] in his theory of ferromagnetism and later rederived by Kramers and Heller [47] in a semiclassical fashion. This theory was employed by Hulthén [48] in studying the small vibrations of simple antiferromagnetic lattices from their classical equilibrium state. His neglect of the zero-point energy and motion however made the results to disagree with the rigorous exact ground state worked out by Bethe [49]. The spin waves theory was used by Anderson in successfully obtaining the ground state energy as well as in the determination of the long range order parameters of an Heisenberg antiferromagnet.

The Anderson ground state energy fell within the rigorous limits derived using the variational principle and was in good agreement with the exact result obtained by Bethe for a spin-1/2 linear chain. Anderson found that the Heisenberg antiferromagnet with nearest neighbour interaction possesses no long range order in one dimension but that long range order exists in two and in three dimensions.

A more recent example of a successful application of the spin wave theory may be found in the work of Gaididei and Büttner [50] where it was shown that the ground state properties of a frustrated compressible antiferromagnet differ qualitatively from that of an Heisenberg antiferromagnet on an anisotropic triangular lattice.

In this section we will adapt the spin waves theory of Anderson to determine the ground state and other properties of the one dimensional ANNNI model.

The one-dimensional ANNNI model is described by the Hamiltonian

$$H = \sum_{i=1}^{N} S_i^z S_{i+1}^z + j \sum_{i=1}^{N} S_i^z S_{i+2}^z \,, \tag{2.1}$$

where i and $i+1$ in the first sum refer to nearest neighbour spins and i and $i+2$ in the second sum denote next nearest neighbour spins, with the summation going over all such pairs. N is the number of lattice sites and j is the next nearest neighbour exchange interaction. We assume periodic boundary conditions, so that $S_{N+1}^z = S_1^z$ and $S_{N+2}^z = S_2^z$.

The basic assumption in the derivation of the semiclassical spin waves is that the antiferromagnetic state is not greatly different from the classical ground state in which the spins on odd sites all point in one direction (say +z), the spins on even lattice sites in the other direction. For convenience we label spins on odd sites with subscript m and those on even numbered sites with n. So we assume

$$S_m^z \cong +\frac{1}{2}, \quad S_n^z \cong -\frac{1}{2}\,. \tag{2.2}$$

Now

$$(S^z)^2 = (S_c)^2 - \left((S^x)^2 + (S^y)^2\right) \,, \tag{2.3}$$

where $S_c = \sqrt{S(S+1)} = \sqrt{3}/2$ is the classical total spin of a spin$-1/2$ atom.

For the odd and even sites we have

$$\begin{aligned} S_m^z &= +\sqrt{S_c^2 - ((S_m^x)^2 + (S_m^y)^2)} \\ &= +S_c\sqrt{1 - \frac{(S_m^x)^2 + (S_m^y)^2}{S_c^2}} \end{aligned} \tag{2.4}$$

and

$$\begin{aligned} S_n^z &= -\sqrt{S_c^2 - ((S_n^x)^2 + (S_n^y)^2)} \\ &= -S_c\sqrt{1 - \frac{(S_n^x)^2 + (S_n^y)^2}{S_c^2}} \end{aligned} \tag{2.5}$$

respectively.

Under assumption (2.2), the binomial theorem allows us to write

$$S_m^z \cong S_c - \left((S_m^x)^2 + (S_m^y)^2\right)/2S_c \,, \tag{2.6}$$

$$S_n^z \cong -S_c + \left((S_n^x)^2 + (S_n^y)^2\right)/2S_c \,. \tag{2.7}$$

For the next nearest neighbour spins we have

$$\begin{aligned} &S_{i+2}^z \equiv S_m^z \text{ if } i \text{ is odd} \\ &S_{i+2}^z \equiv S_n^z \text{ if } i \text{ is even } [1]. \end{aligned} \tag{2.8}$$

Substituting (2.6), (2.7) and (2.8) in the Hamiltonian (2.1), we have

$$H = (j-1)\left\{ NS_c^2 - \sum_m \left((S_m^x)^2 + (S_m^y)^2\right) - \sum_n \left((S_n^x)^2 + (S_n^y)^2\right) \right\} . \tag{2.9}$$

Next we introduce two sets of spin waves, one pair for each sublattice:

$$\begin{aligned} S_m^x &= 1\Big/\sqrt{N}\sum_\lambda \exp(i\lambda m)Q_\lambda \,, \\ S_m^y &= 1\Big/\sqrt{N}\sum_\lambda \exp(-i\lambda m)P_\lambda \end{aligned} \tag{2.10}$$

and

$$S_n^x = 1\Big/\sqrt{N}\sum_\lambda \exp(-i\lambda n)R_\lambda\,,$$
$$S_n^y = -1\Big/\sqrt{N}\sum_\lambda \exp(i\lambda n)S_\lambda \tag{2.11}$$

where in each case the sum runs over $N/2$ values of λ and the wave numbers λ are given by

$$\lambda = 2\pi l/N,\ l = -\tfrac{1}{2}N, -\tfrac{1}{2}N+2, \cdots, -2, 0, 2, \cdots \tfrac{1}{2}N \tag{2.12}$$

The inverse transformations are

$$Q_\lambda = 2\Big/\sqrt{N}\sum_m \exp(-i\lambda m)S_m^x\,,$$
$$P_\lambda = 2\Big/\sqrt{N}\sum_m \exp(i\lambda m)S_m^y \tag{2.13}$$

and

$$R_\lambda = 2\Big/\sqrt{N}\sum_n \exp(i\lambda n)S_n^x\,,$$
$$S_\lambda = -2\Big/\sqrt{N}\sum_n \exp(-i\lambda n)S_n^y \tag{2.14}$$

Clearly, spin waves operators corresponding to spins on different sites commute, so that Q_λ commutes with $Q_{\lambda'}$, $P_{\lambda'}$, $R_{\lambda'}$, and $S_{\lambda'}$; R_λ commutes with $R_{\lambda'}$, $P_{\lambda'}$, $S_{\lambda'}$, and $Q_{\lambda'}$ and so on.

Direct substitution of (2.10) and (2.11) into (2.13) and (2.14) together with the identity

$$\sum_m \exp(i(\lambda-\lambda')m) = \tfrac{1}{2}N\delta_{\lambda\lambda'} \tag{2.15}$$

lead to

$$[Q_\lambda, P_{\lambda'}] = \delta_{\lambda\lambda'} i\sum_m S_m^z \Big/ \tfrac{1}{4}N = i\delta_{\lambda\lambda'} \tag{2.16}$$

and

$$[R_\lambda, S_{\lambda'}] = i\delta_{\lambda\lambda'}\,, \tag{2.17}$$

where we have used the assumption (2.2) to evaluate

$$\sum_m S_m^z = \sum_{m=1}^{N/2}\left(\frac{1}{2}\right) = \frac{N}{4}\,. \tag{2.18}$$

We also have [51]

$$\sum_m (S_m^x)^2 = \tfrac{1}{2}\sum_\lambda Q_\lambda^2 \,,$$
$$\sum_m (S_m^y)^2 = \tfrac{1}{2}\sum_\lambda P_\lambda^2 \,,$$
$$\sum_n (S_n^x)^2 = \tfrac{1}{2}\sum_\lambda R_\lambda^2 \,,$$

and

$$\sum_n (S_n^y)^2 = \tfrac{1}{2}\sum_\lambda S_\lambda^2 \,. \tag{2.19}$$

Substituting the spin waves (2.10) and (2.11) in (2.9), the sums can be easily rewritten in terms of the spin wave operators Q_λ, P_λ, R_λ and S_λ, with the use of the set of equations (2.19).

The Hamiltonian then becomes

$$H = (j-1)\left\{ NS_c^2 - \tfrac{1}{2}\sum_\lambda \left(P_\lambda^2 + Q_\lambda^2 + R_\lambda^2 + S_\lambda^2\right)\right\} \,. \tag{2.20}$$

Let us now introduce a new set of coordinates by defining [51]

$$P_\lambda = (p_{1\lambda} + p_{2\lambda})\Big/\sqrt{2},\ Q_\lambda = (q_{1\lambda} + q_{2\lambda})\Big/\sqrt{2},$$
$$S_\lambda = (p_{1\lambda} - p_{2\lambda})\Big/\sqrt{2},\ R_\lambda = (q_{1\lambda} - q_{2\lambda})\Big/\sqrt{2}\,.$$

This is a canonical transformation of the spin coordinates since $q_{1\lambda}$, $p_{1\lambda}$, $q_{2\lambda}$ and $p_{2\lambda}$ obey the same commutation rules as Q_λ, P_λ, R_λ and S_λ

$$[q_{2\lambda}, p_{2\lambda}] = i$$
$$[q_{2\lambda}, p_{2\lambda}] = i\,, \quad \text{etc} \tag{2.21}$$

The Hamiltonian is now

$$H = (j-1)\left\{ 3N/4 - \tfrac{1}{2}\sum_\lambda \left(q_{1\lambda}^2 + p_{1\lambda}^2 + q_{2\lambda}^2 + p_{2\lambda}^2\right)\right\} \,. \tag{2.22}$$

Since the eigenenergy of the unit-frequency harmonic oscillator $H = p_\lambda^2 + q_\lambda^2$ with $[q_\lambda, p_\lambda] = \mathrm{i}$ is $E = 2n_\lambda + 1$, the Hamiltonian (2.22) therefore has the energies

$$E = (j-1)\left\{3N/4 - \sum_{\lambda}(n_{1\lambda} + n_{2\lambda} + 1)\right\} . \tag{2.23}$$

In the ground state all $n_\lambda = 0$ and we have

$$E_g = (j-1)N/4 . \tag{2.24}$$

2.1.1 Long range order

The long range order parameter is given by the expectation value of total S_z on one site [51] in the ground state. Thus by equation (2.4) we have

$$(S_z)^{(1)}_{tot} = \sum_m S^z_m = NS_c/2 - \sum_m \left((S^x_m)^2 + (S^y_m)^2\right) \Big/ 2S_c . \tag{2.25}$$

Using (2.19) and the canonical transformations (2.21) we have

$$(S_z)^{(1)}_{tot} = \tfrac{1}{2}NS_c - (1/8S_c)\sum_{\lambda}(q^2_{1\lambda} + p^2_{1\lambda} + q^2_{2\lambda} + p^2_{2\lambda} + q_{1\lambda}q_{2\lambda} + p_{1\lambda}p_{2\lambda}) . \tag{2.26}$$

The antiferromagnetic long range order parameter ξ can then be computed by taking the average of $(S_z)^{(1)}_{tot}$ in the ground state. Thus,

$$\begin{aligned}\xi &= \tfrac{1}{2}NS_c - (1/8S_c)\sum_{\lambda} < (q^2_{1\lambda} + p^2_{1\lambda} + q^2_{2\lambda} + p^2_{2\lambda}) > \\ &= \tfrac{1}{2}NS_c - (1/2S_c)\sum_{\lambda} < q^2_{1\lambda} > \\ &= \tfrac{1}{2}NS_c - \frac{N}{8S_c} .\end{aligned} \tag{2.27}$$

We used the fact that the average kinetic and potential energies of a harmonic oscillator are the same and that for a unit frequency oscillator, $2 < q^2_{1\lambda} >= 2 < p^2_{1\lambda} >= 1$. The magnetization per site is therefore

$$\xi/N = \tfrac{1}{2}(\sqrt{3}\Big/2) - \frac{1}{8(\sqrt{3}/2)} = \sqrt{3}\Big/6 . \tag{2.28}$$

Thus we see that the spin waves theory predicts long range order for the one dimensional antiferromagnetic ANNNI model. This is in contrast for example to the Heisenberg model for which there is no long range order, as rigorously demonstrated by Bethe, Hulthén and later Anderson [48, 49, 51].

2.2 The transverse ANNNI model

The Hamiltonian for the transverse ANNNI model is given by

$$H = \sum_i S_i^z S_{i+1}^z - j \sum_i S_i^z S_{i+2}^z - h_x \sum_i S_i^x \,, \tag{2.29}$$

where h_x is the transverse external magnetic field.

Here as in the previous section we assume that the ground state of the classical model $h_x = 0$ is antiferromagnetic. We note that since here only S^z is being measured we cannot say anything about the signs of S_m^x and S_n^x, all we can say is that S_m^x is measured on the sublattice of odd sites and S_n^x is measured on the sublattice of even sites. Thus we use the binomial theorem, as in the preceding section to write

$$S_m^x \cong S_c - \left((S_m^y)^2 + (S_m^z)^2\right)/2S_c \tag{2.30}$$

and

$$S_n^x \cong S_c - \left((S_n^y)^2 + (S_n^z)^2\right)/2S_c \,. \tag{2.31}$$

In terms of even sites and odd sites, the Hamiltonian (2.29) can be written as

$$\begin{aligned} H = 2\sum_{m,n} S_m^z S_n^z + j\left(\sum_m (S_m^z)^2 + \sum_n (S_n^z)^2\right) \\ -h_x\left(\sum_m S_m^x + \sum_n S_n^x\right) \,. \end{aligned} \tag{2.32}$$

Using (2.30) and (2.31) we have

$$\begin{aligned} h_x\left(\sum_m S_m^x + \sum_n S_n^x\right) = h_x N S_c - \frac{h_x}{2S_c}\left(\sum_m (S_m^y)^2 + \sum_n (S_m^z)^2\right) \\ - \frac{h_x}{2S_c}\left(\sum_n (S_n^y)^2 + \sum_n (S_n^z)^2\right) \,. \end{aligned} \tag{2.33}$$

The Hamiltonian now becomes

$$H = -h_x N S_c + 2\sum_{m,n} S_m^z S_n^z + j\left(\sum_m (S_m^z)^2 + \sum_n (S_n^z)^2\right) + \frac{h_x}{2S_c}\left(\sum_m (S_m^y)^2 + \sum_n (S_m^z)^2\right) + \frac{h_x}{2S_c}\left(\sum_m (S_m^y)^2 + \sum_n (S_m^z)^2\right) . \tag{2.34}$$

We now introduce the spin waves

$$\begin{aligned} S_m^y &= 1\Big/\sqrt{N}\sum_\lambda \exp(-i\lambda m) Q_\lambda \,, \\ S_m^z &= 1\Big/\sqrt{N}\sum_\lambda \exp(i\lambda m) P_\lambda \,, \\ S_n^y &= 1\Big/\sqrt{N}\sum_\lambda \exp(i\lambda n) R_\lambda \,, \\ S_n^z &= -1\Big/\sqrt{N}\sum_\lambda \exp(-i\lambda n) S_\lambda \,, \end{aligned} \tag{2.35}$$

with inverse

$$\begin{aligned} Q_\lambda &= 2/\sqrt{N}\sum_m \exp(-i\lambda m) S_m^y \,, \\ P_\lambda &= 2/\sqrt{N}\sum_m \exp(i\lambda m) S_m^z \,, \\ R_\lambda &= 2/\sqrt{N}\sum_n \exp(i\lambda n) S_n^y \,, \\ S_\lambda &= 2/\sqrt{N}\sum_n \exp(-i\lambda n) S_n^z \,. \end{aligned} \tag{2.36}$$

In terms of the spin waves [51],

$$\begin{aligned} \sum_{m,n} S_m^z S_n^z &= -\sum_\lambda P_\lambda S_\lambda \cos\lambda \,, \\ \sum_m (S_m^y)^2 &= \tfrac{1}{2}\sum_\lambda Q_\lambda^2 \,, \\ \sum_m (S_m^z)^2 &= \tfrac{1}{2}\sum_\lambda P_\lambda^2 \,, \\ \sum_n (S_n^y)^2 &= \tfrac{1}{2}\sum_\lambda R_\lambda^2 \,, \end{aligned} \tag{2.37}$$

and

$$\sum_n (S_n^y)^2 = \tfrac{1}{2}\sum_\lambda S_\lambda^2 \,. \tag{2.38}$$

The Hamiltonian (2.34) can now be written in terms of the spin waves operators and we have

$$\begin{aligned} H = -h_x N S_c + \left(\frac{j}{2} + \frac{h_x}{4S_c}\right)\sum_\lambda \left(P_\lambda^2 + S_\lambda^2\right) - 2\sum_\lambda P_\lambda S_\lambda \cos\lambda \\ + \frac{h_x}{4S_c}\sum_\lambda \left(Q_\lambda^2 + R_\lambda^2\right). \end{aligned} \tag{2.39}$$

A canonical transformation which brings H to normal form is

$$\begin{aligned} P_\lambda &= (-p_{1\lambda} + p_{2\lambda})/\sqrt{2}\,, \\ S_\lambda &= (p_{1\lambda} + p_{2\lambda})/\sqrt{2}\,, \\ Q_\lambda &= q_{1\lambda}/\sqrt{2}\,, \\ R_\lambda &= q_{2\lambda}/\sqrt{2}\,. \end{aligned} \tag{2.40}$$

The Hamiltonian (2.39) in normal coordinates is then

$$\begin{aligned} H = -h_x N S_c + \sum_\lambda \left\{ \left(\frac{j}{2} + \frac{h_x}{4S_c} + \cos\lambda\right) p_{1\lambda}^2 + \frac{h_x}{8S_c} q_{1\lambda}^2 \right\} \\ + \sum_\lambda \left\{ \left(\frac{j}{2} + \frac{h_x}{4S_c} - \cos\lambda\right) p_{2\lambda}^2 + \frac{h_x}{8S_c} q_{2\lambda}^2 \right\}. \end{aligned} \tag{2.41}$$

Writing H as a sum of harmonic oscillators

$$H = -h_x N S_c + \sum_\lambda \left(\frac{p_{1\lambda}^2}{m_{1\lambda}} + m_{1\lambda}\omega_{1\lambda}^2 q_{1\lambda}^2\right) + \sum_\lambda \left(\frac{p_{2\lambda}^2}{m_{2\lambda}} + m_{2\lambda}\omega_{2\lambda}^2 q_{2\lambda}^2\right). \tag{2.42}$$

with

$$\begin{aligned} \frac{1}{m_{1\lambda}} &= \left(\frac{j}{2} + \frac{h_x}{4S_c} + \cos\lambda\right), \quad m_{1\lambda}\omega_{1\lambda}^2 = \frac{h_x}{8S_c}\,, \\ \frac{1}{m_{2\lambda}} &= \left(\frac{j}{2} + \frac{h_x}{4S_c} - \cos\lambda\right), \quad m_{2\lambda}\omega_{2\lambda}^2 = \frac{h_x}{8S_c}\,. \end{aligned} \tag{2.43}$$

and with q and p satisfying the commutation relations

$$[q_{1\lambda}, p_{1\lambda}] = i = [q_{2\lambda}, p_{2\lambda}]\,, \tag{2.44}$$

we can write down the eigenvalues E of H

$$E = -h_x N S_c + \sum_\lambda (2n_{1\lambda} + 1)\omega_{1\lambda} + \sum_\lambda (2n_{2\lambda} + 1)\omega_{2\lambda}\,, \tag{2.45}$$

where the frequencies of the spin waves are given by

$$\omega_{1\lambda}^2 = \frac{h_x}{8S_c}\left(\frac{j}{2} + \frac{h_x}{4S_c} + \cos\lambda\right) \quad \omega_{2\lambda}^2 = \frac{h_x}{8S_c}\left(\frac{j}{2} + \frac{h_x}{4S_c} - \cos\lambda\right). \tag{2.46}$$

Since the frequencies $\omega_{1\lambda}$ and $\omega_{2\lambda}$ cannot be negative, h_x and j must fulfil the inequalities

$$\frac{j}{2} + \frac{h_x}{4S_c} > \cos\lambda \text{ and } \frac{j}{2} + \frac{h_x}{4S_c} > -\cos\lambda\,. \tag{2.47}$$

That is

$$-\frac{j}{2} - \frac{h_x}{4S_c} < \cos\lambda < \frac{j}{2} + \frac{h_x}{4S_c} \text{ for all } \lambda\,. \tag{2.48}$$

One way to ensure that this is always the case is to require that

$$\frac{j}{2} + \frac{h_x}{4S_c} = \frac{j}{2} + \frac{h_x\sqrt{3}}{6} \geq 1\,. \tag{2.49}$$

The unfortunate implication of equation (2.49) is that our spin waves theory will be valid only for large values of the transverse field h_x and that we will be kept in the dark concerning the characteristics of the ANNNI model in the presence of a weak transverse external magnetic field. In the ground state, all $n_\lambda = 0$ and we have for the ground state energy

$$E_g = -h_x N S_c + \sum_\lambda \sqrt{\frac{h_x}{8S_c}\left(\frac{j}{2} + \frac{h_x}{4S_c} + \cos\lambda\right)} + \sum_\lambda \sqrt{\frac{h_x}{8S_c}\left(\frac{j}{2} + \frac{h_x}{4S_c} - \cos\lambda\right)}\,. \tag{2.50}$$

Here, as in [51], the frequencies of the spin waves fall into two categories. However, unlike in the Heisenberg model studied by Anderson, $\omega_{1\lambda}$ and $\omega_{2\lambda}$ are not identical and furthermore the dispersion laws are quite different for long wavelengths. In fact, for $\lambda \to 0$, the oscillator frequencies are quadratic in λ as

$$\omega_{1\lambda} \approx \alpha + \beta\lambda^2\,, \tag{2.51}$$

where

$$\alpha = \left(\frac{h_x}{4S_c}\right)^{1/2}\left[\left(\frac{j}{2} + \frac{h_x}{4S_c} + 1\right)^{1/2} + \left(\frac{j}{2} + \frac{h_x}{4S_c} - 1\right)^{1/2}\right]$$

and

$$\beta = \frac{1}{4}\left(\frac{h_x}{4S_c}\right)^{1/2}\left[\left(\frac{j}{2} + \frac{h_x}{4S_c} - 1\right)^{-1/2} - \left(\frac{j}{2} + \frac{h_x}{4S_c} + 1\right)^{-1/2}\right] \tag{2.52}$$

This quadratic dispersion law is rather characteristic of the ground state of the ferromagnetic Heisenberg model [48, 51]. Anderson on the other hand predicted a linear dispersion law for the

Heisenberg antiferromagnet [51].

We are now in a position to calculate the ground state energy for an infinite chain, but first let us calculate the average values of the kinetic and potential energy terms that occur in H since we will need them later for calculating order parameters.

If we write

$$H_1 = \left(\frac{j}{2} + \frac{h_x}{4S_c} + \cos(\lambda)\right) p_{1\lambda}^2 + \frac{h_x}{8S_c} q_{1\lambda}^2 \,, \tag{2.53}$$

with energy $H_{1\lambda} = (2n_{1\lambda} + 1)\omega_{1\lambda}$ and

$$H_2 = \left(\frac{j}{2} + \frac{h_x}{4S_c} + \cos(\lambda)\right) p_{2\lambda}^2 + \frac{h_x}{8S_c} q_{2\lambda}^2 \,, \tag{2.54}$$

with energy $H_{2\lambda} = (2n_{2\lambda} + 1)\omega_{2\lambda}$, then in the ground state

$$\tag{2.55}$$

$$< H_1 >= E_{1g} = \left(\frac{j}{2} + \frac{h_x}{4S_c} + \cos(\lambda)\right) < p_{1\lambda}^2 > + \frac{h_x}{8S_c} < q_{1\lambda}^2 >= \omega_{1\lambda} \,, \tag{2.56}$$

and since

$$< q_{1\lambda}^2 >=< p_{1\lambda}^2 > \,, \tag{2.57}$$

we have

$$\begin{aligned} < p_{1\lambda}^2 > &= \frac{\omega_{1\lambda}}{2\left(\frac{j}{2} + \frac{h_x}{4S_c} + \cos(\lambda)\right)} \\ &= \frac{h_x}{16\omega_{1\lambda} S_c} \end{aligned} \tag{2.58}$$

and

$$< q_{1\lambda}^2 >= \frac{4\omega_{1\lambda} S_c}{h_x} \,. \tag{2.59}$$

That is, substituting the frequencies (2.46)

$$< p_{1\lambda}^2 >= \frac{1}{2}\sqrt{\frac{h_x/8S_c}{\left(\frac{j}{2} + \frac{h_x}{4S_c} + \cos\lambda\right)}} \tag{2.60}$$

and

$$< q_{1\lambda}^2 >= \frac{1}{2}\sqrt{\frac{\left(\frac{j}{2}+\frac{h_x}{4S_c}+\cos\lambda\right)}{h_x/8S_c}} \tag{2.61}$$

in the ground state. Similarly,

$$< p_{2\lambda}^2 >= \frac{1}{2}\sqrt{\frac{h_x/8S_c}{\left(\frac{j}{2}+\frac{h_x}{4S_c}-\cos\lambda\right)}} \tag{2.62}$$

and

$$< q_{2\lambda}^2 >= \frac{1}{2}\sqrt{\frac{\left(\frac{j}{2}+\frac{h_x}{4S_c}-\cos\lambda\right)}{h_x/8S_c}} \tag{2.63}$$

in the ground state.

In order to compute the spin waves theory ground state energy of the spin$-1/2$ ANNNI model in a transverse field, we replace the sum over λ in equation (2.50) by an integral and write

$$E_g = -h_x N S_c + \frac{N}{2}\left(\frac{h_x}{8S_c}\right)^{1/2}\frac{1}{2\pi}\int_{-\pi}^{\pi}\left\{\left(\frac{j}{2}+\frac{h_x}{4S_c}+\cos\lambda\right)^{1/2}+\left(\frac{j}{2}+\frac{h_x}{4S_c}-\cos\lambda\right)^{1/2}\right\}\mathrm{d}\lambda\,. \tag{2.64}$$

The factor of $N/2$ comes from the fact that there are $N/2$ values of the wave number λ. Evaluating the above integral, we obtain

$$E_g = -h_x N S_c + \frac{N}{\pi}\left(\frac{h_x}{8S_c}\right)^{1/2}\left\{(\gamma-1)^{1/2}\,\mathcal{E}\left(i\sqrt{2}\,(\gamma-1)^{-1/2}\right)+(\gamma+1)^{1/2}\,\mathcal{E}\left(\sqrt{2}\,(\gamma+1)^{-1/2}\right)\right\}, \tag{2.65}$$

where $\mathcal{E}$ is an elliptic integral of the second kind and

$$\gamma = \frac{j}{2}+\frac{h_x}{4S_c}\,. \tag{2.66}$$

We note that $\mathcal{E}\left(i\sqrt{2}\,(\gamma-1)^{-1/2}\right)$ is a real function of γ.

2.3 The classical ground state

A useful insight into the nature of the phase diagram of the ANNNI model in the presence of two external magnetic fields, described by the Hamiltonian (1.1)

$$H = \sum_i S_i^z S_{i+1}^z + j \sum_i S_i^z S_{i+2}^z - h_x \sum_i S_i^x - h_z \sum_i S_i^z \ .$$

may be gained by first studying its ground state in a classical fashion. In the classical approximation, spins are represented as three-dimensional vectors [3, 52, 53]. For this purpose let us consider a system of N spins $\frac{1}{2}$. The classical ground state is found from a configuration in which the spin vectors lie in the XZ plane with the N spins pointing respectively at angles φ_1 , φ_2, ... and φ_N with respect to the X axis.

In the absence of the fields h_x and h_z, we have the usual ANNNI model, described by the Hamiltonian

$$H_{ANNNI} = \sum S_i^z S_{i+1}^z + j \sum S_i^z S_{i+2}^z \ . \tag{2.67}$$

The energy corresponding to the Hamiltonian (2.67) in the classical description is given by

$$\begin{aligned} E =& \frac{1}{4} \sin\varphi_N \sin\varphi_1 + \frac{j}{4} \sin\varphi_{N-1} \sin\varphi_1 + \frac{j}{4} \sin\varphi_N \sin\varphi_2 \\ &+ \frac{1}{4} \sum_{i=1}^{N-1} \sin\varphi_i \sin\varphi_{i+1} + \frac{j}{4} \sum_{i=1}^{N-2} \sin\varphi_i \sin\varphi_{i+2} \, , \end{aligned} \tag{2.68}$$

where we have applied periodic boundary conditions for simplicity. It is also convenient to assume, without loss of generality, that N is a multiple of 4.

The energy E as given in (2.68) is a minimum if either

1. $\sin\varphi_i \sin\varphi_{i+1} = -1, \quad i = 1, 2, \ldots, N-1,$ and $\sin\varphi_N \sin\varphi_1 = -1$ or
2. $\sin\varphi_i \sin\varphi_{i+2} = -1, \quad i = 1, 2, \ldots, N-2, \quad \sin\varphi_N \sin\varphi_2 = -1$ and $\sin\varphi_{N-1} \sin\varphi_1 = -1$.

Condition (1) implies that

$$\varphi_i = \begin{cases} \pi/2, & i = 1, 3, 5, \ldots, N-1 \\ \\ -\pi/2, & i = 2, 4, 6, \ldots, N \end{cases} \tag{2.69}$$

This corresponds to antiferromagnetic alignment with the ground state energy given by

$$E_{AF}/N = -1/4\,(1-j)\ . \tag{2.70}$$

The second possibility for a ground state configuration as stated in condition (2) yields the following solution:

$$\begin{aligned}\varphi_{4k+1} =&\varphi_{4k+2} = \pi/2, \quad k = 0,1,2,\ldots,N/4 - 1\\ \varphi_{4k-1} =&\varphi_{4k} = -\pi/2, \quad k = 1,2,\ldots,N/4\,.\end{aligned} \tag{2.71}$$

This is the period 4 antiphase configuration. The corresponding ground state energy is then given by:

$$E_{<2>}/N = -j/4\,. \tag{2.72}$$

Comparing equation (2.70) and equation (2.72) we see that the classical ground state of the one dimensional ANNNI model (2.67) is antiferromagnetic for values of the next nearest neighbour exchange interaction $j < \frac{1}{2}$ and the $< 2 >$ antiphase for $j > \frac{1}{2}$. The ground state is degenerate when $j = \frac{1}{2}$.

The presence of the transverse field h_x or the longitudinal field h_z or both causes the ground state structure to change. The corresponding classical energy to the full Hamiltonian (1.1) is then given by

$$\begin{aligned}E =&\frac{1}{4}\sin\varphi_N\sin\varphi_1 + \frac{j}{4}\sin\varphi_{N-1}\sin\varphi_1 + \frac{j}{4}\sin\varphi_N\sin\varphi_2\\ &+\frac{1}{4}\sum_{i=1}^{N-1}\sin\varphi_i\sin\varphi_{i+1} + \frac{j}{4}\sum_{i=1}^{N-2}\sin\varphi_i\sin\varphi_{i+2}\\ &-\frac{1}{2}\sum_{i=1}^{N}h_x\cos\varphi_i - \frac{1}{2}\sum_{i=1}^{N}h_z\sin\varphi_i\,.\end{aligned} \tag{2.73}$$

When $j < \frac{1}{2}$ the ground state structure changes continuously from the ordered antiferromagnetic states described by $\varphi_1 = \varphi_3 = \ldots = \phi_{N-1} =$ say α and $\varphi_2 = \varphi_4 = \ldots = \phi_N =$ say β to the paramagnetic states having constant magnetization. Thus from equation (2.73) the

antiferromagnetic states have energies given by

$$\begin{aligned} E_{AF}/N =& \frac{1}{4}\sin\alpha\sin\beta + \frac{j}{8}\left(\sin^2\alpha + \sin^2\beta\right) - \frac{h_x}{4}\left(\cos\alpha + \cos\beta\right) \\ & - \frac{h_z}{4}\left(\sin\alpha + \sin\beta\right) . \end{aligned} \tag{2.74}$$

The order parameter, staggered magnetization $M_z^{\pm}$, defined by

$$\begin{aligned} M_z^{\pm} =& \frac{1}{2}\left(\sin\alpha - \sin\beta\right) \\ =& \sin\left(\frac{\alpha-\beta}{2}\right)\cos\left(\frac{\alpha+\beta}{2}\right) , \end{aligned} \tag{2.75}$$

exists everywhere in the antiferromagnetic region and vanishes on the transition line from the antiferromagnetic phase to the paramagnetic phase. Thus, for a given next nearest neighbour exchange interaction $j < \frac{1}{2}$, the transition line is the set of all h_x and h_z for which E_{AF} in equation (2.74) is a minimum, with the additional requirement that the order parameter vanishes, *i.e.* that $\alpha = \beta$ in equation (2.75). Minimizing E_{AF} and taking limit $\alpha \to \beta$ in the resulting critical equations; we find that the antiferro–para phase transition occurs on the line:

$$\begin{aligned} h_x =& (1-j)\cos^3\alpha \\ h_z =& \sin\alpha\left(1 + \cos^2\alpha + j\sin^2\alpha\right) . \end{aligned} \tag{2.76}$$

For $j > \frac{1}{2}$ there is a continuous phase transition from the ordered $< 2 >$ antiphase states described by $\varphi_{4k+1} = \varphi_{4k+2} =$ say α for $k = 0, 1, 2, \ldots, N/4 - 1$ and $\varphi_{4k-1} = \varphi_{4k} =$ say β for $k = 1, 2, \ldots, N/4$ to the paramagnetic states. Thus from equation (2.73) the $< 2 >$ antiphase states have energies given by

$$\begin{aligned} E_{<2>}/N =& \frac{1}{4}\left(\sin\alpha + \sin\beta\right)^2 + \frac{j}{4}\sin\alpha\sin\beta - \frac{h_x}{4}\left(\cos\alpha + \cos\beta\right) \\ & - \frac{h_z}{4}\left(\sin\alpha + \sin\beta\right) . \end{aligned} \tag{2.77}$$

The order parameter,

$$M_z^{++--} = \sin\left(\frac{\alpha-\beta}{2}\right)\cos\left(\frac{\alpha+\beta}{2}\right) , \tag{2.78}$$

remains finite everywhere in the $< 2 >$ antiphase region and vanishes on the transition line. Thus, minimizing equation (2.77) and using the condition $\alpha \to \beta$ in the resulting critical equations,

the antiphase–para phase boundary is given by the line

$$\begin{aligned} h_x &= j\cos^3\alpha\,, \\ h_z &= \sin\alpha\left(1+j(1+\cos^2\alpha)\right)\,. \end{aligned} \tag{2.79}$$

The antiferromagnetic to paramagnetic boundary as given by equation (2.76) is plotted in figure 2.1(a) while the antiphase to paramagnetic boundary as given by equation (2.79) is plotted in figure 2.1(b).

The two lines equation (2.76) and equation (2.79) coincide when $j = \frac{1}{2}$ as expected. We remark also that the special case $j = 0$ (no next nearest neighbour competition) is discussed in [3].

The classical results represent of course only very rough approximations of the true behaviour of the ANNNI model in mixed fields. Thus having gained a useful insight into the nature of the classical ground states and phase transitions of the model, we will now shift attention to the more accurate quantum description.

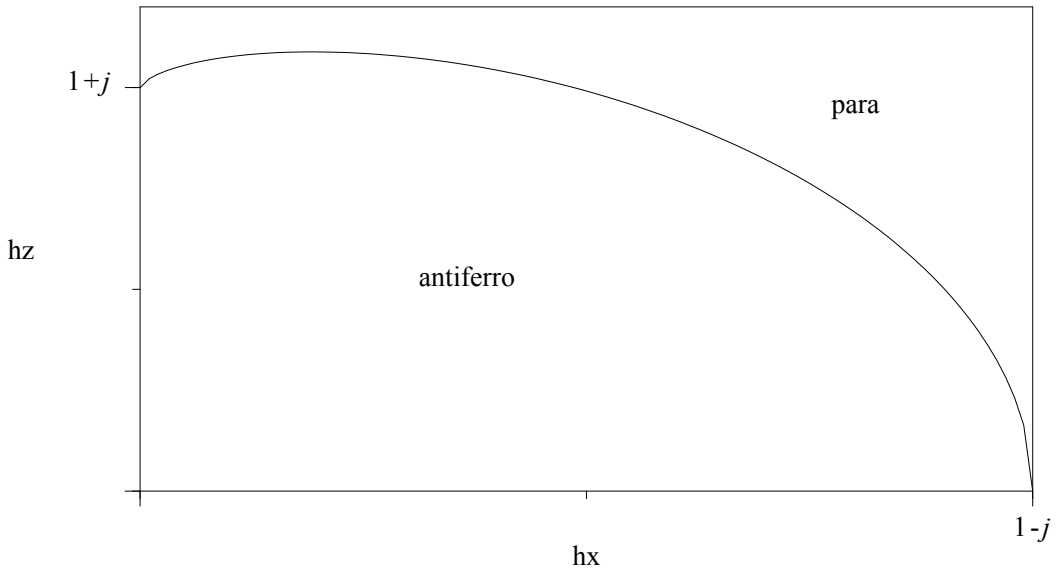

(a) Classical antiferromagnetic to paramagnetic phase boundary in the one dimensional ANNNI model in mixed fields

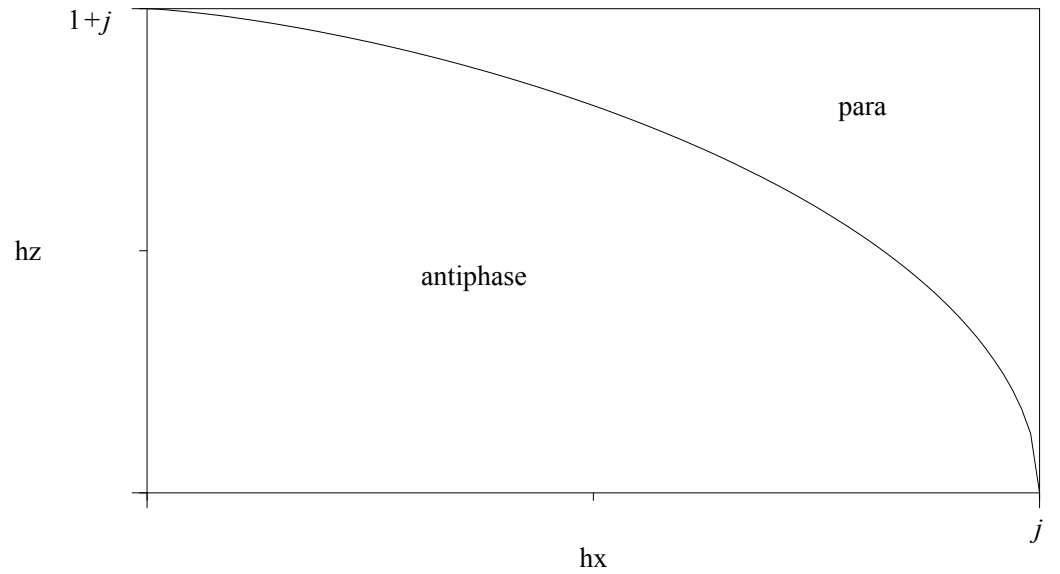

(b) Classical antiphase to paramagnetic phase boundary in the one dimensional ANNNI model in mixed fields

Figure 2.1: Classical phase boundaries in the one dimensional ANNNI model in mixed fields h_x and h_z

Chapter 3

The longitudinal ANNNI model

The ANNNI model in a longitudinal field is described by the Hamiltonian

$$H = \sum_i S_i^z S_{i+1}^z + j \sum_i S_i^z S_{i+2}^z - h_z \sum_i S_i^z \ . \tag{3.1}$$

The Hamiltonian (3.1) describes a *classical model*, in the sense that the Hamiltonian is the sum of commuting quantities. At zero temperature, the structure of the ground state of (3.1) changes, depending on the choice of the parameters j and h_z, so that the model undergoes quantum phase transitions.

In the absence of next nearest neighbour interactions ($j = 0$), the model (3.1) reduces to the Ising model in a uniform longitudinal field

$$H_{j=0} = \sum_i S_i^z S_{i+1}^z - h_z \sum_i S_i^z \, , \tag{3.2}$$

which is exactly solvable, using the transfer matrix technique [54, 55].

The model (3.2) is similar to the classical part of the Hamiltonian discussed in [5] and also to the random-field Ising model believed to capture the essential physics for many systems with discrete symmetry [56]. In fact, with a proper rescaling, the classical part of the model studied in reference [5] can always be rewritten in the form of equation (3.2). The ground state of the model (3.2) is antiferromagnetic for $h_z < 1$ and ferromagnetic for $h_z > 1$. The ground state is highly degenerate at $h_z = 1$.

The case $h_z = 0$ in (3.1) corresponds to the ANNNI chain

$$H_{h_z=0} = \sum_i S_i^z S_{i+1}^z + j \sum_i S_i^z S_{i+2}^z \,, \tag{3.3}$$

whose ground state is also well known [13, 54, 57]. The ground state is antiferromagnetic for values of the next nearest neighbour exchange interaction $j < 1/2$ and the four-fold degenerate antiphase states $\uparrow\uparrow\downarrow\downarrow \cdots \uparrow\uparrow\downarrow\downarrow$ for $j > 1/2$. At $j = 1/2$ the ground state of the model (3.3) is infinitely degenerate with the degeneracy being equal to $\left((1+\sqrt{5})/2\right)^N$ for a chain of length N [13, 22].

In what follows, we will discuss the ANNNI model in a uniform longitudinal field, i.e. we will consider the model (3.1) for finite j and h_z, and it will be shown that there are four candidates for the ground state when j and h_z are both different from zero.

The model (3.1) is diagonal in the S_z representation, and is therefore an exactly solvable system. Although in principle, there are 2^N possible states for a chain of N spins-1/2, translational invariance and reflection symmetry lead to a considerable, in fact drastic, reduction in the dimension of the Hilbert space, as discussed in appendix A. As is shown in appendix A both $\mathcal{R}$ and $\mathcal{T}$ are good quantum numbers, but they however do not mutually commute, that is $[\mathcal{R}, \mathcal{T}] \neq 0$ except in the subspaces $k = 0$ and, when N is even, $k = N/2$ of the eigenstates of $\mathcal{T}$. As proved in appendix A, $\mathcal{T}$ and $\mathcal{R}$ are, in fact, symmetries of the full Hamiltonian (1.1) of the ANNNI model in the presence of both longitudinal and transverse fields h_z and h_x. Another useful operator is the all-spin inversion operator I. I is however not a symmetry of the Hamiltonian (3.1) except in the special case of total $S_z = 0$ or $h_z = 0$. Notwithstanding that I is not a good quantum number, it is still useful because it simplifies the classification of the eigenstates and energies of the model (3.1) since if the energy of a given S_z configuration is known, the energy of the corresponding $-S_z$ state obtained by inversion can be write down immediately, by simply changing the sign of h_z. We also remark that I is a symmetry of the Hamiltonian (1.1) in the special case $h_z = 0$ (that is the transverse ANNNI model), a proof of this statement is included in appendix A. Since the ground state energies are proportional to N, it is also not difficult to generalize the results of finite size exact diagonalization to an infinite system. Furthermore, the states are highly degenerate, so that the number of independent energies among which to search for a minimum is quite few for a given chain length. For example for $N = 12$ there are only 84 independent energies out of which only 4 can be ground state energies (corresponding to 10 states– the two-fold degenerate antiferro states, the three-fold degenerate $\uparrow\uparrow\downarrow \cdots$ states, the

four-fold degenerate antiphase states and the non-degenerate ferromagnetic state). Similarly, for $N = 20$, there are 396 energies out of which only 5 belong to ground state configurations. The number of distinct energies for a given chain length N is tabulated in table 3.1. The values of the dimensions of the reduced Hilbert space can be determined for any N by the Maple procedure *totalcycles*, based on the derivation in appendix A while another procedure carries out the actual diagonalization and classification of energies. The procedure *energy* makes it easy to calculate the eigenenergy of an arbitrary state of any N. The procedures are listed in appendix B

N	Dim. of full Hilbert space	Dim. of reduced Hilbert space ($k = 0$ subspace of $\mathcal{T}$)	No of distinct eigenenergies
2	4	3	3
3	8	4	4
4	16	6	6
5	32	8	8
6	64	14	13
7	128	20	18
8	256	36	26
9	512	60	36
10	1024	108	49
11	2048	188	64
12	4096	352	84
13	8192	632	106
14	1648	1182	133
15	32768	2192	164
16	65536	4116	200
17	131072	7712	240
18	262144	14602	287
19	524288	27596	338
20	1048576	52488	396

Table 3.1: Distinct energies available to the configuration states for given N

In section 3.1 we will discuss the exact diagonalization results for up to 24 sites, while an extrapolation, so to speak, to the thermodynamic limit will be presented in section 3.3.

3.1 Exact Diagonalization of Finite Systems

We have implemented a program consisting of Maple procedures to diagonalize the Hamiltonian (3.1) for finite lattice sizes. We used the S_z representation for the spin operators. In the program, spin up is denoted by $+1$ and spin down by -1. The total S_z direct product basis states are conveniently represented as Maple lists, whose elements consist of a series of 1 and -1. This representation is particularly convenient because the *permute* function from the *combinat* package makes the generation of the 2^N basis states a boon (for large N however, direct permutation is avoided and the *randperm* function is used to generate the independent states (cycles) based on the advance knowledge of the total number of cycles as returned by *totalcycles*). Whenever direct permutation is done, a *procedure* then employs translational invariance to reduce the dimension of the Hilbert space to the value returned by *totalcycles* and another *procedure* computes the states and the corresponding energies. The program listing is given in appendix B.

3.1.1 $N = 4$

Translational invariance reduces the dimension of the Hilbert space from 16 to a maximum of 6 in the $k = 0$ subspace of the eigenstates of $\mathcal{T}$. The remaining subspaces have dimensions $Dim = 3$ for $k = 1$, $Dim = 4$ for $k = 2$ and $Dim = 3$ for $k = 3$. The states and the energies are tabulated in table 3.2. It should be noted that for simplicity and to save space, only the first members (that is only cycles) are listed in the table. For example, by $[-1, -1, 1, -1]$ in table 3.2 we really mean the following:

- In $k = 0$ subspace (corresponding to eigenvalue of $\mathcal{T}$ $exp(2\pi ik/4) = 1$)

  $(|-1,-1,1,-1\rangle + |-1,1,-1,-1\rangle + |1,-1,-1,-1\rangle + |-1,-1,-1,1\rangle)/2$

- In $k = 1$ subspace (corresponding to eigenvalue $exp(2\pi ik/4) = i$)

  $(-|-1,-1,1,-1\rangle + i\,|-1,1,-1,-1\rangle + |1,-1,-1,-1\rangle - i\,|-1,-1,-1,1\rangle)/2$

- In $k = 2$ subspace (corresponding to eigenvalue $exp(2\pi ik/4) = -1$)

  $(-|-1,-1,1,-1\rangle + |-1,1,-1,-1\rangle - |1,-1,-1,-1\rangle + |-1,-1,-1,1\rangle)/2$

  and

- In $k = 3$ subspace (corresponding to eigenvalue $exp(2\pi ik/4) = -i$)

$$(-|-1,-1,1,-1\rangle - i\,|-1,1,-1,-1\rangle + |1,-1,-1,-1\rangle + i\,|-1,-1,-1,1\rangle)/2\,.$$

The eigenvalue of the longitudinal ANNNI model H ((3.1)) in each subspace for this particular example is h_z which is the value tabulated in table 3.2. The value tabulated under 'Degen' is the degeneracy due to translational invariance, and is equal to the period of the cycle, 4 in the example above. The eigenenergy from each subspace is the same because the Hamiltonian (3.1) is diagonal in the total-S_z direct product basis representation.

Of the sixteen states we see that only the ferromagnetic state, with energy $(1 + j - 2h_z)/4$, the antiferromagnetic states $[1,-1,1,-1]$ with energy $-1+j$, the antiphase states $[-1,-1,1,1]$ with energy $-j$, the four-fold degenerate $[1,1,1,-1]$ states and the state $[1,1,-1,1]$ with energy $-h_z$ can be ground states. The resulting phase diagram is as drawn in figure 3.1.

We digress a bit to demonstrate that even for this very short chain of 4 spins, the reflection symmetry already presents an indication of its usefulness for the full H of equation (1.1) in the following way:

In the subspace $k = 0$, all 6 eigenstates of $\mathcal{T}$ belonging to the degenerate eigenvalue 1 are also eigenstates of $\mathcal{R}$ also of eigenvalue 1. In the $k = 0$ subspace therefore, there is no further simplification and the 6×6 matrix must be diagonalized.

In the $k = 2$ subspace however, 3 of the 4 eigenstates of $\mathcal{T}$ belonging to eigenvalue -1 are also eigenstates of $\mathcal{R}$ of eigenvalue -1. The fourth eigenstate of $\mathcal{T}$ is an eigenstate of $\mathcal{R}$ but with eigenvalue 1. Therefore, the 4×4 matrix can be further block-diagonalized as 3×3 and 1×1 matrices.

Explicitly, in the $k = 2$ subspace, the 3 states

$$\begin{aligned}|a\rangle &= (-|-1,-1,1,-1\rangle + |-1,1,-1,-1\rangle - |1,-1,-1,-1\rangle + |-1,-1,-1,1\rangle)/2\,,\\ |b\rangle &= (-|1,-1,1,-1\rangle + |-1,1,-1,1\rangle)/\sqrt{2}\end{aligned}$$

and

$$|\mathrm{c}\rangle = (-|1,1,1,-1\rangle + |1,1,-1,1\rangle - |1,-1,1,1\rangle + |-1,1,1,1\rangle)/2 \tag{3.4}$$

give rise to the matrix

$$H_{-1} = \begin{pmatrix} h_z & h_x/\sqrt{2} & 0 \\ h_x/\sqrt{2} & -1+j & h_x/\sqrt{2} \\ 0 & h_x/\sqrt{2} & -h_z \end{pmatrix} . \tag{3.5}$$

The remaining state

$$|\mathrm{d}\rangle = (-|1,-1,-1,1\rangle + |-1,-1,1,1\rangle - |-1,1,1,-1\rangle + |1,1,-1,-1\rangle)/2 \tag{3.6}$$

gives rise to the 1×1 matrix

$$H_1 = (-j) \ . \tag{3.7}$$

It is interesting to know, for example, that $-j$ is always an eigenenergy of a chain of 4 spins modelled by the Hamiltonian (1.1), under periodic boundary conditions, regardless of the values of the parameters j, h_x and h_z.

SNo	States	$k-$values	S_z	Energy	Degen
1	[-1, -1, -1, -1]	[0]	-2	$1+j+2h_z$	1
2	[-1, -1, 1, -1]	[0, 1, 2, 3]	-1	h_z	4
3	[1, -1, 1, -1]	[0, 2]	0	$-1+j$	2
4	[1, -1, -1, 1]	[0, 1, 2, 3]	0	$-j$	4
5	[1, 1, 1, -1]	[0, 1, 2, 3]	1	$-hz$	4
6	[1, 1, 1, 1]	[0]	2	$1+j-2h_z$	1

Table 3.2: Exact diagonalization of 4 spins.

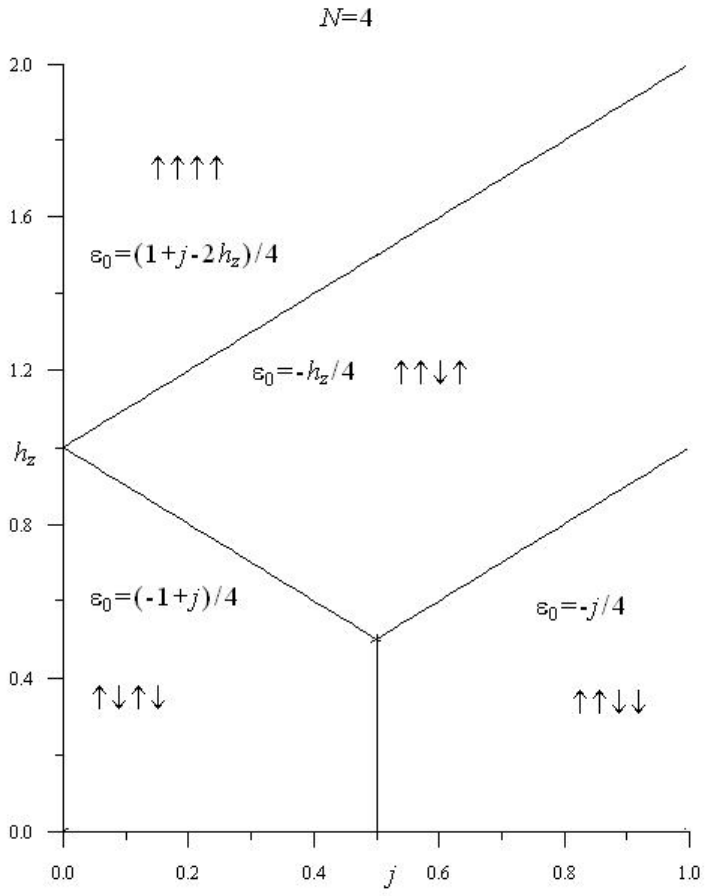

Figure 3.1: $T = 0$ phase diagram of the longitudinal ANNNI model for $N = 4$.

3.1.2 N=5

The reduced Hilbert space of 5 spins-1/2 is of dimension 8 ($k = 0$). The states and corresponding energies are given in table 3.3. The zero temperature phase diagram of the ANNNI model in a longitudinal field is shown in figure 3.2.

SNo	States	$k-$values	S_z	Energy	Degen
1	[-1, -1, -1, -1, -1]	[0]	-5/2	$5/4 + 5j/4 + 5h_z/2$	1
2	[-1, -1, -1, -1, 1]	[0, 1, 2, 3, 4]	-3/2	$1/4 + j/4 + 3h_z/2$	5
3	[-1, -1, -1, 1, 1]	[0, 1, 2, 3, 4]	-1/2	$1/4 - 3j/4 + h_z/2$	5
4	[-1, -1, 1, -1, 1]	[0, 1, 2, 3, 4]	-1/2	$-3/4 + j/4 + h_z/2$	5
5	[-1, -1, 1, 1, 1]	[0, 1, 2, 3, 4]	1/2	$1/4 - 3j/4 - h_z/2$	5
6	[-1, 1, 1, -1, 1]	[0, 1, 2, 3, 4]	1/2	$-3/4 + j/4 - h_z/2$	5
7	[1, -1, 1, 1, 1]	[0, 1, 2, 3, 4]	3/2	$1/4 + j/4 - 3h_z/2$	5
8	[1, 1, 1, 1, 1]	[0]	5/2	$5/4 + 5j/4 - 5h_z/2$	1

Table 3.3: Exact diagonalization of 5 spins.

3.1.3 $N = 6$

For a chain of 6 spins, translational invariance reduces the dimension of the Hilbert space from 64 to a maximum of 14 in the $k = 0$ subspace of eigenstates of $\mathcal{T}$. Furthermore, the states $|6>= [1, -1, 1, 1, -1, -1]$ and $|7>= [-1, -1, 1, 1, -1, 1]$ (here again only cycles are written for simplicity) are degenerate due to the reflection symmetry:

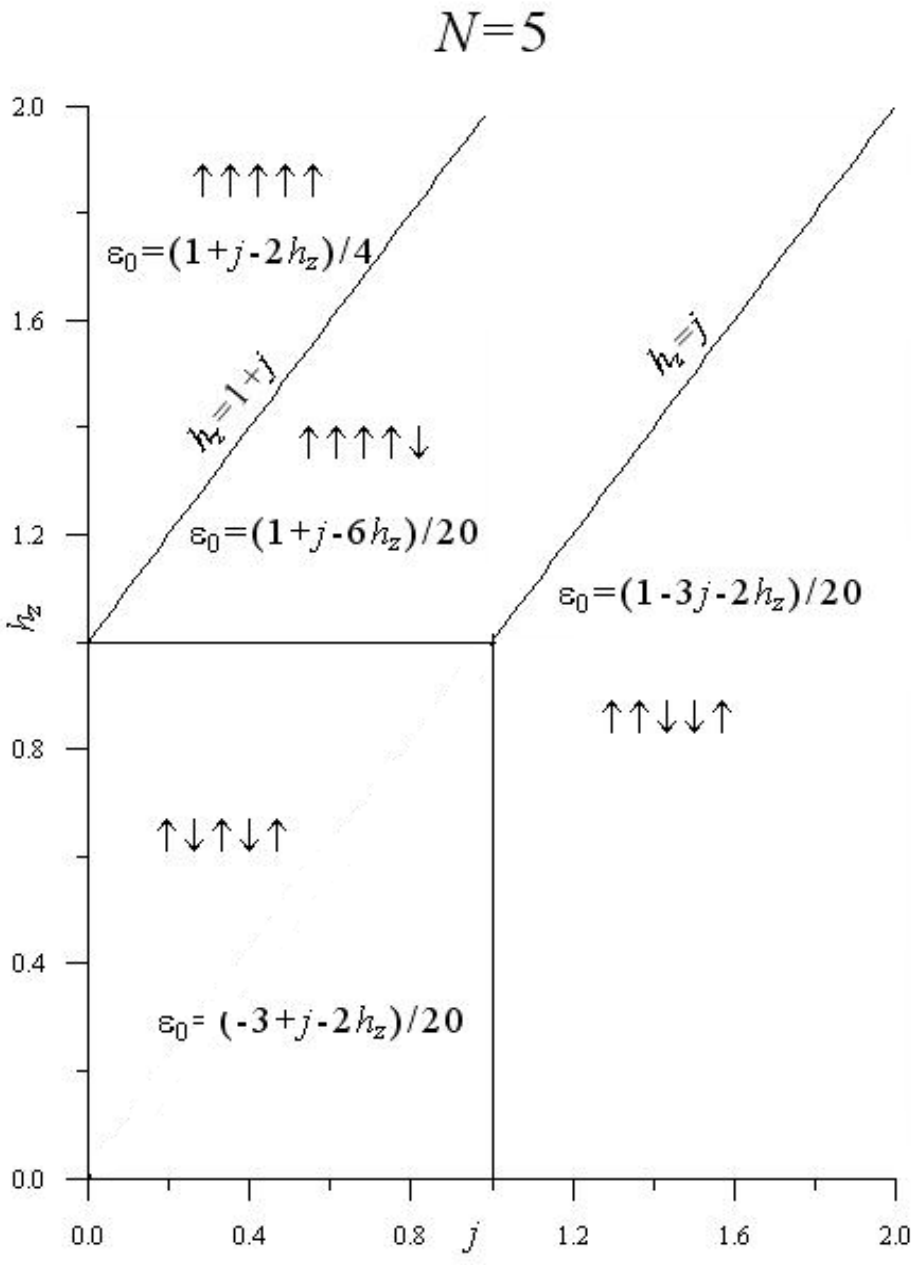

Figure 3.2: $T = 0$ phase diagram of the longitudinal ANNNI model for $N = 5$.

$$\mathcal{R}\,|6\rangle = |7\rangle \ ,$$
$$\mathcal{R}\,|7\rangle = |6\rangle \ . \tag{3.8}$$

The classification is given in table 3.4.

It is clear from table 3.4 that there are only three possible candidates for the ground state – the allspins up ferromagnetic state, the two-fold degenerate anti-ferro configuration with energy $-3/2 + 3j/2$ and the three-fold degenerate $\uparrow\uparrow\downarrow$ configuration with energy $-1/2 - j/2 - h_z$. The ferro state is separated from the $\uparrow\uparrow\downarrow$ states by the line $h_z = 1 + j$ while the antiferro and $\uparrow\uparrow\downarrow$ states are separated by the line $2\,j + h_z = 1$. The phase diagram of the longitudinal ANNNI model for $N = 6$ is drawn in figure 3.3

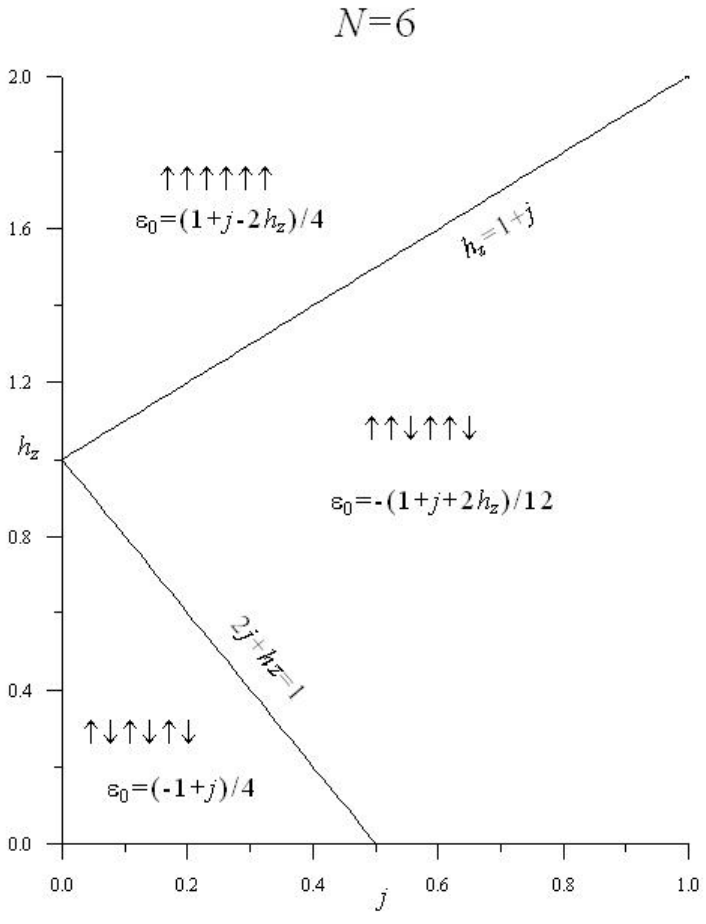

Figure 3.3: $T = 0$ phase diagram of the longitudinal ANNNI model for $N = 6$.

Again for $N = 6$ we have an example of when to take advantage of the symmetries of the system.

SNo	States	$k-$values	S_z	Energies	Degen
1	[-1, -1, -1, -1, -1, -1]	[0]	-3	$3/2 + 3j/2 + 3h_z$	1
2	[1, -1, -1, -1, -1, -1]	[0, 1, 2, 3, 4, 5]	-2	$1/2 + j/2 + 2h_z$	6
3	[1, 1, -1, -1, -1, -1]	[0, 1, 2, 3, 4, 5]	-1	$1/2 - j/2 + h_z$	6
4	[-1, -1, -1, 1, -1, 1]	[0, 1, 2, 3, 4, 5]	-1	$-1/2 + j/2 + hz$	6
5	[-1, -1, 1, -1, -1, 1]	[0, 2, 4]	-1	$-1/2 - j/2 + hz$	3
6	[1, -1, 1, 1, -1, -1]	[0, 1, 2, 3, 4, 5]	0	$-1/2 - j/2$	6
7	[-1, -1, 1, 1, -1, 1]	[0, 1, 2, 3, 4, 5]	0	$-1/2 - j/2$	6
8	[1, 1, -1, -1, -1, 1]	[0, 1, 2, 3, 4, 5]	0	$1/2 - j/2$	6
9	[-1, 1, -1, 1, -1, 1]	[0, 3]	0	$-3/2 + 3j/2$	2
10	[-1, -1, 1, 1, 1, 1]	[0, 1, 2, 3, 4, 5]	1	$1/2 - j/2 - h_z$	6
11	[1, 1, -1, 1, 1, -1]	[0, 2, 4]	1	$-1/2 - j/2 - h_z$	3
12	[1, -1, 1, 1, 1, -1]	[0, 1, 2, 3, 4, 5]	1	$-1/2 + j/2 - h_z$	6
13	[-1, 1, 1, 1, 1, 1]	[0, 1, 2, 3, 4, 5]	2	$1/2 + j/2 - 2hz$	6
14	[1, 1, 1, 1, 1, 1]	[0]	3	$3/2 + 3j/2 - 3h_z$	1

Table 3.4: Exact diagonalization of 6 spins.

First we consider the $k = 0$ subspace of $\mathcal{T}$. We see from equation (3.8) that although $|6\rangle$ and $|7\rangle$ are not eigenstates of $\mathcal{R}$, their linear combinations are, and of course the linear combinations remain eigenstates of $\mathcal{T}$:

$$\mathcal{R}\left(|6\rangle + |7\rangle\right) = \mathcal{R}\,|6\rangle + \mathcal{R}\,|7\rangle = |7\rangle + |6\rangle = 1\left(|6\rangle + |7\rangle\right)\,, \tag{3.9}$$

$$\mathcal{R}\left(|6\rangle - |7\rangle\right) = \mathcal{R}\,|6\rangle - \mathcal{R}\,|7\rangle = |7\rangle - |6\rangle = -1\left(|6\rangle - |7\rangle\right)\,. \tag{3.10}$$

We are therefore able to decompose the matrix of H with respect to the 14 eigenstates of $\mathcal{T}$ in the $k = 0$ subspace to a direct sum of that with respect to the 13 eigenstates of $\mathcal{R}$ of eigenvalue 1 plus 1 eigenstate of $\mathcal{R}$ of eigenvalue -1. In particular, the 1×1 matrix gives eigenvalue $-1/2 - j/2$. Again it is nice to learn that for $N = 6$ in Hamiltonian (1.1), there is an eigenvalue whose value is independent of the values of h_x and h_z.

The situation in the $k = 6/2 = 3$ subspace is similar. We see from table 3.4 that $|3\rangle$, $|10\rangle$ and the linear combination $|6\rangle + |7\rangle$ are eigenstates of $\mathcal{R}$ belonging to eigenvalue 1, while the linear combination $|6\rangle - |7\rangle$ and the remaining states are eigenstates of R with eigenvalue -1. The 10×10 matrix of H in the $k = 3$ subspace can therefore be diagonalized in separate blocks of 3×3 and 7×7.

The 3×3 matrix can be diagonalized "by hand". The 3 states fulfilling $\mathcal{R}\,|u\rangle = |u\rangle$ are:

$$\begin{aligned}
|3\rangle &= \left(-\,|1,1,-1,-1,-1,-1\rangle + - \cdots + |-1,1,1,-1,-1,-1\rangle\right)/\sqrt{6}\,,\\
|10\rangle &= \left(-\,|-1,-1,1,1,1,1\rangle + - \cdots + |1,-1,-1,1,1,1\rangle\right)/\sqrt{6}\,,\\
|6\rangle + |7\rangle &= \left(-\,|1,-1,1,1,-1,-1\rangle + - \cdots\cdots + |-1,1,1,-1,1,-1\rangle\right)/\sqrt{12}\,.
\end{aligned} \tag{3.11}$$

The matrix of H in this subspace of $\mathcal{R}$ is

$$H_1 = \begin{pmatrix} 1/2 - j/2 + h_z & 0 & h_x/\sqrt{2} \\ 0 & 1/2 - j/2 - h_z & h_x/\sqrt{2} \\ h_x/\sqrt{2} & h_x/\sqrt{2} & -1/2 - j/2 \end{pmatrix}\,. \tag{3.12}$$

3.1.4 N=7

There are 18 distinct energies corresponding to the 20 basis states of the reduced Hilbert space. The energies and respective states are tabulated in table 3.5. Reflection symmetry explains the

degeneracy: $|6\rangle$ and $|8\rangle$ are related by reflection and so also are $|12\rangle$ and $|14\rangle$.

There are four ground state candidates: the ferromagnetic state, the two 'almost' $\uparrow\uparrow\downarrow$ configurations $[1,1,-1,1,1,-1,1]$ and $[1,1,-1,1,1,-1,-1]$ with respective energies $-1/4 - j/4 - 3\,h_z/2$ and $-1/4 - 5\,j/4 - h_z/2$ and the hybrid antiferromagnetic-$\uparrow\uparrow\downarrow$ state with energy $-5/4 + 3\,j/4 - h_z/2$. The critical lines are $h_z + j = 1$, $h_z = j$ and $j = 1/2$, just like in the $N = 4$ system. The phase diagram is drawn in figure 3.4

As in the previous cases, the reflection symmetry introduces additional simplification to the diagonalization of H in the $k = 0$ subspace of $\mathcal{T}$. $|6\rangle - |8\rangle$ and $|12\rangle - |14\rangle$ are eigenstates of $\mathcal{R}$ belonging to eigenvalue -1 while $|6\rangle + |8\rangle$ and $|12\rangle + |14\rangle$ are eigenstates of $\mathcal{R}$ with eigenvalue 1. The 20×20 matrix of H can therefore be block-diagonalized as a 18×18 matrix and a 2×2 matrix in the subspace of $\mathcal{R}$ of eigenvalue 1 and of eigenvalue -1 respectively.

We can write down the 2×2 matrix immediately, in the basis

$$\begin{aligned} |u\rangle &= \left(|6\rangle - |8\rangle\right)/\sqrt{14}\,, \\ |v\rangle &= \left(|12\rangle - |14\rangle\right)/\sqrt{14}\,, \end{aligned} \tag{3.13}$$

we have

$$H_{-1} = \begin{pmatrix} -1/4 - j/4 + h_z/2 & h_x/2 \\ h_x/2 & -1/4 - j/4 - h_z/2 \end{pmatrix}. \tag{3.14}$$

It is then an easy matter to write down the eigenenergies and the corresponding eigenstates of the matrix (3.14).

3.1.5 $N = 8$

For 8 spin sites, the reduced Hilbert space ($k = 0$ subspace of $\mathcal{T}$) has dimension 36. Due to degeneracies however, there are only 26 distinct energy eigenvalues. Out of these energies only 5 energies correspond to ground state configurations. They are $2 + 2j - 4h_z$ for the ferro state, $-2h_z$ for the $4 + 8 = 12$-fold degenerate $[1,1,1,-1,1,1,1,-1]$ and $[1,1,-1,1,1,-1,1,1]$ states, $-1 - j$ for the antiferromagnetic ground state, $-2\,j$ for the four-fold degenerate antiphase states, and $-1 - h_z$ for the state $[1,1,-1,1,1,-1,1,-1]$. The distinct energies are tabulated in table 3.6 and the phase diagram is as drawn in figure 3.5.

SNo	States	$k-$values	S_z	Energies	Degen
1	[-1, -1, -1, -1, -1, -1, -1]	[0]	-7/2	$7/4 + 7j/4 + 7h_z/2$	1
2	[-1, -1, -1, -1, -1, -1, 1]	[0, 1, 2, 3, 4, 5, 6]	-5/2	$3/4 + 3j/4 + 5h_z/2$	7
3	[-1, -1, -1, -1, -1, 1, 1]	[0, 1, 2, 3, 4, 5, 6]	-3/2	$3/4 - j/4 + 3h_z/2$	7
4	[-1, -1, -1, -1, 1, -1, 1]	[0, 1, 2, 3, 4, 5, 6]	-3/2	$-1/4 + 3j/4 + 3h_z/2$	7
5	[-1, -1, -1, 1, -1, -1, 1]	[0, 1, 2, 3, 4, 5, 6]	-3/2	$-1/4 - j/4 + 3h_z/2$	7
6	[-1, -1, -1, 1, 1, -1, 1]	[0, 1, 2, 3, 4, 5, 6]	-1/2	$-1/4 - j/4 + h_z/2$	7
7	[-1, -1, -1, -1, 1, 1, 1]	[0, 1, 2, 3, 4, 5, 6]	-1/2	$3/4 - j/4 + h_z/2$	7
8	[-1, -1, 1, -1, 1, 1, -1]	[0, 1, 2, 3, 4, 5, 6]	-1/2	$-1/4 - j/4 + h_z/2$	7
9	[-1, -1, 1, 1, -1, -1, 1]	[0, 1, 2, 3, 4, 5, 6]	-1/2	$-1/4 - 5j/4 + h_z/2$	7
10	[1, -1, -1, 1, -1, 1, -1]	[0, 1, 2, 3, 4, 5, 6]	-1/2	$-5/4 + 3j/4 + h_z/2$	7
11	[-1, -1, -1, 1, 1, 1, 1]	[0, 1, 2, 3, 4, 5, 6]	1/2	$3/4 - j/4 - h_z/2$	7
12	[1, 1, 1, -1, 1, -1, -1]	[0, 1, 2, 3, 4, 5, 6]	1/2	$-1/4 - j/4 - h_z/2$	7
13	[1, 1, -1, 1, 1, -1, -1]	[0, 1, 2, 3, 4, 5, 6]	1/2	$-1/4 - 5j/4 - h_z/2$	7
14	[-1, 1, 1, 1, -1, -1, 1]	[0, 1, 2, 3, 4, 5, 6]	1/2	$-1/4 - j/4 - h_z/2$	7
15	[1, 1, -1, 1, -1, 1, -1]	[0, 1, 2, 3, 4, 5, 6]	1/2	$-5/4 + 3j/4 - h_z/2$	7
16	[1, 1, 1, -1, 1, -1, 1]	[0, 1, 2, 3, 4, 5, 6]	3/2	$-1/4 + 3j/4 - 3h_z/2$	7
17	[-1, 1, 1, 1, -1, 1, 1]	[0, 1, 2, 3, 4, 5, 6]	3/2	$-1/4 - j/4 - 3h_z/2$	7
18	[-1, -1, 1, 1, 1, 1, 1]	[0, 1, 2, 3, 4, 5, 6]	3/2	$3/4 - j/4 - 3h_z/2$	7
19	[1, 1, -1, 1, 1, 1, 1]	[0, 1, 2, 3, 4, 5, 6]	5/2	$3/4 + 3j/4 - 5h_z/2$	7
20	[1, 1, 1, 1, 1, 1, 1]	[0]	7/2	$7/4 + 7j/4 - 7h_z/2$	1

Table 3.5: Energy eigenvalues of 7 spins

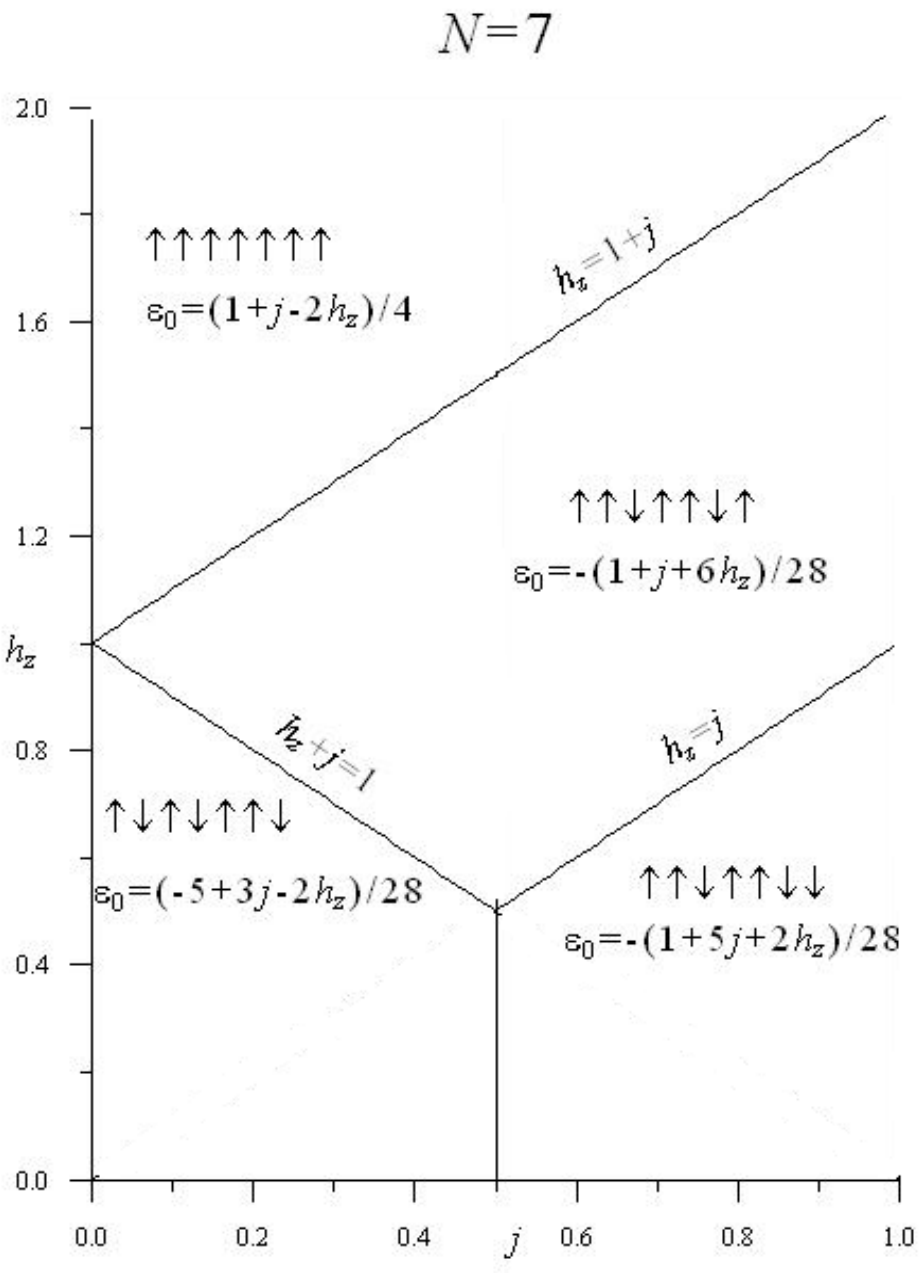

Figure 3.4: $T = 0$ phase diagram of the longitudinal ANNNI model for $N = 7$.

SNo	States	$k-$values	S_z	Energies	Degen
1	[-1, -1, -1, -1, -1, -1, -1, -1]	[0]	-4	$2+2j+4h_z$	1
2	[-1, -1, -1, -1, -1, -1, -1, 1]	[0, 1, 2, 3, 4, 5, 6, 7]	-3	$1+j+3h_z$	8
3	[-1, -1, -1, -1, -1, -1, 1, 1]	[0, 1, 2, 3, 4, 5, 6, 7]	-2	$1+2h_z$	8
4	[-1, 1, -1, 1, -1, -1, -1, -1]	[0, 1, 2, 3, 4, 5, 6, 7]	-2	$j+2h_z$	8
5	[1, -1, -1, -1, -1, 1, -1, -1]	[0, 1, 2, 3, 4, 5, 6, 7]	-2	$2h_z$	8
6	[1, -1, -1, -1, 1, -1, -1, -1]	[0, 2, 4, 6]	-2	$2h_z$	4
7	[-1, -1, -1, -1, -1, 1, 1, 1]	[0, 1, 2, 3, 4, 5, 6, 7]	-1	$1+h_z$	8
8	[-1, -1, 1, 1, -1, 1, -1, -1]	[0, 1, 2, 3, 4, 5, 6, 7]	-1	h_z	8
9	[-1, -1, 1, -1, 1, 1, -1, -1]	[0, 1, 2, 3, 4, 5, 6, 7]	-1	h_z	8
10	[1, 1, -1, -1, 1, -1, -1, -1]	[0, 1, 2, 3, 4, 5, 6, 7]	-1	$-j+h_z$	8
11	[1, -1, -1, 1, 1, -1, -1, -1]	[0, 1, 2, 3, 4, 5, 6, 7]	-1	$-j+h_z$	8
12	[1, -1, 1, -1, -1, -1, 1, -1]	[0, 1, 2, 3, 4, 5, 6, 7]	-1	$-1+j+h_z$	8
13	[1, -1, 1, -1, -1, 1, -1, -1]	[0, 1, 2, 3, 4, 5, 6, 7]	-1	$-1+h_z$	8
14	[-1, 1, -1, -1, 1, 1, -1, 1]	[0, 1, 2, 3, 4, 5, 6, 7]	0	-1	8
15	[1, -1, -1, -1, -1, 1, 1, 1]	[0, 1, 2, 3, 4, 5, 6, 7]	0	1	8
16	[-1, 1, -1, -1, 1, -1, 1, 1]	[0, 1, 2, 3, 4, 5, 6, 7]	0	-1	8
17	[1, -1, -1, 1, 1, 1, -1, -1]	[0, 1, 2, 3, 4, 5, 6, 7]	0	$-j$	8
18	[1, -1, 1, -1, -1, -1, 1, 1]	[0, 1, 2, 3, 4, 5, 6, 7]	0	0	8
19	[1, -1, -1, -1, 1, -1, 1, 1]	[0, 1, 2, 3, 4, 5, 6, 7]	0	0	8
20	[1, -1, -1, -1, 1, 1, -1, 1]	[0, 1, 2, 3, 4, 5, 6, 7]	0	$-j$	8
21	[1, -1, -1, 1, -1, 1, -1, 1]	[0, 1, 2, 3, 4, 5, 6, 7]	0	-1	8
22	[1, 1, -1, -1, 1, 1, -1, -1]	[0, 2, 4, 6]	0	$-2j$	4
23	[1, -1, 1, -1, 1, -1, 1, -1]	[0, 4]	0	$-2+2j$	2
24	[1, 1, -1, -1, 1, 1, -1, 1]	[0, 1, 2, 3, 4, 5, 6, 7]	1	$-j-h_z$	8
25	[1, -1, -1, 1, 1, 1, -1, 1]	[0, 1, 2, 3, 4, 5, 6, 7]	1	$-j-h_z$	8
26	[-1, 1, 1, -1, 1, -1, 1, 1]	[0, 1, 2, 3, 4, 5, 6, 7]	1	$-1-h_z$	8
27	[-1, 1, 1, 1, -1, 1, -1, 1]	[0, 1, 2, 3, 4, 5, 6, 7]	1	$-1+j-h_z$	8
28	[1, 1, 1, -1, -1, 1, -1, 1]	[0, 1, 2, 3, 4, 5, 6, 7]	1	$-h_z$	8
29	[-1, 1, -1, -1, 1, 1, 1, 1]	[0, 1, 2, 3, 4, 5, 6, 7]	1	$-h_z$	8
30	[-1, 1, 1, 1, 1, 1, -1, -1]	[0, 1, 2, 3, 4, 5, 6, 7]	1	$1-h_z$	8
31	[1, 1, 1, 1, -1, -1, 1, 1]	[0, 1, 2, 3, 4, 5, 6, 7]	2	$1-2h_z$	8
32	[1, -1, 1, 1, 1, 1, -1, 1]	[0, 1, 2, 3, 4, 5, 6, 7]	2	$-2h_z$	8
33	[1, -1, 1, -1, 1, 1, 1, 1]	[0, 1, 2, 3, 4, 5, 6, 7]	2	$j-2h_z$	8
34	[-1, 1, 1, 1, -1, 1, 1, 1]	[0, 2, 4, 6]	2	$-2h_z$	4
35	[1, 1, 1, -1, 1, 1, 1, 1]	[0, 1, 2, 3, 4, 5, 6, 7]	3	$1+j-3h_z$	8
36	[1, 1, 1, 1, 1, 1, 1, 1]	[0]	4	$2+2j-4h_z$	1

Table 3.6: Exact diagonalization of 8 spins.

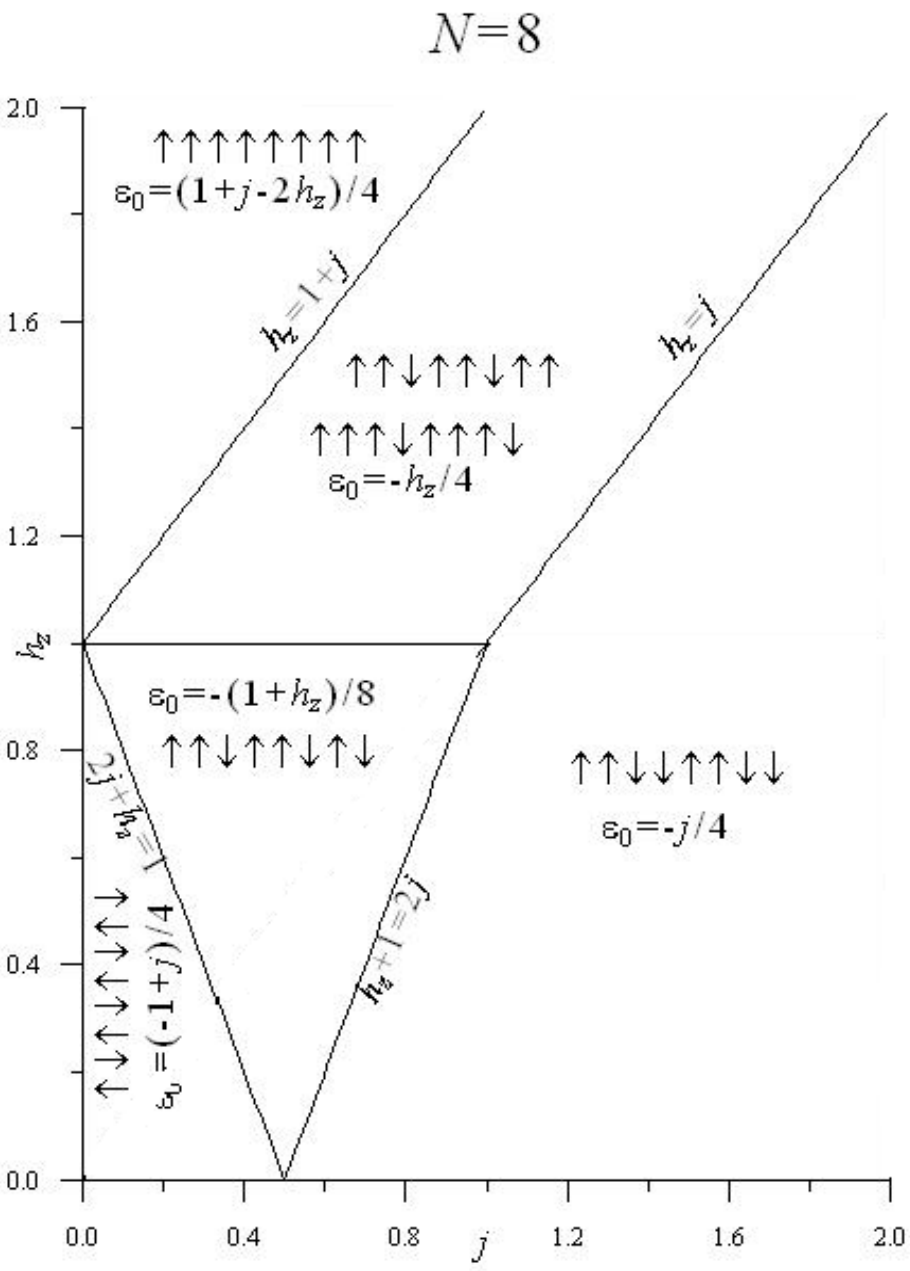

Figure 3.5: $T = 0$ phase diagram of the longitudinal ANNNI model for $N = 8$.

We observe that the degenerate states $|8\rangle$ and $|9\rangle$ are mirror reflections of each other. So also are $|10\rangle$ and $|11\rangle$, $|14\rangle$ and $|21\rangle$, $|18\rangle$ and $|19\rangle$, $|24\rangle$ and $|25\rangle$ and lastly $|28\rangle$ and $|29\rangle$.
We note also that $|17\rangle$ and $|20\rangle$ are degenerate. The two states are not translationally related and they do not posses reflection symmetry. The one state can however be obtained from the other by all-spin inversion (a valid symmetry in this case since total $S_z = 0$) followed by reflection or vice versa, and this explains the degeneracy.

Here as in the previous cases, we can employ the reflection symmetry to further reduce the dimensions of the matices in the $k = 0$ and $k = 8/2 = 4$ subspaces if we are interested in solving the full Hamiltonian of the ANNNI model in the presence of both longitudinal and transverse fields. We take the subspace $k = 0$ as example. The following 6 linear combinations are eigenstates of $\mathcal{R}$ belonging to eigenvalue -1. They are also eigenstates of $\mathcal{T}$ of eigenvalue 1.

$$\begin{aligned}
|u\rangle &= (-|8\rangle + |9\rangle)/\sqrt{16}\,,\\
|v\rangle &= (-|10\rangle + |11\rangle)/\sqrt{16}\,,\\
|w\rangle &= (-|28\rangle + |29\rangle)/\sqrt{16}\,,\\
|u\rangle &= (-|24\rangle + |25\rangle)/\sqrt{16}\,,\\
|u\rangle &= (-|18\rangle + |19\rangle)/\sqrt{16}\,,\\
|u\rangle &= (-|14\rangle + |21\rangle)/\sqrt{16}\,.
\end{aligned} \tag{3.15}$$

The following 6 linear combinations are eigenstates of $\mathcal{R}$ belonging to eigenvalue 1. They are also eigenstates of $\mathcal{T}$ of eigenvalue 1.

$$\begin{aligned}
|u\rangle &= (|8\rangle + |9\rangle)/\sqrt{16}\,,\\
|v\rangle &= (|10\rangle + |11\rangle)/\sqrt{16}\,,\\
|w\rangle &= (|28\rangle + |29\rangle)/\sqrt{16}\,,\\
|u\rangle &= (|24\rangle + |25\rangle)/\sqrt{16}\,,\\
|u\rangle &= (|18\rangle + |19\rangle)/\sqrt{16}\,,\\
|u\rangle &= (|14\rangle + |21\rangle)/\sqrt{16}\,.
\end{aligned} \tag{3.16}$$

The 6 new states in (3.16) can be combined with the 24 states of $k = 0$ that are invariant under reflection to form 30 eigenstates of the subspace of $\mathcal{R}$ of eigenvalue 1 while the 6 new states in (3.15) constitute 6 eigenstates of the subspace of $\mathcal{R}$ of eigenvalue -1. Thus the 36 states of

the subspace $k = 0$ of $\mathcal{T}$ now splits into a union of 6 eigenstates of $\mathcal{R}$ of eigenvalue -1 and 30 eigenstates of $\mathcal{R}$ of eigenvalue 1. The Hamiltonian H of equation (1.1) can now be diagonalized in the 2 subspaces. The 6×6 matrix of H with respect to the basis (3.15) is given below, equation (3.17).

$$H_{-1} = \begin{pmatrix} h_z & 0 & 0 & 0 & h_x/2 & -h_x/2 \\ 0 & -j+h_z & 0 & 0 & -h_x/2 & -h_x/2 \\ 0 & 0 & -h_z & 0 & -h_x/2 & h_x/2 \\ 0 & 0 & 0 & -j-h_z & -h_x/2 & -h_x/2 \\ h_x/2 & -h_x/2 & -h_x/2 & -h_x/2 & 0 & 0 \\ -h_x/2 & -h_x/2 & h_x/2 & -h_x/2 & 0 & -1 \end{pmatrix}. \tag{3.17}$$

3.1.6 N=9

There are 36 energies available to the 60 non translationally-related cycles of a one-dimensional chain of 9 atoms. Of these, only 4 energies belong to ground state configurations. They are $9/4 + 9j/4 - 9h_z/2$ for the ferro state, $-7/4 + 5\,j/4 - h_z/2$ for the antiferro-$\uparrow\uparrow\downarrow$ hybrid state, $-3/4 - 3\,j/4 - 3\,h_z/2$ for the three-fold degenerate $\uparrow\uparrow\downarrow$ configuration and $1/4 - 7j/4 - h_z/2$ for the almost antiphase alignment. The phase diagram is drawn in figure 3.6

3.1.7 $N = 10$

There are 49 distinct energies for a chain of 10 spins, out of which only 5 qualify for ground state configurations. The five lowest energies and the corresponding states are tabulated in table 3.7 and the ground state phase structure at $T = 0$ is depicted in figure 3.7.

3.1.8 N=11

The 186 states of the reduced Hilbert space are highly degenerate and share 64 energies, as contained on the included CD-ROM. The five ground state energies are $11/4 + 11j/4 - 11h_z/2$

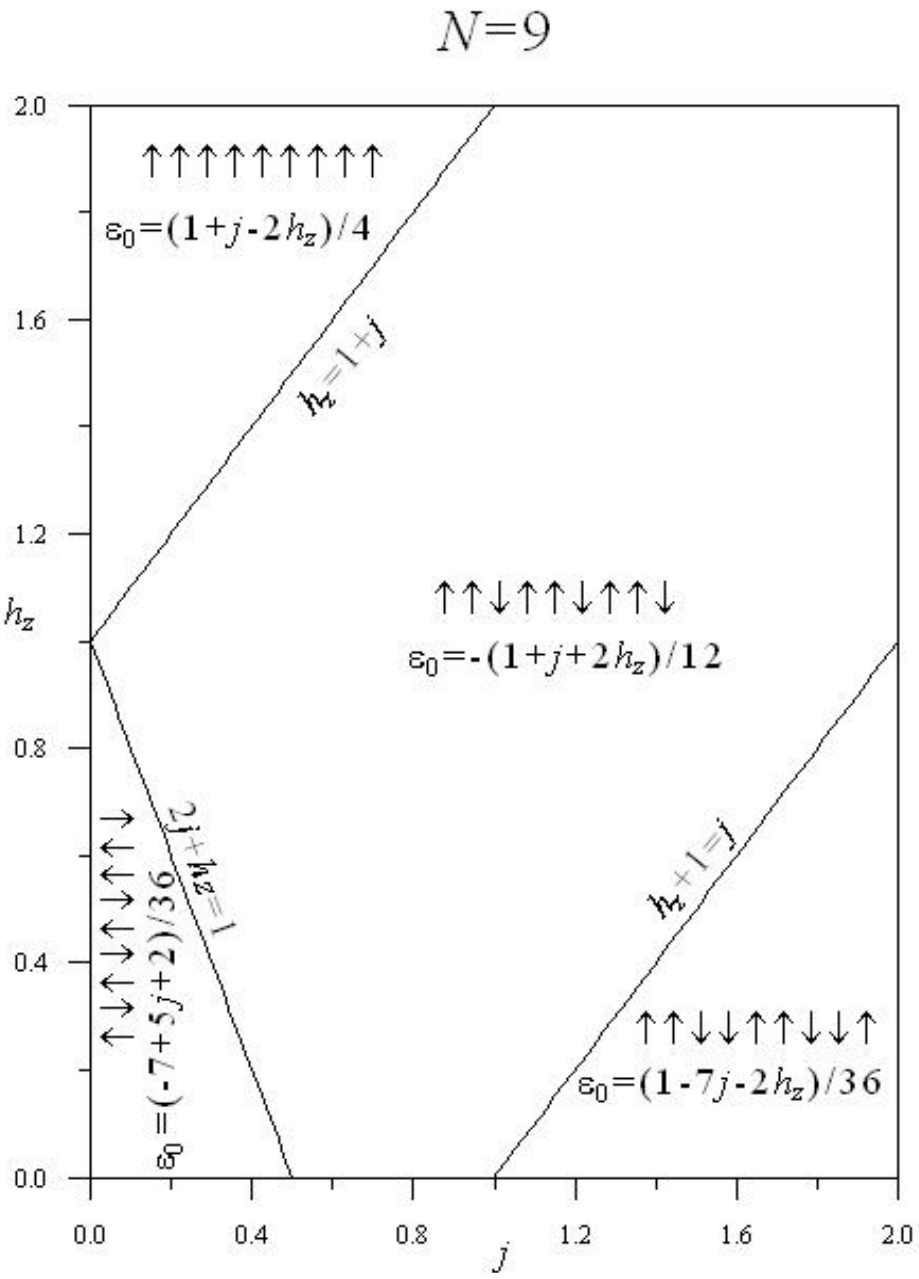

Figure 3.6: $T = 0$ phase diagram of the longitudinal ANNNI model for $N = 9$.

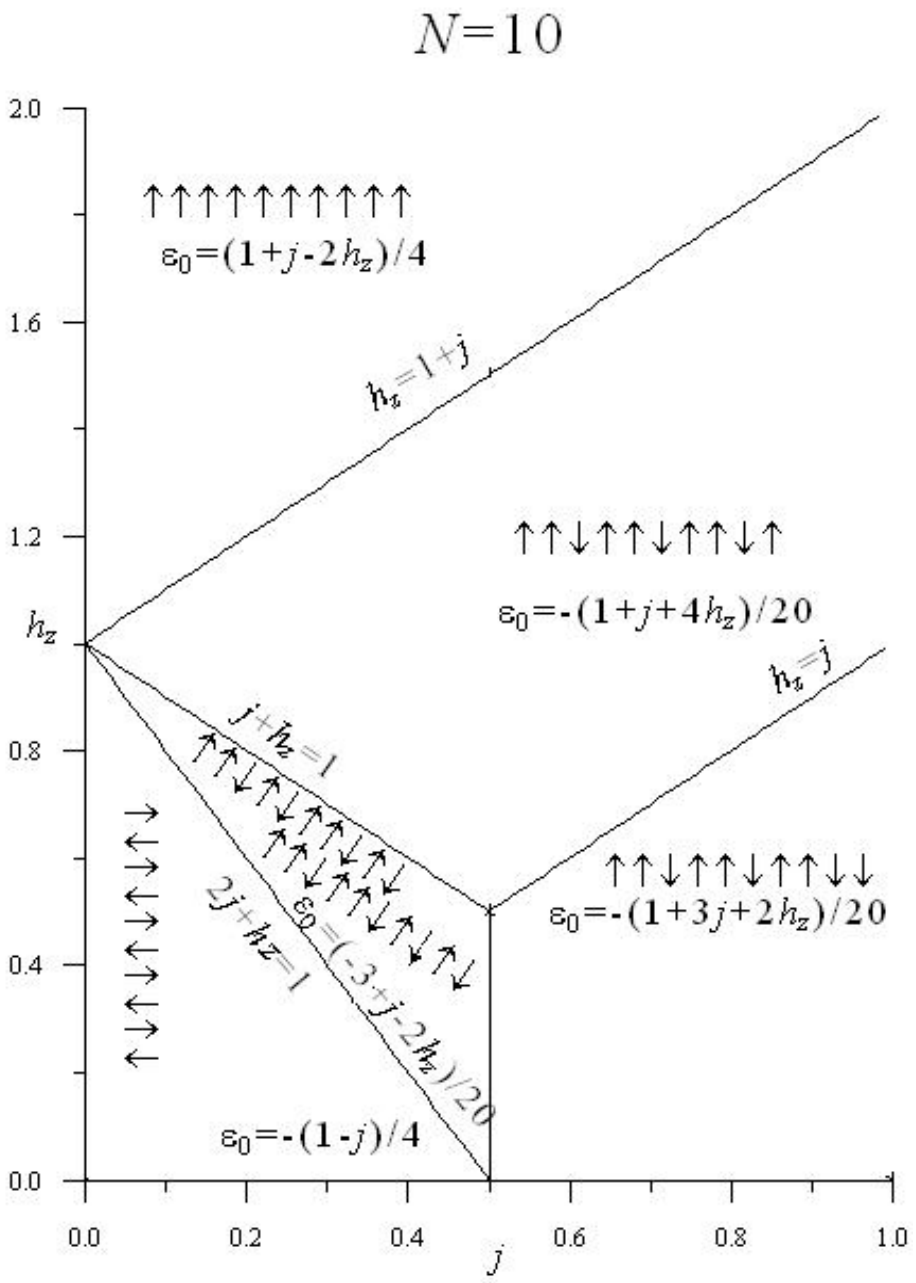

Figure 3.7: $T = 0$ phase diagram of the longitudinal ANNNI model for $N = 10$.

SNo	States	$k-$values	S_z	Energies	Degen
1	[1, -1, 1, -1, 1, -1, 1, -1, 1, -1]	[0, 5]	0	$-5/2-5j/2$	2
2	[-1, -1, 1, 1, -1, 1, 1, -1, 1, 1]	[0, 1, 2, 3, 4, 5, 6, 7, 8, 9]	1	$-1/2-3j/2-h_z$	10
3	[1, -1, 1, 1, -1, 1, -1, 1, -1, 1]	[0, 1, 2, 3, 4, 5, 6, 7, 8, 9]	1	$-3/2+j/2-h_z$	10
4	[1, -1, 1, -1, 1, 1, -1, 1, -1, 1]	[0, 2, 4, 6, 8]	1	$-3/2+j/2-h_z$	5
5	[-1, 1, 1, -1, 1, 1, -1, 1, 1, 1]	[0, 1, 2, 3, 4, 5, 6, 7, 8, 9]	2	$-1/2-j/2-2h_z$	10
6	[1, 1, 1, 1, 1, 1, 1, 1, 1, 1]	[0]	5	$5/2+5j/2-5h_z$	1

Table 3.7: Exact diagonalization of 10 spins. The complete list of energies is contained on the included CD-ROM

for the ferromagnetic state, the 22-fold degenerate $-1/4-j/4-5h_z/2$ for the states indicated in the diagram, $-9/4+7\,j/4-h_z/2$ for the 'almost' antiferro state $[1,-1,1,-1,1,-1,1,-1,1]$, $-5/4-j/4-3\,h_z/2$ for the 'almost' $\uparrow\uparrow\downarrow$ states and $-1/4-9\,j/4-h_z/2$ for the 'almost' antiphase state $[1,1,-1,-1,1,1,-1,-1,1,1,-1]$. The phase diagram is drawn in figure 3.8

3.1.9 N=12

Under translational invariance, the total number of configurations for spins on a chain of 12 spins is 352. The states are highly degenerate and the number of distinct energies is only 84, out of which only 4 correspond to ground state alignments. The 4 ground state structures are the non-degenerate ferromagnetic state with energy $3+3j-6h_z$, the antiferromagnetic states with energy $-3+3\,j$, the antiphase states with energy $-3\,j$ and the period-3 $\uparrow\uparrow\downarrow$ states with energy $-1-j-2\,h_z$. The complete list of energies is contained on the included CD-ROM. The resulting phase diagram is drawn in figure 3.9

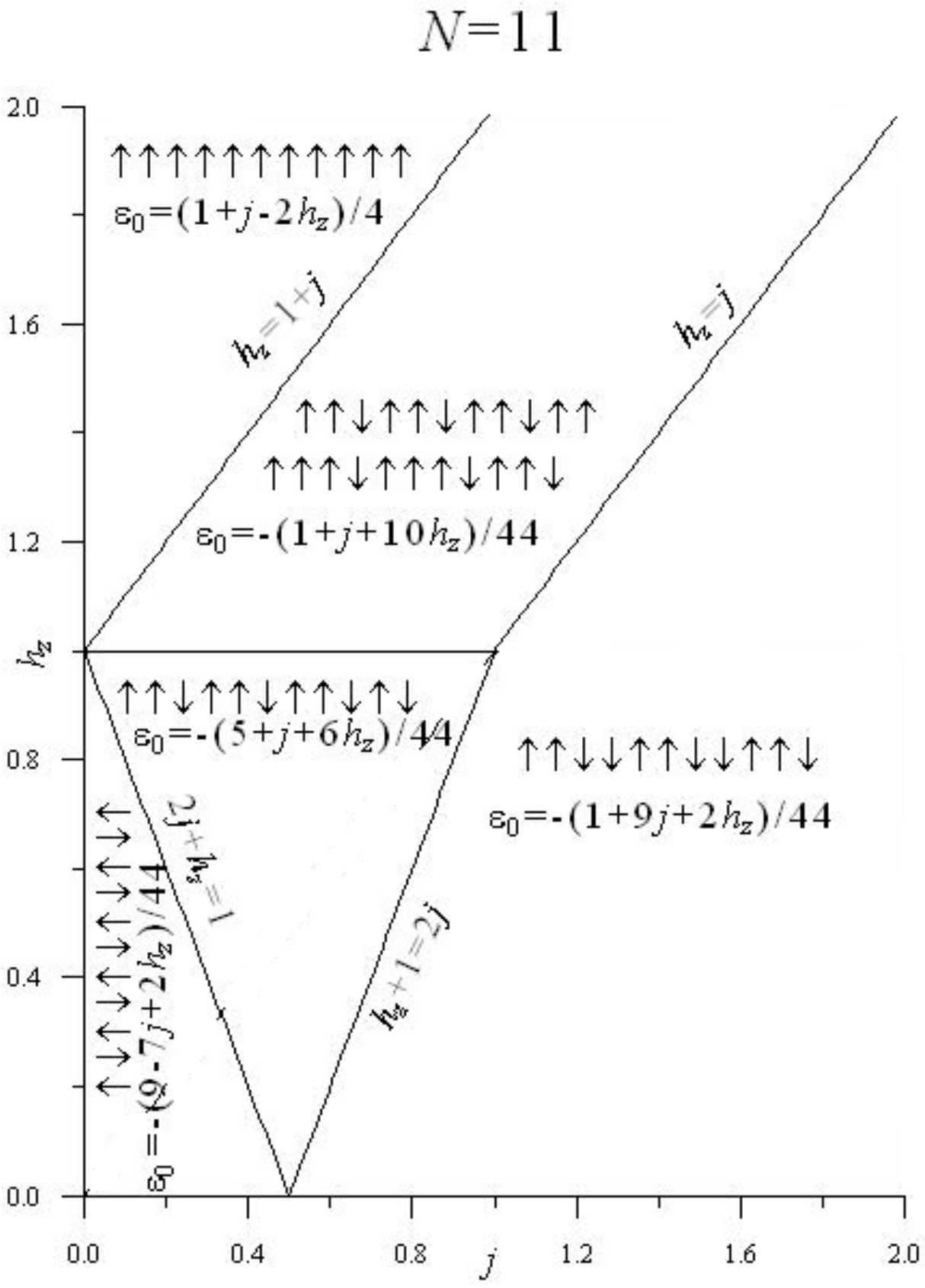

Figure 3.8: $T = 0$ phase diagram of the longitudinal ANNNI model for $N = 11$.

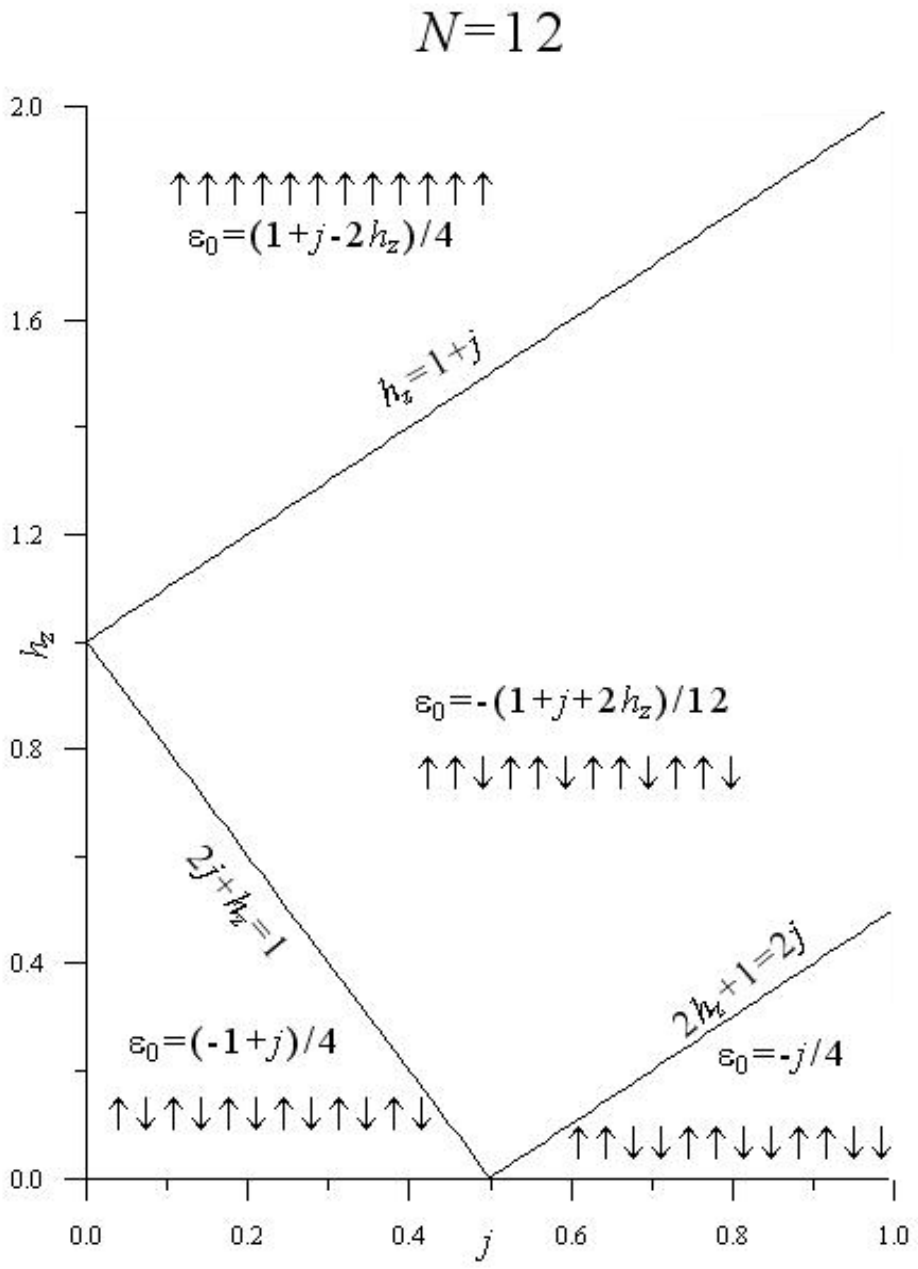

Figure 3.9: $T = 0$ phase diagram of the longitudinal ANNNI model for $N = 12$.

3.1.10 N=13

The total number of translationally non-related cycles corresponding to a lattice of 13 spin sites is 632. For the one-dimensional longitudinal ANNNI model, these 632 states share only 106 energies. Out of the 106 energies, only 6 belong to ground state configurations, as tabulated in table 3.8. Except for the $h_z + 1 = j$ line, the critical lines separating the states are the same as those for $N = 10$. The phase diagram is plotted in figure 3.10.

SNo	States	$k-$values	S_z	Energies	Deg
1	$[1,-1,1,-1,1,-1,1,-1,1,-1,1,-1,1]$	$[0,1,2,\ldots,11,12]$	$1/2$	$-11/4+9j/4-h_z/2$	13
2	$[1,1,-1,-1,1,1,-1,-1,1,1,-1,-1,1]$	$[0,1,2,\ldots,11,12]$	$1/2$	$1/4-11j/4-h_z/2$	13
3	$[1,1,-1,1,1,-1,1,1,-1,1,-1,1,-1]$	$[0,1,2,\ldots,11,12]$	$3/2$	$-7/4+j/4-3h_z/2$	13
4	$[1,1,-1,1,-1,1,1,-1,1,-1,1,1,-1]$	$[0,1,2,\ldots,11,12]$	$3/2$	$-7/4+j/4-3h_z/2$	13
5	$[1,1,-1,1,1,-1,1,1,-1,1,1,-1,-1]$	$[0,1,2,\ldots,11,12]$	$3/2$	$-3/4-7j/4-3h_z/2$	13
6	$[1,1,-1,1,1,-1,1,1,-1,1,1,-1,1]$	$[0,1,2,\ldots,11,12]$	$5/2$	$-3/4-3j/4-5h_z/2$	13
7	$[1,1,1,1,1,1,1,1,1,1,1,1,1]$	$[0]$	$13/2$	$11/4+11j/4-11h_z/2$	1

Table 3.8: Exact diagonalization of 13 spins, showing the lowest energies. The complete list of energies is contained on the included CD-ROM

3.1.11 N=14

The 1182 basis states of the reduced Hilbert space of a chain of 14 atoms share 133 energies. The energies and the corresponding states are as contained on the included CD-ROM. Out of the 133 energy eigenvalues, only 5 make it to the ground state. The lowest energies are given in table 3.9. The critical lines for $N = 14$ are the same as those for $N = 8$. The phase diagram is plotted in figure 3.11

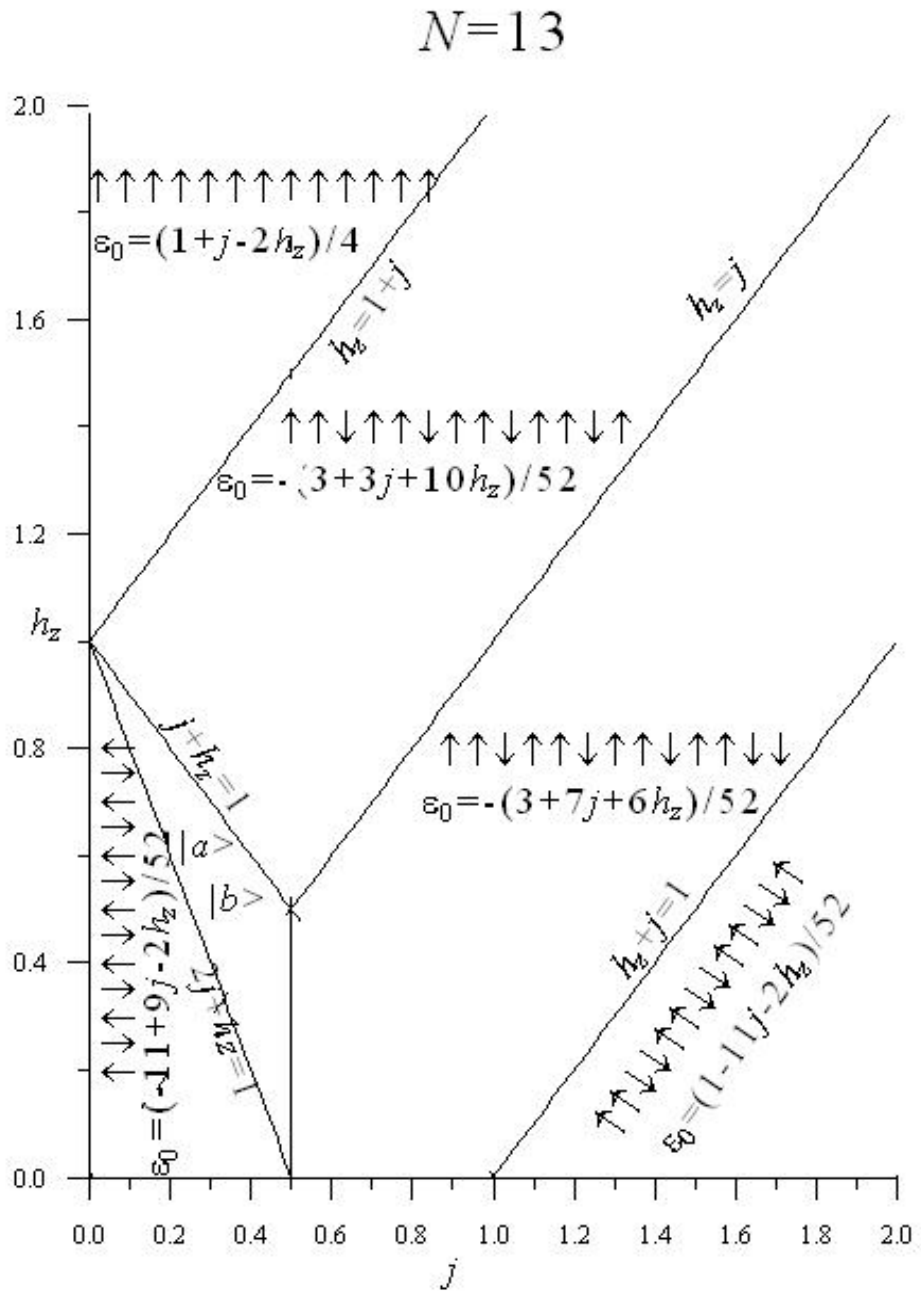

Figure 3.10: $T = 0$ phase diagram of the longitudinal ANNNI model for $N = 13$. $|a\rangle$ and $|b\rangle$ are the degenerate states $\uparrow\uparrow\downarrow\uparrow\uparrow\downarrow\uparrow\uparrow\downarrow\uparrow\downarrow$ and $\uparrow\uparrow\downarrow\uparrow\uparrow\downarrow\uparrow\downarrow\uparrow\uparrow\downarrow\uparrow\downarrow$ with energy per spin $\varepsilon_0 = (-7 + j - 6h_z)/52$.

SNo	States	$k-$values	S_z	Energies	Degen
1	[1,-1,1,-1,1,-1,1,-1,1,-1,1,-1,1,-1]	$[0, 7]$	0	$-7/2 + 7j/2$	14
2	[1,1 -1,-1,1,1,-1,-1,1,1,-1,1,1,-1]	$[0, 1, 2, \ldots, 11, 13]$	1	$-1/2 - 5j/2 - h_z$	14
3	[1,1,-1,-1,1,1,-1,1,1,-1,-1,1,1,-1]	$[0, 2, 4, 6, 8, 10, 12]$	1	$-1/2 - 5j/2 - h_z$	7
4	[1,1,-1,1,1,-1,1,1,-1,1,1,-1,1,-1]	$[0, 1, 2, \ldots, 11, 12, 13]$	2	$-3/2 - j/2 - 2h_z$	14
5	[1,1,1,-1,1,1,-1,1,1,1,-1,1,1,-1]	$[0, 2, 4, 6, 8, 10, 12]$	3	$-1/2 - j/2 - 3hz$	7
6	[1,1,-1,1,1,-1,1,1,-1,1,1,-1,1,1]	$[0, 1, 2, \ldots, 11, 13]$	3	$-1/2 - j/2 - 3hz$	14
7	[1,1,1,-1,1,1,1,-1,1,1,-1,1,1,-1]	$[0, 1, 2, \ldots, 11, 13]$	3	$-1/2 - j/2 - 3hz$	14
8	[1,1,1,1,1,1,1,1,1,1,1,1,1,1]	[0]	13/2	$7/2 + 7j/2 - 7$	1

Table 3.9: Exact diagonalization of 14 spins, showing the lowest 5 energies. The complete list of energies is as contained on the included CD-ROM

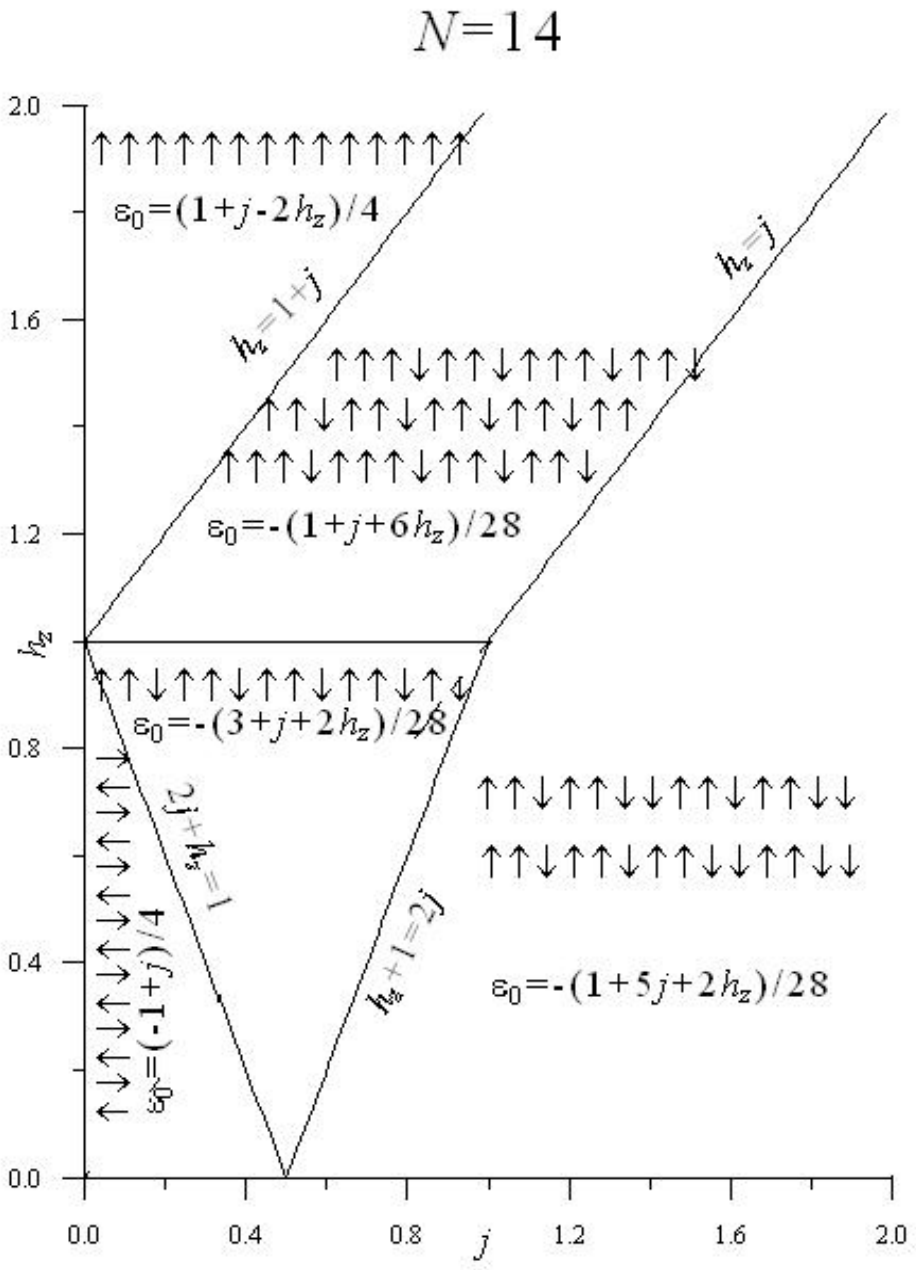

Figure 3.11: $T = 0$ phase diagram of the longitudinal ANNNI model for $N = 14$.

3.1.12 N=16

Using the translation and reflection symmetries as discussed in appendix A, the total number of orientations available to a one-dimensional lattice of 16 spins$-1/2$ atoms is 4116. Due to the high degeneracies, the states share only 200 distinct energies, out of which only 6 actually make it to the ground state. The 6 lowest energies and the respective states are tabulated in table 3.10. The complete list of all the energies can be found on the CD. The corresponding phase diagram is displayed in figure 3.12

SNo	States	$k-$values	S_z	Energies	Degen
1	[1,-1,1,-1,1,-1,1,-1,1,-1,1,-1,1,-1,1,-1]	$[0, 8]$	0	$-4+4j$	2
2	[1,1 -1,-1,1,1,-1,-1,1,1,-1,-1,1,1,-1,-1]	$[0, 4, 8, 12]$	0	$-4j$	4
3	[1,1,-1,1,1,-1,1,1,-1,1,1,-1,1,-1,1,-1]	$[0, 1, \ldots, 14, 15]$	2	$-2-2h_z$	16
4	[1,1,-1,1,1,-1,1,1,-1,1,-1,1,1,-1,1,-1]	$[0, 1, \ldots, 14, 15]$	2	$-2-2h_z$	16
5	[1,1,-1,1,1,-1,1,-1,1,1,-1,1,1,-1,1,-1]	$[0, 2, 4, 6, 8, 10, 12, 14]$	2	$-2-2h_z$	8
6	[1,1,-1,1,1,-1,1,1,-1,1,1,-1,1,1,-1,-1]	$[0, 1, \ldots, 14, 15]$	2	$-1-2j-2h_z$	16
7	[1,1,-1,1,1,-1,1,1,-1,1,1,-1,1,1,-1,1]	$[0, 1, 2, \ldots, 11, 12, 13]$	3	$-1-j-3h_z$	16
8	[1,1,1,1,1,1,1,1,1,1,1,1,1,1,1,1]	$[0]$	8	$4+4j-8h_z$	1

Table 3.10: Exact diagonalization of 16 spins, showing the lowest 6 energies. The complete list of energies is contained on the CD-ROM

3.1.13 N=18

The 14602 translationally invariant cycle states of a chain of 18 atoms share 287 distinct energies out of which only 4 belong to ground state alignment. The four ground state energies are $-9/2-9j/2+9h_z$ for the ferromagnetic state, $-1/2-7j/2-h_z$ for the antiphase-$\uparrow\uparrow\downarrow$ hybrid

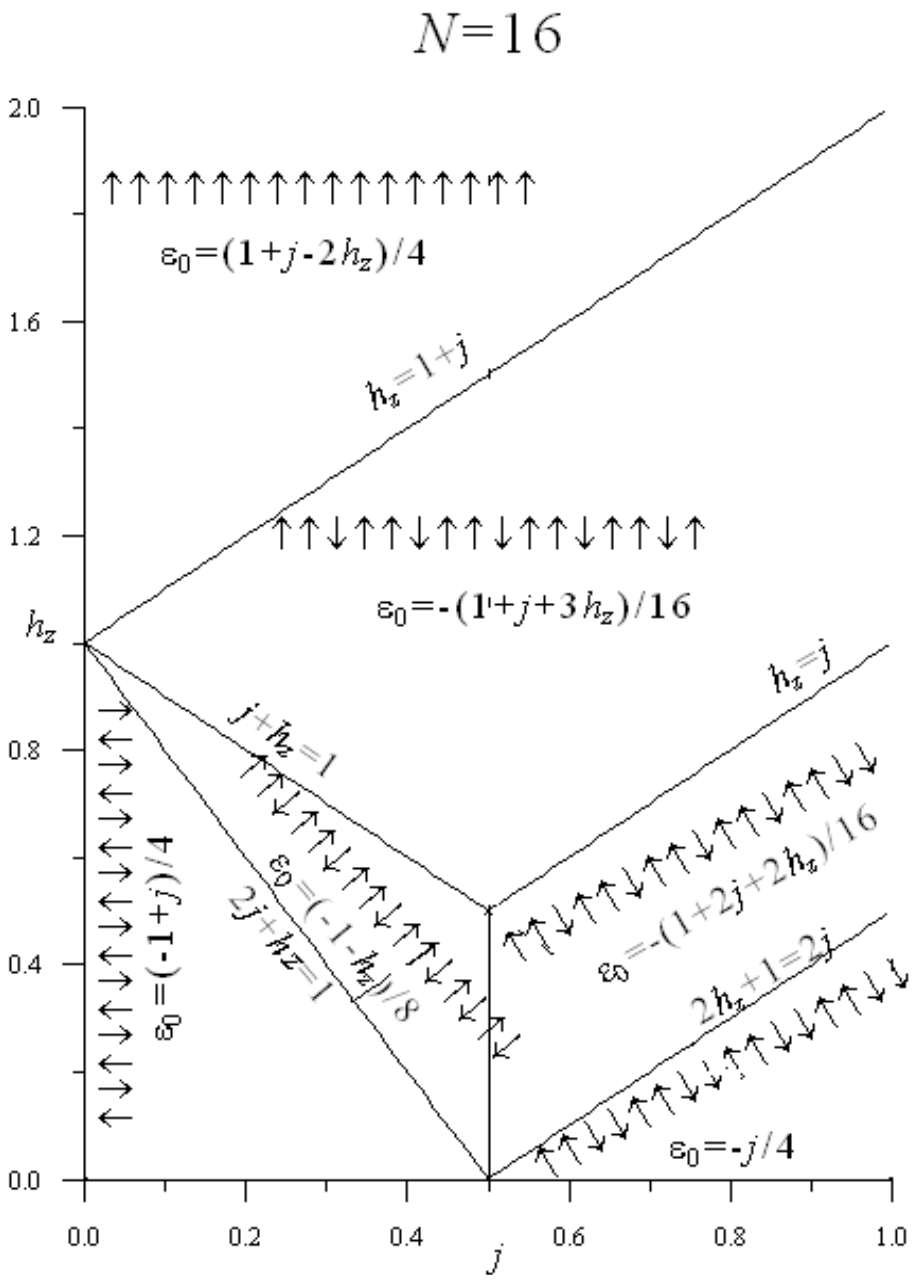

Figure 3.12: $T = 0$ phase diagram of the longitudinal ANNNI model for $N = 16$. Note that the configurations ↑↑↓↑↑↓↑↑↓↑↑↓↑↑↓ and ↑↑↓↑↑↓↑↑↓↑↑↓↑↑↓ also have energy per spin $\varepsilon_0 = (-1 - h_z)/8$ but are not shown in the figure due to space limitation.

SNo	States	$k-$values	S_z	Energies	Degen
1	[1,-1,1,-1,1,-1,1,-1,1,-1,1,-1,1,-1,1,-1,1,-1]	$[0, 9]$	0	$-9/2 + 9j/2$	2
2	[1,1, -1,-1,1,1,-1,-1,1,1,-1,-1,1,1,-1,1,1,-1]	$[0, 1, \ldots, 16, 17]$	1	$-1/2 - 7j/2 - h_z$	18
3	[1,1,-1,-1,1,1,-1,-1,1,1,-1,1,1,-1,-1,1,1,-1]	$[0, 1, \ldots, 16, 17]$	1	$-1/2 - 7j/2 - h_z$	18
4	[1,1,-1,1,1,-1,1,1,-1,1,1,-1,1,1,-1,1,1,-1]	$[0, 6, 12]$	3	$-3/2 - 3j/2 - 3h_z$	3
5	[1,1,1,1,1,1,1,1,1,1,1,1,1,1,1,1,1,1]	$[0]$	9	$9/2 + 9j/2 - 9h_z$	1

Table 3.11: Exact diagonalization of 18 spins, showing the lowest 4 energies. The complete list of energies is contained on the CD.

state $[1, 1, -1, -1, 1, 1, -1, -1, 1, 1, -1, -1, 1, 1, -1, 1, 1, -1]$, $-3/2-3j/2-3\,h_z$ for the $\uparrow\uparrow\downarrow$ states and $-9/2 + 9j/2$ for the antiferromagnetic states (table 3.11). The line $2\,j + h_z = 1$ remains as the boundary separating the antiferromagnetic region from the $\uparrow\uparrow\downarrow$ states. In fact the inequality $2\,j + h_z < 1$ is equivalent to the following ordering of the lowest energies in the antiferromagnetic region:

$$-9/2 + 9j/2 < -7/2 + 5j/2 - h_z < -5/2 + j/2 - 2\,h_z < -3/2 - 3\,j/2 - 3\,h_z\ . \qquad (3.18)$$

As can be seen from the energy list for $N = 18$ on the CD-ROM the energies $-7/2 + 5j/2 - h_z$, $-5/2 + j/2 - 2\,h_z$ and $-3/2 - 3\,j/2 - 3\,h_z$ belong respectively to the first, second and third excited states of the antiferromagnetic states.

Similarly, the line $2\,h_z + 1 = 2\,j$ remains as the boundary separating the $\uparrow\uparrow\downarrow$ phase from the antiphase-$\uparrow\uparrow\downarrow$ hybrid state.

The ground state phase structure of the longitudinal ANNNI model for $N = 18$ at zero temperature is drawn in figure 3.13. It is instructive to observe that $N = 12$ and $N = 18$ share common critical lines.

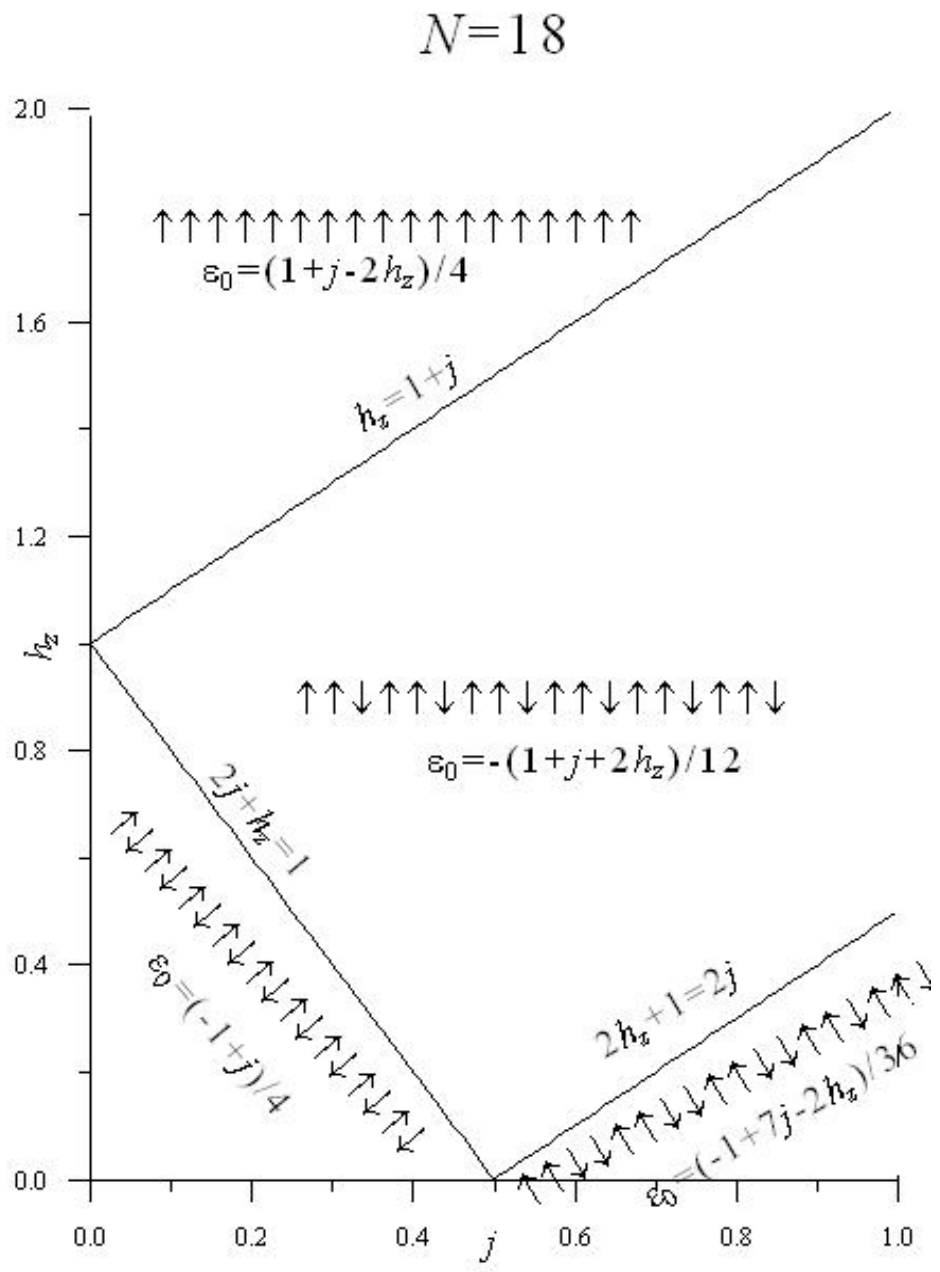

Figure 3.13: $T = 0$ phase diagram of the longitudinal ANNNI model for $N = 18$. Note that the configuration ↑↑↓↓↑↑↓↓↑↑↓↑↑↓↓↑↑↓ also belongs to the per spin energy $\varepsilon_0 = (-1 + 7j - 2h_z)/36$ but is not shown in the figure for lack of space.

3.1.14 N=20

The reduced Hilbert space of 20 spin-1/2 atoms has 52488 states. These states are very highly degenerate, so that they share only 396 energies. Of these energies, only 5 belong to ground state configurations. The 4 lowest energies are tabulated in table 3.12. The ordering of the energies in the antiferro region is as follows:

$$-5+5\,j < -4+3\,j-h_z < -3+j-2\,h_z < -2-j-3\,h_z\ . \tag{3.19}$$

We note that the energies $-4+3\,j-h_z$ and $-3+j-2\,h_z$, energies of the first and second excited states, respectively, never make it to the ground state since there is a lower energy, $-2-j-3\,h_z$, outside the antiferro region. The phase diagram for the longitudinal ANNNI model for $N = 20$ is plotted in figure 3.14

SNo	States	$k-$values	S_z	Energies	Degen
1	[1,-1,1,-1,1,-1,1,-1,1,-1,1,-1,1,-1,1,-1,1,-1,1,-1]	$[0, 10]$	0	$-5+5j$	2
2	[1,1 -1,-1,1,1,-1,-1,1,1,-1,-1,1,1,-1,-1,1,1,-1,-1]	$[0, 5, 10, 15]$	0	$-5j$	4
3	[1,1,-1,1,1,-1,1,1,-1,-1,1,1,-1,1,1,-1,1,1,-1,-1]	$[0, 2, 4, \ldots, 16, 18]$	2	$-1-3j-2h_z$	10
4	[1,1,-1,1,1,-1,1,1,-1,1,1,-1,1,1,-1,-1,1,1,-1,-1]	$[0, 1, \ldots, 18, 19]$	2	$-1-3j-2h_z$	20
5	[1,1,-1,1,1,-1,1,1,-1,1,1,-1,-1,1,1,-1,1,1,-1,-1]	$[0, 1, \ldots, 18, 19]$	2	$-1-3j-2h_z$	20
6	[1,1,-1,1,1,-1,1,1,-1,1,1,-1,1,1,-1,1,1,-1,1,-1]	$[0, 1, \ldots, 18, 19]$	3	$-2-j-3h_z$	20
7	[1,1, -1,1,1,-1,1,1,1,-1,1,1,-1,1,1,-1,1,1,1,-1]	$[0, 2, 4, \ldots, 16, 18]$	4	$-1-j-4h_z$	10
8	[1,1,-1,1,1,-1,1,1,-1,1,1,1,-1,1,1,-1,1,1,1,-1]	$[0, 1, \ldots, 18, 19]$	4	$-1-j-4h_z$	20
9	[1,1,-1,1,1,-1,1,1,-1,1,1,-1,1,1,-1,1,1,-1,1,1]	$[0, 1, \ldots, 18, 19]$	4	$-1-j-4h_z$	20
10	[1,1,-1,1,1,-1,1,1,-1,1,1,-1,1,1,-1,1,1,1,-1,1]	$[0, 1, \ldots, 18, 19]$	4	$-1-j-4h_z$	20
11	[1,1,1,1,1,1,1,1,1,1,1,1,1,1,1,1,1,1,1,1]	$[0]$	10	$5+5j-10h_z$	1

Table 3.12: Exact diagonalization of 20 spins, showing the lowest 6 energies. The complete list of energies is contained on the included CD

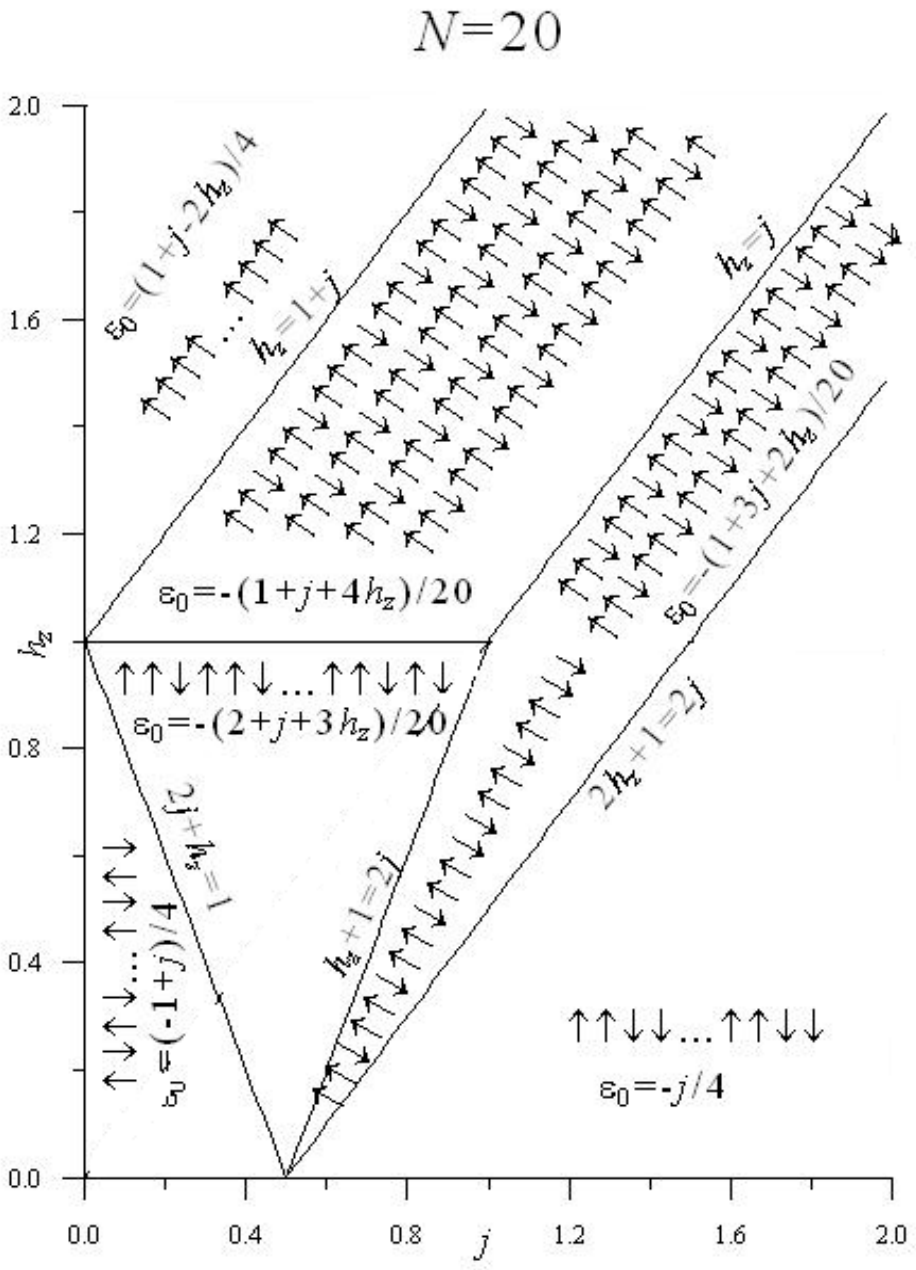

Figure 3.14: $T = 0$ phase diagram of the longitudinal ANNNI model for $N = 20$.

3.2 Exact Diagonalization of Long but Finite Systems

We will now examine the results of section 3.1 and attempt to give a general rule for the classification of the different phases of the longitudinal ANNNI model at zero temperature. We will first consider the case when the chain length N is not a multiple of 3.

3.2.1 N not a multiple of 3

We note that any integer N which is not a multiple of 3 can be written either as $N = 3\,n + 1$ or as $N = 3\,n + 2$ where n is an integer. From the results of the previous section, we can make the following deductions

- The ferromagnetic boundary $h_z = 1 + j$ is always present, regardless of the nature of N.
- Whenever N is of the form $N = 3\,n+1$ (that is $N = 4, 7, 10, 13, 16, \ldots$), the resulting phase diagram always contains the critical lines $2\,j + h_z = 1$, $h_z + j = 1$, $h_z = j$ and $j = 1/2$, with a multicritical point at $j = 1/2 = h_z$. The line $2\,j + h_z = 1$ is absent from the phase diagrams of $N = 4$ and $N = 7$ for reasons that will become clear shortly. Furthermore, if in addition N is a multiple of 4 and $N > 4$, the line $2\,h_z + 1 = 2\,j$ is also a critical line.
- Whenever N is of the form $N = 3\,n+2$ (that is $N = 8, 11, 14, 17, 20, \ldots$), the phase diagram always has as critical lines $h_z = 1$, $2\,j + h_z = 1$ and $2\,j - h_z = 1$. If in addition, N is a multiple of 4 and $N > 8$, then the line $2\,h_z + 1 = 2\,j$ is also a critical line. The reason for the exclusion of $N = 8$ will become apparent shortly.

These observations are not coincidental and in fact, using the fact that the ground state energies are proportional to N, they make it possible for us to determine the phase structure of an arbitrarily long chain. Presently we will obtain expressions for the ground states and their energies and the first excited states and their energies for an arbitrarily long N. This way we will be able to explain or justify the phase structure.

First we consider the case $N = 3n + 1$. There are two possibilities: either N is odd (when n is even) or N is even (that is when n is odd). We note that, of course, in both of these situations, the modulo arithmetic $N = 1 \mod 3$ still holds. We now look at the ground state structure for both situations, in turns:

1. $N = 3n + 1$ and N is odd.

In this case it is easy to write down the ground state configurations and their energies. There are 5 regions, namely the ferromagnetic region, the (pseudo)antiferro states with the last spin pointing up, the (pseudo)$\uparrow\uparrow\downarrow$ state, antiferromagnetic in the last 4, and the two almost $\uparrow\uparrow\downarrow$ states with the one having the last spin pointing up and the other having the last spin pointing down. The states and their energies are tabulated in table 3.13. The energy differences between the states are given by

$$\begin{aligned}
\Delta_{ad} &= E_N^d - E_N^a = (N-7)(1-2j-h_z)/6\,, \\
\Delta_{db} &= E_N^b - E_N^d = 1-j-h_z\,, \\
\Delta_{bc} &= E_N^c - E_N^b = -j+h_z\,, \\
\Delta_{cd} &= E_N^d - E_N^c = -1+2j\,. \qquad (3.20)
\end{aligned}$$

We see from equation (3.20) that, for $N > 7$, $E_N^d > E_N^a$ when $2\,j + h_z < 1$, that is the state(s) with energy E_N^a is the ground state below the line $2\,j + h_z < 1$ while the state(s) with energy E_N^d is the ground state above the line. When $N = 7$, the state $\uparrow\downarrow\uparrow\downarrow\uparrow\downarrow\uparrow$ is actually translationally related to the state $\uparrow\uparrow\downarrow\uparrow\downarrow\uparrow\downarrow$ so that Δ_{ad} is identically zero for $N = 7$ and hence the line $2\,j + h_z = 1$ is absent from the phase diagram of the model for $N = 7$.

We note that $(N-7)/6 = (n-2)/2$ is a positive integer (since n is even) for $n > 2$. This means that the energy E_N^d can be reached by adding an integral multiple of $1-2j-h_z$ to the energy E_N^a. That is, the energy gap between E_N^a and its first excited state is $1-2j-2h_z$.

From equation (3.20), we see that Δ_{db} is independent of N and vanishes on the line $h_z + j = 1$. Similarly Δ_{bc} and Δ_{cd} do not depend on the chain length N. Δ_{bc} disappears on the line $h_z = j$ and Δ_{cd} vanishes on the line $j = 1/2$.

We can therefore conclude that whenever N has the form $N = 3\,n+1$, $n = 4, 6, 8, 10, 12, \ldots$, the critical lines of the one-dimensional longitudinal ANNNI model described by the Hamiltonian (3.1) are $2\,j + h_z = 1$, $h_z = j$, $h_z + 1 = j$, and $j = 1/2$.

2. $N = 3\,n + 1$ and N is even.

This situation is actually not very different from the case when N is odd, since the main point is that $N = 1 \mod 3$.

	Energy	State
E_N^a	$-\left(\frac{N-2}{4}\right)+\left(\frac{N-4}{4}\right)j-\frac{h_z}{2}$	$[\uparrow\downarrow\uparrow\downarrow\uparrow\downarrow\cdots\cdots\uparrow\downarrow\uparrow\downarrow\uparrow]$
E_N^b	$-\left(\frac{N-4}{12}\right)-\left(\frac{N-4}{12}\right)j-\left(\frac{N+2}{6}\right)h_z$	$[\uparrow\uparrow\downarrow\uparrow\uparrow\downarrow\uparrow\uparrow\downarrow\cdots\cdots\uparrow\uparrow\downarrow\uparrow\uparrow\downarrow\uparrow]$
E_N^c	$-\left(\frac{N-4}{12}\right)-\left(\frac{N+8}{12}\right)j-\left(\frac{N-4}{6}\right)h_z$	$[\uparrow\uparrow\downarrow\uparrow\uparrow\downarrow\uparrow\uparrow\downarrow\cdots\cdots\uparrow\uparrow\downarrow\uparrow\uparrow\downarrow\downarrow]$
E_N^d	$-\left(\frac{N+8}{12}\right)+\left(\frac{16-N}{12}\right)j-\left(\frac{N-4}{6}\right)h_z$	$[\uparrow\uparrow\downarrow\uparrow\uparrow\downarrow\uparrow\uparrow\downarrow\cdots\cdots\uparrow\uparrow\downarrow\uparrow\uparrow\downarrow\uparrow\downarrow\uparrow\downarrow]$
E_N^e	$\frac{N}{4}+\frac{Nj}{4}-\frac{Nh_z}{2}$	$\uparrow\uparrow\uparrow\uparrow\uparrow\uparrow\cdots\uparrow\uparrow\uparrow\uparrow\uparrow\uparrow\uparrow\uparrow$

Table 3.13: Ground state energies for the exact diagonalization of N spins fulfilling $N = 3\,n + 1$, $n = 2, 4, 6, 8, \ldots$. We note that because of the degeneracies, the states shown (together with their translationally invariant members) are only representative and not necessarily the only possible configurations. The classification by energy is therefore more reliable.

The first difference is that now we have a true antiferromagnetic region $\uparrow\downarrow\uparrow\downarrow \cdots \uparrow\downarrow$. Table 3.13 is still relevant, but we note that E_N^a is now given by

$$E_N^a = -\frac{N}{4} + \frac{Nj}{4} \; . \tag{3.21}$$

The energy difference between the antiferromagnetic states and the states with energy E_N^d is

$$\begin{aligned} \Delta_{ad} &= E_N^d - E_N^a \\ &= \frac{N-4}{6}\,(1 - 2j - h_z) \; . \end{aligned} \tag{3.22}$$

Again, as in the first case, we see that $(N-4)/6 = (n-1)/2$ is a positive integer for $n = 3, 5, 7, 9, \ldots$, so that the energy gap between the antiferromagnetic states and their first excited state is $1 - 2\,j - h_z$.

The mass gap vanishes on the line $2\,j + h_z = 1$, except when $N = 4$, for which the gap is identically zero.

The second difference between the situations $N = 3\,n+1$, N odd and $N = 3\,n+1$, N even comes when N is not only even, but also a multiple of 4. In this situation, an additional ground state candidate in the name of the period -4 antiphase states $\uparrow\uparrow\downarrow\downarrow \cdots\cdots \uparrow\uparrow\downarrow\downarrow$ emerges. It has the energy

$$E_N^e = -Nj/4 \; . \tag{3.23}$$

The energy difference between the antiphase states and the states with energy E_N^c in table 3.13 is

$$\begin{aligned} \Delta_{ce} &= E_N^e - E_N^c \\ &= \frac{N-4}{12}\,(1 - 2j + 2h_z) \\ &= \frac{n-1}{4}\,(1 - 2j - h_z) \; . \end{aligned} \tag{3.24}$$

This difference Δ_{ce} disappears on the line $2\,h_z + 1 = 2\,j$, except for $N = 4$ when it vanishes identically. Again, this explains why the line $2\,h_z + 1 = 2\,j$ is absent from the phase diagram of $N = 4$.

To summarize, we have found that for an arbitrary system size N of the form $N = 3\,n+1$,

the phase diagram of the one-dimensional longitudinal ANNNI model consists of 5 regions if N is not a multiple of 4 and 6 regions if N is a multiple of 4. The critical lines are $2\,j + h_z = 1$, $h_z = j$, $h_z + j = 1$ and $j = 1/2$. If N is also a multiple of 4, then the line $2\,h_z + 1 = 2\,j$ is also a critical line. The phase diagram of an arbitrarily long system of N spins$-1/2$ such that $N = 3\,n + 1$ is plotted in figure 3.15.

We now consider the second case when N is of the form $N = 3\,n + 2$. Again there are two possibilities: N is even ($n = 2, 4, 6, 8, \ldots$) or N is odd ($n = 1, 3, 5, \ldots$). In both situations, $N = 2$ mod 3. We consider both situations in turn.

1. $N = 3\,n + 2$ and N is odd.

   Exact diagonalization results allow us to deduce that there are 5 ground state energies, as tabulated in table 3.14.

   The energy differences are given by

$$\begin{aligned} \Delta_{ab} &= E_N^b - E_N^a \\ &= (N-5)\,(1 - 2j - h_z)\,/6 \end{aligned} \tag{3.25}$$

   and

$$\begin{aligned} \Delta_{bc} &= E_N^c - E_N^b \\ &= 1 - 2j + h_z\ . \end{aligned} \tag{3.26}$$

   We see from equations (3.25) and (3.26) that the critical lines for $N = 3\,n + 2$, $n = 3, 5, 7, 9, \ldots$, are $2\,j + h_z = 1$ and $2\,j - h_z = 1$. $n = 1$, (that is $N = 5$) is excluded for two reasons. First the state $\uparrow\downarrow\uparrow\downarrow\uparrow$ is translationally related to the state $\uparrow\uparrow\downarrow\uparrow\downarrow$ and hence Δ_{ab} is identically zero for $N = 5$. Secondly, the symmetry of the state with energy E_N^c requires that $N \geq 8$. This explains why there is only one ground state for $N = 5$.

2. $N = 3n + 2$ and N is even

   As in the case of $N = 3n + 1$, the ground state structure with $N = 3n + 2$ with N

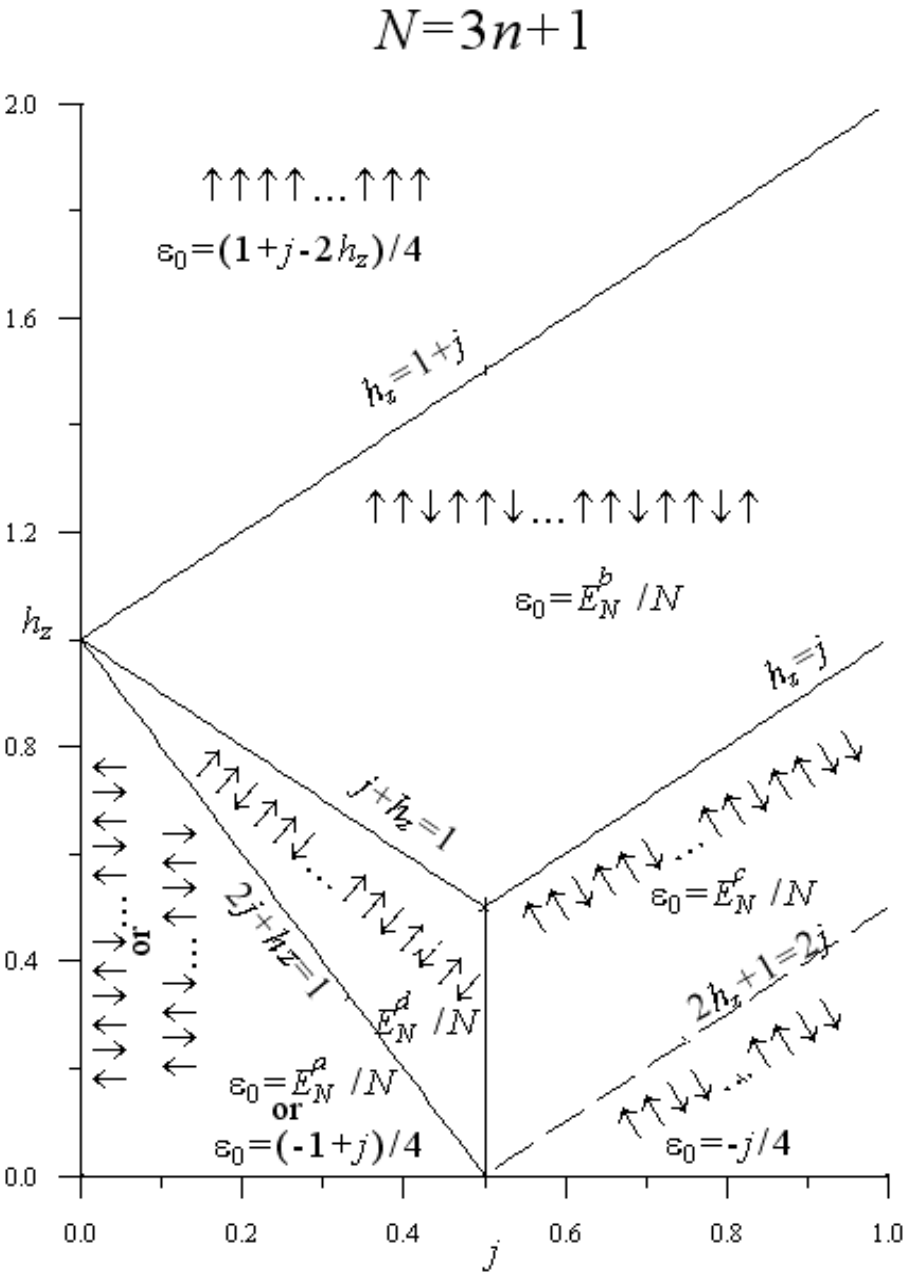

Figure 3.15: $T = 0$ phase diagram of the longitudinal ANNNI model for $N = 3\,n+1$. The dashed line is absent if N is not a multiple of 4. E_N^a etc. are as given in table 3.13

	Energy	State
E_N^a	$-\left(\frac{N-2}{4}\right)+\left(\frac{N-4}{4}\right)j-\frac{h_z}{2}$	$\uparrow\downarrow\uparrow\downarrow\uparrow\downarrow\cdots\uparrow\downarrow\uparrow\downarrow\uparrow$
E_N^b	$-\left(\frac{N+4}{12}\right)-\left(\frac{N-8}{12}\right)j-\left(\frac{N-2}{6}\right)h_z$	$\uparrow\uparrow\downarrow\uparrow\uparrow\downarrow\cdots\uparrow\uparrow\downarrow\uparrow\uparrow\downarrow\uparrow\downarrow$
E_N^c	$-\left(\frac{N-8}{12}\right)-\left(\frac{N+16}{12}\right)j-\left(\frac{N-8}{6}\right)h_z$	$\uparrow\uparrow\downarrow\uparrow\uparrow\downarrow\cdots\uparrow\uparrow\downarrow\uparrow\uparrow\downarrow\uparrow\uparrow\downarrow\uparrow\uparrow\downarrow\downarrow$
E_N^d	$-\left(\frac{N-8}{12}\right)-\left(\frac{N-8}{12}\right)j-\left(\frac{N+4}{6}\right)h_z$	$\uparrow\uparrow\downarrow\uparrow\uparrow\downarrow\cdots\uparrow\uparrow\downarrow\uparrow\uparrow\downarrow\uparrow\uparrow$
E_N^e	$\frac{N}{4}+\frac{Nj}{4}-\frac{Nh_z}{2}$	$\uparrow\uparrow\uparrow\uparrow\uparrow\uparrow\cdots\uparrow\uparrow\uparrow\uparrow\uparrow\uparrow\uparrow\uparrow$

Table 3.14: Ground state energies for the exact diagonalization of N spins fulfilling $N = 3\,n + 2$, $n = 1, 3, 5, 7, \ldots$

even is not different from that with N odd. The states are still as in table 3.14, but with true antiferromagnetic states with energy E_N^a now given by

$$E_N^a = -\frac{N}{4} + \frac{Nj}{4}\ . \tag{3.27}$$

The energy E_N^b remains as given in table 3.14, so that the energy difference is now

$$\begin{aligned}\Delta_{ab} &= E_N^b - E_N^a \\ &= (N-2)\,(1-2j-h_z)\,/6\ .\end{aligned} \tag{3.28}$$

$(N-2)/6 = n/2$ is an integer since n is even. As discussed above, this implies that the energy gap between the antiferromagnetic state and its first excited state is $1-2j-h_z$. This gap disappears on the critical line $2\,j + h_z = 1$.

If in addition to being even, N is also a multiple of 4, then the antiphase states also become contenders for the ground state. The antiphase energy $E_N^d = -N\,j/4$, together

with the energy E_N^c in table 3.14 give the energy difference

$$\begin{aligned}\Delta_{cd} &= E_N^d - E_N^c \\ &= \frac{N-8}{12}\,(1-2j+2h_z) \\ &= \frac{n-2}{4}\,(1-2j+2h_z)\ . \end{aligned} \tag{3.29}$$

Clearly $(n-2)/4$ is an integer whenever N is a multiple of 4 (that is whenever $n = 2, 6, 10, 14, 18, 22, \ldots$). Thus the ground state of the longitudinal ANNNI model is antiphase for $N = 3\,n+2$ below the line $2\,h_z = 2\,j-1$ and the state with energy E_N^c of table 3.14 above, whenever N is a multiple of 4. The case $N = 8$, corresponding to $n = 2$ is excluded because then Δ_{cd} becomes identically zero. This explains why the line $2\,h_z = 2\,j-1$ is absent from the phase diagram of the model for $N = 8$.

We are now in a position to draw the zero temperature phase diagram of the one-dimensional longitudinal ANNNI model for $N = 3\,n+2$. The different phases are exhibited in figure 3.16.

3.2.2 N a multiple of 3

Next we will study the phase transitions in the one dimensional longitudinal ANNNI model for the case 3 divides N.
Exact diagonalization results show that there are 4 ground state energies. The 4 lowest energies available to a chain of $N = 3n$ and the representative states are as tabulated in table 3.15

If N is odd, the energy differences are given by

$$\begin{aligned}\Delta_{ab} &= E_N^b - E_N^a \\ &= (N-3)\,(1-2j-h_z)\,/6 \\ &= (n-1)\,(1-2j-h_z)\,/2 \end{aligned} \tag{3.30}$$

and

$$\begin{aligned}\Delta_{bc} &= E_N^c - E_N^b \\ &= 1-2j+2h_z \end{aligned} \tag{3.31}$$

We see that for $N = 3n$, N odd, the lines $h_z = j+1$, $2j+h_z = 1$ and $2h_z+1 = 2j$ are critical lines for the model described by the Hamiltonian 3.1. We note that the line $2h_z+1 = 2j$ is

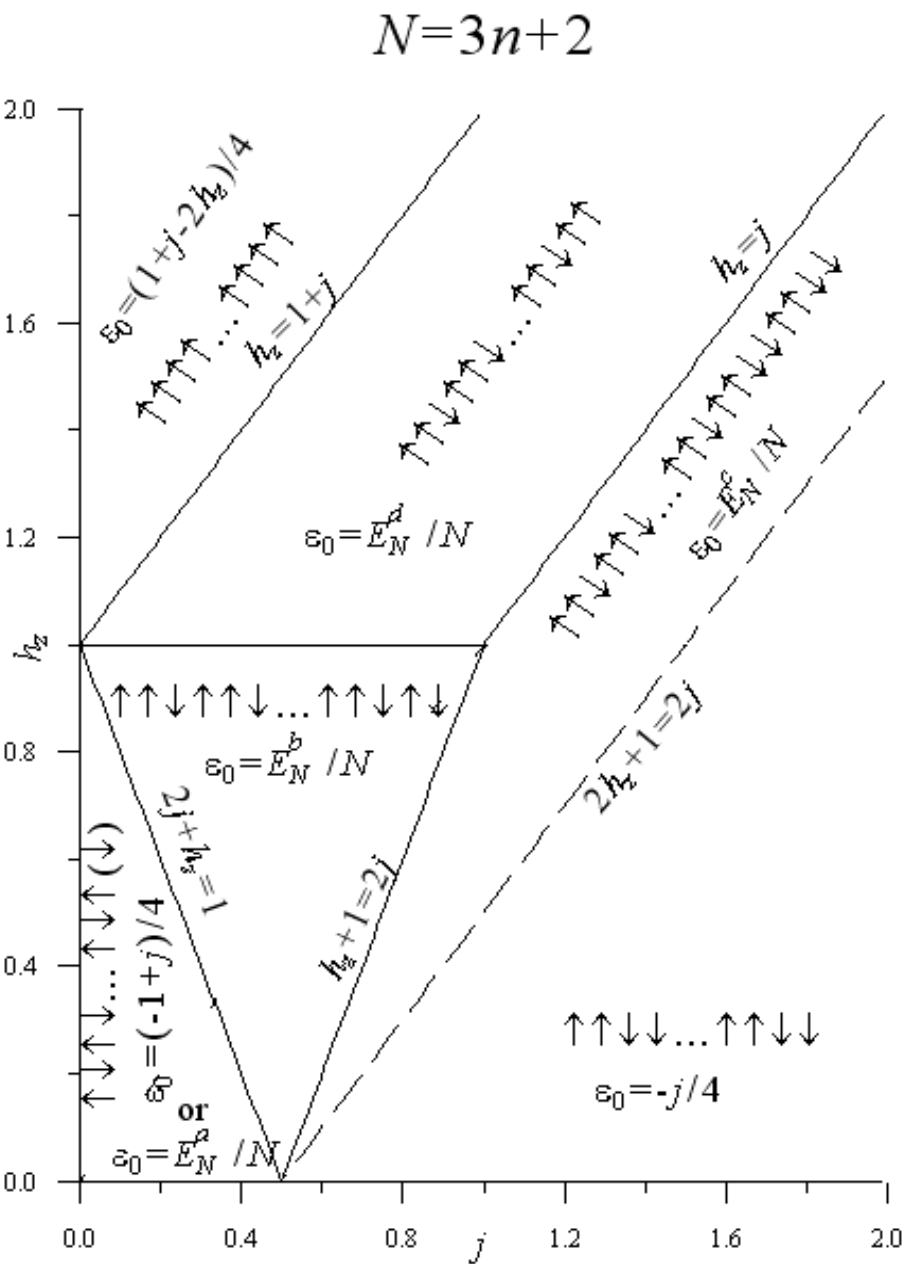

Figure 3.16: $T = 0$ phase diagram of the longitudinal ANNNI model for $N = 3\,n+2$. The dashed line is absent if N is not a multiple of 4

missing in the phase diagrams for $N = 6$ and for $N = 9$. The reason for this is that, as can be seen from the table, the symmetry of the states require that N be greater than 12.

If N is even, the energy differences are given by (table 3.15)

$$\begin{aligned}\Delta_{ab} &= E_N^b - E_N^a \\ &= N\left(1 - 2j - h_z\right)/6 \\ &= n\left(1 - 2j - h_z\right)/2 \end{aligned} \tag{3.32}$$

and

$$\begin{aligned}\Delta_{bc} &= E_N^c - E_N^b \\ &= 1 - 2j + 2h_z\ . \end{aligned} \tag{3.33}$$

Again, the critical lines are $h_z = 1 + j$, $2j + h_z = 1$ and $2h_z + 1 = 2j$.

If N is a multiple of 4, we have for the second energy difference,

$$\begin{aligned}\Delta_{bc} &= E_N^c - E_N^b \\ &= n(1 - 2j + 2h_z)/4\,, \end{aligned} \tag{3.34}$$

establishing the line $2h_z + 1 = 2j$.

The conclusion in this section is that when $N = 3n$, there are three critical lines $h_z = 1 + j$, $2j + h_z = 1$ and $2h_z + 1 = 2j$ and they are always present regardless of whether or not N is even or odd or a multiple of 4 (except the trivial cases $N = 6$ and $N = 9$ due to the aforementioned reasons). The phase diagram of $N = 3n$ is plotted in figure 3.17.

3.3 Exact Diagonalization of an Infinite System

We are now in a position to write down the ground state structures and their energies for the one-dimensional spin-1/2 ANNNI model in a longitudinal field. The role of the longitudinal field h_z is to break the all-spins inversion symmetry which the Hamiltonian (3.1) otherwise possesses. As mentioned earlier and proved in the appendix A, the inversion symmetry exists even in the presence of an external transverse magnetic field.

	Energy	State	Comment
E_N^a	$-\left(\frac{N-2}{4}\right)+\left(\frac{N-4}{4}\right)j-\frac{h_z}{2}$	$\uparrow\downarrow\uparrow\downarrow\uparrow\downarrow\cdots\uparrow\downarrow\uparrow\downarrow\uparrow$	N odd
	$-\frac{N}{4}+\frac{Nj}{4}$	$\uparrow\downarrow\uparrow\downarrow\uparrow\downarrow\cdots\uparrow\downarrow\uparrow\downarrow$	N even
E_N^b	$-\frac{N}{12}-\frac{Nj}{12}-\frac{Nh_z}{6}$	$\uparrow\uparrow\downarrow\uparrow\uparrow\downarrow\cdots\uparrow\uparrow\downarrow$	
E_N^c	$-\left(\frac{N-12}{12}\right)-\left(\frac{N+24}{12}\right)j-\left(\frac{N-12}{6}\right)h_z$	$\uparrow\uparrow\downarrow\uparrow\uparrow\downarrow\cdots\uparrow\uparrow\downarrow \mid \uparrow\uparrow\downarrow\downarrow\uparrow\uparrow\downarrow\downarrow\uparrow\uparrow\downarrow\downarrow$	
	$\frac{-Nj}{4}$	$\uparrow\uparrow\downarrow\downarrow\cdots\uparrow\uparrow\downarrow\downarrow\uparrow\uparrow\downarrow\downarrow$	4 divides N
E_N^d	$\frac{N}{4}+\frac{Nj}{4}-\frac{Nh_z}{2}$	$\uparrow\uparrow\uparrow\uparrow\ldots\uparrow\uparrow\uparrow\uparrow$	

Table 3.15: Ground state energies for the exact diagonalization of N spins fulfilling $N = 3\,n$, $n = 1, 2, 3, 4, \ldots$

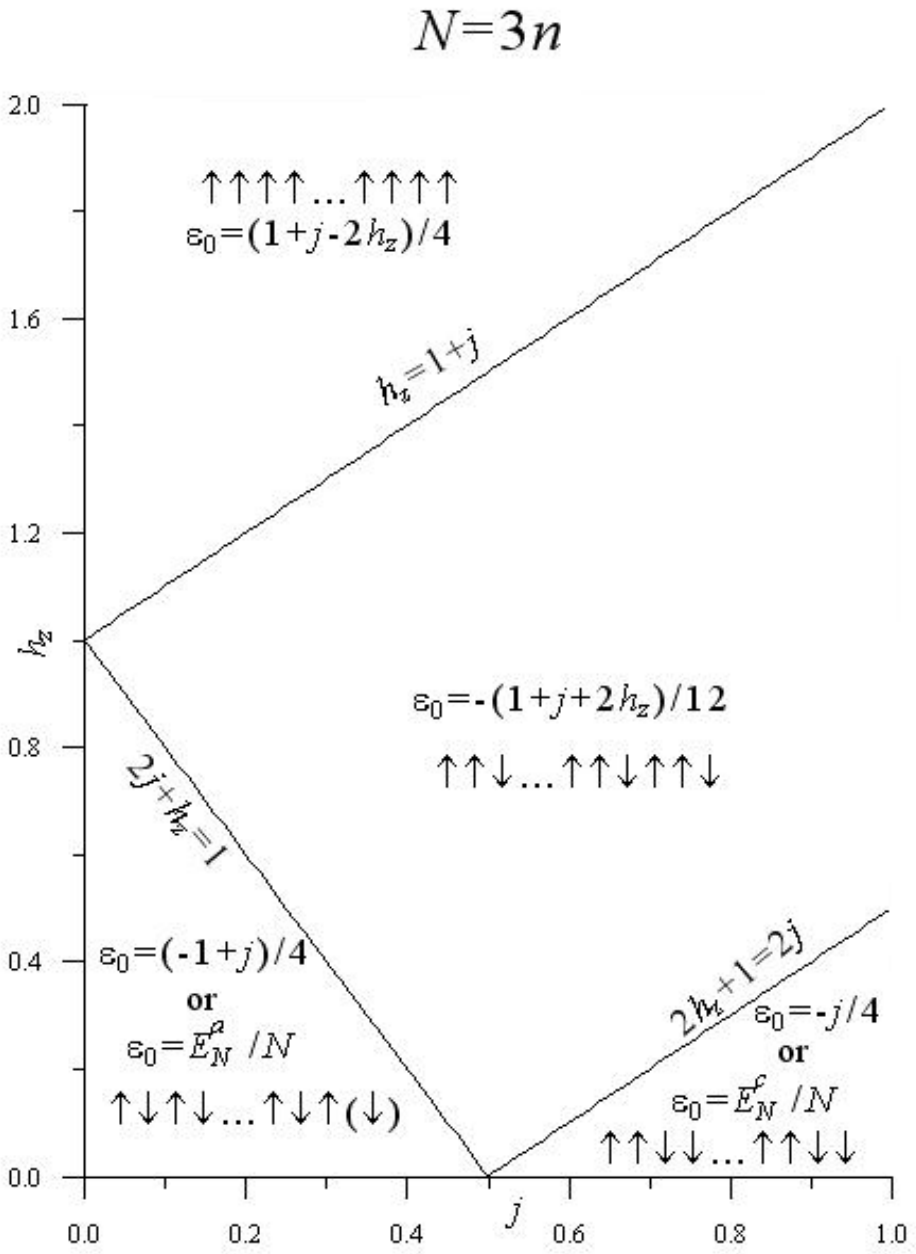

Figure 3.17: $T = 0$ phase diagram of the longitudinal ANNNI model for $N = 3n$.

The discussions of the penultimate section exhaust all possible one-dimensional lattice size N and we see from tables 3.13, 3.14 and 3.15 that in the thermodynamic limit $N \to \infty$, there are only 4 candidates for the ground state.

We have for the antiferromagnetic states

$$\lim_{N\to\infty} E_N^a/N = -(1-j)/4 \tag{3.35}$$

and

$$\lim_{N\to\infty} E_N^b/N = -(1+j+2h_z)/12 \tag{3.36}$$

for the 3-fold degenerate $\uparrow\uparrow\downarrow$ states.

The four-fold degenerate antiphase states have energy per spin given by

$$\lim_{N\to\infty} E_N^c/N = -j/4\ . \tag{3.37}$$

Lastly, the non-degenerate ferromagnetic state has ground state energy per spin

$$\lim_{N\to\infty} E_N^d/N = (1+j-2h_z)/4\ . \tag{3.38}$$

The phase boundaries separating these phases are as shown in figure 3.18.

Viewed as eigenstates of the direct product total S_z basis, the antiferromagnetic states cannot be more than 2-fold degenerate because they preserve the translation, reflection and inversion symmetries. The same argument holds for the four-fold degenerate antiphase states. The three-fold degenerate $\uparrow\uparrow\downarrow$ states do not preserve the inversion symmetry, but this is not a problem since the $\downarrow\downarrow\uparrow$ states that result after inversion are always higher in energy as long as h_z is finite.

3.4 Chapter Summary

The effect of an external longitudinal field h_z on the ground state structure of the ANNNI model has been investigated. In the absence of the field, there are only two possible configurations for the ground state of the ANNNI model: antiferromagnetic for values of the next nearest neighbour exchange interactions $j < 0.5$ and the four-fold degenerate antiphase states for $j > 0.5$. With the introduction of the field however, the story changed. Two new configurations

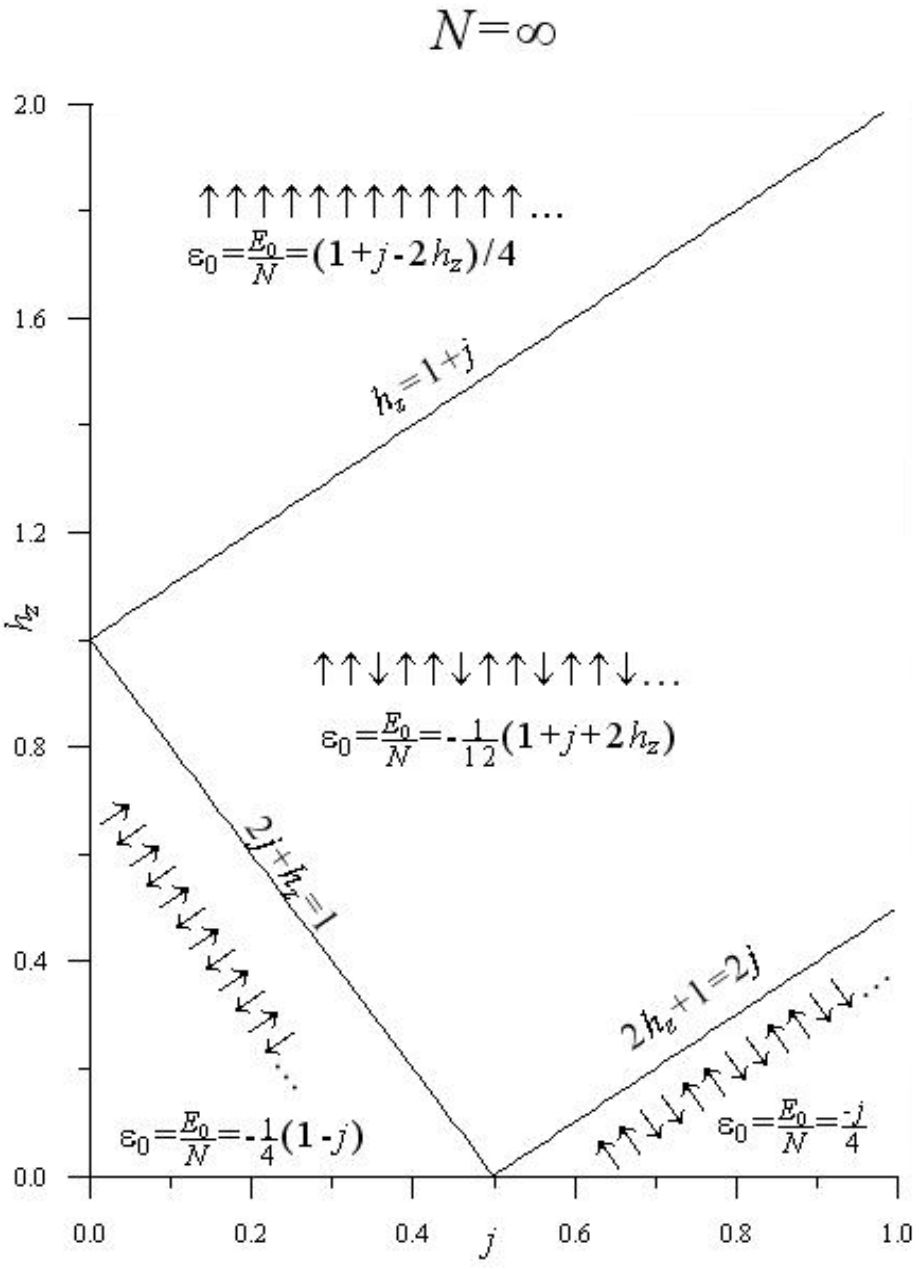

Figure 3.18: $T = 0$ phase diagram of the longitudinal ANNNI model.

emerged as contenders for the ground state structure in the thermodynamic limit. Using exact diagonalization of finite spin systems and deductions based on the results we have been able to establish that in the region bounded by the lines $h_z = 1 + j$, $2j + 1 = h_z$ and $2h_z + 1 = 2j$ the ground state is the three-fold degenerate $\uparrow\uparrow\downarrow$ alignment, with ground state energy per spin $\varepsilon_0 = -(1 + j + 2h_z)/12$. Above the line $h_z = 1 + j$ and bounded by the h_z axis in the $h_z - j$ plane, we found the ground state to be the non-degenerate allspins up ferromagnetic state with ground state energy per spin $\varepsilon_0 = (1 + j - 2h_z)/12$. We note that the external longitudinal field did more than simply breaking the inversion symmetry which the ANNNI model otherwise possessed. In fact the model studied here is antiferromagnetic, so that only an external field could have altered the ground state structure to become ferromagnetic. The $\uparrow\uparrow\downarrow$ state is even more interesting, in the sense that it is the ground state only if both the external longitudinal field h_z and the next nearest neighbour exchange interaction j are both finite. We also pointed out the tremendous simplifications which arise when the various symmetries of the Hamiltonian– reflection, translation and inversion are employed. It is hoped that these observations will be found useful in future research.

We wish to remark that results similar to ours have been obtained in the past by Morita and Horiguchi [58], [59]. Exact diagonalzations were however not performed in the said reference and the deep connectivity of the various symmetries were not discussed therein. The aim in the said paper was simply to give a proof of the spin orderings ot the one-dimensional ANNNI model in a field.

Having obtained the phase diagram of the longitudinal ANNNI model, we are now in a position to investigate the effect, on the phases, of frustration arising from the introduction of an external transverse field h_x. This will be the subject of investigation in the next chapter.

Chapter 4

Perturbation approach to the ANNNI model in mixed fields

We recall that the one dimensional ANNNI model in the presence of a perpendicular external magnetic field h_x and a longitudinal field h_z is described by the Hamiltonian

$$\begin{aligned} H &= \sum_i S_i^z S_{i+1}^z + j \sum_i S_i^z S_{i+2}^z - h_z \sum_i S_i^z - h_x \sum_i S_i^x \\ &= H_z + H_x \,, \end{aligned}$$

where

$$H_z = \sum_i S_i^z S_{i+1}^z + j \sum_i S_i^z S_{i+2}^z - h_z \sum_i S_i^z \tag{4.1}$$

and

$$H_x = -h_x \sum_i S_i^x \,. \tag{4.2}$$

The (sub)Hamiltonian H_z, describing the ANNNI model in a longitudinal field is diagonal in both the total S_z basis as well as in the eigenbases of the orthogonal subspaces of the translation operator. As discussed in chapter 3, the ground state of H_z is antiferromagnetic in the region bounded by $2j + h_z < 1$, the non-degenerate ferromagnetic state in the region bounded by the h_z axis and the line $h_z = j + 1$, the four-fold degenerate antiphase states in the region bounded by $2h_z + 1 = 2j$ and the j axis, and the three-fold degenerate $\uparrow\uparrow\downarrow$ in the region bounded by the three lines $2h_z + 1 = 2j$, $2j + h_z < 1$ and $h_z = 1 + j$. All this information is contained in figure 3.18.

In this chapter we will restrict ourselves to an even number N of spins. Since the ANNNI model in a longitudinal field is diagonal in the S_z and $\mathcal{T}$ bases, it is therefore natural to treat

$H_x = -h_x \sum_i S_i^x$ as a perturbation on H_z for $h_x < 1$.

In section 4.2 we will investigate the effect of h_x on the longitudinal ANNNI model in the region $2j + h_z < 1$. In section 4.3 we apply the perturbation treatment to the ferromagnetic ground state. In section 4.4, similar investigations will be made for the antiphase ground states, while the perturbation effects on the $\uparrow\uparrow\downarrow$ states will be examined in section 4.5

4.1 Feynman's theorem

Before continuing with obtaining the perturbation expansions, we shall first prove a useful theorem which is due to Feynman [60]. Hamiltonian (1.1) as a function of the parameters j, h_x and h_z (and the real use of the theorem will come when we introduce yet another parameter in the Hamiltonian) is in a very convenient form for the application of Feynman's theorem (also known in the literature as Feynman-Hellman theorem) to calculate various physical quantities such as the order parameters and the respective magnetic susceptibilities. The theorem states that: given the eigenvalue equation $H|\psi\rangle = E|\psi\rangle$ and with λ any of the parameters on which the Hamiltonian H depends, then

$$\frac{\partial E}{\partial \lambda} = \langle\psi| \frac{\partial H}{\partial \lambda} |\psi\rangle = \left\langle \frac{\partial H}{\partial \lambda} \right\rangle , \tag{4.3}$$

provided that $|\psi\rangle$ is a normalized eigenstate of H. The Feynman theorem is proved as follows: Since

$$E = \langle\psi| H |\psi\rangle \tag{4.4}$$

we have

$$\frac{\partial E}{\partial \lambda} = \langle\psi| \frac{\partial H}{\partial \lambda} |\psi\rangle + \left\langle \frac{\partial \psi}{\partial \lambda} \right| H |\psi\rangle + \langle\psi| H \left| \frac{\partial \psi}{\partial \lambda} \right\rangle . \tag{4.5}$$

But H is Hermitian, so that

$$\left\langle \psi \left| H \frac{\partial \psi}{\partial \lambda} \right\rangle = \left\langle H\psi \left| \frac{\partial \psi}{\partial \lambda} \right\rangle , \right. \tag{4.6}$$

and

$$\langle H\psi| = E\langle\psi| . \tag{4.7}$$

Therefore we can write

$$\frac{\partial E}{\partial \lambda} = \langle\psi| \frac{\partial H}{\partial \lambda} |\psi\rangle + E \left\langle \frac{\partial \psi}{\partial \lambda} \right| \psi\rangle + E \left\langle \psi \left| \frac{\partial \psi}{\partial \lambda} \right\rangle . \right. \tag{4.8}$$

The last two terms cancel each other, since

$$E\left\langle \frac{\partial\psi}{\partial\lambda} \,\middle|\, \psi \right\rangle + E\left\langle \psi \,\middle|\, \frac{\partial\psi}{\partial\lambda} \right\rangle = E\frac{\partial}{\partial\lambda}\langle\psi \mid \psi\rangle = E\frac{\partial}{\partial\lambda}(1) = 0\ . \tag{4.9}$$

We have thus proved that

$$\frac{\partial E}{\partial\lambda} = \langle\psi|\,\frac{\partial H}{\partial\lambda}\,|\psi\rangle \tag{4.10}$$

whenever $H\,|\psi\rangle = E\,|\psi\rangle$ and $\langle\psi \mid \psi\rangle = 1$.
In Feynman's own words:

> Equation (4.10) is true, regardless of the nature of H, (whether for spin, or nuclear forces, etc.)

4.2 The antiferromagnetic ground state

Our exact diagonalization results show that the ground state of H_z in the region $2j + hz < 1$ consists of the two-fold degenerate antiferromagnetic states. We will denote these states by $|AF^+\rangle$ and $|AF^-\rangle$, where

$$\left|AF^+\right\rangle = |+-+-\cdots+-+-\rangle \tag{4.11a}$$

and

$$\left|AF^-\right\rangle = |-+-+\cdots-+-+\rangle\ . \tag{4.11b}$$

The degenerate antiferromagnetic ground state energy is

$$E^{(0)}_{AF^+} = E^{(0)}_{AF^-} = -\tfrac{N}{4}(1-j)\ . \tag{4.12}$$

In order to facilitate the calculation of physical quantities like the order parameter and the associated susceptibility, we introduce a field $\alpha > 0$ and write the unperturbed Hamiltonian H_z (4.1) as

$$H_z = \sum_{i=1}^{N} S^z_i S^z_{i+1} + j\sum_{i=1}^{N} S^z_i S^z_{i+2} - h_z\sum_{i=1}^{N} S^z_i - \alpha\sum_{i=1}^{N/2}(S^z_{2i-1} - S^z_{2i})\ . \tag{4.13}$$

This way, it will then be possible to compute the long range antiferromagnetic order (staggered magnetization) ρ_{AF} and the susceptibility χ_{AF} from

$$\rho_{AF} = -\frac{2}{N}\left.\frac{\partial E_{AF}(\alpha)}{\partial \alpha}\right|_{\alpha=0} \tag{4.14}$$

and

$$\chi_{AF} = -\frac{2}{N}\left.\frac{\partial^2 E_{AF}(\alpha)}{\partial \alpha^2}\right|_{\alpha=0} . \tag{4.15}$$

We note that the introduction of α breaks the translational invariance symmetry and thus removes the ground state degeneracy, now giving

$$E^{(0)}_{AF^{\pm}} = -N(1 - j \pm 2\alpha)/4\,, \tag{4.16}$$

with $E^{(0)}_{AF^+}$ being the non-degenerate ground state energy belonging to the state $|AF^+\rangle = |+-+-+-\cdots+-\rangle$.

4.2.1 Energy corrections

First order correction

Since the degeneracy remains at $\alpha = 0$ we will apply degenerate perturbation theory to obtain the corrections to the ground state energy.

The operator $H_x = -\sum_{i=1}^{N} S_i^x$, acting on an eigenstate of total S_z generates a linear combination of N states with the ith spin flipped in the ith member, with each spin flip costing ± 1 in the total S_z quantum number of the ith member state. This means that a necessary (but not sufficient) condition for the matrix element of H_x between any two states $|a\rangle$ and $|b\rangle$ not to vanish is that the absolute value of the total S_z quantum number of $|a\rangle$ and that of $|b\rangle$ must be 1. That is

$$\langle b|\, H_x\, |a\rangle = 0 \tag{4.17a}$$

whenever

$$|S_z(|a\rangle) - S_z(|b\rangle)| \neq 1\,, \tag{4.17b}$$

where $|a\rangle$ and $|b\rangle$ are eigenstates of total S_z. In particular

$$\langle a|\, H_x\, |a\rangle = 0 \tag{4.18}$$

for any $|a\rangle$ an eigenstate of S_z.

To first order in h_x, the perturbation matrix, V, of H_x is

$$V = \begin{pmatrix} \langle AF^+| H_x |AF^+\rangle & \langle AF^+| H_x |AF^-\rangle \\ \\ \langle AF^-| H_x |AF^+\rangle & \langle AF^-| H_x |AF^-\rangle \end{pmatrix}, \tag{4.19}$$

and since both $|AF^+\rangle$ and $|AF^-\rangle$ are total $S_z = 0$ states, it follows from (4.17) that V is a null matrix, so that there is no first order correction to the antiferromagnetic ground state energy.

Second order correction

The 2×2 perturbation matrix for the second order correction to the ground state energy has elements

$$V_{11} = \sum_m \frac{\langle AF^+| H_x |m\rangle \langle m| H_x |AF^+\rangle}{E^{(0)}_{AF} - E^{(0)}_m},$$
$$V_{12} = \sum_m \frac{\langle AF^+| H_x |m\rangle \langle m| H_x |AF^-\rangle}{E^{(0)}_{AF} - E^{(0)}_m},$$
$$V_{21} = \sum_m \frac{\langle AF^-| H_x |m\rangle \langle m| H_x |AF^+\rangle}{E^{(0)}_{AF} - E^{(0)}_m}$$

and

$$V_{22} = \sum_m \frac{\langle AF^-| H_x |m\rangle \langle m| H_x |AF^-\rangle}{E^{(0)}_{AF} - E^{(0)}_m}. \tag{4.20}$$

Each of the summations over m above extends over the total S_z direct-product basis states $|m\rangle$ of the Hamiltonian, but excluding the states $|AF^+\rangle$ and $|AF^-\rangle$.

By inspection of the definitions (4.11), it is clear that any state whose H_x matrix element with $|AF^-\rangle$ does not vanish must have a vanishing matrix element with $|AF^+\rangle$ and vice versa.

That is

$$\langle AF^-| H_x |m\rangle = 0 \text{ whenever } \langle AF^+| H_x |m\rangle \neq 0$$

and

$$\langle AF^+| H_x |m\rangle = 0 \text{ whenever } \langle AF^-| H_x |m\rangle \neq 0 \tag{4.21}$$

for any $|m\rangle$ in the Hilbert space of H.

The conditions in (4.21) imply that the off-diagonal matrix elements V_{12} and V_{21} are zero.

In V_{11}, there are only N non-vanishing matrix elements $\langle m| H_x |AF^+\rangle$ contributed by states $|m\rangle$ such that

$$|m\rangle \in \{|--+-+-\cdots+-\rangle, |+++-+-\cdots+-\rangle, \cdots, |+-+-\cdots++\rangle\} \ . \tag{4.22}$$

$N/2$ of these states (corresponding to $N/2-1$ configurations with 3 consecutive spins down and 1 configuration with first two spins up and the last spin up, with total $S_z(|m\rangle) = -1$) contribute

$$\frac{N}{2}\frac{h_x^2}{4}\frac{-1}{1-j+\alpha+h_z} \tag{4.23}$$

to V_{11} while $N/2$ states (corresponding to $N/2-1$ states with 3 consecutive spins up and 1 configuration with first two spins down and the last spin down, with total $S_z(|m\rangle) = +1$) contribute

$$\frac{N}{2}\frac{h_x^2}{4}\frac{-1}{1-j+\alpha-h_z} \ . \tag{4.24}$$

The diagonal element V_{11} therefore evaluates to

$$V_{11} = -\frac{Nh_x^2}{8}\left(\frac{1}{1-j+\alpha+h_z}+\frac{1}{1-j+\alpha-h_z}\right) \ . \tag{4.25}$$

Similarly, we have

$$V_{22} = -\frac{Nh_x^2}{8}\left(\frac{1}{1-j-\alpha+h_z}+\frac{1}{1-j-\alpha-h_z}\right) \ . \tag{4.26}$$

In the limit $\alpha \to 0$, V_{11} and V_{22} give the second order corrections to the antiferromagnetic ground state energy to be

$$\begin{aligned} E^{(2)}_{AF^+} = E^{(2)}_{AF^-} &= -\frac{Nh_x^2}{8}\left(\frac{1}{1-j+h_z}+\frac{1}{1-j-h_z}\right) \\ &= -\frac{Nh_x^2}{4}\frac{(1-j)}{(1-j)^2-h_z^2} \ . \end{aligned} \tag{4.27}$$

We see that, to second order in perturbation, the degeneracy in the ground state energy is not lifted by the application of an external magnetic field h_x. This is probably a manifestation of the translational invariance which exists for $\alpha = 0$. As shown in Appendix A, translation invariance

is a symmetry of our general Hamiltonian (1.1), even in the presence of an external transverse magnetic field. One should therefore expect the two-fold degeneracy of the antiferromagnetic states to remain to any order in perturbation. This is in fact known to be the case in the thermodynamic limit, at least for the transverse Ising model ($j = 0 = h_z$) for $h_x < \frac{1}{2}$ [3].

As expected, the second order correction to the ground state energy (equation (4.27)) is negative since $1 - j > 0$ (because $2j + h_z < 1$) and $(1-j)^2 - h_z^2 = (1 - j - h_z)(1 - j + h_z)$ is clearly a positive quantity in the region $2j - h_z < 1$ for which the perturbation is carried out ($2j + h_z < 1 \Rightarrow 1 - j > j + h_z \Rightarrow 1 - j > \pm h_z$ since $j, h_z > 0$).

From (4.12) and (4.27) we have that the antiferromagnetic ground state energy to second order in h_x is given by

$$E_{AF} = -\frac{N(1-j)}{4}\left(1 + \frac{h_x^2}{(1-j)^2 - h_z^2}\right) . \tag{4.28}$$

So that the antiferromagnetic ground state energy per spin is

$$\varepsilon_{AF} = -\frac{(1-j)}{4}\left(1 + \frac{h_x^2}{(1-j)^2 - h_z^2}\right) . \tag{4.29}$$

From (4.16) and (4.25) we have

$$E_{AF^+}(\alpha) = -\frac{N(1-j+2\alpha)}{4} - \frac{Nh_x^2}{4}\frac{1-j+\alpha}{(1-j+\alpha)^2 - h_z^2} , \tag{4.30}$$

where for the sake of definiteness we have taken $|AF^+\rangle = |+-+-+-\cdots+-\rangle$ as the definition of the antiferromagnetic ground state. Results for $|AF^-\rangle$ can be obtained from those for $|AF^+\rangle$ by replacing α with $-\alpha$.

The staggered magnetization is then obtained as

$$\begin{aligned}\rho_{AF^+} &= -\frac{2}{N}\frac{\partial}{\partial\alpha}\left(E_{AF^+}(\alpha)\right)\Big|_{\alpha=0} \\ &= 1 + \frac{1}{2}\frac{h_x^2}{(1-j)^2 - h_z^2}\left(1 - \frac{2(1-j)}{(1-j)^2 - h_z^2}\right) .\end{aligned} \tag{4.31}$$

We observe that

$$\frac{(1-j)}{(1-j)^2 - h_z^2} = \frac{1}{1-j}\left(\frac{1}{1 - \frac{h_z}{(1-j)^2}}\right) > 1 , \tag{4.32}$$

so that $\rho_{AF^+} < 1$ which is consistent with the requirement that the staggered magnetization attain its maximum value of unity in zero external transverse field.

The magnetic susceptibility is obtained from equation (4.15) as

$$\chi_{AF^+} = -\frac{h_x^2(1-j)}{((1-j)^2-h_z^2)^2}\left(3-\frac{4(1-j)^2}{(1-j)^2-h_z^2}\right) . \tag{4.33}$$

We notice that the bracketed term is always negative, which means that χ_{AF^+} is always a positive quantity. This is consistent with the inequality proved by Ferrell [61, 62] for a Hamiltonian with a linear dependence on a parameter λ for the ground state energy, namely that

$$\frac{\partial^2 E}{\partial \lambda^2} \leq 0 . \tag{4.34}$$

Third order correction

The third order correction to the ground state energy contains terms of the form

$$E^{(3)}_{AF^+} = \sum_{k,m} \frac{\langle AF^+| H_x |m\rangle \langle m| H_x |k\rangle \langle k| H_x |AF^+\rangle}{(E_{AF^+}-E_m)(E_{AF^+}-E_k)} - \left\langle AF^+\right| H_x \left|AF^+\right\rangle \sum_m \frac{|\langle AF^+| H_x |m\rangle|^2}{(E_{AF^+}-E_m)^2} . \tag{4.35}$$

First we note that the second term in the above sum vanishes because of (4.18). Also, when $k = m$ in the above sum, the first sum contains $\langle m| H_x |m\rangle$ which is zero for the same reason. If we now consider terms in the first sum such that $k \neq m$ we have the following situations

$$\left\langle AF^+\right| H_x |m\rangle \neq 0 \Rightarrow S_z(|m\rangle) = \pm 1 \tag{4.36a}$$

and

$$\langle k| H_x \left|AF^+\right\rangle \neq 0 \Rightarrow S_z(|k\rangle) = \pm 1 . \tag{4.36b}$$

If the above set of equations hold, then we have

$$|S_z(|m\rangle) - S_z(|k\rangle)| = 0 \text{ or } 2 \tag{4.37}$$

For the first sum in equation (4.35) not to vanish, we must have, for every m and k :

$$\langle m| H_x |k\rangle \neq 0 . \tag{4.38}$$

This is possible only if (4.17)

$$|S_z(|m\rangle) - S_z(|k\rangle)| = 1 , \tag{4.39}$$

which contradicts equation (4.37).

We therefore have that

$$E^{(3)}_{AF^+} = 0\,. \tag{4.40}$$

In fact, it is clear there can be no odd-order contributions to the energy corrections due to the following reason. The lead sum in mth order perturbation has a product of m matrix elements in the numerator for any combination of the summation indices. If m is odd, then if the first $(m-1)/2$ matrix elements, as well as the last $(m-1)/2$ matrix elements are non-vanishing, then the remaining matrix element (in the $(m+1)/2$ position) has the form $\langle r|\, H_x\, |s\rangle$ such that

$$S_z(|r\rangle) = \pm S_z(|s\rangle) = \pm\frac{m-1}{2}\,. \tag{4.41}$$

This matrix element $\langle r|\, H_x\, |s\rangle$ will therefore be zero by virtue of (4.17).
The remaining terms in the expression for the mth order correction to the energy will be proportional to odd order correction terms and hence will vanish on account of this present arguement.

Fourth order correction

The fourth order correction to the antiferromagnetic energy is given by

$$\begin{aligned} E^{(4)}_{AF^+} = &\sum_{ijk} \frac{\langle AF^+|\, H_x\, |i\rangle\, \langle i|\, H_x\, |j\rangle\, \langle j|\, H_x\, |k\rangle\, \langle k|\, H_x\, |AF^+\rangle}{(E^{(0)}_{AF^+} - E^{(0)}_i)(E^{(0)}_{AF^+} - E^{(0)}_j)(E^{(0)}_{AF^+} - E^{(0)}_k)} \\ &- E^{(2)}_{AF^+} \sum_k \frac{\langle AF^+|\, H_x\, |k\rangle\, \langle k|\, H_x\, |AF^+\rangle}{(E^{(0)}_{AF^+} - E^{(0)}_k)^2}\,. \end{aligned} \tag{4.42}$$

If $\{|a_r\rangle\,, r = 1, 2, \ldots, N\}$ be the set of states with non-vanishing matrix element with $|AF^+\rangle$, that is, such that

$$\left\langle AF^+\right|\, H_x\, |a_r\rangle \neq 0\,, \tag{4.43}$$

then the expression for $E^{(4)}_{AF^+}$ simplifies to

$$\begin{aligned} E^{(4)}_{AF^+} = &\sum_{rs} \left(\frac{\langle AF^+|\, H_x\, |a_r\rangle\, \langle a_s|\, H_x\, |AF^+\rangle}{(E^{(0)}_{AF^+} - E^{(0)}_{a_r})(E^{(0)}_{AF^+} - E^{(0)}_{a_s})} \sum_j \frac{\langle a_r|\, H_x\, |j\rangle\, \langle j|\, H_x\, |a_s\rangle}{E^{(0)}_{AF^+} - E^{(0)}_j} \right) \\ &- E^{(2)}_{AF^+} \sum_r \frac{|\langle AF^+|\, H_x\, |a_r\rangle|^2}{(E^{(0)}_{AF^+} - E^{(0)}_{a_r})^2}\,. \end{aligned} \tag{4.44}$$

A Maple procedure which evaluates the above sums was written and is included in Appendix B. The first sum evaluates to

$$\begin{aligned}
&\sum_{rs}\left(\frac{\langle AF^+|\,H_x\,|a_r\rangle\,\langle a_s|\,H_x\,|AF^+\rangle}{(E^{(0)}_{AF^+}-E^{(0)}_{a_r})(E^{(0)}_{AF^+}-E^{(0)}_{a_s})}\sum_j\frac{\langle a_r|\,H_x\,|j\rangle\,\langle j|\,H_x\,|a_s\rangle}{E^{(0)}_{AF^+}-E^{(0)}_j}\right)=\\
&\frac{Nh_x^4}{32}\frac{1}{(-1+j-\alpha-h_z)^2}\left\{\frac{2}{-1+2j-2\alpha}+\frac{N/4-1}{-1+j-\alpha}+\frac{N/4-3/2}{-1+j-h_z-\alpha}+\frac{2}{-2+j-2\alpha-2h_z}\right\}\\
&+\frac{Nh_x^4}{32}\frac{1}{(-1+j-\alpha+h_z)^2}\left\{\frac{2}{-1+2j-2\alpha}+\frac{N/4-1}{-1+j-\alpha}+\frac{N/4-3/2}{-1+j+h_z-\alpha}+\frac{2}{-2+j-2\alpha+2h_z}\right\}\\
&+\frac{Nh_x^4}{16}\left\{\frac{1}{(-1+j-\alpha+h_z)^2(-2+j-2\alpha+2h_z)}+\frac{1}{(-1+j-\alpha-h_z)^2(-2+j-2\alpha-2h_z)}\right\}\\
&+\frac{N(N-6)h_x^4}{128}\left\{\frac{1}{(-1+j-\alpha+h_z)^3}+\frac{1}{(-1+j-\alpha-h_z)^3}\right\}\\
&+\frac{Nh_x^4}{16}\frac{1}{(-1+j-\alpha-h_z)(-1+j-\alpha+h_z)}\left\{\frac{N/4-1}{-1+j-\alpha}+\frac{2}{-1+2j-2\alpha}\right\}, \qquad (4.45)
\end{aligned}$$

while the second sum yields

$$\begin{aligned}
&-E^{(2)}_{AF^+}\sum_r\frac{|\langle AF^+|\,H_x\,|a_r\rangle|^2}{(E^{(0)}_{AF^+}-E^{(0)}_r)^2}\\
&=-\frac{N^2h_x^4}{64}\left(\frac{1}{(-1+j-\alpha+h_z)^2}+\frac{1}{(-1+j-\alpha-h_z)^2}\right)\left(\frac{1}{(-1+j-\alpha+h_z)}+\frac{1}{(-1+j-\alpha-h_z)}\right). \qquad (4.46)
\end{aligned}$$

Substituting (4.45) and (4.46) for the sums in equation (4.44), and noting that the terms proportional to N^2 cancel out, we have

$$\begin{aligned}
E^{(4)}_{AF^+}=&\frac{Nh_x^4}{32}\frac{1}{(-1+j-\alpha-h_z)^2}\left\{\frac{2}{-1+2j-2\alpha}+\frac{1}{1-j+\alpha}+\frac{3/2}{1-j+h_z+\alpha}-\frac{2}{2-j+2\alpha+2h_z}\right\}\\
&+\frac{Nh_x^4}{32}\frac{1}{(-1+j-\alpha+h_z)^2}\left\{\frac{2}{-1+2j-2\alpha}+\frac{1}{1-j+\alpha}+\frac{3/2}{1-j-h_z+\alpha}-\frac{2}{2-j+2\alpha-2h_z}\right\}\\
&-\frac{Nh_x^4}{16}\frac{1}{(-1+j-\alpha-h_z)(-1+j-\alpha+h_z)}\left\{\frac{1}{-1+j-\alpha}-\frac{2}{-1+2j-2\alpha}\right\}\\
&+\frac{Nh_x^4}{16}\left\{\frac{1}{(-1+j-\alpha+h_z)^2(-2+j-2\alpha+2h_z)}+\frac{1}{(-1+j-\alpha-h_z)^2(-2+j-2\alpha-2h_z)}\right\}\\
&-\frac{3Nh_x^4}{64}\left\{\frac{1}{(-1+j-\alpha+h_z)^3}+\frac{1}{(-1+j-\alpha-h_z)^3}\right\}. \qquad (4.47)
\end{aligned}$$

Substituting $\alpha = 0$ in (4.47) and dividing by N, we find the fourth order correction to the antiferromagnetic ground state energy per spin to be

$$\begin{aligned}
\varepsilon^{(4)}_{AF^+} &= \frac{h_x^4}{32}\frac{1}{(-1+j-h_z)^2}\left\{\frac{2}{-1+2j}+\frac{1}{1-j}+\frac{3/2}{1-j+h_z}-\frac{2}{2-j+2h_z}\right\} \\
&+ \frac{h_x^4}{32}\frac{1}{(-1+j+h_z)^2}\left\{\frac{2}{-1+2j}+\frac{1}{1-j}+\frac{3/2}{1-j-h_z}-\frac{2}{2-j-2h_z}\right\} \\
&- \frac{h_x^4}{16}\frac{1}{(-1+j-h_z)(-1+j+h_z)}\left\{\frac{1}{-1+j}-\frac{2}{-1+2j}\right\} \\
&+ \frac{h_x^4}{16}\left\{\frac{1}{(-1+j+h_z)^2(-2+j+2h_z)}+\frac{1}{(-1+j-h_z)^2(-2+j-2h_z)}\right\} \\
&- \frac{3h_x^4}{64}\left\{\frac{1}{(-1+j+h_z)^3}+\frac{1}{(-1+j-h_z)^3}\right\}. \qquad (4.48)
\end{aligned}$$

From equations (4.16), (4.25) and (4.47), we have

$$\begin{aligned}
\varepsilon_{AF^+}(\alpha,j,h_x,h_z) &= -\frac{(1-j+2\alpha)}{4} - \frac{h_x^2}{8}\left\{\frac{1}{1-j+\alpha+h_z}+\frac{1}{1-j+\alpha-h_z}\right\} \\
&+ \frac{h_x^4}{32}\frac{1}{(-1+j-\alpha-h_z)^2}\left\{\frac{2}{-1+2j-2\alpha}+\frac{1}{1-j+\alpha}+\frac{3/2}{1-j+h_z+\alpha}-\frac{2}{2-j+2\alpha+2h_z}\right\} \\
&+ \frac{h_x^4}{32}\frac{1}{(-1+j-\alpha+h_z)^2}\left\{\frac{2}{-1+2j-2\alpha}+\frac{1}{1-j+\alpha}+\frac{3/2}{1-j-h_z+\alpha}-\frac{2}{2-j+2\alpha-2h_z}\right\} \\
&- \frac{h_x^4}{16}\frac{1}{(-1+j-\alpha-h_z)(-1+j-\alpha+h_z)}\left\{\frac{1}{-1+j-\alpha}-\frac{2}{-1+2j-2\alpha}\right\} \\
&+ \frac{h_x^4}{16}\left\{\frac{1}{(-1+j-\alpha+h_z)^2(-2+j-2\alpha+2h_z)}+\frac{1}{(-1+j-\alpha-h_z)^2(-2+j-2\alpha-2h_z)}\right\} \\
&- \frac{3h_x^4}{64}\left\{\frac{1}{(-1+j-\alpha+h_z)^3}+\frac{1}{(-1+j-\alpha-h_z)^3}\right\}. \qquad (4.49)
\end{aligned}$$

The antiferromagnetic ground state energy per spin, to the fourth order in h_x is therefore given by

$$\begin{aligned}\varepsilon_{AF^+}(0,j,h_x,h_z) = &-\frac{(1-j)}{4} - \frac{h_x^2}{8}\left\{\frac{1}{1-j+h_z}+\frac{1}{1-j-h_z}\right\} \\ &+\frac{h_x^4}{32}\frac{1}{(-1+j-h_z)^2}\left\{\frac{2}{-1+2j}+\frac{1}{1-j}+\frac{3/2}{1-j+h_z}-\frac{2}{2-j+2h_z}\right\} \\ &+\frac{h_x^4}{32}\frac{1}{(-1+j+h_z)^2}\left\{\frac{2}{-1+2j}+\frac{1}{1-j}+\frac{3/2}{1-j-h_z}-\frac{2}{2-j-2h_z}\right\} \\ &-\frac{h_x^4}{16}\frac{1}{(-1+j-h_z)(-1+j+h_z)}\left\{\frac{1}{-1+j}-\frac{2}{-1+2j}\right\} \\ &+\frac{h_x^4}{16}\left\{\frac{1}{(-1+j+h_z)^2(-2+j+2h_z)}+\frac{1}{(-1+j-h_z)^2(-2+j-2h_z)}\right\} \\ &-\frac{3h_x^4}{64}\left\{\frac{1}{(-1+j+h_z)^3}+\frac{1}{(-1+j-h_z)^3}\right\} . \end{aligned} \tag{4.50}$$

The simplest case of equation (4.50) is the transverse Ising model, $h_z = 0 = j$, and the ground state energy per spin is

$$\varepsilon_{AF^+} = -\frac{1}{4} - \frac{h_x^2}{4} - \frac{h_x^4}{16} . \tag{4.51}$$

The exact ground state energy per spin of the transverse Ising model is ([15, 63, 64]

$$\begin{aligned}\frac{E_0}{N} &= -\frac{(1+2h_x)}{2\pi}\mathcal{E}\left(\frac{\sqrt{8h_x}}{(1+2h_x)}\right) \\ &= -\frac{1}{4} - \frac{h_x^2}{4} - \frac{h_x^4}{16} + \mathrm{O}(h_x^6) . \end{aligned} \tag{4.52}$$

Thus we see that the perturbation expansion (4.51) gives the correct energy per spin for the Ising model in a transverse field to the fourth order in h_x.

4.3 The ferromagnetic ground state

The ground state of the longitudinal ANNNI model (4.1) is the non-degenerate allspins-up ferromagnetic state in the region bounded by the h_z axis and the line $h_z = 1 + j$ in the $h_z - j$ plane. That is, the unperturbed ground state is

$$|F\rangle = |+++++\cdots++\rangle , \tag{4.53}$$

with corresponding energy

$$E_F^{(0)} = \frac{N(1+j)}{4} - \frac{Nh_z}{2} . \tag{4.54}$$

We note that the ground state is ferromagnetic only for finite h_z, this is in contrast to the situation in a ferromagnetic model. The inversion symmetry which makes the allspins up and allspins down state to be degenerate is removed by the presence of a finite longitudinal field, h_z, so that the ground state is the allspins up nondegenerate state in the indicated region. The longitudinal field h_z however does not break the translational invariance symmetry of the Hamiltonian. We see also that the presence of h_z makes the Hamiltonian to already be in a form where can apply the Feynman technique directly to calculate the various physical quantities. We recall

$$H = H_z + H_x \,, \tag{4.55}$$

where

$$H_z = \sum_i S_i^z S_{i+1}^z + \sum_i S_i^z S_{i+2}^z - h_z \sum_i S_i^z \tag{4.56}$$

and

$$H_x = -h_x \sum_i S_i^x \ . \tag{4.57}$$

4.3.1 Energy corrections

The first order correction $E_F^{(0)}$ to the ferromagnetic ground state energy is

$$E_F^{(0)} = \langle F | \, H_x \, | F \rangle \ . \tag{4.58}$$

This quantity vanishes, on account of equation (4.18).

Second order correction

The second order correction to the ground state energy is given by

$$\begin{aligned} E_F^{(2)} &= \sum_j \frac{\langle F | \, H_x \, | j \rangle \, \langle j | \, H_x \, | F \rangle}{E_F^{(0)} - E_j^{(0)}} \\ &= \sum_j \frac{|\langle F | \, H_x \, | j \rangle|^2}{E_F^{(0)} - E_j^{(0)}} \ . \end{aligned} \tag{4.59}$$

The only non-vanishing matrix elements in the above sum are those contributed by the N-fold degenerate $N-1$ spins up, 1 spin down states, $|m\rangle$, any linear combination of which is also a first excited state of the ferromagnetic ground state. The degenerate unperturbed energy of $|m\rangle$ is

$$E_{|m\rangle}^{(0)} = \left(\frac{N}{4} - 1 \right) (1 + j) - \left(\frac{N}{2} - 1 \right) h_z \,, \tag{4.60}$$

with

$$|m\rangle \in \{|++++\cdots+-\rangle, |+++\cdots+-+\rangle, \cdots, |-+++\cdots++\rangle\} \ . \tag{4.61}$$

We therefore have from equation (4.54) and (4.60) that the energy shift is

$$E_F^{(0)} - E_m^{(0)} = 1 + j - h_z \ . \tag{4.62}$$

The second order correction to the ferromagnetic ground state energy is therefore

$$E_F^{(2)} = \frac{Nh_x^2}{4} \frac{1}{(1+j-h_z)} \ . \tag{4.63}$$

The first order correction to the ferromagnetic ground state is

$$\begin{aligned} |0\rangle^{(1)} &= \frac{H_{x_{0a}}}{\hbar\omega_{0a}} |a\rangle \\ &= \frac{h_x/2}{(1+j-h_z)} \left(|++++\cdots++++-\rangle + \cdots + |-+++\cdots++++\rangle\right) \ . \end{aligned} \tag{4.64}$$

We remark that perturbation expansions with terms similar to that in equation (4.63) have been obtained in a quantum modelling of the two-dimensional ANNNI model by Barber and Duxbury [22], for a ferromagnetic model. The said paper was not concerned with the longitudinal ANNNI model and in fact the longitudinal field was introduced merely as an artifice to enable the calculation of the ferromagnetic order parameter and the associated susceptibility.

With argument similar to that in the previous section, we find that the third order correction to the ferromagnetic ground state energy vanishes.

Next we will compute the fourth-order correction to the ferromagnetic ground state energy.

Fourth order correction

The fourth-order correction to the ground state energy is given by

$$\begin{aligned} E_F^{(4)} = &\sum_{ijk} \frac{\langle F| H_x |i\rangle \langle i| H_x |j\rangle \langle j| H_x |k\rangle \langle k| H_x |F\rangle}{(E_F^{(0)} - E_i^{(0)})(E_F^{(0)} - E_j^{(0)})(E_F^{(0)} - E_k^{(0)})} \\ &- E_F^{(2)} \sum_k \frac{\langle F| H_x |k\rangle \langle k| H_x |F\rangle}{(E_F^{(0)} - E_k^{(0)})^2} \ . \end{aligned} \tag{4.65}$$

If $\{|a_r\rangle, r = 1, 2, \ldots, N\}$ (equivalent to the set $\{|m\rangle\}$ of equation (4.61)) be the set of states with non-vanishing matrix element with $|F\rangle$, that is, such that

$$\langle F| H_x |a_r\rangle \neq 0 \, , \tag{4.66}$$

then the expression for $E_F^{(4)}$ simplifies to

$$E_F^{(4)} = \sum_{rs} \left(\frac{\langle F| H_x |a_r\rangle \langle a_s| H_x |F\rangle}{(E_F^{(0)} - E_{a_r}^{(0)})(E_F^{(0)} - E_{a_s}^{(0)})} \sum_j \frac{\langle a_r| H_x |j\rangle \langle j| H_x |a_s\rangle}{E_F^{(0)} - E_j^{(0)}} \right) - E_F^{(2)} \sum_r \frac{|\langle F| H_x |a_r\rangle|^2}{(E_F^{(0)} - E_{a_r}^{(0)})^2} \, . \tag{4.67}$$

A Maple procedure computes $E_F^{(4)}$ as

$$E_F^{(4)} = \frac{Nh_x^4}{16(1+j-h_z)^2} \left(\frac{2}{1+2j-2h_z} + \frac{2}{2+j-2h_z} + \frac{(N-5)/2}{1+j-h_z} \right) + \frac{Nh_x^4}{8(1+j-h_z)^2} \left(\frac{1}{(1+2j-2h_z)} + \frac{1}{2+j-2h_z} \right) + \frac{h_x^4 N(N-5)}{32(1+j-h_z)^3} - \frac{N^2 h_x^4}{16(1+j-h_z)^3} \, . \tag{4.68}$$

We observe that the terms proportional to N^2 cancel out and we are left with

$$E_F^{(4)} = \frac{Nh_x^4}{16(1+j-h_z)^2} \left(\frac{-5}{(1+j-h_z)} + \frac{4}{(2+j-2h_z)} + \frac{4}{(1+2j-2h_z)} \right) \, . \tag{4.69}$$

The expression (4.69) is always positive. This is easy to see when we recall that the ground state of the longitudinal ANNNI model is ferromagnetic for $h_z > j+1$. Substitution of $h_z = j+1+\delta$ in (4.69) (δ a positive quantity) gives

$$E_F^{(4)} = \frac{Nh_x^4}{16\delta^2} \left(\frac{5j + 6\delta + 6j\delta + 4\delta^2}{\delta(j+2\delta)(1+2\delta)} \right) \, , \tag{4.70}$$

which is clearly a positive quantity.

Combining equations (4.54), (4.63) and (4.69), we therefore have that to fourth-order in the transverse field h_x, the ferromagnetic ground state energy of the ANNNI model in mixed field is given by

$$E_F = \frac{Nh_x^4}{16(1+j-h_z)^2} \left(\frac{-5}{(1+j-h_z)} + \frac{4}{(2+j-2h_z)} + \frac{4}{(1+2j-2h_z)} \right) + \frac{Nh_x^2}{4(1+j-h_z)} + \frac{N(1+j-2h_z)}{4} \, . \tag{4.71}$$

4.3.2 Physical quantities

Having obtained the approximate ferromagnetic ground state energy, we are now in a position to calculate various quantities of physical interest, the ferromagnetic order parameter, the magnetic susceptibility and the specific heat. The form of the Hamiltonian makes it easy to compute these quantities using Feynman's theorem [60]

Ferromagnetic order parameter

Using Feynman's theorem

$$\langle F| \frac{\partial H}{\partial h_z} |F\rangle = \frac{\partial E_F}{\partial h_z}\,, \tag{4.72}$$

the ferromagnetic order parameter of the ANNNI model in mixed fields is given by

$$\begin{aligned}
\eta_F &= 2 < \sum_i S_i^z > /N \\
&= -2/N \partial E_F/\partial h_z \\
&= -2\partial \varepsilon_F/\partial h_z \\
&= 1 - \frac{1}{2}\frac{h_x^2}{(1+j-h_z)^2} - \frac{1}{4}\frac{h_x^4}{(1+j-h_z)^3}\left(\frac{-5}{1+j-h_z} + \frac{4}{2+j-2h_z} + \frac{4}{1+2j-2h_z}\right) \\
&\quad - \frac{1}{8}\frac{h_x^4}{(1+j-h_z)^2}\left(\frac{-5}{(1+j-h_z)^2} + \frac{8}{(2+j-2h_z)^2} + \frac{8}{(1+2j-2h_z)^2}\right)\,.
\end{aligned} \tag{4.73}$$

The susceptibility is given by

$$\begin{aligned}
\chi_F &= \partial^2 \varepsilon_F/\partial h_z^2 \\
&= -\frac{h_x^2}{(1+j-h_z)^3} - \frac{3}{4}\frac{h_x^4}{(1+j-h_z)^4}\left(\frac{-5}{1+j-h_z} + \frac{4}{2+j-2h_z} + \frac{4}{1+2j-2h_z}\right) \\
&\quad - \frac{1}{2}\frac{h_x^4}{(1+j-h_z)^3}\left(\frac{-5}{(1+j-h_z)^2} + \frac{8}{(2+j-2h_z)^2} + \frac{8}{(1+2j-2h_z)^2}\right) \\
&\quad - \frac{1}{4}\frac{h_x^4}{(1+j-h_z)^2}\left(\frac{-5}{(1+j-h_z)^3} + \frac{16}{(2+j-2h_z)^3} + \frac{16}{(1+2j-2h_z)^3}\right)\,.
\end{aligned} \tag{4.74}$$

Specific Heat

The specific heat of the ferromagnetic ground state ANNNI model in non-commuting fields is given by

$$c = -\frac{1}{N}\frac{\mathrm{d}^2 E_0}{\mathrm{d}y^2}$$

(where $y = h_x^{-1}$ [20])

$$= -\frac{3}{2}\frac{h_x^4}{1+j-h_z} - \frac{5}{4}\frac{h_x^6}{(1+j-h_z)^2}\left(\frac{-5}{1+j-h_z} + \frac{4}{2+j-2h_z} + \frac{4}{1+2j-2h_z}\right)\,. \tag{4.75}$$

4.4 The antiphase ground state

The ground state of the longitudinal ANNNI model (4.1) in the region bounded by the line $2h_z+1 = 2j$ and the j axis is the four-fold degenerate antiphase states, with two spins up followed by two spins down. Classified by translational invariance, the states occur in the subspaces $k = 0$, $k = N/4$, $k = N/2$ and $k = 3N/4$ of the eigenstates of $\mathcal{T}$ (one linear combination in each subspace). In order to simulate the antiphase states correctly, we will assume that N is a multiple of 4. The degenerate energy is

$$E^{(0)}_{<2>} = -\frac{Nj}{4}\,, \tag{4.76}$$

belonging to each of the 4 states

$$\begin{aligned} |<2>\rangle_a &= |++--\cdots++--\rangle\ , \\ |<2>\rangle_b &= |+--+\cdots+--+\rangle\ , \\ |<2>\rangle_c &= |--++\cdots--++\rangle\ , \end{aligned}$$

and

$$|<2>\rangle_d = |-++-\cdots-++-\rangle\ . \tag{4.77}$$

In order to facilitate the calculation of the order parameter and the susceptibility, we introduce in the unperturbed Hamiltonian (4.1), a field, $\beta > 0$, and write the unperturbed Hamiltonian as

$$\begin{aligned} H_z = &\sum_{i=1}^{N} S^z_i S^z_{i+1} + \sum_{i=1}^{N} S^z_i S^z_{i+2} - h_z \sum_{i=1}^{N} S^z_i \\ &- \beta \sum_{k=1}^{N/4} \left(S^z_{4k-3} + S^z_{4k-2} - S^z_{4k-1} - S^z_{4k} \right)\ . \end{aligned} \tag{4.78}$$

This way, the antiphase order parameter, $\rho_{<2>}$, and the associated susceptibility, $\chi_{<2>}$ can be calculated from

$$\rho = -\frac{2}{N} \frac{\partial E_{<2>}}{\partial \beta}\bigg|_{\beta=0}$$

and

$$\chi = -\frac{2}{N} \frac{\partial^2 E_{<2>}}{\partial \beta^2}\bigg|_{\beta=0}\ . \tag{4.79}$$

We note that the field β breaks the translational invariance symmetry of the Hamiltonian (1.1). A finite β also lifts the degeneracy of the antiphase states, although not completely. $|< 2 >\rangle_b$ and $|< 2 >\rangle_d$ are not sensitive to the field β, and so they remain degenerate, with the energy remaining the same as in (4.76), while $|< 2 >\rangle_a$ and $|< 2 >\rangle_c$ now have energies given by

$$E^{(0)}_{<2>_a} = -\frac{N(j+2\beta)}{4} \tag{4.80a}$$

and

$$E^{(0)}_{<2>_c} = -\frac{N(j-2\beta)}{4} \ . \tag{4.80b}$$

We see that $|< 2 >\rangle_a$ is the non-degenerate ground state of the unperturbed Hamiltonian (4.78) in the region between the j axis and the line $2h_z + 1 = 2j$, for a finite β.

4.4.1 Energy corrections

First order correction

In zero field β, the ground state of Hamiltonian (4.78) is four-fold degenerate, so that the 4×4 perturbation matrix V, has elements

$$V_{ij} = \langle < 2 >_i | \, H_x \, | < 2 >_j \rangle \ . \tag{4.81}$$

where the states $|< 2 >_s\rangle$ are given in (4.77). All sixteen elements of V vanish on account of (4.18), so that as in the previous cases, the first order correction to the ground state energy of the antiphase states is zero.

Second order correction

The perturbation matrix for the second order correction to the antiphase ground state energy has elements

$$V_{ij} = \sum_m \frac{\langle < 2 >_i | \, H_x \, |m\rangle \, \langle m| \, H_x \, | < 2 >_j \rangle}{E^{(0)}_{<2>} - E^{(0)}_m} \ . \tag{4.82}$$

It is clear that it is impossible to have a state $|m\rangle$ in the 2^N dimensional Hilbert space of the Hamiltonian of N spins simultaneously having nonzero matrix element with two different members of the four-fold degenerate $|< 2 >\rangle$ states. In other words, the matrix V is diagonal, with

$$V_{ii} = \sum_m \frac{|\langle < 2 >_i | \, H_x \, |m\rangle|^2}{E^{(0)}_{<2>_i} - E^{(0)}_m} \ , \tag{4.83}$$

which are just the Rayleigh-Schrödinger expressions for second-order corrections to the energy in non-degenerate perturbation theory.

Putting $i = a, b, c, d$ in turns in (4.83), we have

$$E^{(2)}_{<2>_a} = -\frac{Nh_x^2}{8}\left(\frac{1}{j+h_z+\beta}+\frac{1}{j-h_z+\beta}\right), \tag{4.84}$$

$$E^{(2)}_{<2>_b} = -\frac{Nh_x^2}{16}\left(\frac{1}{j+h_z+\beta}+\frac{1}{j-h_z-\beta}+\frac{1}{j-h_z+\beta}+\frac{1}{j+h_z-\beta}\right) = E^{(0)}_{<2>_d} \tag{4.85}$$

and

$$E^{(2)}_{<2>_c} = -\frac{Nh_x^2}{8}\left(\frac{1}{j+h_z-\beta}+\frac{1}{j-h_z-\beta}\right). \tag{4.86}$$

Equations (4.84), (4.85) and (4.86) contain an interesting summary of the properties of the general Hamiltonian (1.1) of the ANNNI model in mixed fields. We note that although the introduction of the field β breaks the translational invariance symmetry of the Hamiltonian, it does leave the reflection symmetry intact, and as proved in Appendix A, reflection is a symmetry of the Hamiltonian. In fact every eigenstate of the reflection operator $\mathcal{R}$ is also an eigenstate of the operator $\beta\sum_{i=1}^{N/4}\left(\mathrm{S^z_{4k-3}}+\mathrm{S^z_{4k-2}}-\mathrm{S^z_{4k-1}}-\mathrm{S^z_{4k}}\right)$ with eigenvalue 0. That is, for any $|\psi\rangle$ an eigenstate of total S_z, we have

$$\left(\beta\sum_{i=1}^{N/4}\left(\mathrm{S^z_{4k-3}}+\mathrm{S^z_{4k-2}}-\mathrm{S^z_{4k-1}}-\mathrm{S^z_{4k}}\right)\right)|\psi\rangle = 0\,, \tag{4.87}$$

whenever

$$\mathcal{R}\,|\psi\rangle = \pm\,|\psi\rangle\ . \tag{4.88}$$

In other words, eigenstates of $\mathcal{R}$ do not sense the presence of the field β.

Each of the two states (and hence their linear combination)

$$|<2>\rangle_b = |+--+\cdots+--+\rangle \tag{4.89a}$$

and

$$|<2>\rangle_d = |-++-\cdots-++-\rangle \tag{4.89b}$$

is an eigenstate of $\mathcal{R}$. This explains their degeneracy at zeroth-order perturbation and why the second order energy corrections in these states are the same. Since $[H, \mathcal{R}] = 0$, it is expected that their degeneracy will not be lifted, to any order in perturbation. It is also noteworthy that

$|< 2 >\rangle_b$ and $|< 2 >\rangle_d$ are related by the inversion symmetry, which however is not a symmetry of H for finite h_z.

As for

$$|< 2 >\rangle_a = |++--\cdots++--\rangle \tag{4.90a}$$

and

$$|< 2 >\rangle_c = |--++\cdots--++\rangle \tag{4.90b}$$

the translational invariance which connects the two states is removed by the field β and they cease to be degenerate. We observe also that the two states are related by the inversion symmetry, but this is not a symmetry of the Hamiltonian (Appendix A), except at $h_z = 0$ (corresponding to the ANNNI model in a transverse field). Results for one state can be obtained from the other by replacing β in one with $-\beta$ in the other.

Putting $\beta = 0$ in (4.84), (4.85) and (4.86) we see that the degeneracy in the antiphase states remain to second order in perturbation in h_x.

Fourth order correction

For simplictity we will drop the subscript a on $|< 2 >_a\rangle$ henceforth and simply refer to the antiphase ground state by $|< 2 >\rangle$. The fourth-order correction to the ground state energy of the antiphase ground state is given by

$$\begin{aligned} E^{(4)}_{<2>} = \sum_{ijk} \frac{\langle< 2 >| H_x |i\rangle \langle i| H_x |j\rangle \langle j| H_x |< 2 >\rangle}{(E^{(0)}_{<2>} - E^{(0)}_i)(E^{(0)}_{<2>} - E^{(0)}_j)(E^{(0)}_{<2>} - E^{(0)}_k)} \\ - E^{(2)}_{<2>} \sum_k \frac{\langle< 2 >| H_x |k\rangle \langle k| H_x |< 2 >\rangle}{(E^{(0)}_{<2>} - E^{(0)}_k)^2} \, . \end{aligned} \tag{4.91}$$

If $\{|a_r\rangle\}, r = 1, 2, \cdots, N$ denotes the set of states with non-vanishing matrix elements with $|< 2 >\rangle$, then the above expression simplifies to

$$E^{(4)}_{<2>} = \sum_{rs}\left(\frac{\langle <2>|\, H_x\,|a_r\rangle\,\langle a_r|\, H_x\,|<2>\rangle}{(E^{(0)}_{<2>}-E^{(0)}_{a_r})(E^{(0)}_{<2>}-E^{(0)}_{a_s})}\sum_j \frac{\langle a_r|\, H_x\,|j\rangle\,\langle j|\, H_x\,|a_s\rangle}{E^{(0)}_{<2>}-E^{(0)}_j}\right) - E^{(2)}_{<2>}\sum_r \frac{|\langle <2>|\, H_x\,|a_r\rangle|^2}{(E^{(0)}_{<2>}-E^{(0)}_{a_r})^2}\,. \tag{4.92}$$

The Maple procedure *fourthorder* evaluates the above sum to

$$\begin{aligned}
E^{(4)}_{<2>} = &-\frac{Nh_x^4}{32}\frac{1}{(j+\beta+h_z)^2}\left(\frac{1}{2j+2\beta+1+2h_z}+\frac{2}{j+2\beta}+\frac{1}{2j+2\beta-1}+\frac{N/4-1}{j+\beta+h_z}+\frac{N/4-3/2}{j+\beta}\right)\\
&-\frac{Nh_x^4}{32}\frac{1}{(j+\beta-h_z)^2}\left(\frac{1}{2j+2\beta+1-2h_z}+\frac{2}{j+2\beta}+\frac{1}{2j+2\beta-1}+\frac{N/4-1}{j+\beta-h_z}+\frac{N/4-3/2}{j+\beta}\right)\\
&-\frac{Nh_x^4}{32}\left(\frac{1}{(j+\beta+h_z)^2(2j+2\beta+1+2h_z)}+\frac{1}{(j+\beta-h_z)^2(2j+2\beta+1-2h_z)}\right)\\
&-\frac{Nh_x^4}{32}\frac{1}{(j+\beta+h_z)(j+\beta-h_z)}\left(\frac{2}{2j+2\beta-1}+\frac{(N/2-3)}{j+\beta}+\frac{4}{j+2\beta}\right)\\
&-\frac{Nh_x^4}{32}\left(\frac{N}{4}-1\right)\left(\frac{1}{(j+\beta+h_z)^3}+\frac{1}{(j+\beta-h_z)^3}\right)\\
&+\frac{Nh_x^4}{64}\left(\frac{1}{(j+\beta+h_z)^2}+\frac{1}{(j+\beta-h_z)^2}\right)\left(\frac{1}{(j+\beta+h_z)}+\frac{1}{(j+\beta-h_z)}\right)\,.
\end{aligned}\tag{4.93}$$

If we denote the terms proportional to N^2 in the above equation by s_{N^2}, then

$$\begin{aligned}
s_{N^2} = &-\frac{N^2h_x^4}{64}\frac{1}{(j+\beta+h_z)^3}-\frac{N^2h_x^4}{128}\frac{1}{(j+\beta+h_z)^2}\frac{1}{j+\beta}\\
&-\frac{N^2h_x^4}{64}\frac{1}{(j+\beta-h_z)^3}-\frac{N^2h_x^4}{128}\frac{1}{(j+\beta-h_z)^2}\frac{1}{j+\beta}\\
&-\frac{N^2h_x^4}{64}\frac{1}{(j+\beta+h_z)(j+\beta-h_z)(j+\beta)}\\
&+\frac{N^2h_x^4}{64}\frac{1}{(j+\beta+h_z)^3}+\frac{N^2h_x^4}{64}\frac{1}{(j+\beta+h_z)^2}\frac{1}{(j+\beta-h_z)}\\
&+\frac{N^2h_x^4}{64}\frac{1}{(j+\beta-h_z)^2}\frac{1}{(j+\beta+h_z)}+\frac{N^2h_x^4}{64}\frac{1}{(j+\beta-h_z)^3}\\
= &\,0\,.
\end{aligned}\tag{4.94}$$

We therefore have that the fourth order correction to the antiphase ground state is given by

$$
\begin{aligned}
E^{(4)}_{<2>} = &-\frac{Nh_x^4}{32}\frac{1}{(j+\beta+h_z)^2}\left(\frac{1}{2j+2\beta+1+2h_z}+\frac{2}{j+2\beta}+\frac{1}{2j+2\beta-1}-\frac{1}{j+\beta+h_z}-\frac{3/2}{j+\beta}\right)\\
&-\frac{Nh_x^4}{32}\frac{1}{(j+\beta-h_z)^2}\left(\frac{1}{2j+2\beta+1-2h_z}+\frac{2}{j+2\beta}+\frac{1}{2j+2\beta-1}-\frac{1}{j+\beta-h_z}-\frac{3/2}{j+\beta}\right)\\
&-\frac{Nh_x^4}{32}\left(\frac{1}{(j+\beta+h_z)^2(2j+2\beta+1+2h_z)}+\frac{1}{(j+\beta-h_z)^2(2j+2\beta+1-2h_z)}\right)\\
&-\frac{Nh_x^4}{32}\frac{1}{(j+\beta+h_z)(j+\beta-h_z)}\left(\frac{2}{2j+2\beta-1}-\frac{3}{j+\beta}+\frac{4}{j+2\beta}\right)\\
&+\frac{Nh_x^4}{32}\left(\frac{1}{(j+\beta+h_z)^3}+\frac{1}{(j+\beta-h_z)^3}\right)\ . \qquad (4.95)
\end{aligned}
$$

The antiphase ground state energy per spin, to fourth order in the transverse field h_x is therefore given by (equations (4.80a), (4.84) and (4.95))

$$
\begin{aligned}
\varepsilon_{<2>}(\beta=0) = &\left\{-\frac{h_x^4}{32}\frac{1}{(j+\beta+h_z)^2}\left(\frac{1}{2j+2\beta+1+2h_z}+\frac{2}{j+2\beta}+\frac{1}{2j+2\beta-1}-\frac{1}{j+\beta+h_z}-\frac{3/2}{j+\beta}\right)\right.\\
&-\frac{h_x^4}{32}\frac{1}{(j+\beta-h_z)^2}\left(\frac{1}{2j+2\beta+1-2h_z}+\frac{2}{j+2\beta}+\frac{1}{2j+2\beta-1}-\frac{1}{j+\beta-h_z}-\frac{3/2}{j+\beta}\right)\\
&-\frac{h_x^4}{32}\left(\frac{1}{(j+\beta+h_z)^2(2j+2\beta+1+2h_z)}+\frac{1}{(j+\beta-h_z)^2(2j+2\beta+1-2h_z)}\right)\\
&-\frac{h_x^4}{32}\frac{1}{(j+\beta+h_z)(j+\beta-h_z)}\left(\frac{2}{2j+2\beta-1}-\frac{3}{j+\beta}+\frac{4}{j+2\beta}\right)\\
&+\frac{h_x^4}{32}\left(\frac{1}{(j+\beta+h_z)^3}+\frac{1}{(j+\beta-h_z)^3}\right)\\
&\left.-\frac{h_x^2}{8}\left(\frac{1}{(j+\beta+h_z)}+\frac{1}{(j+\beta-h_z)}\right)-\frac{(j+2\beta)}{4}\right\}\ \Big|_{\beta=0}\ . \qquad (4.96)
\end{aligned}
$$

That is

$$\begin{aligned}
\varepsilon_{<2>} = & -\frac{h_x^4}{32}\frac{1}{(j+h_z)^2}\left(\frac{1}{2j+1+2h_z}+\frac{1}{2j}+\frac{1}{2j-1}-\frac{1}{j+h_z}\right) \\
& -\frac{h_x^4}{32}\frac{1}{(j-h_z)^2}\left(\frac{1}{2j+1-2h_z}+\frac{1}{2j}+\frac{1}{2j-1}-\frac{1}{j-h_z}\right) \\
& -\frac{h_x^4}{32}\left(\frac{1}{(j+h_z)^2(2j+1+2h_z)}+\frac{1}{(j-h_z)^2(2j+1-2h_z)}\right) \\
& -\frac{h_x^4}{32}\frac{1}{(j+h_z)(j-h_z)}\left(\frac{2}{2j-1}+\frac{1}{j}\right) \\
& +\frac{h_x^4}{32}\left(\frac{1}{(j+h_z)^3}+\frac{1}{(j-h_z)^3}\right) \\
& -\frac{h_x^2}{8}\left(\frac{1}{(j+h_z)}+\frac{1}{(j-h_z)}\right)-\frac{j}{4}\,. \qquad (4.97)
\end{aligned}$$

In particular the ground state energy per spin of the antiphase state for the ANNNI model in a transverse field ($h_z = 0$), to the fourth order in h_x is

$$\varepsilon_{<2>_{tANNNI}} = -\frac{j}{4}-\frac{h_x^2}{4j}-\frac{1}{16j^3}\left(\frac{8j^2}{4j^2-1}-1\right)h_x^4\,. \qquad (4.98)$$

$\varepsilon_{<2>_{tANNNI}}$ is always negative since $j > 0.5$. The ground state energy per spin for the transverse ANNNI model is plotted as a function of h_x in figure 4.1 for three different values of j.

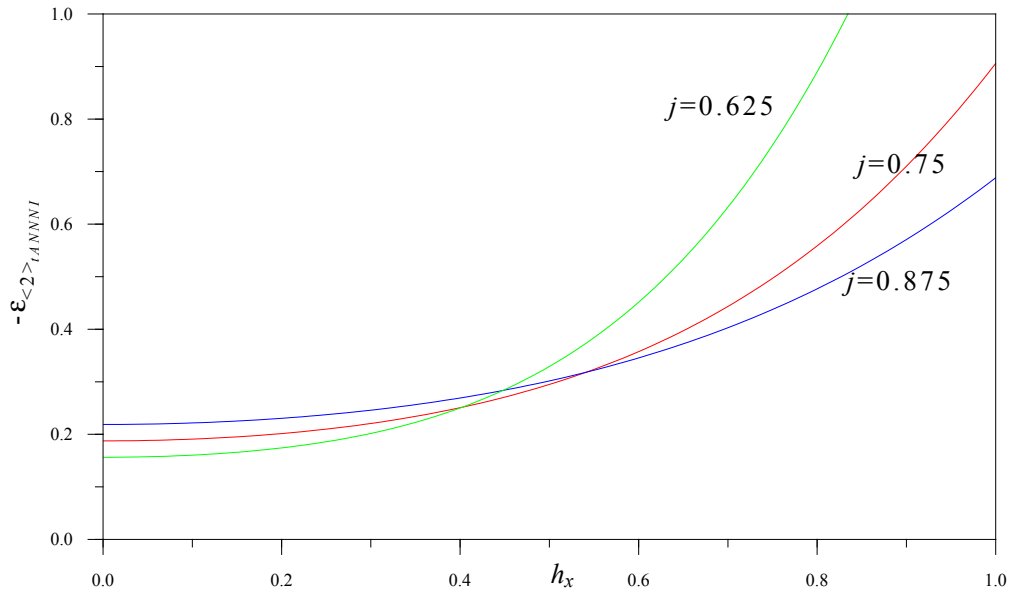

Figure 4.1: Transverse field antiphase ANNNI ground state energy per spin as a function of h_x, to the fourth order, for selected values of j.

4.4.2 Physical quantities of the antiphase ground state

Order parameter

The antiphase long range order parameter is obtained from

$$\begin{aligned}
\rho_{<2>} &= \lim_{N\to\infty} 2\left\langle \sum_{k=1}^{N/4}\left(S^z_{4k-3}+S^z_{4k-2}+S^z_{4k-1}+S^z_{4k}\right)\right\rangle /N = -2\left.\frac{\partial\varepsilon_{<2>}}{\partial\beta}\right|_{\beta=0} \\
&= 1-\frac{h_x^2}{4}\left(\frac{1}{(j+h_z)^2}+\frac{1}{(j-h_z)^2}\right) \\
&-\frac{1}{8}\frac{h_x^4}{(j+h_z)^3}\left(\frac{1}{2j+1+2h_z}+\frac{1}{2j}+\frac{1}{2j-1}-\frac{1}{j+h_z}\right) \\
&-\frac{1}{8}\frac{h_x^4}{(j-h_z)^3}\left(\frac{1}{2j+1-2h_z}+\frac{1}{2j}+\frac{1}{2j-1}-\frac{1}{j-h_z}\right) \\
&-\frac{1}{16}\frac{h_x^4}{(j+h_z)^2}\left(\frac{2}{(2j+1+2h_z)^2}+\frac{5}{2j^2}+\frac{2}{(2j-1)^2}-\frac{1}{(j+h_z)^2}\right) \\
&-\frac{1}{16}\frac{h_x^4}{(j+h_z)^2}\left(\frac{2}{(2j+1-2h_z)^2}+\frac{5}{2j^2}+\frac{2}{(2j-1)^2}-\frac{1}{(j-h_z)^2}\right) \\
&-\frac{h_x^4}{8}\left(\frac{1}{(j+h_z)^3(2j+1+2h_z)}+\frac{1}{(j+h_z)^2(2j+1+2h_z)^2}\right) \\
&-\frac{h_x^4}{8}\left(\frac{1}{(j-h_z)^3(2j+1-2h_z)}+\frac{1}{(j-h_z)^2(2j+1-2h_z)^2}\right) \\
&-\frac{h_x^4}{16}\left(\frac{2}{2j-1}+\frac{1}{j}\right)\left(\frac{1}{(j+h_z)^2(j-h_z)}+\frac{1}{(j+h_z)(j-h_z)^2}\right) \\
&-\frac{h_x^4}{16}\frac{1}{(j+h_z)(j-h_z)}\left(\frac{4}{(2j-1)^2}+\frac{5}{j^2}\right)+\frac{3h_x^4}{16}\left(\frac{1}{(j+h_z)^4}+\frac{1}{(j-h_z)^4}\right) . \qquad (4.99)
\end{aligned}$$

The antiphase order parameter for the transverse ANNNI model is given by

$$\rho_{<2>_{tANNNI}} = 1-\frac{1}{2j^2}h_x^2-\left(\frac{1-16j^2+112j^4}{8(4j^2-1)^2j^4}\right)h_x^4 . \qquad (4.100)$$

$\rho_{<2>_{tANNNI}}$ is plotted in figure 4.2 as a function of h_x for three different values of j. We observe that both the second order and the fourth order contributions to the order parameter are negative, so that the antiphase order parameter drops in value. The vanishing of the order parameter is well depicted in figure 4.2. The application of an external transverse magnetic field h_x is therefore expected to destroy the $< 2 >$ antiphase spin ordering which exists at $j > 0.5$ for $h_x = 0$. This expectation turns out to be correct as finite size scaling shows that the model undergoes a transition to paramagnetic phase.

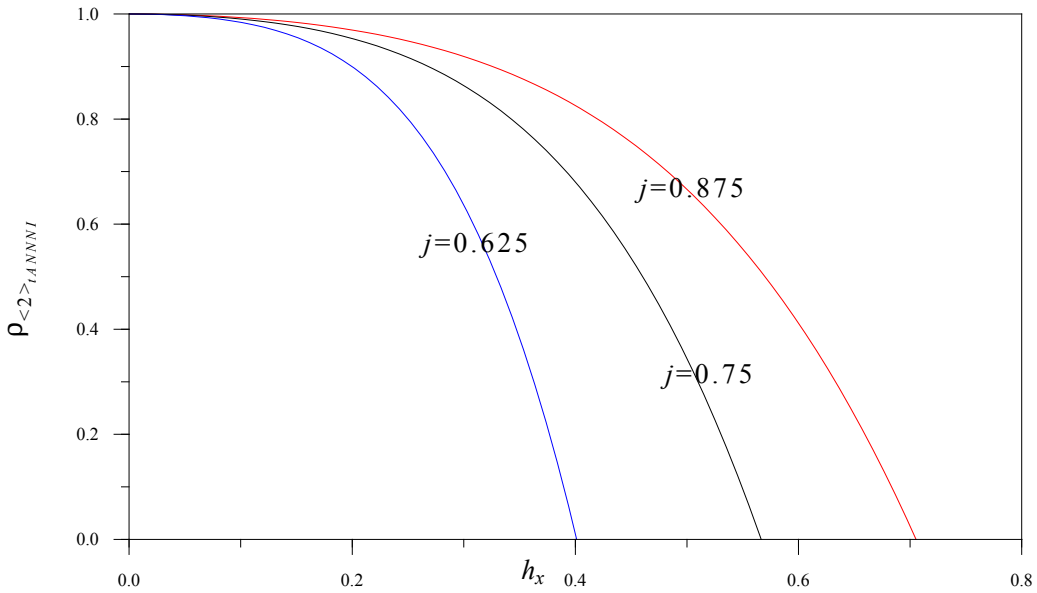

Figure 4.2: Transverse field antiphase ANNNI order parameter as a function of h_x, to the fourth order, for selected values of j.

Susceptibility

The magnetic susceptiblity of the antiphase ground state under the influence of a weak transverse external magnetic field is

$$
\begin{aligned}
\chi_{<2>} &= -2\frac{\partial^2 \varepsilon_{<2>}}{\partial \beta^2}\bigg|_{\beta=0} \\
&= \frac{1}{2}\left(\frac{1}{(j+h_z)^3}+\frac{1}{(j-h_z)^3}\right)h_x^2 \\
&+\left\{\frac{3}{8}\frac{1}{(j+h_z)^4}\left(\frac{1}{2j+1+2h_z}+\frac{1}{2j}+\frac{1}{2j-1}-\frac{1}{j+h_z}\right)\right. \\
&+\frac{3}{8}\frac{1}{(j-h_z)^4}\left(\frac{1}{2j+1-2h_z}+\frac{1}{2j}+\frac{1}{2j-1}-\frac{1}{j-h_z}\right) \\
&+\frac{1}{4}\frac{1}{(j+h_z)^3}\left(\frac{2}{(2j+1+2h_z)^2}+\frac{5}{2j^2}+\frac{2}{(2j-1)^2}-\frac{1}{(j+h_z)^2}\right) \\
&+\frac{1}{4}\frac{1}{(j-h_z)^3}\left(\frac{2}{(2j+1-2h_z)^2}+\frac{5}{2j^2}+\frac{2}{(2j-1)^2}-\frac{1}{(j-h_z)^2}\right) \\
&+\frac{1}{16}\frac{1}{(j+h_z)^2}\left(\frac{2}{(2j+1+2h_z)^3}+\frac{13}{j^3}+\frac{8}{(2j-1)^3}-\frac{2}{(j+h_z)^3}\right) \\
&+\frac{1}{16}\frac{1}{(j-h_z)^2}\left(\frac{2}{(2j+1-2h_z)^3}+\frac{13}{j^3}+\frac{8}{(2j-1)^3}-\frac{2}{(j-h_z)^3}\right) \\
&+\frac{3}{8}\left(\frac{1}{(j+h_z)^4(2j+1+2h_z)}+\frac{1}{(j-h_z)^4(2j+1-2h_z)}\right) \\
&+\frac{1}{2}\left(\frac{1}{(j+h_z)^3(2j+1+2h_z)^2}+\frac{1}{(j-h_z)^3(2j+1-2h_z)^2}\right) \\
&+\frac{1}{2}\left(\frac{1}{(j+h_z)^2(2j+1+2h_z)^3}+\frac{1}{(j-h_z)^2(2j+1-2h_z)^3}\right) \\
&+\frac{1}{8}\frac{1}{(j+h_z)(j-h_z)}\left(\frac{1}{j+h_z}+\frac{1}{j-h_z}\right)\left(\frac{4}{(2j-1)^2}+\frac{5}{j^2}\right) \\
&+\frac{1}{8}\frac{1}{(j+h_z)(j-h_z)}\left(\frac{1}{(j+h_z)^2}+\frac{1}{(j-h_z)^2}\right)\left(\frac{2}{2j-1}+\frac{1}{j}\right) \\
&+\frac{1}{8}\frac{1}{(j+h_z)^2(j-h_z)^2}\left(\frac{2}{2j-1}+\frac{1}{j}\right) \\
&\left.+\frac{1}{(j+h_z)(j-h_z)}\left(\frac{1}{(2j-1)^3}+\frac{13}{8j^3}\right)-\frac{3}{4}\left(\frac{1}{(j+h_z)^5}+\frac{1}{(j-h_z)^5}\right)\right\}h_x^4\,. \qquad (4.101)
\end{aligned}
$$

A particular case of equation (4.4.2) is the ANNNI model in a transverse field ($h_z = 0$), for which the magnetic susceptiblity is

$$\chi_{<2>_{tANNNI}} = \frac{1}{j^3}h_x^2 + \frac{1}{2j^5}\frac{(-384j^4+88j^2+832j^6-7)}{(4j^2-1)^3}\,. \qquad (4.102)$$

Again we note that $\chi_{<2>_{tANNNI}}$ is a positive quantity for $j > 0.5$. The transverse ANNNI model susceptiblity, to fourth order in h_x is plotted in figure 4.3.

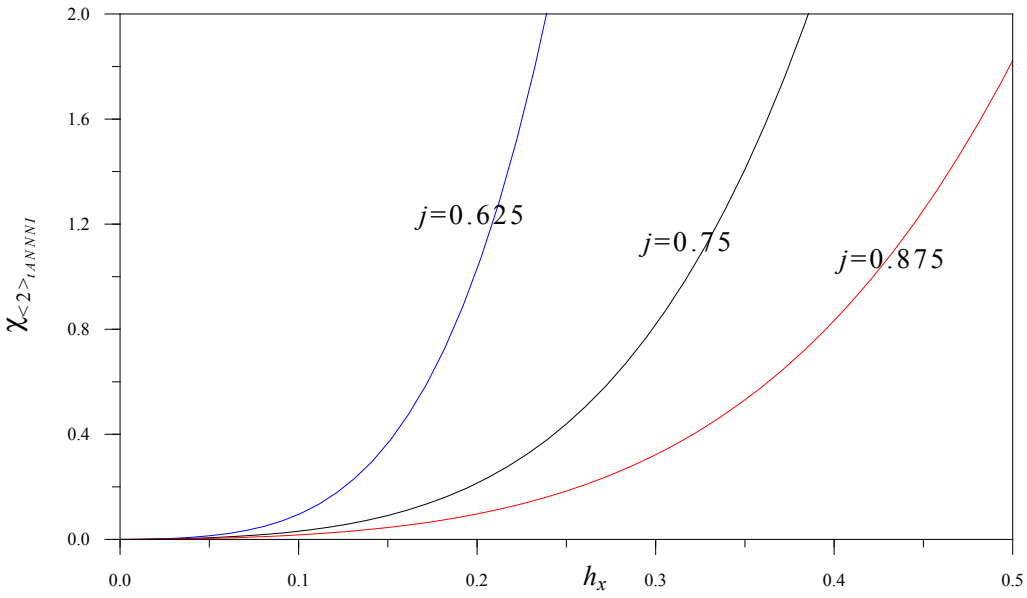

Figure 4.3: Transverse antiphase ANNNI magnetic susceptiblity as a function of h_x, to the fourth order, for selected values of j.

Specific heat

The specific heat of the ANNNI model in the presence of a longitudinal field h_z and a weak transverse field h_x, to second order in h_x is given by

$$\begin{aligned} c_{<2>} &= -\frac{\partial^2 \varepsilon_{<2>}(\beta=0)}{\partial y^2} \quad (\text{ where } y = h_x^{-1}) \\ &= \frac{3h_x^4}{4}\left(\frac{1}{j+h_z}+\frac{1}{j-h_z}\right)+\frac{5}{8}\left\{\frac{1}{(j+h_z)^2}\left(\frac{1}{2j+1+2h_z}+\frac{1}{2j}+\frac{1}{2j-1}-\frac{1}{j+h_z}\right)\right. \\ &\quad +\frac{1}{(j-h_z)^2}\left(\frac{1}{2j+1-2h_z}+\frac{1}{2j}+\frac{1}{2j-1}-\frac{1}{j-h_z}\right) \\ &\quad +\left(\frac{1}{(j+h_z)^2(2j+1+2h_z)}+\frac{1}{(j-h_z)^2(2j+1-2h_z)}\right) \\ &\quad \left.-\left(\frac{1}{(j+h_z)^3}+\frac{1}{(j-h_z)^3}\right)+\frac{1}{(j+h_z)(j-h_z)}\left(\frac{2}{2j-1}+\frac{1}{j}\right)\right\}h_x^6 \,. \end{aligned} \tag{4.103}$$

In particular, we have for the ANNNI model in a transverse field, (corresponding to $h_z = 0$ here)

$$c_{<2>_{tANNNI}} = \frac{3h_x^4}{2j}+\frac{5}{4}\frac{1}{j^3}\left(\frac{4j^2+1}{4j^2-1}\right)h_x^6 \,. \tag{4.104}$$

We observe that equation (4.104) always gives a positive value for the specific heat of the model. We also remark that contrary to the appearance of equation (4.104), there are no singularities.

The condition $2h_z + 1 < 2j$ reduces to $j > 0.5$ for the unperturbed Hamiltonian (ANNNI model), so that there must be next nearest neighbour interactions and hence j cannot be zero. At $j = 0.5$, the ground state of the ANNNI model is highly degenerate [22], so that formula (4.104) is then not valid. The specific heat as a function of h_x is plotted in figure 4.4 for three different values of j.

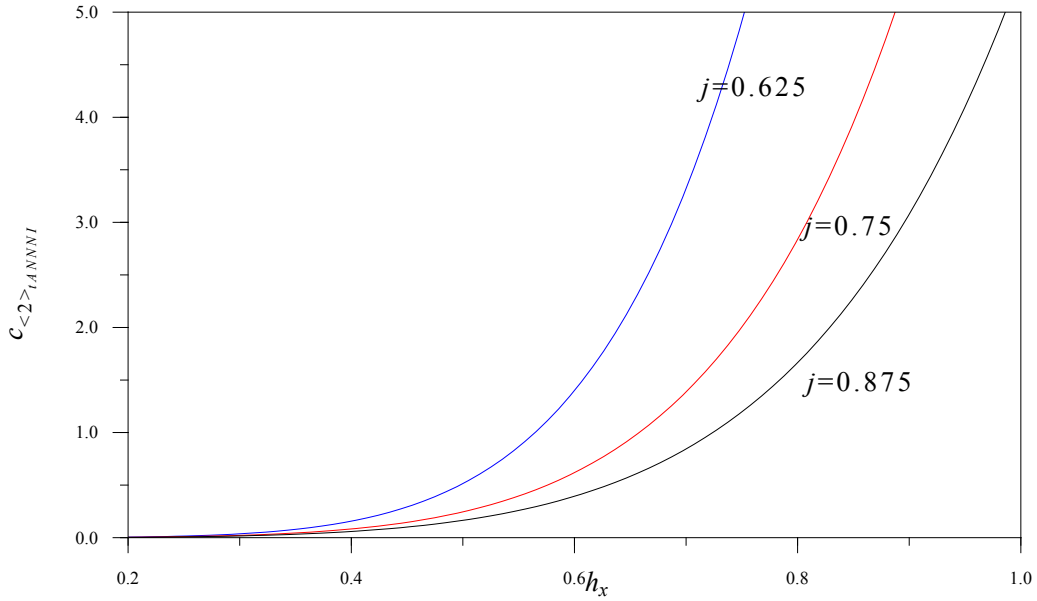

Figure 4.4: Transverse antiphase ANNNI specific heat as a function of h_x, to the sixth order, for selected values of j.

4.5 The ↑↑↓ ground state

The ground state of the longitudinal ANNNI model described by the Hamiltonian (4.1) in the region bounded by the lines $h_z = 1$, $2j + 1 = 2h_z$ and $2j + 1 = h_z$ is the three-fold degenerate two spins up followed by one spin down state, eigenstates of total S_z with eigenvalue $S_z = N/6$. Classified by translational invariance, these states occur in the $k = 0$, $k = N/3$ and $k = 2N/3$ subspaces of the space of eigenstates of the translation operator $\mathcal{T}$. Here we assume that N is a multiple of 3.
Explicitly, the degenerate states are

$$|a\rangle = \frac{1}{\sqrt{3}} \left(|\uparrow\uparrow\downarrow \cdots \uparrow\uparrow\downarrow\rangle + |\uparrow\downarrow\uparrow \cdots \uparrow\downarrow\uparrow\rangle + |\downarrow\uparrow\uparrow \cdots \downarrow\uparrow\uparrow\rangle \right) , \tag{4.105}$$

having translational invariance quantum number $k = 0$, i.e. the zero momentum state (eigenstate of $\mathcal{T}$ of eigenvalue $\exp(0) = 1$).

$$|b\rangle = \frac{1}{\sqrt{3}} \left(|\uparrow\uparrow\downarrow \cdots \uparrow\uparrow\downarrow\rangle + \exp(-\frac{2\pi i}{3}) \, |\uparrow\downarrow\uparrow \cdots \uparrow\downarrow\uparrow\rangle + \exp(-\frac{4\pi i}{3}) \, |\downarrow\uparrow\uparrow \cdots \downarrow\uparrow\uparrow\rangle \right) , \tag{4.106}$$

the $2\pi/3$ -momentum state with $k = N/3$ (eigenstate of $\mathcal{T}$ of eigenvalue $\exp(2\pi \mathrm{i}/3)$).
and

$$|c\rangle = \frac{1}{\sqrt{3}} \left(|\uparrow\uparrow\downarrow \cdots \uparrow\uparrow\downarrow\rangle + \exp(\frac{2\pi i}{3}) \, |\uparrow\downarrow\uparrow \cdots \uparrow\downarrow\uparrow\rangle + \exp(\frac{4\pi i}{3}) \, |\downarrow\uparrow\uparrow \cdots \downarrow\uparrow\uparrow\rangle \right) , \tag{4.107}$$

the $4\pi/3$ -momentum state with $k = 2N/3$ (eigenstate of $\mathcal{T}$ of eigenvalue $\exp(4\pi \mathrm{i}/3)$).

The degenerate energy is

$$E_{|a\rangle} = E_{|b\rangle} = E_{|c\rangle} = \frac{-N(1 + j + 2h_z)}{12} . \tag{4.108}$$

As in the previous section, it is useful to include a symmetry breaking, order parameter term to the Hamiltonian (4.1) by including a field $\gamma > 0$ and write the unperturbed Hamiltonian as follows:

$$H_z = \sum_{i=1}^{N} S_i^z S_{i+1}^z + j \sum_{i=1}^{N} S_i^z S_{i+2}^z - h_z \sum_{i=1}^{N} S_i^z - \gamma \sum_{k=1}^{N/3} \left(S_{3k-2}^z + S_{3k-1}^z - S_{3k}^z \right) . \tag{4.109}$$

γ breaks the translational invariance symmetry of H_z, so that the states $|\uparrow\uparrow\downarrow \cdots \uparrow\uparrow\downarrow\rangle$, $|\uparrow\downarrow\uparrow \cdots \uparrow\downarrow\uparrow\rangle$ and $|\downarrow\uparrow\uparrow \cdots \downarrow\uparrow\uparrow\rangle$ are no longer degenerate and can therefore no longer be classified as eigenstates of $\mathcal{T}$. The state $|\uparrow\uparrow\downarrow \cdots \uparrow\uparrow\downarrow\rangle$ (which we shall henceforth denote by $|\uparrow\uparrow\downarrow\rangle$, with a similar notation for the remaining two states) is now the non-degenerate ground state of H_z.

The long range order parameter $\rho_{\uparrow\uparrow\downarrow}$ and the magnetic susceptibility $\chi_{\uparrow\uparrow\downarrow}$ can now be calculated by computing

$$\rho_{\uparrow\uparrow\downarrow} = -\frac{2}{N}\frac{\partial E_{\uparrow\uparrow\downarrow}(j, h_x, h_z, \gamma)}{\partial \gamma}\bigg|_{\gamma=0} \tag{4.110}$$

and

$$\chi_{\uparrow\uparrow\downarrow} = -\frac{2}{N}\frac{\partial^2 E_{\uparrow\uparrow\downarrow}(j, h_x, h_z, \gamma)}{\partial \gamma^2}\bigg|_{\gamma=0}, \tag{4.111}$$

where $E_{\uparrow\uparrow\downarrow}(\gamma = 0)$ is the ground state energy of $H = H_z + H_x$ and $\varepsilon_{\uparrow\uparrow\downarrow}(\gamma = 0)$ the ground state energy per spin. To zeroth order then,

$$E^{(0)}_{\uparrow\uparrow\downarrow}(j, h_x = 0, h_z, \gamma) = \frac{-N(1 + j + 2h_z)}{12} - \frac{N\gamma}{2} \tag{4.112}$$

and

$$E^{(0)}_{\uparrow\downarrow\uparrow}(j, 0, h_z, \gamma) = \frac{-N(1 + j + 2h_z)}{12} + \frac{N\gamma}{6} = E^{(0)}_{\downarrow\uparrow\uparrow}(j, 0, h_z, \gamma)\ . \tag{4.113}$$

4.5.1 Energy corrections

First order correction to the ground state energy

Since the three states $|\uparrow\uparrow\downarrow\rangle$, $|\uparrow\downarrow\uparrow\rangle$ and $|\downarrow\uparrow\uparrow\rangle$ are degenerate for $\gamma = 0$, we can consider γ to be small and attempt to apply degenerate perturbation theory to determine the first order corrections to the energies. The 3×3 perturbation matrix $V^{(1)}$ is given by

$$V^{(1)} = \begin{pmatrix} \langle\uparrow\uparrow\downarrow| H_x |\uparrow\uparrow\downarrow\rangle & \langle\uparrow\uparrow\downarrow| H_x |\uparrow\downarrow\uparrow\rangle & \langle\uparrow\uparrow\downarrow| H_x |\downarrow\uparrow\uparrow\rangle \\ \langle\uparrow\downarrow\uparrow| H_x |\uparrow\uparrow\downarrow\rangle & \langle\uparrow\downarrow\uparrow| H_x |\uparrow\downarrow\uparrow\rangle & \langle\uparrow\downarrow\uparrow| H_x |\downarrow\downarrow\uparrow\rangle \\ \langle\downarrow\uparrow\uparrow| H_x |\uparrow\uparrow\downarrow\rangle & \langle\downarrow\uparrow\uparrow| H_x |\uparrow\downarrow\uparrow\rangle & \langle\downarrow\uparrow\uparrow| H_x |\downarrow\uparrow\uparrow\rangle \end{pmatrix}. \tag{4.114}$$

But the three states $|\uparrow\uparrow\downarrow\rangle$, $|\uparrow\downarrow\uparrow\rangle$ and $|\downarrow\uparrow\uparrow\rangle$ are all eigenstates of total S_z with the same eigenvalue of $S_z = N/6$ for a chain of N spins, it follows from equation (4.18) that $V^{(1)}$ is a null matrix, so that there are no first order contributions to the energies.

Second order correction to the ground state energy

Treating γ as a small parameter and the states $\{|\uparrow\uparrow\downarrow\rangle, |\uparrow\downarrow\uparrow\rangle, |\downarrow\uparrow\uparrow\rangle\}$ as nearly degenerate, the 3×3 second order perturbation matrix $V^{(2)}$ has elements of the form

$$V^{(2)}_{ij} = \sum_k \frac{\langle i| H_x |k\rangle \langle k| H_x |j\rangle}{E^{(0)}_i - E^{(0)}_k}, \tag{4.115}$$

where

$$i, j \in \{|\uparrow\uparrow\downarrow\rangle, |\uparrow\downarrow\uparrow\rangle, |\downarrow\uparrow\uparrow\rangle\},$$

and k runs over the 2^N basis states of the Hilbert space excluding $|i\rangle$ and $|j\rangle$. Clearly, for $i \neq j$, any state $|k\rangle$ whose H_x matrix element with $|i\rangle$ must have a vanishing matrix element with $|j\rangle$. Therefore the matrix $V^{(2)}$ is diagonal, with the diagonal elements giving the second order corrections to the ground state energies. That is

$$V_{11}^{(2)} = E_{\uparrow\uparrow\downarrow}^{(2)} = \sum_k \frac{|\langle\uparrow\uparrow\downarrow| H_x |k\rangle|^2}{E_{\uparrow\uparrow\downarrow}^{(0)} - E_k^{(0)}} , \tag{4.116}$$

$$V_{22}^{(2)} = E_{\uparrow\downarrow\uparrow}^{(2)} = \sum_k \frac{|\langle\uparrow\downarrow\uparrow| H_x |k\rangle|^2}{E_{\uparrow\downarrow\uparrow}^{(0)} - E_k^{(0)}} \tag{4.117}$$

and

$$V_{33}^{(2)} = E_{\downarrow\uparrow\uparrow}^{(2)} = \sum_k \frac{|\langle\downarrow\uparrow\uparrow| H_x |k\rangle|^2}{E_{\downarrow\uparrow\uparrow}^{(0)} - E_k^{(0)}} . \tag{4.118}$$

We note that there are only N non-vanishing contributions in each of the above sums, so that the evaluation of each sum is almost trivial. We have

$$E_{\uparrow\uparrow\downarrow}^{(2)}(j, h_x, h_z, \gamma) = -\frac{Nh_x^2}{12}\left(\frac{2}{h_z+\gamma} + \frac{1}{1+j-h_z+\gamma}\right) \tag{4.119}$$

and

$$E_{\uparrow\downarrow\uparrow}^{(2)}(j, h_x, h_z, \gamma) = -\frac{Nh_x^2}{12}\left(\frac{1}{h_z+\gamma} + \frac{1}{1+j-h_z-\gamma} + \frac{1}{h_z-\gamma}\right) = E_{\downarrow\uparrow\uparrow}^{(2)}(\gamma) . \tag{4.120}$$

We see here that the degeneracy in the states $|\uparrow\downarrow\uparrow\rangle$ and $|\downarrow\uparrow\uparrow\rangle$ is not lifted to second order in h_x.

Fourth order correction

The fourth order correction to the energy of the $|\uparrow\uparrow\downarrow\rangle$ state is given by

$$\begin{aligned} E_{\uparrow\uparrow\downarrow}^{(4)} = &\sum_{ijk} \frac{\langle\uparrow\uparrow\downarrow| H_x |i\rangle \langle i| H_x |j\rangle \langle j| H_x |k\rangle \langle k| H_x |\uparrow\uparrow\downarrow\rangle}{(E_{\uparrow\uparrow\downarrow}^{(0)} - E_i^{(0)})(E_{\uparrow\uparrow\downarrow}^{(0)} - E_j^{(0)})(E_{\uparrow\uparrow\downarrow}^{(0)} - E_k^{(0)})} \\ &- E_{\uparrow\uparrow\downarrow}^{(2)} \sum_k \frac{\langle\uparrow\uparrow\downarrow| H_x |k\rangle \langle k| H_x |\uparrow\uparrow\downarrow\rangle}{(E_{\uparrow\uparrow\downarrow}^{(0)} - E_k^{(0)})^2} . \end{aligned} \tag{4.121}$$

If we let $\{|a_r\rangle, r = 1, 2, \cdots, N\}$ be the set of states such that

$$\langle\uparrow\uparrow\downarrow| H_x |a_r\rangle \neq 0 , \tag{4.122}$$

that is if

$$\begin{aligned} |a_r\rangle \in \{ &|\uparrow\uparrow\downarrow\cdots\uparrow\uparrow\downarrow\uparrow\uparrow\uparrow\rangle, |\uparrow\uparrow\downarrow\cdots\uparrow\uparrow\downarrow\uparrow\downarrow\downarrow\rangle, |\uparrow\uparrow\downarrow\cdots\uparrow\uparrow\downarrow\downarrow\uparrow\downarrow\rangle, \\ &\cdots|\uparrow\downarrow\downarrow\uparrow\uparrow\downarrow\cdots\uparrow\uparrow\downarrow\uparrow\uparrow\downarrow\rangle, |\downarrow\uparrow\downarrow\uparrow\uparrow\downarrow\cdots\uparrow\uparrow\downarrow\uparrow\uparrow\downarrow\rangle \} , \end{aligned} \tag{4.123}$$

then equation (4.121) simplifies to

$$E^{(4)}_{\uparrow\uparrow\downarrow} = \sum_{rs}\left(\frac{\langle\uparrow\uparrow\downarrow|\,H_x\,|a_r\rangle\,\langle a_r|\,H_x\,|\uparrow\uparrow\downarrow\rangle}{(E^{(0)}_{\uparrow\uparrow\downarrow}-E^{(0)}_{a_r})(E^{(0)}_{\uparrow\uparrow\downarrow}-E^{(0)}_{a_s})}\sum_j\frac{\langle a_r|\,H_x\,|j\rangle\,\langle j|\,H_x\,|a_s\rangle}{E^{(0)}_{\uparrow\uparrow\downarrow}-E^{(0)}_j}\right) - E^{(2)}_{\uparrow\uparrow\downarrow}\sum_r\frac{|\langle\uparrow\uparrow\downarrow|\,H_x\,|a_r\rangle|^2}{(E^{(0)}_{\uparrow\uparrow\downarrow}-E^{(0)}_{a_r})^2}\,. \tag{4.124}$$

The procedures *fourthorder1* and *fourthorder2* evaluate the above sums as s_1 and s_2, respectively, where

$$\begin{aligned}\frac{16s_1}{h_x^4} &= \frac{2N}{3}\frac{1}{(-h_z-\gamma)^2}\left\{\frac{1}{-1-2h_z-2\gamma}+\frac{1}{-1-2\gamma}+\frac{1}{-j-2\gamma}+\frac{2N/3-3}{-2h_z-2\gamma}\right.\\ &\left.+\frac{N/3-2}{-1-j-2\gamma}+\frac{1}{-j-2h_z-2\gamma}\right\}+\frac{N/3(N/3-1)}{(-1-j+h_z-\gamma)^2(-2-2j+2h_z-2\gamma)}\\ &+\frac{N}{3}\frac{1}{(-1-j+h_z-\gamma)^2}\left\{\frac{2}{-1-2\gamma}+\frac{2}{-j-2\gamma}+\frac{2N/3-4}{-1-j-2\gamma}+\frac{N/3-1}{-2-2j+2h_z-2\gamma}\right\}\\ &+\frac{1}{(-h_z-\gamma)^2}\left\{\frac{2N/3}{-1-2h_z-2\gamma}+\frac{2N/3(2N/3-3)}{-2h_z-2\gamma}+\frac{2N/3}{-j-2h_z-2\gamma}\right\}\\ &+\frac{1}{(-h_z-\gamma)(-1-j+h_z-\gamma)}\left\{\frac{4N/3}{-1-2\gamma}+\frac{4N/3(N/3-2)}{-1-j-2\gamma}+\frac{4N/3}{-j-2\gamma}\right\}\end{aligned} \tag{4.125}$$

and

$$\frac{16s_2}{h_x^4} = -\left(\frac{2N}{3}\frac{1}{(-h_z-\gamma)^2}+\frac{N}{3}\frac{1}{(-1-j+h_z-\gamma)^2}\right)\left(\frac{2N}{3}\frac{1}{-h_z-\gamma}+\frac{N}{3}\frac{1}{-1-j+h_z-\gamma}\right)\,. \tag{4.126}$$

Upon adding equations (4.125) and (4.126) and noting the cancellation of the terms proportional to N^2, we obtain

$$\begin{aligned}\varepsilon^{(4)}_{\uparrow\uparrow\downarrow}(j,h_x,h_z,\gamma) &= \frac{h_x^4}{12}\frac{1}{(h_z+\gamma)^2}\left\{-\frac{1}{(1+2h_z+2\gamma)}+\frac{3}{2h_z+2\gamma}-\frac{1}{j+2h_z+2\gamma}\right\}\\ &+\frac{h_x^4}{24}\left\{\frac{1}{(h_z+\gamma)^2}+\frac{1}{(1+j-h_z+\gamma)^2}+\frac{2}{(h_z+\gamma)(1+j-h_z+\gamma)}\right\}\times\\ &\left\{-\frac{1}{1+2\gamma}-\frac{1}{j+2\gamma}+\frac{2}{1+j+2\gamma}\right\}+\frac{h_x^4}{48}\frac{1}{(1+j-h_z+\gamma)^3}\,,\end{aligned} \tag{4.127}$$

so that the fourth order correction to the ground state energy per spin of the $\uparrow\uparrow\downarrow$ state is given

by

$$\varepsilon^{(4)}_{\uparrow\uparrow\downarrow}(j,h_x,h_z,0) = \frac{h_x^4}{12}\frac{1}{h_z^2}\left\{-\frac{1}{1+2h_z}+\frac{3}{2h_z}-\frac{1}{j+2h_z}\right\} + \frac{h_x^4}{24}\left\{\frac{1}{h_z^2}+\frac{1}{(1+j-h_z)^2}+\frac{2}{h_z(1+j-h_z)}\right\}\left\{-1-\frac{1}{j}+\frac{2}{1+j}\right\} + \frac{h_x^4}{48}\frac{1}{(1+j-h_z)^3}\,. \tag{4.128}$$

Combining equations (4.112), (4.119) and (4.127), we have

$$\varepsilon_{\uparrow\uparrow\downarrow}(j,h_x,h_z,\gamma) = \frac{h_x^4}{12}\frac{1}{(h_z+\gamma)^2}\left\{-\frac{1}{(1+2h_z+2\gamma)}+\frac{3}{2h_z+2\gamma}-\frac{1}{j+2h_z+2\gamma}\right\} + \frac{h_x^4}{24}\left\{\frac{1}{(h_z+\gamma)^2}+\frac{1}{(1+j-h_z+\gamma)^2}+\frac{2}{(h_z+\gamma)(1+j-h_z+\gamma)}\right\}\times \left\{-\frac{1}{1+2\gamma}-\frac{1}{j+2\gamma}+\frac{2}{1+j+2\gamma}\right\}+\frac{h_x^4}{48}\frac{1}{(1+j-h_z+\gamma)^3} - \frac{h_x^2}{12}\left\{\frac{2}{h_z+\gamma}+\frac{1}{1+j-h_z+\gamma}\right\}-\frac{(1+j+2h_z)}{12}-\frac{\gamma}{2}\,. \tag{4.129}$$

The ground state energy of the longitudinal ANNNI model in the region bounded by the lines $2j+h_z=1$, $h_z=1$ and $2h_z+1=2j$, to fourth order in h_x is therefore given by

$$\varepsilon_{\uparrow\uparrow\downarrow}(j,h_x,h_z,0) = \frac{h_x^4}{12}\frac{1}{h_z^2}\left\{-\frac{1}{1+2h_z}+\frac{3}{2h_z}-\frac{1}{j+2h_z}\right\} + \frac{h_x^4}{24}\left\{\frac{1}{h_z^2}+\frac{1}{(1+j-h_z)^2}+\frac{2}{h_z(1+j-h_z)}\right\}\left\{-1-\frac{1}{j}+\frac{2}{1+j}\right\} + \frac{h_x^4}{48}\frac{1}{(1+j-h_z)^3}-\frac{h_x^2}{12}\left(\frac{2}{h_z}+\frac{1}{1+j-h_z}\right)-\frac{(1+j+2h_z)}{12}\,. \tag{4.130}$$

As noted earlier, the $\uparrow\uparrow\downarrow$ state as an eigenstate of the unperturbed Hamiltonian h_z has the unique property that it can be ground state only for finite h_z and finite j (in fact $j>0.5$). If $j=0$, the ground state is ferromagnetic for $h_z>1$ and antiferromagnetic otherwise. If $h_z=0$ the ground state is the four-fold degenerate antiphase configuration for $j>0.5$ and the two-fold degenerate configuration if $j<0.5$. One implication of this remark is that there are no special cases of equation (4.130).

Typical behaviour of $\varepsilon_{\uparrow\uparrow\downarrow}(j,h_x,h_z,0)$ as a function of h_x is plotted in figures 4.5(a) and 4.5(b). Comparing the two curves, it appears that $\varepsilon_{\uparrow\uparrow\downarrow}(j,h_x,h_z,0)$ is more sensitive to changes in j than in h_z.

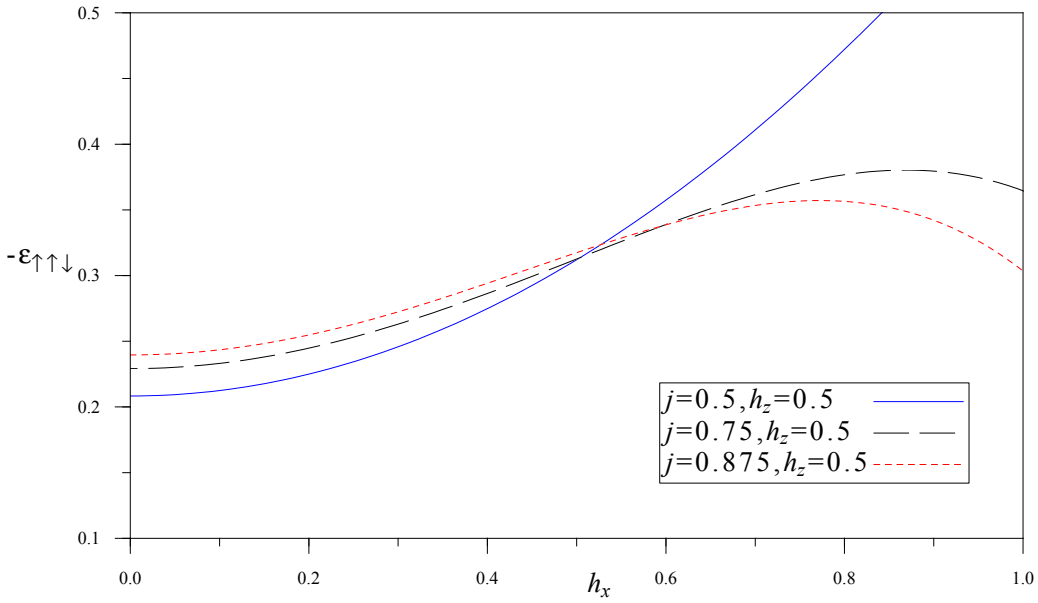

(a) $\varepsilon_{\uparrow\uparrow\downarrow}(j, h_x, h_z, 0)$ as a function of h_x for $h_z = 0.5$

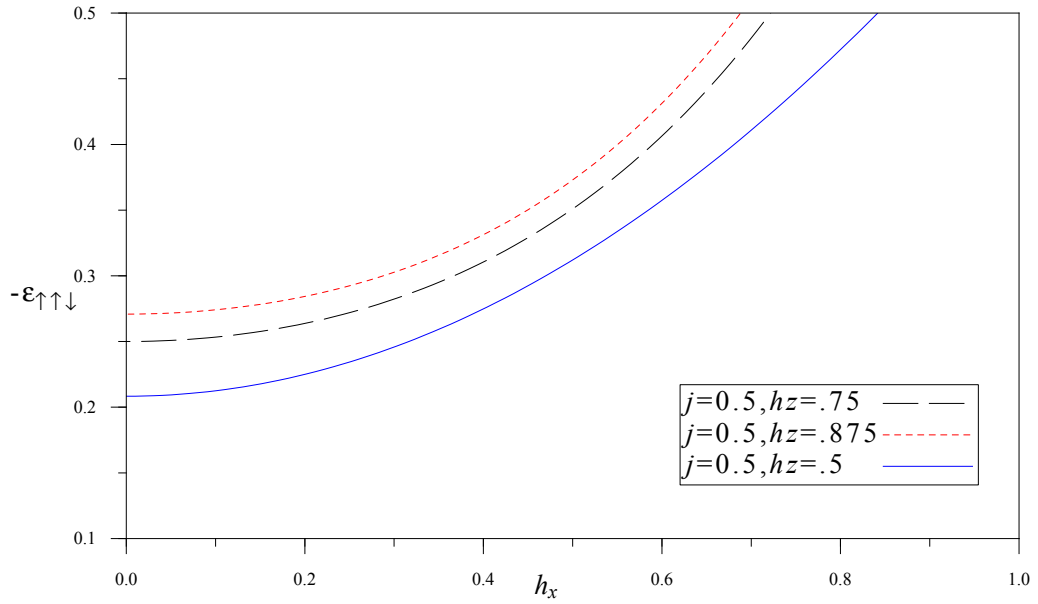

(b) $\varepsilon_{\uparrow\uparrow\downarrow}(j, h_x, h_z, 0)$ as a function of h_x for $j = 0.5$

Figure 4.5: $\varepsilon_{\uparrow\uparrow\downarrow}(j, h_x, h_z, 0)$ as a function of h_x

4.5.2 Physical quantities

Long range order parameter

From equations (4.111), (4.110) and (4.129) we obtain the long range order parameter $\rho_{\uparrow\uparrow\downarrow}$ of the $\uparrow\uparrow\downarrow$ state to fourth order in the perturbation h_x as

$$\begin{aligned}\rho_{\uparrow\uparrow\downarrow} = 1 &- \frac{h_x^2}{6}\left(\frac{2}{h_z^2}+\frac{1}{(1+j-h_z)^2}\right)+\frac{h_x^4}{3h_z^3}\left(-\frac{1}{1+2h_z}+\frac{3}{2h_z}-\frac{1}{j+2h_z}\right)\\ &-\frac{h_x^4}{6h_z^2}\left(\frac{2}{(1+2h_z)^2}-\frac{3}{2h_z^2}+\frac{2}{(j+2h_z)^2}\right)+\frac{1}{8}\frac{h_x^4}{(1+j-h_z)^4}\\ &-2h_x^4\left(\frac{1}{h_z^3}+\frac{1}{(1+j-h_z)^3}+\frac{1}{h_z^2(1+j-h_z)}+\frac{1}{h_z(1+j-h_z)^2}\right)\left(-1-\frac{1}{j}+\frac{2}{1+j}\right)\\ &-\frac{h_x^4}{6}\left(\frac{1}{h_z^2}+\frac{1}{(1+j-h)^2}+\frac{2}{h_z(1+j-h_z)}\right)\left(1+\frac{1}{j^2}-\frac{2}{(1+j)^2}\right)\end{aligned} \tag{4.131}$$

A typical behaviour of the long range order parameter is depicted in figure 4.6. To fourth order in perturbation, we see that the $\uparrow\uparrow\downarrow$ order of the ANNNI model in mixed fields vanish. That the model indeed does not possess long range order in the thermodynamic limit was confirmed by our finite size scaling results which showed that the model indeed undergoes a phase transition from the $\uparrow\uparrow\downarrow$ state to a paramagnetic phase.

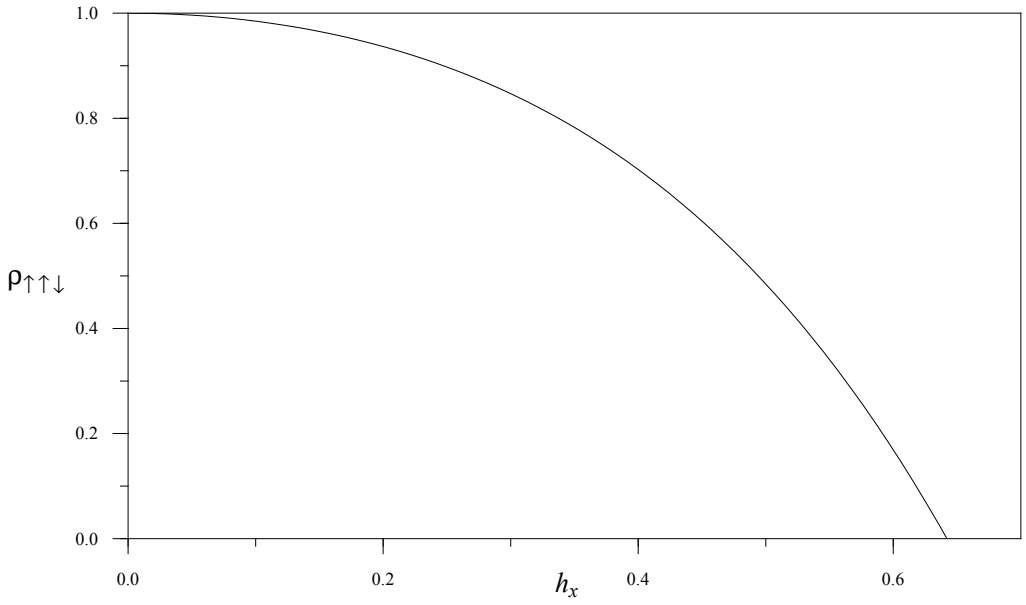

Figure 4.6: $\rho_{\uparrow\uparrow\downarrow}$ as a function of h_x to fourth order in h_x

Chapter 5

Finite size scaling

5.1 Introduction

In investigating the model (1.1)

$$H = \sum_i S_i^z S_{i+1}^z + j \sum_i S_i^z S_{i+1}^z - h_z \sum_i S_i^z - h_x \sum_i S_i^x$$

we have carried out finite-lattice calculations using the finite size scaling technique. The method introduced by the authors of reference [65] and later developed and generalized by the authors of reference [7] has turned out to be a valuable tool in evaluating critical behaviour from numerical results by extrapolating information obtained from a finite system to the thermodynamic limit [66, 67]. The technique gives reliable results for quite different models and different types of critical behaviour [66]. The main idea behind finite size scaling is the assumption that the operator corresponding to finite-size effects has a critical index equal to one or to put it differently, if a thermodynamic quantity diverges in the thermodynamic limit at some critical temperature $T = T_C$, then its behaviour as a function of $|T - T_C|$ can be parametrized for finite, but large, N by the same function of $1/N$ at the critical point

$$f\left(|T - T_C|\right) = f\left(\frac{1}{N}\right)\Big|_{T=T_C} . \tag{5.1}$$

A direct implementation of the finite-size scaling technique was applied to the transfer matrix by Nightingale [68] who recognized the strength of the method and showed how it can be reinterpreted as a renormalization group transformation of the infinite system [67]. The phenomenological renormalization equation for finite systems of sizes N and N' with respective correlation lengths ξ_N and $\xi_{N'}$ is given by [67]

$$\frac{\xi_N(T)}{N} = \frac{\xi_{N'}(T')}{N} \tag{5.2}$$

and has a fixed point at $T^{(N,N')}$. It is expected that the succession of points $\left\{T^{(N,N')}\right\}$ will converge to the true critical temperature T_C in the infinite size limit.

Equation (5.2) gives an implicit definition of a unique relationship between the original and renormalized temperatures T and T'.
The critical temperature, T_C is thus obtained from

$$N\Delta_N(T_C) = N'\Delta_{N'}(T_C) \tag{5.3}$$

where Δ_N and $\Delta_{N'}$ are the respective mass gaps (inverses of the correlation lengths ξ_N and $\xi_{N'}$). The critical exponent, ν_T, is obtained from

$$\nu_T = \frac{\partial N\Delta_N(T)}{\partial T} \Big/ \left.\frac{\partial N'\Delta_{N'}(T')}{\partial T'}\right|_{T=T'=T_C^{(N,N')}} \tag{5.4}$$

The finite size scaling method was employed to study quantum spin systems by Hamer and Barber [34] who established that finite size scaling is exact for the mass gap of the transverse Ising chain in the limit $N \to \infty$.

In a recent study of the field-induced magnetic order in cubic lattices of dimers with antiferromagnetic Heisenberg interactions, the authors of [69] obtained finite size scaling results which they believe to be of direct relevance to the spin-dimer systems $TlCuCl_3$ and $KCuCl_3$. Specifically, they found that the physical properties of the two coupled-dimer systems possess the same universal scaling behaviour despite large quantitative differences in their magnon dispersion relations.

A list of references on numerous successful applications of the finite size scaling technique (at nonzero temperature) to various quite different models is found in reference [66].

The finite size scaling technique is also gaining popularity in the study of quantum phase transitions (that is, phase transitions at zero temperature) that are driven by competition and quantum fluctuations alone, as opposed to conventional, thermally driven phase transitions. The author of reference [5] employed the finite size scaling technique to investigate the quantum phase transitions in the Ising model in spatially modulated field and obtained the ferromagnetic to paramagnetic phase transition diagram of the model. The model was found to belong to the

universality class of the two dimensional Ising model. In reference [67], the finite size scaling was employed directly (that is without making explicit analogy to classical statistical mechanics) to study the critical behaviour of quantum Hamiltonians. The authors also reported their success in an earlier study where the critical charges for two- and three-electron atoms were obtained by combining finite size scaling with transfer matrix calculations of a classical pseudosystem.

The general idea behind the finite size scaling technique, as applied to quantum systems is the following. Let λ be a parameter of the quantum Hamiltonian playing the role of temperature and which has as its critical value λ_C. The correlation length $\xi \backsim |\delta\lambda|^{-\nu}$, where the reduced coordinate $\delta\lambda$ is defined by $\delta\lambda = (\lambda - \lambda_C)/\lambda_C$, diverges with the critical exponent ν. At the transition point, the mass gap $\Delta(\lambda)$ vanishes inversely as the correlation length and for finite sizes the mass gap variation is given by [4]

$$\Delta(\lambda, N) \backsim N^{-1} f\left(\delta\lambda N^{1/\nu}\right) \tag{5.5}$$

where $f(x) \backsim x^{\nu}$ as $x \to 0$. Hence for two system sizes N and N' we obtain at the critical point

$$N\Delta(\lambda_C, N) = N'\Delta(\lambda_C, N') \tag{5.6}$$

We have employed the finite size scaling ansatz (5.6) to determine the critical points (h_{x_C}, h_{z_C}) of the one dimensional ANNNI model in non-commuting external magnetic fields, described by Hamiltonian (1.1)

$$H = \sum_{i=1}^{N} S_i^z S_{i+1}^z + j \sum_{i=1}^{N} S_i^z S_{i+2}^z - h_x \sum_{i=1}^{N} S_i^x - h_z \sum_{i=1}^{N} S_i^z$$

We took advantage of the translational symmetry of the Hamiltonian under periodic boundary conditions to drastically reduce the dimensions of the Hilbert space of the spin systems in the total S_z basis. The Hamiltonian H was diagonalized in the orthogonal subspaces of the translation operator. This is discussed in some detail in appendix A.

We recall from the phase diagram of the one-dimensional ANNNI model in a longitudinal field figure 3.18 that there are four different ground state structure of the model in the absence of the transverse field h_x. We have investigated the effect of the quantum fluctuations introduced by the perpendicular field on the existing order in three of the four regions, excluding the ferromagnetic region, and our findings are reported in the following sections.

One of the reasons our model (1.1) is interesting to study is the fact that it is an embodiment of various models (depending on the choice of j, h_x and h_z). Some of these models are exactly

solvable (for example the Ising model in a transverse field, corresponding to $j = 0 = h_z$ and the ANNNI model ($h_x = h_z = 0$)), while the phase diagrams of the others (the ANNNI model in a transverse field or the model studied in reference [3] for example) can only be estimated using approximation techniques. We applied the finite scaling technique to obtain the phase diagram of our model, Hamiltonian (1.1) (the ANNNI model with non-commuting fields). In addition to our new results, we were also able to verify the ones known in the literature.

5.2 The transverse Ising model

With $j = 0 = h_z$ in the Hamiltonian (1.1), the resulting Hamiltonian is

$$H = \sum_i S_i^z S_{i+1}^z - h_x \sum_i S_i^x \tag{5.7}$$

which describes the one-dimensional Ising model in a transverse field h_x. The model (5.7), an exactly-solvable one-dimensional model, is well studied. At zero temperature, the antiferromagnetic order in the ground state is destroyed at $h_x = 0.5$ [3, 15]. An application of the finite size scaling method confirms this result, giving the critical value of $h_x = 0.5002$ with the critical exponent $\nu = 1.074$ (compared with the exact value of $\nu = 1$). The variation of the energy gap with h_x is plotted in figure 5.1(a) while the scaling of the energy gaps is depicted in figure 5.1(b). The dependence of the energy gap on h_x for 12 spin sites, $\Delta 12$, in the neighbourhood of the critical point $h_x = .5002$ may be approximated by the fourth degree polynomial

$$12\Delta_{12} = c_0 + c_1 h_x + c_2 h_x^2 + c_3 h_x^3 + c_4 h_x^4 \tag{5.8}$$

where the coefficients are $c_0 = -20.284843$, $c_1 = 182.9425$, $c_2 = -608.25998$, $c_3 = 873.91558$ and $c_4 = -447.48087$. The standard error in the fit is 0.0002142 and the correlation coefficient is 0.9999999.

5.3 The Ovchinnikov model

Next we applied the finite size scaling ansatz to another model whose phase diagram has been obtained; the antiferromagnetic Ising model in the presence of two mutually perpendicular fields described by the Hamiltonian

$$H = \sum_i S_i^z S_{i+1}^z - h_x \sum_i S_i^x - h_z \sum_i S_i^z \tag{5.9}$$

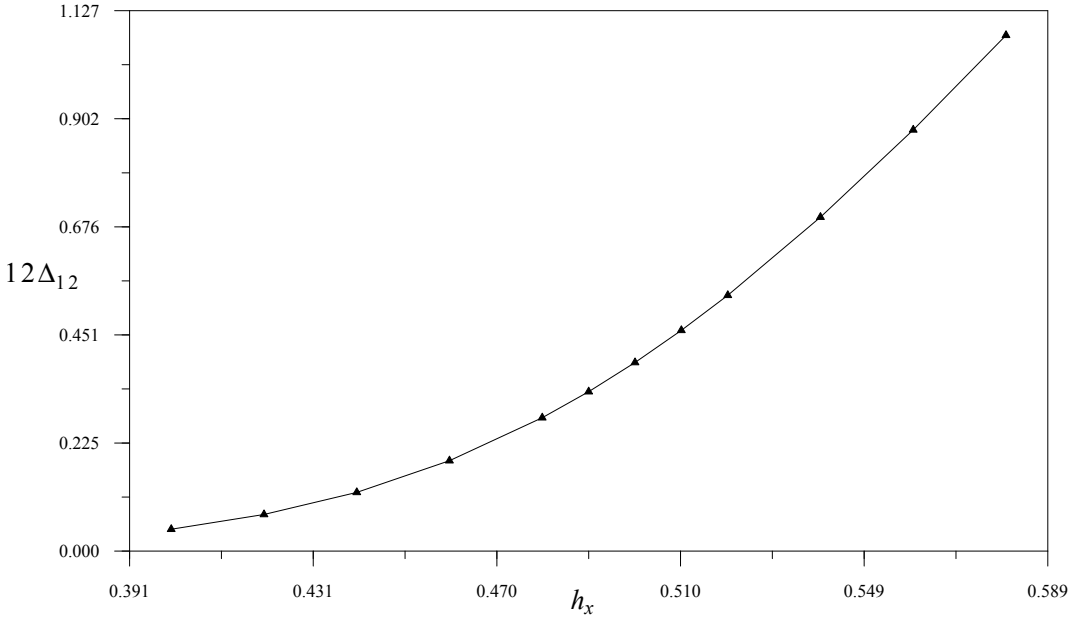

(a) The scaled mass gap as a function of h_x for $j = 0$ and $h_z = 0$

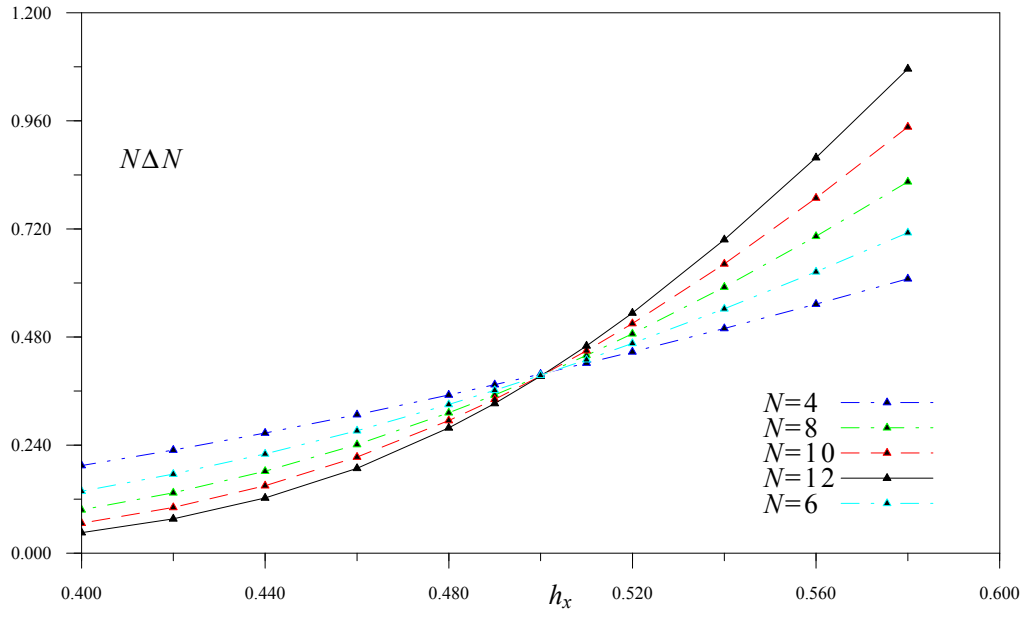

(b) The scaled mass gap vs. h_x for various system sizes for $j = 0$ and $h_z = 0$

Figure 5.1: Scaled mass gap. The points of intersection give the critical points h_{x_C}

This model corresponds to our model without next nearest neighbour spins interactions, that is $j = 0$ in the Hamiltonian (1.1). The authors of reference [3] carried out density matrix renormalization group (DMRG) calculations and obtained the critical line of the model. The authors also concluded that the antiferromagnetic Ising model in mixed field is in the same universality class as the classical two-dimensional Ising model. Our finite size scaling results reproduced the phase diagram for this model, as expected. The scaled mass gap is plotted in figure 5.2 while the resulting phase diagram for $j = 0$, based on the collection of points (h_{x_C}, h_{z_C}) is displayed in figure 5.3.

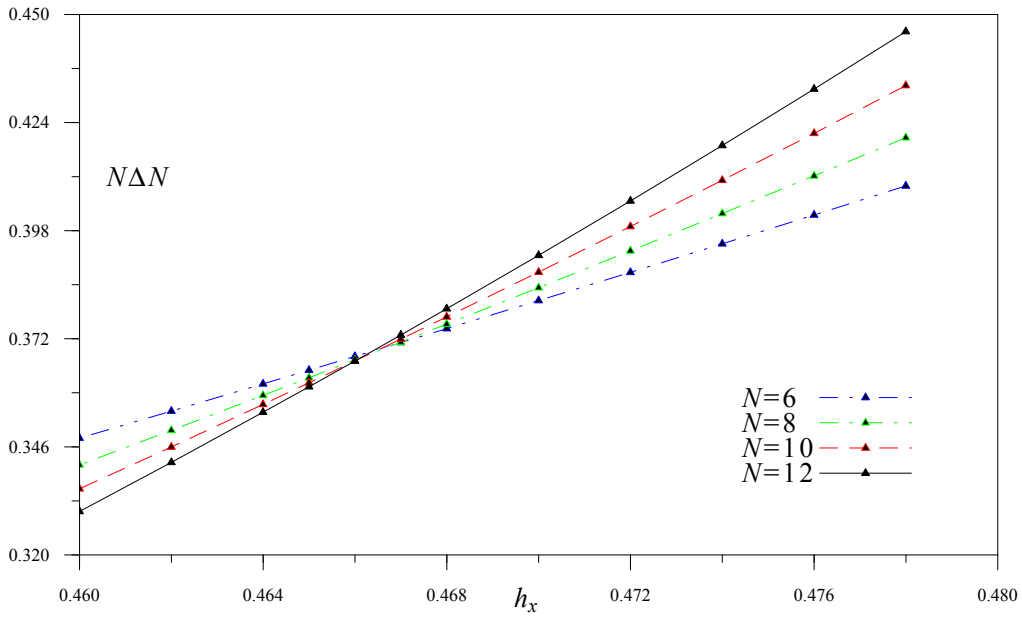

Figure 5.2: Typical scaled mass gap for various system sizes for $j = 0$. The points shown here are taken at $h_z = 0.3$. The point of intersection gives the critical point h_{x_C}

5.4 The antiferromagnetic ANNNI model in non-commuting fields

After having reproduced the phase diagram of the antiferromagnetic Ising model in mixed fields ($j = 0$, $0 < h_z < 1$), we next considered the effect of next nearest neighbour interactions. We investigated the Hamiltonian (1.1) for $j = 0.2$, $0 < h_z < 0.6$ and $j = 0.4$, $0 < h_z < 0.2$. In each case the critical line separating the antiferromagnetic phase from the paramagnetic phase was obtained. The resulting phase diagrams for $j = 0.2$ and $j = 0.4$ based on the collection of critical

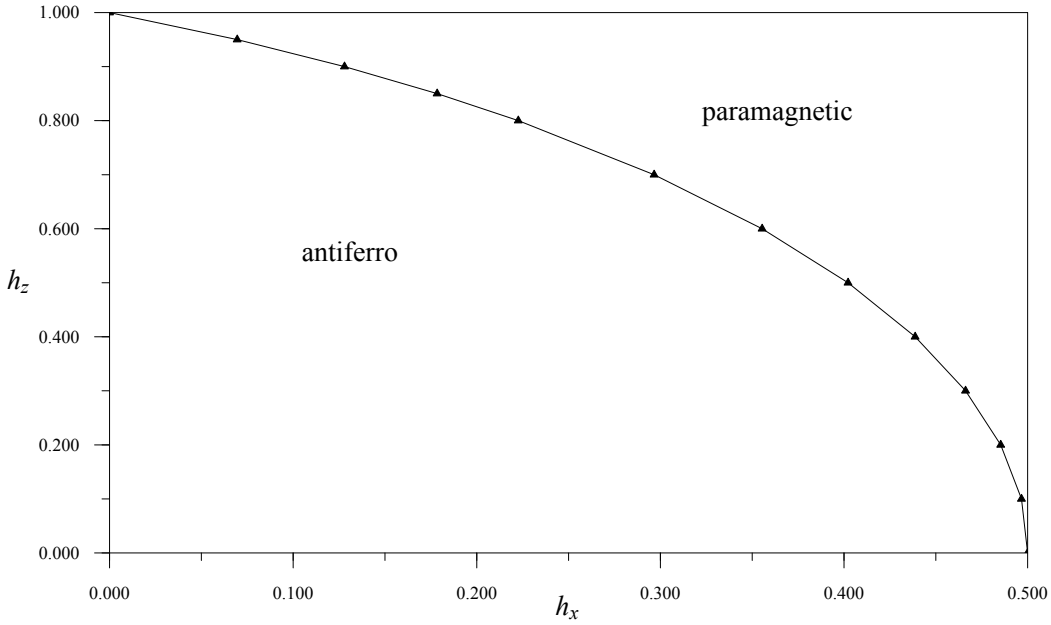

Figure 5.3: Phase boundary separating the paramagnetic from the antiferromagnetic states for $j = 0$

points (h_x, h_z) from finite size scaling are displayed in figure 5.4. In both cases the transition is from the ordered antiferromagnetic to paramagnetic phase.
There is no qualitative difference in the phase diagrams for $j = 0.2$ and $j = 0.4$ and that of the model studied in Reference [3] (corresponding to $j = 0$). This is probably not surprising since in the absence of the perpendicular field h_x, the ground state of Hamiltonian (1.1) is antiferromagnetic in the region $2j + hz < 1$ as can be seen from the $h_x = 0$ phase diagram. We remark that although the classical phase diagrams in figure 2.1 turned out not surprisingly to be inaccurate, they indeed provided a good insight into the correct phase diagrams of figure 5.4.

5.5 The ANNNI model in a transverse field: $h_z = 0$

The one-dimensional transverse ANNNI model is another model whose phase diagram has been obtained using various methods. Arizmendi et. al. [37] used Monte Carlo simulations to obtain the continuous phase boundary separating the ferromagnetic states from the paramagnetic phase, and that separating the paramagnetic states from the four-fold degenerate $< 2 >$ antiphase states. Sen [25] applied the interface approach to the model and obtained similar diagrams. There were

also speculations concerning the existence of floating phases close to the antiphase regions [4, 25]. Recently, Guimarães et. al. [33] employed the finite size scaling technique to obtain the second order phase transitions in the same model. We remark that all the above references investigated the ferromagnetic model. We have applied the finite size scaling technique to obtain the phase diagram of the antiferromagnetic ANNNI model in a transverse field. The Hamiltonian is given by $h_z = 0$ in equation (1.1), that is

$$H = \sum_i S_i^z S_{i+1}^z + j \sum_i S_i^z S_{i+2}^z - h_x \sum_i S_i^x \tag{5.10}$$

The application of an external magnetic field h_x destroys the existing antiferromagnetic order which exists for $j < 0.5$ in zero field. The critical line between the antiferromagnetic phase and the disordered states was obtained. As j is increased beyond 0.5 under the influence of the external perpendicular field h_x, the ground state of the system became ordered and the continuous transition line separating the paramagnetic phase from the antiphase region was also determined. The phase diagram of the antiferromagnetic ANNNI model in a transverse field based on the finite size scaling data points is exhibited in figure 5.5

5.6 The ANNNI model in non-commuting fields: $h_z = 0.2$

As discussed in the preceding section, there are three main regions in the phase diagram of the transverse ANNNI model– the ordered antiferromagnetic region, the paramagnetic region and the ordered period-4 $< 2 >$ antiphase region as shown in figure 5.5.

The introduction of a finite external longitudinal field h_z changes this picture completely! A third ordered phase appears and the phase diagram becomes richer. First the antiferromagnetic order gives way to the disordered paramagnetic region. Order begins to set in again as j is increased beyond 0.4 (for $h_z = 0.2$) and the new ground state is the period 3 $\uparrow\uparrow\downarrow\uparrow\uparrow\downarrow$ spin configuration. For low values of the field h_x the period 3 ground state order disappears and antiphase order appears. For relatively high values of h_x however, there is a small paramagnetic area between the period 3 phase and the period 4 antiphase ground state as can be seen in figure 5.6.

The critical exponents were calculated and tabulated in table 5.1. From the table $\nu \approx 1$, so that the ANNNI model in mixed fields is still in the same universality class as the zero field classical two-dimensional ANNNI model. The phase diagram obtained from the finite size scaling data points is shown in figure 5.6.

The richness of the phase diagram is not surprising when one examines the phase diagram of the one-dimensional ANNNI model in longitudinal field as discused under section 3. The ground state is the two-fold degenerate antiferromagnetic state for $2j + h_z < 1$, the four-fold degenerate antiphase states for $2h_z + 1 < 2j$, and the period 3 $\uparrow\uparrow\downarrow\uparrow\uparrow\downarrow \cdots$ in the region bounded by the lines $2j + h_z < 1$ and $2h_z + 1 < 2j$ in the $h_z - j$ plane. Thus in the absence of the longitudinal field ($h_z = 0$, transverse ANNNI model), only the antiferromagnetic order (for $j < 0.5$) and the antiphase order (for $j > 0.5$) exist. In this situation the frustration introduced by the presence of the transverse field destroys the antiferromagnetic order for $j < 0.5$ while as the next nearest neighbour interactions become stronger $j > 0.5$ the competition combines with the frustration to produce a new order, the antiphase alignment. For a finite longitudinal field h_z however, there is the additional period 3 ground state structure to consider.

As far as the estimation of continuous phase boundaries is concerned therefore, the exact solvability of the longitudinal ANNNI model already gives one a rough idea of what to expect in the presence of quantum fluctuations. The main point is then the accurate determination of the transition lines, a task which the finite size scaling technique handles very well.

j	h_{x_c}	ν
0	0.48518	1.07281
0.1	0.397037	1.064492
0.2	0.30105	1.042743
0.3	0.19032	0.964838
0.5	0.265	0.907053
0.6	0.39016	1.0762272
0.7	0.498	1.191895

Table 5.1: Critical field and corresponding critical exponent for the phase boundary of the ANNNI model in non-commuting fields.

5.7 The ANNNI model in non-commuting fields: $h_z = 0.5$

Increasing the strength of the longitudinal field h_z to 0.5 produced an interesting effect on the phase diagram of the ANNNI model in mixed fields. It became possible to determine accurately

the phase boundary where the period 3 ground state structure disappears. This can be easily seen in the phase diagram shown in figure 5.7 where around $j > 0.7$ the critical line takes a downward turn. The convergence and smoothness of the data points indicate that this is clearly a second order phase transition. This however does not rule out the possibility of the existence of floating phases in the region as well. This will have to be investigated using other means, since the finite size scaling works well and gives accurate results only in the determination of continuous phase boundaries.

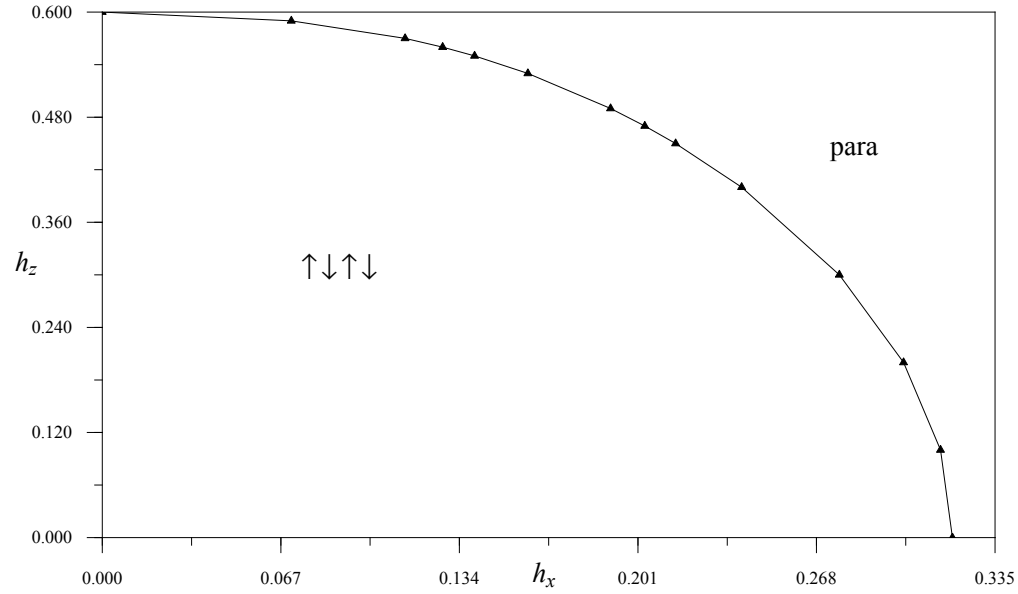

(a) Critical line between antiferromagnetic phase and paramagnetic phase for $j = 0.2$

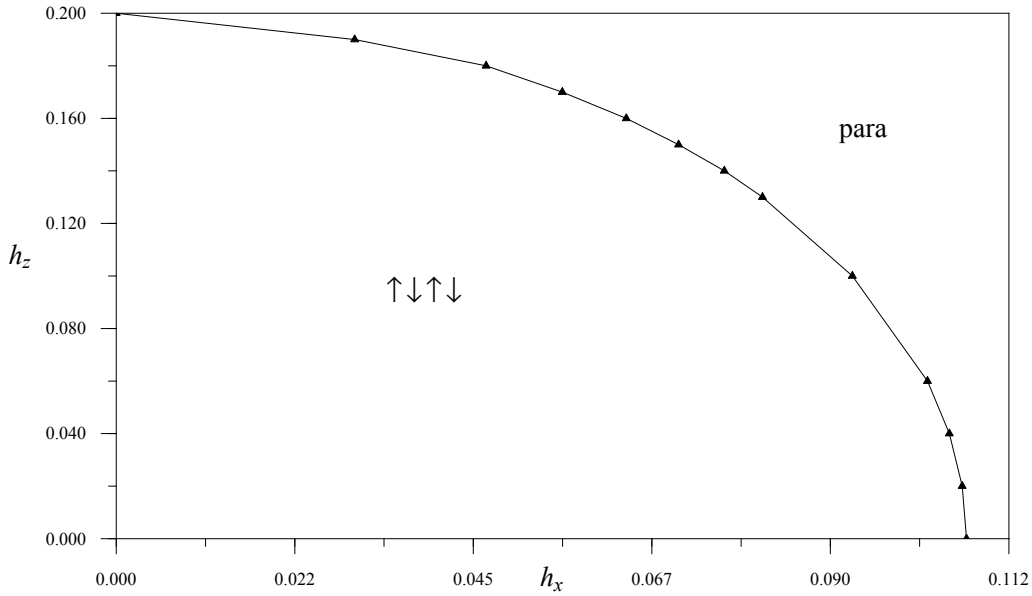

(b) Critical line between antiferromagnetic phase and paramagnetic phase for $j = 0.4$

Figure 5.4: Phase boundary between antiferromagnetic and paramagnetic regions for the one dimensional ANNNI model in mixed longitudinal field h_z and transverse field h_z

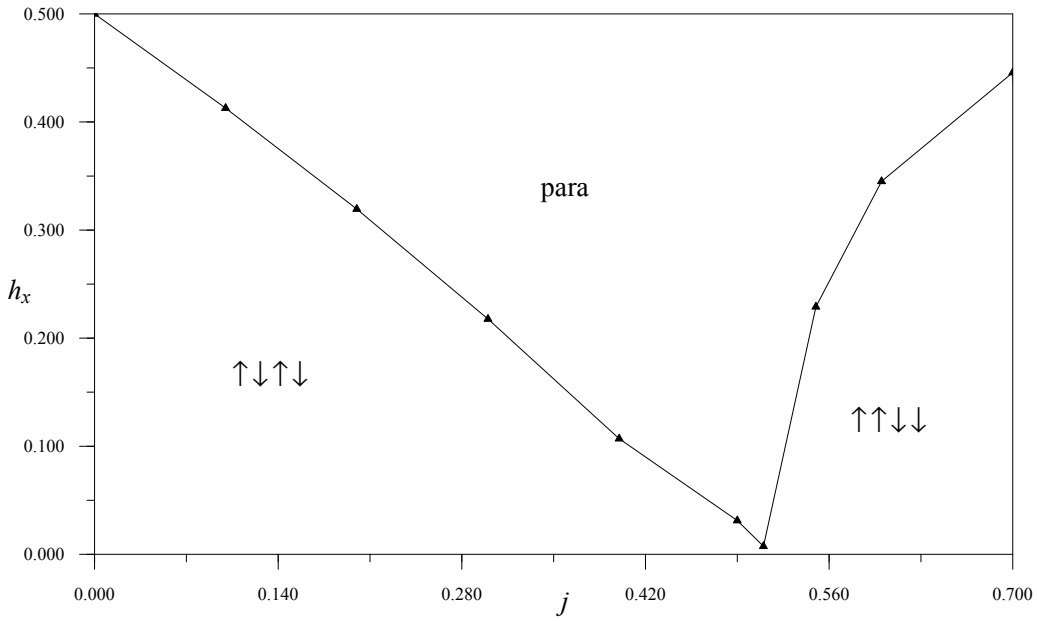

Figure 5.5: $T = 0$ phase diagram of the transverse ANNNI model

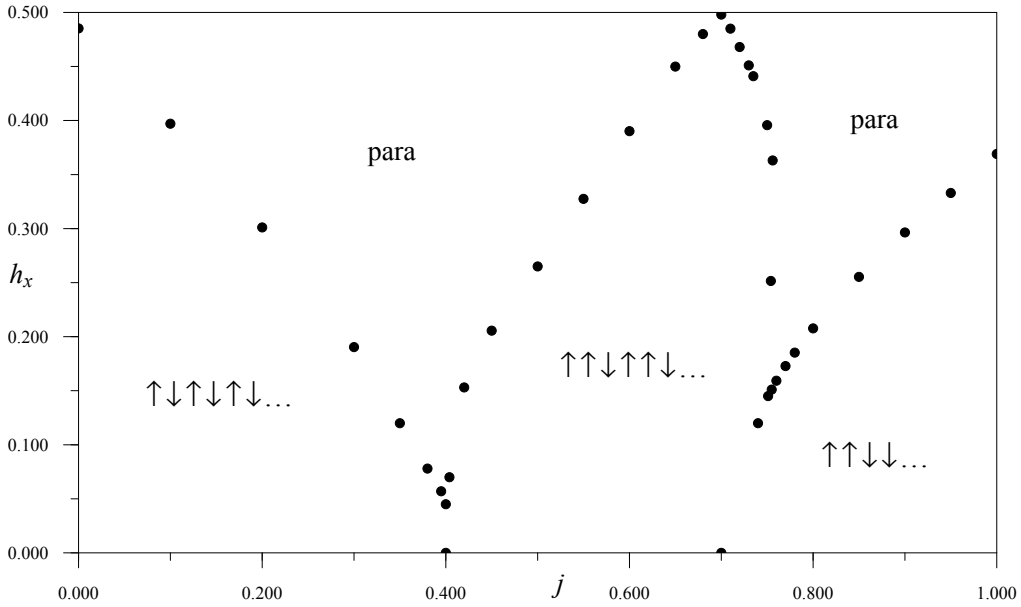

Figure 5.6: $T = 0$ phase diagram of the ANNNI model in mixed fields for $h_z = 0.2$

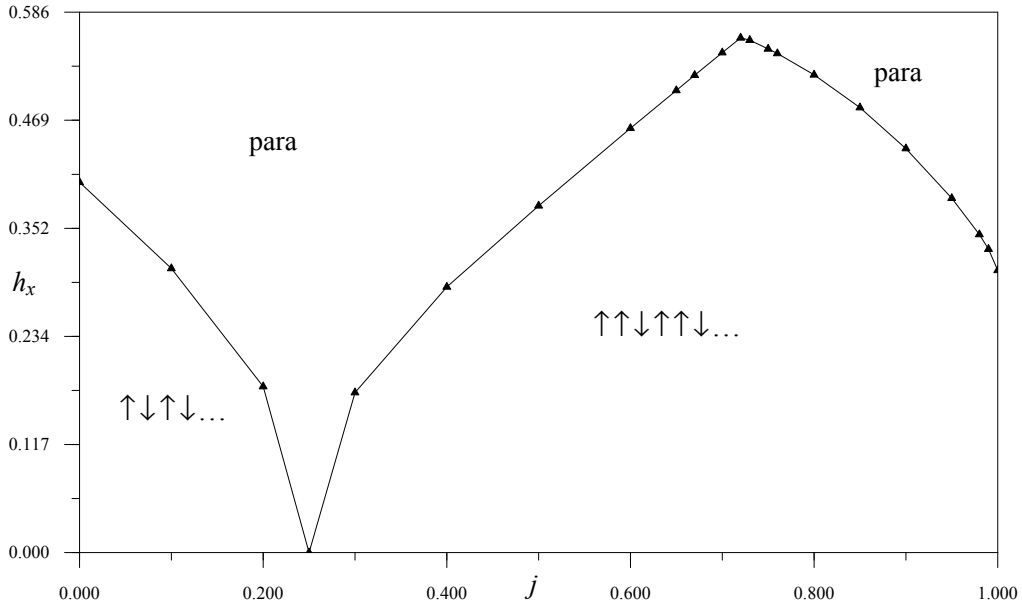

Figure 5.7: $T = 0$ phase diagram of the ANNNI model in mixed fields for $h_z = 0.5$

Chapter 6

Summary

In this thesis we have investigated the ANNNI model in noncommuting magnetic fields h_x and h_y, described by the Hamiltonian

$$H(j, h_x, h_z) = \sum_i S_i^z S_{i+1}^z + j \sum_i S_i^z S_{i+2}^z - h_x \sum_i S_i^x - h_z \sum_i S_i^z$$

where the parameters j, h_x and h_z are all nonnegative.

In the first part of chapter 2 we gave a spin wave treatment of the ANNNI model and of the transverse ANNNI model respectively. The ground state energy was calculated in both cases and antiferromagnetic long range order was predicted for the ANNNI model. In the second part, the spins were treated as classical vectors and the configurations minimizing the energy were sought, in order to gain an insight into the nature of the ground state of the model. As it turned out, the resulting phase diagram was not accurate. This is of course not surprising, since a classical model can probably not be expected to simulate a quantum system correctly.

In chapter 3, the nature of the zero temperature ground state of the one-dimensional spin-1/2 ANNNI model in a longitudinal magnetic field was investigated. The original intention was to prepare the stage for a systematic perturbation expansion of the full Hamiltonian, treating the quantum fluctuation term $-h_x \sum_i S_i^x$ as a perturbation. It turned out that the longitudinal ANNNI model in itself and on its own account was worth being studied. We found that there are four different possible ground state configurations in the thermodynamic limit. In the region above the line $h_z = 1 + j$ and bounded by the h_z axis in the $h_z - j$ plane, the ground state of the longitudinal ANNNI model is the nondegenerate ferromagnetic state, with ground state energy per spin $(1 + j - 2h_z)/4$. Below the ferromagnetic region and bounded by the two lines $2j + 1 = h_z$ and $2h_z + 1 = 2j$, the ground state was found to be the three-fold degenerate $\uparrow\uparrow\downarrow$

configuration with energy per spin $-(1+j+h_z)/12$. This region is rather interesting because it exists only when h_z and j are both finite. The ground state of the longitudinal ANNNI model is the two-fold degenerate antiferromagnetic configuration in the region below the line $2j+h_z=1$ and bounded by the j axis and the h_z axis. The antiferromagnetic ground state energy per spin is $(-1+j)/4$. Below the line $2h_z+1=2j$ and bounded by the j axis the longitudinal ANNNI model has as its ground state the four-fold degenerate $\uparrow\uparrow\downarrow\downarrow$ configuration as the ground state (the so-called antiphase states denoted $<2>$), with energy per spin $-j/4$. The points $j=1/2$ and $h_z=1$ are multiphase points of the model. The zero temperature phase diagram of the longitudinal ANNNI model is plotted in figure 3.18. In addition to obtaining the $T=0$ phase diagram of the model, the various symmetries (translation, reflection and sometimes inversion) and their interconnections and ways of gainfully employing them to reduce the dimension of the Hilbert space for exact diagonalization of large systems were also discussed in considerable detail. It is hoped that these will be found useful in future research.

Chapter 4 was concerned with developing Rayleigh-Schrödinger perturbation series for the ground state energy of the ANNNI model in noncommuting fields. Naturally, the longitudinal ANNNI model was taken as the unperturbed Hamiltonian and the quantum fluctuation term $-h_x\sum_i S_i^x$ was treated as the perturbation. The expansions were carried out in each of the four regions that were established in Chapter 3. The knowledge of the ground state energy of our Hamiltonian was sufficient for calculating the order parameters and other quantities since the necessary expectation values could be obtained using Feynman's theorem [60]. Whenever necessary, an additional field was introduced in the unperturbed Hamiltonian to ensure that the order parameter terms were correctly simulated (as suggested by Barber [22]).

The ANNNI model in noncommuting fields was investigated numerically in chapter 5 using the finite size scaling technique to understand the effect of quantum fluctuations introduced by the transverse field h_x on the existing order (as established in chapter 3). The full Hamiltonian (finite j, h_x and h_z) was investigated, as well as special cases, in order to be able to compare with known results. The finite size method turned out to be rather very accurate. For the Ising model ($h_z=0=j$), our finite size scaling gave the critical value of $h_{x_C}=0.5002$ for the vanishing of the mass gap, which is in very good agreement with the exact resul of $h_{x_C}=0.5$ [3, 15]. The critical exponent was also found to be $\nu=1.074$, which compares well with the exact result of $\nu=1$. For the model studied by Ovchinnikov et al. [3], that is $j=0$ in our model, the agreement is also excellent. In fact we were able to reproduce the phase diagram for the antiferromagnetic Ising model as obtained in reference [3]. The phase diagram which we obtained for the ANNNI model in a transverse field $h_z=0$ in our model is similar to the ones obtained by previous

researchers, with the ferro region replaced by antiferro in our case. For the full Hamiltonian, we found that all the three types of order considered (antiferro, antiphase and $\uparrow\uparrow\downarrow$) vanish on certain critical lines (See figure 5.6). The ferromagnetic region was not investigated in this thesis.

6.1 Suggestions

We have investigated the ANNNI model in noncommuting longitudinal and transverse fields h_x and h_z. Our results are as summarized above. Due to time limitation, there are a number of aspects which may be interesting, but which were not investigated.

- It is believed that the technique of linked clusters is more efficient for making perturbation expansions for many body systems, as it handles divergences in a smart way [64, 70]. It would be nice to carry out a linked cluster expansion in the future, for the Hamiltonian studied in this model.

- As we have demonstrated in this thesis, finite size scaling is a powerful technique which yields accurate results. The shortcoming of the method is that it is capable of describing only second-order phase transitions. A workaround has been suggested by Xavier et al. [71] which will make it possible to also estimate first order transitions. It would be nice to have this implemented.

- Part of our results is that the longitudinal ANNNI model has a ferromagnetic ground state in the region above the line $h_z = 1 + j$. In the finite-size scaling calculations, we have not investigated what happens to this spin order when the longitudinal ANNNI model is perturbed with a transverse field.

Chapter 7

Zussamenfassung

Gegenstand dieser Arbeit war die Untersuchung des eindimensionalen Spin-1/2 Ising Modells mit Übernächster - Nachbar Wechselwirkung (das sog. ANNNI Modell) in nichtkommutierenden magnetischen Feldern.

Als Ausgangspunkt behandelten wir die Spins als klassische Vektoren um eine Abschaetzung des Phasendiagramms zu erhalten. Diesem folgte eine Untersuchung des T=0 Grundzustandes des eindimensionalen Spin-1/2 ANNNI Modells mit longitudinalem Feld. Durch Ausnutzen der Symmetrieeigenschaften des Hamiltonians, war es möglich das longitudinale Modell exakt zu diagonalisieren. Wir fanden heraus, dass es im thermodynamischen Limes vier mögliche, voneinander verschiedene Grundzustandskonfigurationen gibt.

Dann wurde für das ANNNI Modell mit nichtkommutierenden Feldern die Grundzustandsenergie in den vier geordneten Regionen mittels Raleigh Schrödinger Störungsentwicklung entwickelt. Sowohl Ordnugsparameter mit zugehörigen Suszeptibilitäten als auch spezifische Wärmen wurden berechnet. Durch Anwendung der finite-size scaling Technik war es möglich die Phasengrenzen des Modells numerisch zu erhalten. Für gewisse Grenzfälle des gesamten Hamiltonians wurde ein Vergleich mit Literaturdaten durchgeführt und gute Übereinstimmung erzielt.

Appendix A

Symmetries

The Hilbert space corresponding to a system of N spins $\frac{1}{2}$ atoms is 2^N dimensional. Exact diagonalization of such systems can be quite formidable, due to the exponential increase in the dimensions of the Hamiltonian matrix with increasing N. When the symmetries of the system are gainfully employed however, the diagonalization process can be considerably simplified, since a Hamiltonian can be diagonalized in the degenerate-eigenvalued subspaces of its symmetries. In this appendix we will discuss the symmetries of our Hamiltonian, the ANNNI model in the presence of a longitudinal field h_z and a transverse field h_x. We recall equation (1.1)

$$H = \sum_i S_i^z S_{i+1}^z + j \sum_i S_i^z S_{i+2}^z - h_z \sum_i S_i^z - h_x \sum_i S_i^x \tag{1.1}$$

It is convenient to choose a system of basis vectors in which S_i^z is diagonal.

For a single spin$-1/2$ particle, with $S = \pm 1$ and S_z basis states $|S\rangle$ and $|-S\rangle$, the spin operators S_x, S_y and S_z satisfy

$$S^x |S\rangle = |-S\rangle$$
$$S^y |S\rangle = iS |-S\rangle$$

and

$$S^z |S\rangle = S |S\rangle \tag{A.1}$$

We can therefore write the S_i^z direct product basis vectors, spanning the 2^N-dimensional Hilbert space associated with the Hamiltonian, in the form $|S_1 S_2 \cdots\cdots S_i \cdots S_N\rangle$ so that

$$S_i^z \left|S_1 S_2 \cdots\cdots S_i \cdots S_N\right\rangle = S_i \left|S_1 S_2 \cdots\cdots S_i \cdots S_N\right\rangle \tag{A.2}$$

where $S_i = \pm 1$.

In this work, we have exploited the translational invariance of the Hamiltonian and the spin reflection symmetry to simplify the diagonalization of the Hamiltonian. When $h_z = 0$, we have also used all-spins inversion symmetry. These symmetries will be discussed in the following sections. In particular we will have more to say on the translational symmetry because it simplified the diagonalization processes tremendously.

A.1 The spin reflection symmetry $\mathcal{R}$

Definition 1. We define the spin reflection operator $\mathcal{R}$ by its action on an arbitrary direct-product state $|S_1 S_2 \cdots S_i \cdots S_{N-1} S_N\rangle$ as follows:

$$\mathcal{R}\left|S_1 S_2 \cdots S_i \cdots S_{N-1} S_N\right\rangle = \left|S_N S_{N-1} \cdots S_{N-i+1} \cdots S_2 S_1\right\rangle \tag{A.3}$$

Clearly, $\mathcal{R}^2 = \mathbb{1}$, so that the eigenvalues of $\mathcal{R}$ are ± 1. If any two states $|u\rangle$ and $|v\rangle$ (each of which may be linear combinations of the direct-product basis states) are related by reflection, then we must have

$$R\left|u\right\rangle = \left|v\right\rangle$$

and

$$R\left|v\right\rangle = \left|u\right\rangle \tag{A.4}$$

The usefulness of equation (A.4) stems from the fact that although $|u\rangle$ and $|v\rangle$ may separately not be eigenstates of $\mathcal{R}$, their linear combinations always are.

$$\begin{aligned} \mathcal{R}\left(\left|u\right\rangle + \left|v\right\rangle\right) &= 1\left(\left|u\right\rangle + \left|v\right\rangle\right) \\ \mathcal{R}\left(\left|u\right\rangle - \left|v\right\rangle\right) &= -1\left(\left|u\right\rangle - \left|v\right\rangle\right) \end{aligned} \tag{A.5}$$

As will be proved in section A.3, $\mathcal{R}$ and $\mathcal{T}$ commute in the $k = 0$ and $k = N/2$ subspaces of the eigenstates of $\mathcal{T}$. In the $k = 0$ and $k = N/2$ subspaces, R can be diagonalized, and thereafter

H can then be diagonalized in the two subspaces of the eigenstates of $\mathcal{R}$ (corresponding to eigenvalues $+1$ and -1). Examples of the simplification which arises from the combined use of the symmetries $\mathcal{R}$ and $\mathcal{T}$ are given in chapter 3 for $N = 6$, $N = 7$ and $N = 8$.

Presently we prove that $\mathcal{R}$ is a symmetry of the Hamiltonian H given by equation (1.1).

Theorem A.1.1.

$$[\mathcal{R}, H] = 0$$

Proof. Since H and $\mathcal{R}$ are linear operators and the S_z direct product states form a complete orthonormal basis for the Hilbert space of N spins, it is sufficient to prove that

$$\mathcal{R}H\,|\psi\rangle = H\mathcal{R}\,|\psi\rangle \tag{A.6}$$

for any arbitrary $|\psi\rangle = |S_1 S_2 \cdots S_{N-1} S_N\rangle$.
We write

$$H = H_1 + H_2 + H_3 + H_4\,, \tag{A.7}$$

where

$$H_1 = \sum_{i=1}^{N} S_i^z S_{i+1}^z\,, \tag{A.8}$$

$$H_2 = j \sum_{i=1}^{N} S_i^z S_{i+2}^z\,, \tag{A.9}$$

$$H_3 = -h_z \sum_{i=1}^{N} S_i^z\,, \tag{A.10}$$

and

$$H_4 = -h_x \sum_{i=1}^{N} S_i^x\,. \tag{A.11}$$

$$\begin{aligned} H_1\,|\psi\rangle &= H_1\,|S_1 S_2 \cdots S_{N-1} S_N\rangle \\ &= \sum_{i=1}^{N} \left(S_i^z S_{i+1}^z\,|S_1 S_2 \cdots S_i S_{i+1} \cdots S_{N-1} S_N\rangle \right) \end{aligned}$$

using the third of equation (A.1)

$$
\begin{aligned}
&= \sum_{i=1}^{N} \left(S_i^z S_{i+1} \left|S_1 S_2 \cdots S_i S_{i+1} \cdots S_{N-1} S_N\right\rangle\right) \\
&= \sum_{i=1}^{N} \left(S_{i+1} S_i^z \left|S_1 S_2 \cdots S_i S_{i+1} \cdots S_{N-1} S_N\right\rangle\right) \\
&= \sum_{i=1}^{N} \left(S_i S_{i+1} \left|S_1 S_2 \cdots S_i S_{i+1} \cdots S_{N-1} S_N\right\rangle\right) \\
&= \sum_{i=1}^{N} \left(S_i S_{i+1}\right) \left|S_1 S_2 \cdots S_i S_{i+1} \cdots S_{N-1} S_N\right\rangle \\
&= \left(\sum_{i=1}^{N} S_i S_{i+1}\right) |\psi\rangle
\end{aligned} \tag{A.12}
$$

Similarly,

$$
H_2 |\psi\rangle = \left(j \sum_{i=1}^{N} S_i S_{i+1}\right) |\psi\rangle \tag{A.13}
$$

and

$$
H_3 |\psi\rangle = \left(-h_z \sum_{i=1}^{N} S_i\right) |\psi\rangle \tag{A.14}
$$

As for H_4, we have

$$
H_4 |\psi\rangle = -h_x \sum_{i=1}^{N} \left(S_i^x \left|S_1 S_2 \cdots S_i \cdots S_{N-1} S_N\right\rangle\right)
$$

using the first of equation (A.1)

$$
= -h_x \sum_{i=1}^{N} \left|S_1 S_2 \cdots (-S_i) \cdots S_{N-1} S_N\right\rangle \tag{A.15}
$$

Operating on both sides of equation (A.12) with $\mathcal{R}$ gives

$$
\begin{aligned}
\mathcal{R} H_1 |\psi\rangle &= \left(\sum_{i=1}^{N} S_i S_{i+1}\right) \mathcal{R} \left|S_1 S_2 \cdots S_k \cdots S_{N-1} S_N\right\rangle \\
&= \left(\sum_{i=1}^{N} S_i S_{i+1}\right) \left|S_N S_{N-1} \cdots S_{N-k+1} \cdots S_2 S_1\right\rangle
\end{aligned} \tag{A.16}
$$

While

$$\begin{aligned} H_1 R\,|\psi\rangle &= \left(\sum_{i=1}^{N} S_i^z S_{i+1}^z\right) |S_N S_{N-1}\cdots S_{N-k+1}\cdots S_2 S_1\rangle \\ &= \sum_{i=1}^{N} \left(S_i^z S_{i+1}^z\,|S_N S_{N-1}\cdots S_{N-k+1}\cdots S_2 S_1\rangle\right) \\ &= \left(\sum_{i=1}^{N-1} S_{N-i+1} S_{N-i}\right) |S_N S_{N-1}\cdots S_{N-k+1}\cdots S_2 S_1\rangle \\ &= \left(\sum_{i=1}^{N} S_i S_{i+1}\right) |S_N S_{N-1}\cdots S_{N-k+1}\cdots S_2 S_1\rangle \end{aligned} \tag{A.17}$$

Comparing (A.17) and (A.16), we find that $[H_1, \mathcal{R}] = 0$.
In a similar way, we find that $[H_2, \mathcal{R}] = 0$.

Now

$$R H_3\,|\psi\rangle = \left(\sum_{i=1}^{N} S_i\right) |S_N S_{N-1}\cdots S_{N-k+1}\cdots S_2 S_1\rangle \tag{A.18}$$

and

$$\begin{aligned} H_3 R\,|\psi\rangle &= \sum_{i=1}^{N} \left(S_i^z\,|S_N S_{N-1}\cdots S_{N-k+1}\cdots S_2 S_1\rangle\right) \\ &= \left(\sum_{i=1}^{N-1} S_{N-i+1}\right) |S_N S_{N-1}\cdots S_{N-k+1}\cdots S_2 S_1\rangle \\ &= \left(\sum_{i=1}^{N} S_i\right) |S_N S_{N-1}\cdots S_{N-k+1}\cdots S_2 S_1\rangle \end{aligned} \tag{A.19}$$

Comparing (A.18) and (A.19), we find that $[H_3, \mathcal{R}] = 0$.

Finally, we turn attention to H_4. We will drop the constant factor $-h_x$. Using equation (A.15), we have

$$\begin{aligned} \mathcal{R} H_4\,|\psi\rangle &= \sum_{i=1}^{N} \left(\mathcal{R}\,|S_1 S_2\cdots(-S_i)\cdots S_{N-1} S_N\rangle\right) \\ &= \sum_{i=1}^{N} |S_N S_{N-1}\cdots(-S_{N-i+1})\cdots S_2 S_1\rangle \end{aligned} \tag{A.20}$$

and

$$H_4\mathcal{R}\,|\psi\rangle = \sum_{i=1}^{N} S_i^x\,|S_N S_{N-1}\cdots S_{N-i+1}\cdots S_2 S_1\rangle$$
$$= \sum_{i=1}^{N} |S_N S_{N-1}\cdots(-S_{N-i+1})\cdots S_2 S_1\rangle \tag{A.21}$$

From (A.18) and (A.19), we see that $[H_4, \mathcal{R}] = 0$.

Therefore, we have proved that $[\mathcal{R}, H] = 0$, that is that spin reflection is a symmetry of the ANNNI model in the presence of an external longitudinal field and an external transverse field. □

A.2 All spin inversion operator $\mathcal{I}$

Another useful operator which we have employed to advantage is the inversion operator $\mathcal{I}$ defined in the notations of the previous section by

$$\mathcal{I}\,|S_1 S_2\cdots S_{N-1}S_N\rangle = |(-S_1)(-S_2)\cdots(-S_{N-1})(-S_N)\rangle \tag{A.22}$$

Again we note that $\mathcal{I}^2 = \mathbb{1}$, so that the eigenvalues of $\mathcal{I}$ are ± 1.

We hasten to emphasize that $\mathcal{I}$ is *not* a symmetry of the general Hamiltonian (1.1), for a finite h_z. Nonetheless $\mathcal{I}$ is very useful even when $h_z \neq 0$. $\mathcal{I}$ is a symmetry of the Ising model, the ANNNI model and the transverse ANNNI model, as will be proved shorty. When $h_x = 0$, the model (1.1) reduces to the ANNNI model in a longitudinal field (3.1). In this case $\mathcal{I}$ is useful in writing down immediately the energy of any state obtained from another state by inversion since then one merely has to change the sign of h_z in the energy of the former state. In other words, the use of $\mathcal{I}$ makes it possible to restrict the discussion of the eigenstates of $H(j, h_x = 0, h_z)$ to only those with total $S_z \geq 0$ or total $S_z \leq 0$. On the other hand, when $h_z = 0$, the Hamiltonian (1.1) reduces to that of the transverse ANNNI model and in this case, $\mathcal{I}$ is a symmetry. Combined with the translation symmetry and the reflection symmetry, exact diagonalization of the transverse ANNNI model can be significantly simplified.

Theorem A.2.1. *$\mathcal{I}$ is a symmetry of the ANNNI model, i.e. $[H_1 + H_2, \mathcal{I}] = 0$.*

Proof.

$$\begin{aligned} H_1\mathcal{I}\,|\psi\rangle &= \left(\sum_{i=1}^{N} S_i^z S_{i+1}^z\right)\mathcal{I}\,|S_1S_2\cdots S_{N-1}S_N\rangle \\ &= \sum_{i=1}^{N}\left(S_i^z S_{i+1}^z\,|(-S_1)(-S_2)\cdots(-S_{N-1})(-S_N)\rangle\right) \\ &= \sum_{i=1}^{N}\left((-S_i)(-S_{i+1})\,|(-S_1)(-S_2)\cdots(-S_{N-1})(-S_N)\rangle\right) \\ &= \left(\sum_{i=1}^{N} S_iS_{i+1}\right)|(-S_1)(-S_2)\cdots(-S_{N-1})(-S_N)\rangle \end{aligned} \tag{A.23}$$

On the other hand,

$$\begin{aligned} \mathcal{I}H_1\,|\psi\rangle &= \mathcal{I}\left(\sum_{i=1}^{N} S_iS_{i+1}\right)|S_1S_2\cdots S_{N-1}S_N\rangle \\ &= \left(\sum_{i=1}^{N} S_iS_{i+1}\right) I\,|S_1S_2\cdots S_{N-1}S_N\rangle \\ &= \left(\sum_{i=1}^{N} S_iS_{i+1}\right)|(-S_1)(-S_2)\cdots(-S_{N-1})(-S_N)\rangle \end{aligned} \tag{A.24}$$

Comparing equation (A.23) and (A.24) we see that $[H_1, \mathcal{I}] = 0$. In a similar way we obtain $[H_2, \mathcal{I}] = 0$.
We have thus proved that $\mathcal{I}$ is a symmetry of the ANNNI model. □

Next we will prove that $\mathcal{I}$ is a symmetry of the transverse ANNNI model.

Theorem A.2.2.

$$[H_1 + H_2 + H_4, \mathcal{I}] = 0$$

Proof. Since we have proved that $\mathcal{I}$ is a symmetry of the ANNNI model, it is sufficient to prove that $\mathcal{I}$ commutes with the transverse field term, H_4. We drop the constant $-h_x$ in the proof.

$$\begin{aligned} \mathcal{I}H_4\,|\psi\rangle &= \sum_{i=1}^{N}\left(\mathcal{I}\,|S_1S_2\cdots(-S_i)\cdots S_{N-1}S_N\rangle\right) \\ &= \sum_{i=1}^{N}|(-S_1)(-S_2)\cdots(S_i)\cdots(-S_{N-1})(-S_N)\rangle \end{aligned} \tag{A.25}$$

Likewise,

$$\begin{aligned} H_4\mathcal{I}\,|\psi\rangle &= \left(\sum_{i=1}^{N} S_i^x\right)|(-S_1)(-S_2)\cdots(-S_i)\cdots(-S_{N-1})(-S_N)\rangle \\ &= \sum_{i=1}^{N} S_i^x\,|(-S_1)(-S_2)\cdots(-S_i)\cdots(-S_{N-1})(-S_N)\rangle \\ &= \sum_{i=1}^{N} |(-S_1)(-S_2)\cdots(S_i)\cdots(-S_{N-1})(-S_N)\rangle \end{aligned} \tag{A.26}$$

Comparing equation (A.26) and (A.25) we see that $[H_4, \mathcal{I}] = 0$ and we have proved that inversion is a symmetry of the transverse ANNNI model. □

Now we will prove that $\mathcal{I}$ is not a symmetry of the longitudinal ANNNI model (3.1).

Theorem A.2.3.

$$[H_1 + H_2 + H_3, \mathcal{I}] \neq 0$$

Proof. We have already proved (Theorem A.2.1) that $[H_1 + H_2, \mathcal{I}] = 0$, therefore it is sufficient here to prove that $[H_3, \mathcal{I}] \neq 0$.

$$\begin{aligned} IH_3\,|\psi\rangle &= I\left(-h_z\sum_{i=1}^{N} S_i\right)|S_1S_2\cdots S_{N-1}S_N\rangle \\ &= \left(-h_z\sum_{i=1}^{N} S_i\right) I\,|S_1S_2\cdots S_{N-1}S_N\rangle \\ &= \left(-h_z\sum_{i=1}^{N} S_i\right)|(-S_1)(-S_2)\cdots(-S_{N-1})(-S_N)\rangle \end{aligned} \tag{A.27}$$

On the other hand,

$$\begin{aligned} H_3I\,|\psi\rangle &= \left(-h_z\sum_{i=1}^{N} S_i^z\right) I\,|S_1S_2\cdots S_{N-1}S_N\rangle \\ &= -h_z\sum_{i=1}^{N}\left(S_i^z\,|(-S_1)(-S_2)\cdots(-S_{N-1})(-S_N)\rangle\right) \\ &= -h_z\sum_{i=1}^{N}\left((-S_i)\,|(-S_1)(-S_2)\cdots(-S_{N-1})(-S_N)\rangle\right) \\ &= \left(h_z\sum_{i=1}^{N} S_i\right)|(-S_1)(-S_2)\cdots(-S_{N-1})(-S_N)\rangle \end{aligned} \tag{A.28}$$

Comparing equation (A.27) and equation (A.28), we see that $[H_3, \mathcal{I}] = 0$ only if $h_z = 0$ or total $S_z = 0$, so that $\mathcal{I}$ is not a symmetry of the longitudinal ANNNI model. □

Next we prove that $\mathcal{I}$ and $\mathcal{R}$ are compatible operators.

Theorem A.2.4.

$$[\mathcal{R}, \mathcal{I}] = 0$$

Proof. We recall,

$$\begin{aligned} \mathcal{I}\,|\psi\rangle &= \mathcal{I}\,|S_1 S_2 \cdots S_{N-1} S_N\rangle \\ &= |(-S_1)(-S_2)\cdots(-S_i)\cdots(-S_{N-1})(-S_N)\rangle \end{aligned} \tag{A.29}$$

and

$$\begin{aligned} \mathcal{R}\,|\psi\rangle &= \mathcal{R}\,|S_1 S_2 \cdots S_i \cdots S_{N-1} S_N\rangle \\ &= |S_N S_{N-1} \cdots S_{N-i+1} \cdots S_2 S_1\rangle \end{aligned} \tag{A.30}$$

which lead to

$$\mathcal{R}\mathcal{I}\,|\psi\rangle = |(-S_N)(-S_{N-1})\cdots(-S_{N-i+1})\cdots(-S_2)(-S_1)\rangle$$

and

$$\mathcal{I}\mathcal{R}\,|\psi\rangle = |(-S_N)(-S_{N-1})\cdots(-S_{N-i+1})\cdots(-S_2)(-S_1)\rangle \tag{A.31}$$

From which we conclude that the order in which $\mathcal{R}$ and $\mathcal{I}$ operate on an arbitrary state is unimportant so that the subspaces of $\mathcal{R}$ can always be further classified into the subspaces of $\mathcal{I}$ (for systems for which $\mathcal{I}$ and $\mathcal{R}$ are symmetries).

□

Before leaving this section, we give a simple non-trivial example of how one can take advantage of the inversion symmetry; we will diagonalize a four-spin transverse ANNNI system.

Classified by translation (Section A.3), the 6 eigenstates of $\mathcal{T}$ in the $k = 0$ subspaces of $\mathcal{T}$

belonging to the degenerate eigenvalue +1 are:

$$\begin{aligned}
|a\rangle &= |++++\rangle \\
|b\rangle &= |----\rangle \\
|c\rangle &= \left(|+-+-\rangle + |-+-+\rangle\right)/\sqrt{2} \\
|d\rangle &= \left(|++--\rangle + |+--+\rangle + |--++\rangle + |-++-\rangle\right)/2 \\
|e\rangle &= \left(|+++-\rangle + |++-+\rangle + |+-++\rangle + |-+++\rangle\right)/2
\end{aligned}$$

and

$$|f\rangle = \left(|---+\rangle + |--+-\rangle + |-+--\rangle + |+---\rangle\right)/2 \tag{A.32}$$

We note that these 6 states are also eigenstates of $\mathcal{R}$ belonging to eigenvalue +1, so that in this subspace, $\mathcal{R}$ provides no further simplification. For the transverse ANNNI model, inversion is a good quantum number. In the present example,$|c\rangle$ and $|d\rangle$ are eigenstates of $\mathcal{I}$ belonging to eigenvalue +1, $|b\rangle$ can be obtained from $|a\rangle$ by inversion, and likewise $|f\rangle$ from $|e\rangle$. $|a\rangle + |b\rangle$ and $|e\rangle + |f\rangle$ are eigenstates of I belonging to eigenvalue +1 while $|a\rangle - |b\rangle$ and $|e\rangle - |f\rangle$ are eigenstates of I belonging to eigenvalue −1. The 6 eigenstates of $\mathcal{T}$ in the subspace $k = 0$ can therefore be further reclassified into 4 eigenstates of $\mathcal{I}$ of eigenvalue +1 and 2 eigenstates of $\mathcal{I}$ of eigenvalue −1. The 6×6 matrix of the H in this subspace can therefore be block-diagonalized as a 2×2 matrix and a 4×4 matrix.

A.3 The Translation invariance symmetry $\mathcal{T}$

Consider *any* basis vector $|u\rangle = |S_1 S_2 \cdots S_{N-1} S_N\rangle$ of the direct product total S_z basis of a system of N spins 1/2; where as before $S_i = \pm 1$. The Translation operator $\mathcal{T}$ whose action on $|u\rangle$ produces another basis vector $|v\rangle$ of the total S_z basis belonging to the same value of total S_z as $|u\rangle$ is defined by

$$\begin{aligned}
|v\rangle =& \mathcal{T}\,|u\rangle \\
=& |S_2 S_3 \cdots S_{N-1} S_N S_1\rangle
\end{aligned} \tag{A.33}$$

Definition 2. Two vectors $|u\rangle$ and $|v\rangle$ are translationally related if $T^n\,|u\rangle = |v\rangle$ for some integer $n \leq N$.

Definition 3. A set of m translationally related vectors $\{|u_1\rangle, |u_2\rangle, \cdots, |u_k\rangle, \cdots, |u_m\rangle\}$ such that for any member $|u_k\rangle$, the relationship

$$T^m |u_k\rangle = |u_k\rangle \tag{A.34}$$

holds is called a cycle of period m.

Oridinarily one can build and diagonalize the matrix of H in the basis defined in equation (A.2). However, as noted earlier, even with the fastest computer, a direct diagonalization of a $2^N \times 2^N$ matrix even for a relatively small system is quite inefficient and impractical and as such should be avoided. We take advantage of the fact that the S_i^z basis vectors can be sorted into cycles, as long as periodic boundary conditions are imposed. We will prove shortly that although total S_z is not a symmetry of the Hamiltonian (1.1), $\mathcal{T}$ is. We are then able to use the translation symmetry, together with the reflection symmetry and in some special cases, the inversion symmetry, discussed in the previous sections to simplify the diagonalization process. Following the convention of [6] cycles will be called *proper cycles* if they have period N, otherwise they will be called *epicycles*. A more detailed discussion of how one can gainfully employ the symmetries of a Hamiltonian can be found in [6, 72, 73]. We note however that some important observations that are made here are not discussed in [6, 72, 73], nor in fact anywhere else.

We will now prove that $\mathcal{T}$ is a symmetry of Hamiltonian (1.1).

Theorem A.3.1.

$$[H, \mathcal{T}] = 0$$

Proof. In the notations of section A.1 and from the definition (A.33)

$$\begin{aligned} H_1 \mathcal{T} |\psi\rangle &= \sum_{i=1}^{N} \left(S_i^z S_{i+1}^z |S_2 S_3 \cdots S_N S_1\rangle \right) \\ &= \left(\sum_{i=1}^{N} S_{i+1} S_{i+2} \right) |S_2 S_3 \cdots S_N S_1\rangle \end{aligned} \tag{A.35}$$

Because of the periodic boundary condition, $S_N S_{N+1} = S_N S_1$ and $S_{N+1} S_{N+2} = S_1 S_2$ in the above summation and we therefore have

$$\begin{aligned} H_1 \mathcal{T} |\psi\rangle &= \left(\sum_{i=1}^{N} S_i S_{i+1} \right) |S_2 S_3 \cdots S_N S_1\rangle \\ &= \left(\sum_{i=1}^{N} S_i S_{i+1} \right) |\psi\rangle \end{aligned} \tag{A.36}$$

On the other hand,

$$\begin{aligned}\mathcal{T}H_1\left|\psi\right\rangle &= \left(\sum_{i=1}^{N} S_iS_{i+1}\right)\mathcal{T}\left|S_1S_2\cdots S_{N-1}S_N\right\rangle \\ &= \left(\sum_{i=1}^{N} S_iS_{i+1}\right)\left|S_2S_3\cdots S_NS_1\right\rangle \\ &= \left(\sum_{i=1}^{N} S_iS_{i+1}\right)\left|\psi\right\rangle \end{aligned} \tag{A.37}$$

and we have proved that $[H_1, \mathcal{T}] = 0$. The proof of $[H_2, \mathcal{T}] = 0$ is similar, and that $[H_3, \mathcal{T}] = 0$ is trivial. We have now only to prove that $[H_4, \mathcal{T}] = 0$. Now

$$\begin{aligned}\mathcal{T}H_4\left|\psi\right\rangle &= \sum_{i=1}^{N}\left(\mathcal{T}\left|S_1S_2\cdots(-S_i)\cdots S_{N-1}S_N\right\rangle\right) \\ &= \sum_{i=1}^{N}\left|S_2S_3\cdots - S_{i+1}\cdots S_NS_1\right\rangle \end{aligned} \tag{A.38}$$

and

$$\begin{aligned}H_4\mathcal{T}\left|\psi\right\rangle &= \left(\sum_{i=1}^{N} S_i^x\right)\left|S_2S_3\cdots S_{i+1}\cdots S_NS_1\right\rangle \\ &= \sum_{i=1}^{N}\left(S_i^x\left|S_2S_3\cdots S_{i+1}\cdots S_NS_1\right\rangle\right) \\ &= \sum_{i=1}^{N}\left|S_2S_3\cdots - S_{i+1}\cdots S_NS_1\right\rangle \end{aligned} \tag{A.39}$$

Comparing (A.38) and (A.39) we find that $[H_4, \mathcal{T}] = 0$.

This completes the proof that $\mathcal{T}$ is a symmetry of the Hamiltonian (1.1).

□

Next we prove that $\mathcal{T}$ and $\mathcal{I}$ commute. The commutation makes it possible to further reduce the dimension of the Hilbert space as mentioned in the previous section.

Theorem A.3.2.

$$[\mathcal{T}, \mathcal{I}] = 0$$

Proof.

$$\begin{aligned}\mathcal{I}\mathcal{T}\left|\psi\right\rangle &= \mathcal{I}\left|S_2S_3\cdots S_NS_1\right\rangle \\ &= \left|(-S_2)(-S_3)\cdots(-S_N)(-S_1)\right\rangle\end{aligned} \tag{A.40}$$

and

$$\begin{aligned}\mathcal{T}\mathcal{I}\left|\psi\right\rangle &= \mathcal{T}\left|(-S_1)(-S_2)\cdots(-S_{N-1})(-S_N)\right\rangle \\ &= \left|(-S_2)(-S_3)\cdots(-S_N)(-S_1)\right\rangle\end{aligned} \tag{A.41}$$

and the proof is complete. □

Next we will prove that although $\mathcal{I}$ and $\mathcal{T}$ are both symmetries of the Hamiltonian (1.1), they do not commute, in general.

Theorem A.3.3.

$$[\mathcal{T},\mathcal{R}] \neq 0$$

Proof.

$$\begin{aligned}\mathcal{R}\mathcal{T}\left|\psi\right\rangle &= \mathcal{R}\left|S_2S_3\cdots S_NS_1\right\rangle \\ &= \left|S_1S_N\cdots S_{N-i+2}\cdots S_3S_2\right\rangle\end{aligned} \tag{A.42}$$

and

$$\begin{aligned}\mathcal{T}\mathcal{R}\left|\psi\right\rangle &= \mathcal{T}\left|S_NS_{N-1}\cdots S_{N-i+1}S_2S_1\right\rangle \\ &= \left|S_{N-1}S_{N-2}\cdots S_{N-i}\cdots S_1S_N\right\rangle\end{aligned} \tag{A.43}$$

We see from equation (A.42) and equation (A.43) that $\mathcal{R}$ and $\mathcal{T}$ do not commute.
We will show however, that $[\mathcal{T},\mathcal{R}] = 0$ in the subspaces of T of eigenvalues of $\mathcal{T} = \pm 1$.

□

Theorem A.3.4. $[\mathcal{T},\mathcal{R}] = 0$ in the $k = 0$ subspace of the eigenstates of $\mathcal{T}$

Proof. Let $\{|\gamma_i\rangle\}$ and $\{|\lambda_i\rangle\}$ be two period-D cycles which are related by reflection, that is, such that

$$\mathcal{R}\left|\gamma_i\right\rangle = \left|\lambda_i\right\rangle,\ i = 1, 2, \cdots, D$$

and

$$\mathcal{R}\,|\lambda_i\rangle = |\gamma_i\rangle \ . \tag{A.44}$$

Then $\sum_{i=1}^{D} |\gamma_i\rangle = |\gamma\rangle$ and $\sum_{i=1}^{D} |\lambda_i\rangle = |\lambda\rangle$ are eigenstates of $\mathcal{T}$ of eigenvalue 1. That is

$$\mathcal{T}\,|\gamma\rangle = |\gamma\rangle$$

and

$$\mathcal{T}\,|\lambda\rangle = |\lambda\rangle \tag{A.45}$$

We see from equation (A.44) that

$$\mathcal{R}\,|\lambda\rangle = \mathcal{R}\sum_{i=1}^{D} |\lambda_i\rangle = \sum_{i=1}^{D} \mathcal{R}\,|\lambda_i\rangle = \sum_{i=1}^{D} |\gamma_i\rangle = |\gamma\rangle$$

and

$$\mathcal{R}\,|\gamma\rangle = \mathcal{R}\sum_{i=1}^{D} |\gamma_i\rangle = \sum_{i=1}^{D} \mathcal{R}\,|\gamma_i\rangle = \sum_{i=1}^{D} |\lambda_i\rangle = |\lambda\rangle \tag{A.46}$$

From (A.45) and (A.46), it follows that

$$\mathcal{T}\mathcal{R}\,|\lambda\rangle = \mathcal{T}\,|\gamma\rangle = |\gamma\rangle$$
$$\mathcal{R}\mathcal{T}\,|\lambda\rangle = \mathcal{R}\,|\lambda\rangle = |\gamma\rangle$$

and

$$\mathcal{T}\mathcal{R}\,|\gamma\rangle = \mathcal{T}\,|\lambda\rangle = |\lambda\rangle$$
$$\mathcal{R}\mathcal{T}\,|\gamma\rangle = \mathcal{R}\,|\gamma\rangle = |\lambda\rangle \tag{A.47}$$

From (A.47) we have that $[\mathcal{R}, \mathcal{T}] = 0$ for any $|\gamma\rangle$ and $|\lambda\rangle$ eigenstates of $\mathcal{T}$ of eigenvalue 1, and such that $|\gamma\rangle = R\,|\lambda\rangle$.

□

The proof that $[\mathcal{T}, \mathcal{R}] = 0$ *in the* $k = N/2$ *subspace of the eigenstates of* $\mathcal{T}$ is similar to the above proof.

A.4 Matrix representation of the translation operator

For D vectors that are translationally related the action of the translation operator $\mathcal{T}$ may be represented by

$$\begin{aligned} \mathcal{T}\left|m\right\rangle &= \left|m+1\right\rangle, \qquad m = 1, 2, \ldots, D-1 \\ \mathcal{T}\left|D\right\rangle &= \left|1\right\rangle \end{aligned} \tag{A.48}$$

The $D \times D$ matrix representation of $\mathcal{T}$ is therefore

$$T = \begin{pmatrix} 0 & 0 & 0 & & \cdots & & 1 \\ 1 & 0 & 0 & & \cdots & & 0 \\ 0 & 1 & 0 & & \cdots & & 0 \\ \vdots & & & & & & \\ 0 & 0 & 0 & & 1 & 0 & 0 \\ 0 & 0 & 0 & \cdots & 0 & 1 & 0 \end{pmatrix} \tag{A.49}$$

Thus, the eigenvalues x_k of T are the $D\,Dth$ roots of unity, *i.e.*

$$x_k = \exp\left(\frac{2\pi i k}{D}\right) \quad k = 0, 1, \ldots, D-1 \tag{A.50}$$

The corresponding eigenvectors of T are

$$\left|x_k\right\rangle = \frac{1}{\sqrt{D}} \sum_{m=1}^{D} x_k^{-m} \left|m\right\rangle \quad k = 0, 1, \ldots, D-1 \tag{A.51}$$

As a simple illustration, let us consider four arbitrary orthonormal vectors $|1\rangle$, $|2\rangle$, $|3\rangle$ and $|4\rangle$ that are translationally related *i.e.* such that $\mathcal{T}\left|1\right\rangle = \left|2\right\rangle$, $\mathcal{T}\left|2\right\rangle = \left|3\right\rangle$, $\mathcal{T}\left|3\right\rangle = \left|4\right\rangle$ and $\mathcal{T}\left|4\right\rangle = \left|1\right\rangle$. The matrix of T is

$$T = \begin{pmatrix} 0 & 0 & 0 & 1 \\ 1 & 0 & 0 & 0 \\ 0 & 1 & 0 & 0 \\ 0 & 0 & 1 & 0 \end{pmatrix} \tag{A.52}$$

The eigenvalues and corresponding eigenvectors of T for the four translationally related vectors are as given in the table A.1 on the following page. As another example let us consider a period- 6 cycle $\{\left|1\right\rangle, \left|2\right\rangle, \left|3\right\rangle, \left|4\right\rangle, \left|5\right\rangle, \left|6\right\rangle\}$.

Eigenvalue	Corresponding Eigenvector
1	$\frac{1}{2}\left(\left\|1\right\rangle + \left\|2\right\rangle + \left\|3\right\rangle + \left\|4\right\rangle\right)$
-1	$\frac{1}{2}\left(-\left\|1\right\rangle + \left\|2\right\rangle - \left\|3\right\rangle + \left\|4\right\rangle\right)$
i	$\frac{1}{2}\left(\left\|1\right\rangle - i\left\|2\right\rangle - \left\|3\right\rangle + i\left\|4\right\rangle\right)$
$-i$	$\frac{1}{2}\left(\left\|1\right\rangle + i\left\|2\right\rangle - \left\|3\right\rangle - i\left\|4\right\rangle\right)$

Table A.1: Eigenstates of T for a period 4 cycle

The matrix representation of $\mathcal{T}$ in this case is then

$$T = \begin{pmatrix} 0 & 0 & 0 & 0 & 0 & 1 \\ 1 & 0 & 0 & 0 & 0 & 0 \\ 0 & 1 & 0 & 0 & 0 & 0 \\ 0 & 0 & 1 & 0 & 0 & 0 \\ 0 & 0 & 0 & 1 & 0 & 0 \\ 0 & 0 & 0 & 0 & 1 & 0 \end{pmatrix} \tag{A.53}$$

The eigenvalues of T for the six translationally related vectors are the 6 6th roots of unity and the respective eigenvectors are linear combinations of the six vectors, as expressed in equation (A.51).

As a final explicit example, for a period 2 cycle $\{\left|1\right\rangle, \left|2\right\rangle\}$, the translation operator $\mathcal{T}$ has the representation

$$T = \begin{pmatrix} 0 & 1 \\ 1 & 0 \end{pmatrix} \tag{A.54}$$

The eigenvalues and respective eigenvectors are $[1, \frac{1}{\sqrt{2}}\left(\left|1\right\rangle + \left|2\right\rangle\right)]$ and $[-1, \frac{1}{\sqrt{2}}\left(-\left|1\right\rangle + \left|2\right\rangle\right)]$.

$2S_z$	Cycle	Period
4	$\{\|++++\rangle\}$	1
2	$\{\|+++-\rangle, \|-+++\rangle, \|+-++\rangle, \|++-+\rangle\}$	4
0	$\{\|++--\rangle, \|-++-\rangle, \|--++\rangle, \|+--+\rangle\}$	4
	$\{\|+-+-\rangle, \|-+-+\rangle\}$	2
-2	$\{\|+---\rangle, \|-+--\rangle, \|--+-\rangle, \|---+\rangle\}$	4
-4	$\|----\rangle$	1

Table A.2: The cycles of a 4-spin system

A.4.1 The total S_z basis and translational symmetry

The set of 2^N basis vectors in (A.2) can be sorted first into $N+1$ subsets with constant total S_z. Each subset has $\binom{N}{r} = N!/(r!(N-r)!)$ vectors for fixed values of total S_z such that $2S_z(r) = N - 2r$ for $r = 0, 1, \ldots, N$. The $\binom{N}{r}$ vectors in each subset can then be sorted into cycles. Clearly, the periods of the cycles are factors of N. As a very simple illustration, let us consider a system of 4 spins 1/2. The sixteen basis vectors of the direct product Hilbert space can be grouped into five subsets corresponding respectively to values of total $2S_z = 4, 2, 0, -2$ and -4. The classification into translationally related subsets *i.e.* cycles is displayed in table A.2.

A.4.2 Some characteristics of the translational invariance with respect to spin systems

The number of cycles to a given period.

Let N_1 and N_2 be certain spin system sizes, the configuration space of each being a direct product basis of S_z.

Lemma A.4.1. *If m is a positive integer and if $m|N_1$ and $m|N_2$, then every cycle of N_1 of period m is also a cycle of N_2 having period m.*

Proof. We recall that the cycles of each space have only periods which are factors of the number of spins.

Let $\left|S_1 S_2 \ldots S_m S_{m+1} \ldots S_{2m} \ldots S_{(k-1)m+1} \ldots S_{km}\right\rangle$ together with the $m-1$ translationally related vectors be a cycle of period m for system size $N_1 = km$, k some integer.

Clearly $\left|S_1 S_2 \ldots S_m S_{m+1} \ldots S_{2m} \ldots S_{(\lambda-1)m+1} \ldots S_{\lambda m}\right\rangle$ together with its $m-1$ translationally related vectors is also a cycle of period m for system size $N_2 = \lambda m$, λ some integer. □

Example A.4.1. *As an example,* $|++--++--\rangle$ *and its three translationally related vectors constitute a cycle of period* 4 *for* $N = 8$ *while* $|++--++--++--\rangle$ *and its three translationally related vectors form a period* 4 *cycle for system size* $N = 12$*. In this example* $k = 2$ *and* $\lambda = 3$*.*

Theorem A.4.1. *The number of cycles having a given period is independent of the system size* N*.*

Example A.4.2. *There are always two period-one cycles regardless of the number of spins. They are, of course, the vectors with total* $2S_z = \pm N$ i.e. $|+++\cdots++\rangle$ *and* $|---\cdots--\rangle$*. There is always one period-two cycle, namely* $\{|+-+-\cdots+-\rangle, |-+-+\cdots-+\rangle\}$*. A less obvious example would be the fact that there are always* 30 *cycles with period* 8 *regardless of chain length or that there are always* 14602 *period-*18 *cycles. By "regardless of system size", we assume of course that the size allows the particular period* i.e. *that the period is a factor of the system size in question.*

Proof. By Lemma A.4.1, if there are q cycles of system N_1 having period m, there must also be q cycles of system N_2 with period m. This completes the proof. □

A recursion relation for the number of cycles to a period

Let $X(m)$ be the number of cycles to a given period m. From the results from the last paragraphs we have immediately that $X(1) = 2$ and $X(2) = 1$. Now since the number of cycles is independent of system size, in order to determine $X(m)$ it is sufficient to consider system size $N = m$. This is a straightforward task since, due to the fact that the periods are factors of N we have that

$$\sum (\text{period} \times \text{number of cycles}) = 2^N \tag{A.55}$$

.

The simplest case is when m is prime, since in this case, we have that for $N = m$ there are only cycles of period 1 and cycles of period m. The number of period m cycles is then determined by solving

$$1 \times 2 + m \times X(m) = 2^m$$

for $X(m)$. Thus if m is prime, the number of period m cycles for any system size is

$$X(m) = \frac{2^m - 2}{m}$$

For a general m we have from equation (A.55) the following recursion relation for the number of cycles having period m:

$$X(m) = \frac{2^m - \sum_{k=1}^{\gamma-1} \lambda_k X(\lambda_k)}{m} \tag{A.56}$$

with $X(1) = 2$, $\lambda_k = k$th factor of m and $\gamma =$ total number of factors of m. The factors of m must be arranged in ascending order.
The total number of cycles of a chain of N spins is then given by

$$Totalcycles(N) = \sum_{i=1}^{\alpha} X(\beta_i) \tag{A.57}$$

where β_i is the ith factor of N and α is the total number of factors of N.

Dimensions of the subspaces of the space of eigenstates of $\mathcal{T}$

The orthogonal subspaces of $\mathcal{T}$ eigenstates contain eigenvector contributions from proper cycles as well as from epicycles of the total S_z basis vectors of the Hilbert space of a system of N spins. In this section we will derive a criterion for determining which cycles contribute eigenvectors to a subspace of $\mathcal{T}$ (corresponding to a fixed eigenvalue of $\mathcal{T}$). This way we will be able to determine in advance the dimensions of the subspaces of $\mathcal{T}$.
Let D be the period of an epicycle $\{|u\rangle\}$ and N the system size ($\equiv$ the period of a proper cycle $\{|v\rangle\}$).
We have $\mathcal{T}^D |u\rangle = |u\rangle$ for an epicycle and $\mathcal{T}^N |v\rangle = |v\rangle$ for a proper cycle.
Every solution of $\mathcal{T}^D = 1$ is also a solution of $\mathcal{T}^N = 1$. This is so because

$$\mathcal{T}^N = \left(\mathcal{T}^D\right)^{N/D} = 1 \text{ whenever } \mathcal{T}^D = 1$$

Thus all the eigenvalues of the translation operator $\mathcal{T}$ for proper cycles, as well as for epicycles are contained in the solutions of $\mathcal{T}^N = 1$. These are the N Nth roots of unity, $\exp(2\pi i/N)$, $k = 0, 1, \ldots, N-1$. The N orthogonal subspaces of the eigenstates of $\mathcal{T}$ may then be labelled as $k = 0$ subspace, $k = 1$ subspace, ..., and $k = N - 1$ subspace.

The eigenvalue of $\mathcal{T}$ from an epicycle will be one of the D Dth roots of unity, $\exp(2\pi i\lambda/D)$, $\lambda = 0, 1, \ldots, D-1$.

Thus an epicycle contributes an eigenvector to a given k-subspace provided that a $\lambda \in \{0, 1, \ldots, D-1\}$ exists such that

$$\frac{2\pi i\lambda}{D} = \frac{2\pi ik}{N} \tag{A.58}$$

That is, an epicycle of period $D \leq N$ contributes an eigenvector to the k-subspace only if kD/N is an integer or zero.

As an example of the application of the results of sections A.4.2 and A.4.2 let us consider a system of 10 spins $\frac{1}{2}$. Since the dividers of 10 are $1, 2, 5$ and 10, the total S_z basis vectors belong to cycles which have periods $1, 2, 5$ and 10.

From the recursion relation (A.56) we find that there are 2 period 1 cycles, 1 period 2 cycle, 6 period 5 cycles and 99 period 10 cycles. Thus there are 108 cycles altogether.

Let us now determine the dimensions of the subspaces of the eigenstates of $\mathcal{T}$, *i.e.* the k subspaces. We recall that according to equation (A.58) an epicycle of period $D \leq N$ contributes an eigenvector to the k-subspace only if kD/N is an integer or zero.

- $k = 0$

  Since $0 \times D/10 = 0$ for all epicycles, it follows that all 108 cycles contribute to the $k = 0$ subspace, and therefore the dimension of this subspace is 108.

- $k = 1$

  $D/10$ is an integer only if $D = 10$. This implies that only the 99 proper cycles contribute eigenvectors to the $k = 1$ subspace. The dimension of this subspace is therefore 99.

k	0	1	2	3	4	5	6	7	8	9
dimension	108	99	105	99	105	100	105	99	105	99

Table A.3: Dimensions of the k subspaces of $\mathcal{T}$ for $N = 10$

- $k = 2$

  $2D/10$ is an integer when $D = 5$ and when $D = 10$. Thus the dimension of the $k = 2$ subspace is made up of 6 eigenvectors from the period 5 epicycles and 99 eigenvectors from the proper cycles. The dimension of this subspace is therefore 105.

Continuing in this way, we determine the dimension of each of the 10 subspaces. This is summarized in table A.3.

A.5 $\left[S^2, H\right] \neq 0$

In this work we have gainfully employed translational invariance, reflection and in some special cases ($h_z = 0$)inversion symmetries of the ANNNI model in mixed fields (1.1). This led to significant reduction in the dimension of the Hilbert space considered in carrying out exact diagonalization. The symmetries also shed lights on the properties of the model as discussed throughout this work. Further simplification would also have been possible if H had been invariant under rotation. This turned out not to be the case.

To conclude this appendix, we will now prove that the Hamiltonian (1.1) does not possess rotational symmetry.

Proof. We write H as

$$H = H_1 + H_2 + H_3 + H_4 \tag{A.59}$$

where

$$\begin{aligned} H_1 &= \sum_i S_i^z S_{i+1}^z, \quad H_2 = j \sum_i S_i^z S_{i+2}^z \\ H_3 &= -h_z \sum_i S_i^z \quad \text{and} \quad H_4 = -h_z \sum_i S_i^x \end{aligned} \tag{A.60}$$

The total spin angular momentum operator of a system of N spin-1/2 particles is given by:

$$\begin{aligned} S^2 &= 3N\mathbb{1}/4 + \sum_{m\neq k} (S_m^x S_k^x + S_m^y S_k^y + S_m^z S_k^z) \\ &= S_0 + S_1 + S_2 + S_3 \end{aligned} \tag{A.61}$$

where

$$\begin{aligned} S_0 &= \frac{3N\mathbb{1}_N}{4}, \quad S_1 = \sum_{m\neq k} S_m^x S_k^x \\ S_2 &= \sum_{m\neq k} S_m^y S_k^y \text{ and } S_3 = \sum_{m\neq k} S_m^z S_k^z \end{aligned} \tag{A.62}$$

clearly $[H, S_0] = 0$, so we need be concerned only with S_1, S_2 and S_3.

$$[H, S^2] = \sum_{i=1}^{3}\sum_{j=1}^{3} [H_i, S_j] \tag{A.63}$$

We will evaluate the sums in turns

$$\begin{aligned} [H_1, S_1] &= \left[\sum_i S_i^z S_{i+1}^z, \sum_{m\neq k} S_m^x S_k^x\right] \\ &= \sum_i \sum_{m\neq k} \left(\left[S_i^z S_{i+1}^z, S_m^x S_k^x\right]\right) \end{aligned} \tag{A.64}$$

Using the commutator identities

$$[A, BC] = B[A, C] + [A, B]C \tag{A.65a}$$

$$[AB, C] = A[B, C] + [A, C]B \tag{A.65b}$$

and the commutation relations for spin operators

$$\begin{aligned} [S_{i+1}^z, S_k^x] &= S_k^y \delta_{k,i+1}, \quad [S_i^z, S_k^x] = S_k^y \delta_{ik} \\ [S_{i+1}^z, S_m^x] &= S_m^y \delta_{i+1,m} \text{ and } [S_i^z, S_m^x] = S_m^y \delta_{im} \end{aligned} \tag{A.66}$$

The sum in equation (A.64) evaluates to

$$[H_1, S_1] = 2 \sum_{\substack{k\neq i \\ k\neq i+1}} S_k^x \left(S_i^z S_{i+1}^y + S_i^y S_{i+1}^z\right) \tag{A.67}$$

A similar calculation gives

$$[H_1, S_2] = -2 \sum_{\substack{k \neq i \\ k \neq i+1}} S_k^y \left(S_i^z S_{i+1}^x + S_i^x S_{i+1}^z \right) \tag{A.68}$$

Clearly $[H_1, S_3] = 0$.
We therefore have that

$$[H_1, S^2] \neq 0 \tag{A.69}$$

$[H_2, S_1]$, $[H_2, S_2]$ and $[H_2, S_3]$ give results similar to the ones above, with $i+1$ replaced with $i+2$, so that we also have

$$[H_2, S^2] \neq 0 \tag{A.70}$$

$$\begin{aligned}
[H_3, S_1] &= \left[-h_z \sum_i S_i^z, \sum_{m \neq k} S_m^x S_k^x \right] \\
&= -h_z \sum_i \sum_{m \neq k} [S_i^z, S_m^x S_k^x] \\
&= -h_z \sum_i \sum_{m \neq k} S_m^x [S_i^z, S_k^x] - h_z \sum_i \sum_{m \neq k} [S_i^z, S_m^x] S_k^x
\end{aligned} \tag{A.71}$$

Now

$$[S_i^z, S_k^x] = S_k^y \delta_{ik} \text{ and } [S_i^z, S_m^x] = S_m^y \delta_{im} \tag{A.72}$$

so that

$$\begin{aligned}
[H_3, S_1] &= -h_z \sum_i \sum_{m \neq k} S_m^x S_k^y \delta_{ik} - h_z \sum_i \sum_{m \neq k} S_m^y S_k^x \delta_{im} \\
&= -h_z \sum_{i \neq m} S_m^x S_i^y - h_z \sum_{i \neq k} S_i^y S_k^x \\
&= -h_z \sum_{i \neq m} (S_m^x S_i^y + S_i^y S_m^x) \\
&= -h_z \sum_{i \neq m} \{S_m^x, S_i^y\}
\end{aligned} \tag{A.73}$$

A similar calculation yields

$$[H_3, S_2] = h_z \sum_{i \neq m} \{S_i^x, S_m^y\} \tag{A.74}$$

Clearly

$$[H_3, S_3] = 0 \tag{A.75}$$

Adding equations (A.73), (A.74) and (A.75) we therefore have

$$[H_3, S^2] = 0 \tag{A.76}$$

Finally we evaluate the commutator of $H_4 = -h_x \sum_i S_i^x$ and S^2.

$$\begin{aligned}
[H_4, S_1] &= \left[-h_x \sum_i S_i^x, \sum_{m \neq k} S_m^x S_k^x \right] \\
&= -h_x \sum_i \sum_{m \neq k} [S_i^x, S_m^x S_k^x] \\
&= 0
\end{aligned} \tag{A.77}$$

$$\begin{aligned}
[H_4, S_2] &= \left[-h_x \sum_i S_i^x, \sum_{m \neq k} S_m^y S_k^y \right] \\
&= -h_x \sum_i \sum_{m \neq k} [S_i^x, S_m^y S_k^y]
\end{aligned} \tag{A.78}$$

Expanding the commutator and using the relations

$$[S_i^x, S_k^y] = S_i^z \delta_{ik} \text{ and } [S_i^x, S_m^y] = S_i^z \delta_{im} \tag{A.79}$$

yields

$$[H_4, S_2] = -h_x \sum_{m \neq k} (S_m^y S_k^z + S_m^z S_k^y) \tag{A.80}$$

Similarly,

$$[H_4, S_3] = h_x \sum_{m \neq k} (S_m^z S_k^y + S_m^y S_k^z) \tag{A.81}$$

Adding equations (A.77), (A.80) and (A.81) we see again that

$$[H_4, S^2] = 0 \tag{A.82}$$

Collecting the results together (equations (A.69), (A.70), (A.76) and (A.82)), we conclude that the general Hamiltonian H does not commute with the total angular momentum operator S^2, that is

$$[H, S_2] \neq 0 \tag{A.83}$$

The non-commutativity is a result of both nearest-neighbour and next-nearest-neighbour interactions. It therefore turns out that total angular momentum is not a good quantum number for the ANNNI model in the presence of two fields.

□

Appendix B

Program Listing

```
# SUBROUTINES (procedures)

# factorsN accepts an integer N and creates a list
# of the factors of N

factorsN:=proc(N)
local factorsN1, k;
factorsN1:=[]:
for k to N do
if irem(N,k)=0 then
factorsN1:=[op(factorsN1),k] fi
od: factorsN1 end:

# EvenfactorsN accepts an integer N and creates a list
# of the even factors of N

EvenfactorsN:=proc(N)
local factorsN1, k;
factorsN1:=[]:
for k to N do
if irem(N,k)=0 and irem(k,2)=0 then
factorsN1:=[op(factorsN1),k] fi
od: factorsN1 end:
```

```
 # zerocycles(N) returns the number of cycles having total Sz=0 for a given N

 zerocycles:=proc (N) local x, m, k; option remember; x[2] := 1; for m from 2 to N
 by 2 do x[m] := (binomial(m,m/2)-sum(EvenfactorsN(m)[k]*x[EvenfactorsN(m)[k]],k = 1 ..
ops(EvenfactorsN(m))-1))/m od; x[N] end:

 # cycles(N) calculates the number of cycles
 # having period N e.g. cycles(4) returns 3

 cycles:=proc(N) option remember;
 local x, m, k;
 x[1]:=2:
 for m from 2 to N do
 x[m]:=(2^m-sum(factorsN(m)[k]*x[factorsN(m)[k]],
 `k`=1..nops(factorsN(m))-1))/m od: x[N] end:

 # totalcycles(N) determines the total number of
 # cycles in a chain of length N (this is also the
 # dimension of the largest matrix block). It makes
 # a call to cycles(N).e.g.totalcycles(6) returns 14.

 totalcycles:=proc(N)
 local totalcycles1, k;
 totalcycles1:=0:
 for k to nops(factorsN(N)) do
 totalcycles1:=totalcycles1 + cycles(factorsN(N)[k])
 od: totalcycles1 end:

 # totalzerocycles(N) determines the total number of
 # zero cycles in a chain of length N. It makes
 # a call to zerocycles(N).e.g.totalzerocycles(6) returns 4.

 totalzerocycles:=proc(N)
 local totalcycles1, k;
```

```
totalcycles1:=0:
for k to nops(EvenfactorsN(N)) do
totalcycles1:=totalcycles1 + zerocycles(EvenfactorsN(N)[k])
od: totalcycles1 end:

# T acts on a list and returns the next list
# that is translationally related to the given list
# e.g. T([1,1,-1,1]) returns [1,1,1,-1]

T:=proc(l::list) option remember; [op(l[2..nops(l)]),l[1]] end:

T_element:=proc(l1::list,l2::list)
if T(l2)=l1 then 1 else 0 fi end:


# Tmatrix(M) produces an M by M representation of T
# This is useful because the eigenstates of T for
# cycles having the same period are identical,
# so that one does not have to repeat the
# calculations.

Tmatrix:=proc(M)
local i,j,T1;
T1:=matrix(M,M,0):
for i to M do
for j to M-1 do
T1[i,i]:=0:
if i=j+1 then
T1[i,j]:=1 fi
od od:
T1[1,M]:=1:
evalm(T1) end:

# Sx(k,l) gives the action of Skx on a list
# e.g. Sx(2,[1,-1,1,-1]) returns [1,1,1,-1]
```

```
Sx:=proc(k,l::list) local l1;
l1:=l:
l1[k]:=-l[k]:
l1 end:


# hhx(list1,list2) computes the matrix element of Hx
# between two lists e.g. hhx([1,1,1,-1],[1,1,1,1])
# returns -hx/2

hhx:=proc(sj::list,ri::list)
option remember;
local hxri,k,hhhx;
hxri:={seq(Sx(k,ri),k=1..nops(ri))}:
if member(sj,hxri) then
hhhx:=-hx/2 else
hhhx:=0 fi: hhhx end:

# newhhx is the 'normalized' version of hhhx
# it returns 0 or 1

newhhx:=proc(sj::list,ri::list)
option remember;
local hxri,k,hhhx;
hxri:={seq(Sx(k,ri),k=1..nops(ri))}:
if member(sj,hxri) then
hhhx:=1 else
hhhx:=0 fi: hhhx end:

# nearsum(list) computes the nearest neighbour
# interaction of a list e.g. nearsum([-1,-1,-1,-1]) # returns  1

nearsum:=proc(l::list)
local nearsum1, i;
```

```
nearsum1:=0:
for i to nops(l)-1 do
nearsum1:=nearsum1+l[i]*l[i+1] od:
nearsum1:=nearsum1+l[1]*l[nops(l)]:
evalf(nearsum1/4) end:

# nextsum computes the next nearest neighbour
# sum of a list e.g nextsum([-1,-1,-1,-1]) returns 1

nextsum:=proc(l::list)
local nextsum1, i;
nextsum1:=0:
for i to nops(l)-2 do
nextsum1:=nextsum1+l[i]*l[i+2] od:
nextsum1:=nextsum1+l[nops(l)-1]*l[1]+
l[nops(l)]*l[2]:evalf(nextsum1/4) end:

# fieldsum computes the negative of total Sz
# of a list e.g fieldsum([-1,-1,-1,-1]) returns 2

fieldsum:=proc(l::list)
local fieldsum1,i;
fieldsum1:=0.:
for i to nops(l) do
fieldsum1:=fieldsum1-1./2*l[i] od:
fieldsum1 end:

# szstagger computes the staggered total Sz
# of a list e.g szstagger([-1,-1,-1,-1]) returns 0

szstagger:=proc(l::list)
local fieldsum1,i;
fieldsum1:=0.:
for i to nops(l) do
fieldsum1:=fieldsum1-(-1)^i*1./2*l[i] od:
```

```
fieldsum1 end:

antiphase:=proc (l::list)
local f,x,y,list1,k,newlist,retval,t;
f:=(x,y)->x*y:
list1:=[]:
for k to nops(l)/4 do
list1:=[op(list1),1,1,-1,-1] od:
newlist:=zip(f,list1,l):
retval:=0.5*add(t,t=newlist):
retval end:

energy:=proc(L::list)local k,i,Enn,Ennn,Ehz;
Enn:=0: Ennn:=0:
for k to nops(L)-1 do
Enn:=Enn+L[k]*L[k+1] od:
Enn:=Enn+L[nops(L)]*L[1]:
for k to nops(L)-2 do
Ennn:=Ennn+L[k]*L[k+2] od:
Ennn:=Ennn+L[nops(L)]*L[2]+L[nops(L)-1]*L[1]:
Ehz:=add(i,i=L):
Enn/4+j*Ennn/4-hz/2*Ehz end:

period:=proc(L::list) option remember;
local k;
for k while (T@@k)(L)<>L do od:
k end:

Tstates:=proc(tt) option remember; local i;
{seq((T@@i)(tt),i=1..nops(tt))} end:


trelated:=proc(L1::list,L2::list) local deter,k;
for k while (T@@k)(L1)<>L2 and k<=nops(L1) do od:
if (T@@k)(L1)=L2 then deter:=1 else deter:=0 fi:
```

```
deter end:

truehx:=proc(l1::list,l2::list,k) local toadd,i,s,coff;
toadd:=0:
for i to period(l1) do
for s to period(l2) do

coff:=exp(2*Pi*I*k/nops(l1)*(i-s)):
toadd:=toadd + coff*newhhx((T@@(i-1))(l1),(T@@(s-1))(l2))
od od:
toadd/sqrt(period(l1)*period(l2)) end:

prune:=proc(l::list) local i, toret;

toret:={}:
for i to nops(l) do
toret:=toret minus Tstates(l[i]) union {l[i]} od:
convert(toret,list) end:

# same as prune, but possibly slower

pruned:=proc(Qx::list) local F,F1,G,k,F2,newF,newF1,newG;
F:=convert(Qx,set):
G:={}:
while F<>{} do
F1:=F[1]:
newF1:={seq((T@@(k-1))(F1),k=1..period(F1))}:
F2:=`intersect`(newF1,F):
newF:=F minus F2:
unassign('F'):
F:=newF:
newG:=G union {F1}:
unassign('G'):
G:=newG  od:
convert(G,list) end:
```

```
secondorder:=proc(ketn::list,allkets::list,k)
local summe,toadd,m,fsumme;
summe:=0:
for m to nops(allkets) do

if abs(add(t,t=ketn)-add(t,t=allkets[m]))=2 then
toadd:=simplify(abs(truehx(ketn,allkets[m],k)*
        conjugate(truehx(ketn,allkets[m],k))))
        /(energy(ketn)-energy(allkets[m])):
summe:=summe+toadd fi od: hx^2/4*summe
end:


perturbmat:=proc(degkets::list,allkets::list,k)
local Vee,n,m,summe,q,toadd;
Vee:=matrix(nops(degkets),nops(degkets),0):

for n to nops(degkets) do
for m from n to nops(degkets) do

summe:=0:

for q to nops(allkets) do

if abs(add(t,t=degkets[n])-add(t,t=allkets[q]))=2
and abs(add(t,t=allkets[q])-add(t,t=degkets[m]))=2
then

toadd:=truehx(degkets[n],allkets[q],k)
       *truehx(allkets[q],degkets[m],k)
       /(energy(degkets[n])-energy(allkets[q]))
else

toadd:=0 fi:
```

```
summe:=summe+toadd od:

Vee[n,m]:=hx^2/4*summe:
Vee[m,n]:=hx^2/4*conjugate(summe)

od od: evalm(Vee) end:

comp:=proc(L::list) local k;
[seq(subsop(k=-L[k],L),k=1..nops(L))]
end:

relevant:=proc(L::list)
prune(comp(L)) end:

lowestn:=proc(a,b,c,A::matrix,n)

global j,hx,hz;
local Matblock, Hvalues1, Hvalues, sorted, toreturn;
Matblock:=matrix(rowdim(A),rowdim(A),(i,s)->evalf(subs(j=a,
hz=c,hx=b,A[i,s]))):
Hvalues1:=convert(Matlab[eig](Matblock),list):
if nops(Hvalues1)=2 then
Hvalues:=convert(Hvalues1[1],list)
else
Hvalues:=Hvalues1 fi:
sorted:=sort(Hvalues):
toreturn:=sorted[1..n]: toreturn end:



lowestn_wv:=proc(a,b,c,A::matrix)

 global j,hx,hz;
 local Matblock, Hvalues1, Hvalues, mvalue,t,r,uu1,uu2,vv1,vv2
```

```
,vects,vals,mvect,thevects;
 Matblock:=matrix(rowdim(A),rowdim(A),(i,s)->evalf(subs(j=a,
 hz=c,hx=b,A[i,s]))):
 (vects, vals) := Matlab[eig](Matblock, 'eigenvectors'='true'):


if nops(vals)=2 then vv1:=convert(op(1,vals),array): vv2:=convert(op(2,vals),array):
Hvalues1:=evalm(vv1+I*vv2)
else
 Hvalues1:=convert(vals,array) fi:

if nops(vects)=2 then uu1:=convert(op(1,vects),array): uu2:=convert(op(2,vects),array)
thevects:=evalm(uu1+I*uu2)
else
 thevects:=convert(vects,array) fi:

 Hvalues:=[]:

 for t to rowdim(Hvalues1) do
 Hvalues:=[op(Hvalues),Re(Hvalues1[t,t])] od:
 r:=1:
 mvalue:=Hvalues[1]:
 for t to nops(Hvalues) do
 if Hvalues[t]<mvalue then mvalue:=Hvalues[t]: r:=t fi od:
  [mvalue,col(thevects,r)] end:

sisjx:=proc(i,j,l::list) local u1,u2;
u1:=subsop(i=-l[i],l):
u2:=subsop(j=-l[j],u1):
[1/2,u2] end:

sisjy:=proc(i,j,l::list) local u1,u2;
u1:=subsop(i=-l[i],l):
u2:=subsop(j=-l[j],u1):
[-l[i]*l[j]/2,u2] end:
```

```
sisjz:=proc(i,j,l::list)
[l[i]*l[j]/2,l] end:

ssquared:=proc(l::list) local sssum,i,k,newl,multipl,s,output;
sssum:=[[3*nops(l)/4,l]]:

for i from 2 to nops(l) do
for k from 1 to i-1 do
sssum:=[op(sssum),sisjx(i,k,l),sisjy(i,k,l),sisjz(i,k,l)]
od od:

newl:={}:
for k to nops(sssum) do
newl:=newl union {sssum[k][2]} od:

newl:=convert(newl,list):

output:=[]:
for i to nops(newl) do
multipl:=0:

for s to nops(sssum) do

if sssum[s][2]=newl[i] then
multipl:=multipl+sssum[s][1] fi od:

if multipl<>0 then
output:=[op(output),[multipl,newl[i]]] fi od:
output:
end:

ssquared_element:=proc(l1::list,l2::list) local uv,i,bsum;
uv:=ssquared(l2):
bsum:=0:
```

```
for i to nops(uv) do

if uv[i][2]=l1 then
bsum:=bsum+uv[i][1] fi od:
bsum end:

flipall:=proc(l::list) local i;
[seq(-l[i],i=1..nops(l))] end:

flipall_element:=proc(l1::list,l2::list)
if flipall(l2)=l1 then 1 else 0 fi end:

xchange:=proc(l::list) local k;
[seq(l[-k],k=1..nops(l))] end:

xchange_element:=proc(l1,l2)
if l1=xchange(l2) then 1 else 0 fi end:

totalsz:=proc(l::list) local t;
add(t,t=l)/2 end:

rrelated:=proc(l1::list,l2::list)
if `intersect`({xchange(l1)},Tstates(l2))={} then 0 else 1 fi end:

hxelt:=proc(l1::list,l2::list)
if member(l1,{op(comp(l2))}) then 1 else 0 fi end:

energy_af:=proc(l::list)
local l1,l2,s1,s2,t,k;
global a0;
l1:=[seq(l[2*k-1],k=1..nops(l)/2)]:
l2:=[seq(l[2*k],k=1..nops(l)/2)]:
s1:=add(t,t=l1):
s2:=add(t,t=l2):
```

```
(s1-s2)*a0/2 end:

energy_fe:=proc(l::list) global a0; local t;
a0/2*add(t,t=l) end:

energy_ap:=proc(l::list)
local l1,l2,l3,l4,s1,s2,s3,s4,t,k;
global a0;
l1:=[seq(l[4*k-3],k=1..nops(l)/4)]:
l2:=[seq(l[4*k-2],k=1..nops(l)/4)]:
l3:=[seq(l[4*k-1],k=1..nops(l)/4)]:
l4:=[seq(l[4*k],k=1..nops(l)/4)]:
s1:=add(t,t=l1):
s2:=add(t,t=l2):
s3:=add(t,t=l3):
s4:=add(t,t=l4):
(s1+s2-s3-s4)*a0/2 end:

energy_uud:=proc(l::list)
local l1,l2,l3,s1,s2,s3,t,k;
global a0;
l1:=[seq(l[3*k-2],k=1..nops(l)/3)]:
l2:=[seq(l[3*k-1],k=1..nops(l)/3)]:
l3:=[seq(l[3*k],k=1..nops(l)/3)]:
s1:=add(t,t=l1):
s2:=add(t,t=l2):
s3:=add(t,t=l3):
(s1+s2-s3)*a0/2 end:

new_energy:=proc(l::list,xx)
if xx=0 then energy(l)-energy_fe(l)
elif xx=1 then energy(l)-energy_af(l)
elif xx=2 then energy(l)-energy_ap(l)
else
energy(l)-energy_uud(l) fi end:
```

```
 sec_order:=proc(gstate::list,xx) local i,second_cor,survivors;
 survivors:=comp(gstate):
 second_cor:=0:
 for i to nops(survivors) do
 second_cor:=second_cor+1/(new_energy(gstate,xx)-new_energy(survivors[i],xx)) od:
econd_cor end:

 corr2_degen:=proc(keta::list,ketb::list,xx)
 local l1,l2,k,l,asum;
 l1:=comp(keta):
 l2:=comp(ketb):

 l:={op(l1),op(l2)}:
 l:=convert(l,list):

 asum:=0:

 for k to nops(l) do
 if hxelt(keta,l[k])=1 and hxelt(ketb,l[k])=1 then
 asum:=asum+1/(new_energy(keta,xx)-new_energy(l[k],xx))
 fi od: asum end:

 fourth_corr1:=proc(gstate,xx)
 local all_ar,allar_r,allar_s,comp_ar,comp_as,comp_aras,asum,fsum,r,s,i;
 all_ar:=comp(gstate):

 fsum:=0:

 for r to nops(all_ar) do
 for s to nops(all_ar) do

 allar_r:=all_ar[r]:
 allar_s:=all_ar[s]:
```

```
comp_ar:=comp(allar_r):
comp_as:=comp(allar_s):

comp_aras:={op(comp_ar)} union {op(comp_as)} minus {gstate}:
comp_aras:=convert(comp_aras,list):




asum:=0:

for i to nops(comp_aras) do

asum:=asum+hxelt(allar_r,comp_aras[i])*hxelt(allar_s,comp_aras[i])
      /(new_energy(gstate,xx)-new_energy(comp_aras[i],xx)) od:

fsum:=fsum+1/(new_energy(gstate,xx)-new_energy(allar_r,xx))
      *1/(new_energy(gstate,xx)-new_energy(allar_s,xx))*asum od od:
fsum end:

fourth_corr2:=proc(gstate::list,xx) local i,second_cor,survivors;
survivors:=comp(gstate):
second_cor:=0:
for i to nops(survivors) do
second_cor:=second_cor+1/(new_energy(gstate,xx)-new_energy(survivors[i],xx))^2 od:
second_cor*sec_order(gstate,xx) end:

##############################################################################

# Create the subspaces of the space of eigenstates of the translation operator T

st:=time():
N:=8:
lamma:=[]:
for i to N do
```

```
 lamma:=[op(lamma),1,-1] od:
 lammb:=permute(lamma,N):
 cyclesonly:=prune(lammb):

 for k to N do
 subspace[k]:=[]:

 for i to nops(cyclesonly) do
 if irem((k-1)*period(cyclesonly[i]),N)=0 then
 subspace[k]:=[op(subspace[k]),cyclesonly[i]] fi od od:
 et:=time():
 duration:=(et-st)/60:

#############################################################################
# Build the matrices Hx and Hz

st:=time():
 NN:=N:
 MM:=1:

 Hz:=vector(N):
 Hx:=vector(N):
 H:=vector(N):
 for k from MM to NN do


 Hz[k]:=matrix(nops(subspace[k]),nops(subspace[k]),0):
 for i to nops(subspace[k]) do
 Hz[k][i,i]:=energy(subspace[k][i]) od od:

 for k from MM to NN do

 Hx[k]:=matrix(nops(subspace[k]),nops(subspace[k]),0):
 for i to nops(subspace[k]) do
 for s from i+1 to nops(subspace[k]) do
```

```
rsumm:=add(t,t=subspace[k][i]):
ssumm:=add(t,t=subspace[k][s]):
diffsum:=rsumm-ssumm:
if abs(diffsum)=2 then

xelement:=truehx(subspace[k][i],subspace[k][s],k-1):
Hx[k][i,s]:=-hx/2*xelement:
Hx[k][s,i]:=-hx/2*conjugate(xelement) fi od od od:

for k from MM to NN do

H[k]:=evalm(Hx[k]+Hz[k]) od:
et:=time():
duration:=(et-st)/60:
```

Appendix C

Exact diagonalization results

The results are contained in the included CDROM.

Bibliography

[1] H. Rieger and G. Uimin, Z. Phys B **101**, 597 (1996).

[2] P. Sen and B. K. Chakrabarti, Phys. Rev. B **43**, 559 (1991).

[3] A. Ovchinnikov, D. V. Dmitriev, V. Y. Krivnov, and V. O. Cheranovskii, Phys. Rev. B **68**, 214406 (2003).

[4] B. K. Chakrabarti, A. Dutta, and P. Sen, *Quantum Ising phases and Transitions in Transverse Ising models* (Springer-Verlag, 1996).

[5] P. Sen, Phys. Rev. E **63**, 016112 (2001).

[6] K. Bärwinkel, H. Schmidt, and J. Schnack, J. Magn. Magn. Mater. **212**, 240 (2000).

[7] M. E. Fisher and H. N. Barber, Phys. Rev. Lett. **28**, 1516 (1972).

[8] R. J. Elliot, Phys. Rev. **124**, 346 (1961).

[9] M. N. Barber and P. M. Duxbury, J. Phys. A: Math. Gen. **14**, L251 (1981).

[10] M. R. Hornreich, R. Liebmann, H. G. Schuster, and W. Selke, Z. Physik B **35**, 91 (1979).

[11] W. Selke and M. E. Fisher, Z. Phys. B **40**, 71 (1980).

[12] J. Villain and P. Bak, J. Phys. (Paris) **42**, 657 (1981).

[13] W. Selke, Phys. Rep. **170**, 213 (1988).

[14] J. Yeomans, *Solid State Physics*, vol. 41 (Academic Press, New York, 1987).

[15] P. Pfeuty, Ann. Phys. **57**, 79 (1970).

[16] E. Lieb, T. Schultz, and D. Mattis, Ann. Phys. (N.Y.) **16**, 407 (1961).

[17] B. M. McCoy, Phys. Rev. **173**, 531 (1968).

[18] M. Suzuki, ed., *Quantum Monte Carlo Methods* (Springer-Verlag, Heidelberg, 1986).

[19] J. B. Kogut, Rev. Mod. Phys. **51**, 659 (1979).

[20] L. G. Marland, J. Phys. A.: Math. Gen. **14**, 2047 (1981).

[21] E. Fradkin and L. Susskind, Phys. Rev. D **17**, 2637 (1978).

[22] M. N. Barber and P. M. Duxbury, J. Stat. Phys. **29**, 427 (1982).

[23] W. Pesch and J. Kroemer, Z. Physik B **59**, 317 (1984).

[24] P. Ruján, Phys. Rev. B **24**, 6620 (1981).

[25] P. Sen and B. K. Chakrabarti, Phys. Rev. B **40**, 760 (1989).

[26] D. Wolf and J. Zittartz, Z. Phys. B **43** (1981).

[27] B. Hu, Phys. Lett. A **71**, 83 (1982).

[28] P. Pfeuty, R. Jullien, and K. A. Penson, *Real Space Renormalization, Topics in Current Physics* (Springer-Verlag, Heidelberg, 1982).

[29] D. Drell, M. Weinstein, and S. Yankiclowicz, Phys. Rev. D **16**, 1769 (1977).

[30] R. Jullien, P. Pfeuty, J. N. Fields, and S. Doniac, Phys. Rev. B **18**, 3568 (1978).

[31] T. Garel and P. Pfeuty, J. Phys. C **9**, L245 (1976).

[32] C. J. Hamer and M. N. Barber, J. Phys. A: Math. Gen. **13**, L169 (1980).

[33] P. R. C. Guimarães, J. A. Plascak, F. C. S. Barreto, and J. Florencio, Phys. Rev. B **66**, 064413 (2002).

[34] C. J. Hamer and M. N. Barber, J. Phys. A: Math. Gen. **14**, 241 (1981).

[35] J. Igarashi and T. Tonegawa, Phys. Rev. B **40**, 756 (1989).

[36] V. J. Emery and C. Noguera, Phys. Rev. Lett. **60**, 631 (1988).

[37] C. M. Arizmendi, A. H. Rizzo, L. N. Epele, and C. A. G. Canal, Z. Phys. B **83**, 273 (1991).

[38] S. N. Coopersmith, D. S. Fisher, B. I. Halperin, P. A. Lee, and W. F. Brinkman, Phys. Rev. Lett. (1981).

[39] I. Peschel and V. J. Emery, Z. Phys. B. **43**, 241 (1981).

[40] P. Sen, Phys. Rev. B **55** (1997).

[41] I. Affleck and M. Oshikawa, Phys. Rev. B **60**, 1038 (1999).

[42] A. Langari and S. Mahdavifar, Phys. Rev. B **73**, 054410 (2006).

[43] M. Kenzelmann, R. Coldea, D. A. Tennant, D. Visser, M. Hofmann, P. Smeibidl, and Z. Tylczynski, Phys. Rev B. **65**, 144432 (2002).

[44] D. V. Dmitriev and V. Y. Krivnov, Phys. Rev. B **70**, 144414 (2004).

[45] S. R. White, Phys. Rev. B **48**, 10345 (1993).

[46] F. Bloch, Z. Physik **61**, 206 (1930).

[47] G. Heller and H. A. Kramers, Proc. Roy. Acad. Sci. Amsterdam **37**, 378 (1934).

[48] L. Hulthén, Proc Roy. Acad. Sci. Amsterdam **39**, 190 (1936).

[49] H. A. Bethe, Z. Physik **21**, 205 (1931).

[50] Y. Gaididei and H. Büttner, Phys.Rev. B **62**, 8604 (2000).

[51] P. W. Anderson, Phys. Rev. **86** (1952).

[52] A. Dutta and D. Sen, Phys. Rev. B **67**, 094435 (2003).

[53] B. Yavorsky and A. Detlaf, *Handbook of Physics* (Mir Publishers, Moscow, 1977).

[54] C. Domb, Adv. Phys. **9** (1960).

[55] A. Aharony, *Critical Phenomena, Lecture Notes in Physics*, vol. 186 (Springer-Verlag, Berlin, 1983).

[56] J. P. H. et. al., Phys. Rev. B **55**, 356 (1997).

[57] R. Liebemann, *Statistical Mechanics of Periodic Frustrated Ising Systems, Lecture Notesin Physics*, vol. 251 (Springer-Verlag, 1986).

[58] T. Morita and T. Horiguchi, Phys. Lett. A **38**, 223 (1972).

[59] C. S. O. Yokoi, M. D. Coutinho-Filho, and S. R. Salinas, Phys. Rev. B **24**, 4047 (1981).

[60] R. Feynmann, Phys. Rev. **56**, 340 (1939).

[61] L. F. Lemmens and F. Brosens, Phys. Rev.B **12**, 4316 (1975).

[62] R. A. Ferrell, Phys. Rev. Lett. **1**, 443 (1958).

[63] Y. Hieida, K. Okunishi, and Y. Akutsu, Phys. Rev. B **64**, 224422 (2001).

[64] J. Rosenfeld and N. E. Ligterink, Phys. Rev. B **62**, 308 (2000).

[65] H. A. Kramers and G. H. Wannier, Phys. Rev **B 60**, 252 (1941).

[66] G. O. Williams, P. Ruján, and H. L. Frisch, Phys. Rev. B **24**, 6632 (1981).

[67] P. Serra, J. P. Neirotti, and S. Kais, J. Phys. Chem. A **102**, 9518 (1998).

[68] M. P. Nightingale, Phys. Lett. A **59**, 486 (1977).

[69] O. Nohadani, S. Wessel, B. Normand, and S. Haas, Phys. Rev **B 69**, 220402(R) (2004).

[70] H. L. Davis, Phys. Rev. **120**, 789 (1960).

[71] J. C. Xavier, F. C. Alcaraz, and J. A. Plascak, Phys. Rev. B **57**, 575 (1998).

[72] D. Kouzoudis, J. Magn. Magn. Mater. **173**, 259 (1997).

[73] D. Kouzoudis, J. Magn. Magn. Mater. **189**, 366 (1998).

Erklärung

Hiermit erkläre ich, dass es von mir keine früheren Promotionsversuche gibt.

Außerdem erkläre ich, dass ich die vorliegende Doktorarbeit mit dem Titel „The one-dimensional spin-1/2 ANNNI model in non-commuting magnetic fields“ selbständig verfasst habe und keine anderen als die angegebenen Quellen und Hilfsmittel benutzt habe.

Bayreuth, den 05.06.2006

Adekunle M. Adegoke

Credits

I am most grateful to my supervisor, Prof. Dr. Helmut Büttner, for being such a marvellous Doktorvater. It is not always that one has the priviledge of working under the supervision of a master in the field! Prof. Gbenga Jegede provided the motivation and established my Bayreuth link. He is a wonderful mentor who would support and encourage you with all his resources! Special thanks to Prof. Dr. F. G. Mertens who wrote recommendation letters for me for scholarship extensions. Special thanks to Prof. Dr. W. Pesch who showed me some advanced techniques in theoretical Physics. Special thanks to Juniorprofessur Dr. Cord Müller who extended a warm hand of friendship to me. My wonderful friend Dr. Christian Schuster and his girlfriend Christina made integration and settling down pleasant tasks for me. They are a wonderful people! Dr. Luis Morales Molina and I had a wonderful time together, a cool friend! I acknowledge the kindness of Mrs. Sigrid Glas, the departmental secretary. My friends Jochen Endrejat and Christian Brunhuber helped with the Logistics of last minute preparations. Dr. Denis Sheka showed me some nice LaTeX tips and tricks. Endrejat, Brunhuber, Christopher Gaul, Christian Hörhammer, Dr. Olivier Sigwarth and Dr. Pullakart made very useful suggestions that helped improve my presentation. My friend and fellow scholar Dr. Jonathan Guevarra (Tani) and his family and my family had wonderful moments together in Bayreuth. Thanks Tani, also for answering all my numerous questions on the required procedure while I was bringing my research to a conclusion. Tobias Kercher and Christopher Gaul took the Promotion pictures. Thanks again! Dr. Pramod Pullakart and his family are a wonderful people. We had a nice time together in Bayreuth. The Weick family (Klaus and Rowena and their son Andreas) contributed in no small way to our happiness in Bayreuth. The institute of Physics Bayreuth provided the facility with which I carried out my research. My coming to Germany and subsequent doctoral research would have remained a dream without funding. I am most grateful to the DAAD (German academic exchange service) for awarding me a scholarship. My former teachers and erstwhile supervisors Prof. Oluwole Odundun and Prof. Akin Ojo recommended me to the DAAD. My friends Drs. Waheed Adeagbo, Dele Oluwade and Wole Yewande were with me all the way. Of course I have not forgotten the homefront: The support and presence of my loving wife Funmilade and my wonderful children Adenike and Oyinlola made living in Germany a lot of fun! I would like to thank all members of staff of the Institut of Physics of the University of Bayreuth. You are all a wonderful people! We had nice times with the Africans in Bayreuth too, in particular with the families of Dr. Sola Ajibade, Rev. Selome Kuponu, Dr. Afe Adogame, brother Sam Owiredu, Dr Taiwo Oloruntobaoju and Dr. Ayantayo and Elijah Yenyor.
I thank my mother, Omoseeke Famoroti, who continued to encourage me, and for being my mother!

The constraints of time and space do not allow me to mention by name everybody who must have contributed in one way or another to the success of this research. I can only count on your understanding!

Kunle Adegoke
Bayreuth, July 2006.